Equilibre acide-base lors de l'hémodiafiltration en ligne : modélisation, analyses in vitro et clinique des transferts de bicarbonate

H. Morel

UNIVERSITE DE TECHNOLOGIE DE COMPIEGNE

Laboratoire UMR6600 : BioMécanique et BioIngénierie (BMBI)

Equilibre acide-base lors de l'hémodiafiltration en ligne : modélisation, analyses *in vitro* et clinique des transferts de bicarbonate

THESE

présentée pour l'obtention du grade de

Docteur de l'Université de Technologie de Compiègne

Discipline : Bio-Ingénierie Biomécanique Biomatériaux

par

Hélène MOREL

Soutenance effectuée le 1 décembre 2009 devant le jury composé de :

Patrice Bacchin	Université Paul Sabatier de Toulouse (Rapporteur)
Michel Jaffrin	Université de Technologie de Compiègne (Directeur de thèse)
Eric Leclerc	Université de Technologie de Compiègne
Cécile Legallais	Université de Technologie de Compiègne (Directrice de thèse)
Philippe Morinière	CHU Amiens
Thierry Petitclerc	AURA - CHU Pitié Salpêtrière
Raymond Vanholder	Ghent University (Rapporteur)
Jörg Vienken	Fresenius Medical Care

Je remercie les membres du jury pour la lecture minutieuse de mon manuscrit et pour les différents commentaires constructifs.
Je remercie l'ensemble des partenaires du projet, pour leur aide précieuse et pour leur soutien technique et financier :

Prof. Vienken, and Dr. Nier, Fresenius Medical Care (Germany)
Dr. Morinière, CHU Amiens
Prof. Petitclerc, AURA Paris
Patrick Paullier, UTC
Henri Fournier, Fresenius Medical Care (France)
Pharmacy department, CHU Amiens
Technical assistance from Laon slaughterhouse
Nurses and dialysed patients from Amiens hospital

Table of Content

Nomenclature

A	Hemodialyzer area	m^2
C	Concentration	mmol/L
cO_2/cCO_2	Oxygen/Carbon dioxide concentration	mmol/L
CL	Clearance	mL/min
CLd	Diffusive clearance	mL/min
D	Dialysance	mL/min
Dp	Dialysance (patient)	mL/min
Ds	Solute diffusivity	cm^2/min
e	Membrane thickness	m
H	Hematocrit	%
Hb	Hemoglobin	g/dL
J_F	Volumetric flux of water	mL/h/m^2
Js_c	Solute flux by convection	mmol/m^2/h
Js_d	Solute flux by diffusion	mmol/cm^2/min
K	Partition coefficient	-
K_0	Mass transfer coefficient	cm/min
K_{UF}	Ultrafiltration coefficient	mL/h/mmHg
L	Fibre/hemodialyzer length	m
Lp	Hydraulic membrane permeability	mL/h/m^2/mmHg
M	Mass transfer per unit time	mmol/min
Mbh	(Hemodialyzer) mass flow rate in blood	mmol/min
Mdh	(Hemodialyzer) mass flow rate in dialysis fluid	mmol/min
Mbp	(Patient blood) mass flow rate	mmol/min
N	Number of fibres	-
P	Pressure	mmHg
pO_2/pCO_2	Oxygen/Carbone dioxide partial pressure	mmHg
Q	Flow rate	mL/min
Qf	Ultrafiltration rate	mL/min
Qr	Reinjection rate	mL/min
Qs_c	Convective mass transfer	mmol/h
Qs_d	Diffusive mass transfer	mmol/min
Qw	Weigh loss rate	mL/min
Qpw	Plasma water flow rate	mL/min
r	Fibre radius	m
R	Rejection coefficient	-
R_M	Membrane diffusion resistance	min/cm
S	Sieving coefficient	-
t	Time	min
TMP	Transmembrane pressure	mmHg
TProt	Total protein concentration	g/L
V	Volume	L
Vbin	Initial blood volume	L
W	Body weight	kg
αO_2/ αCO_2	Oxygen/Carbone dioxide solubility	mmol/L/mmHg
μ	Viscosity	Pa.s
σ	Staverman's coefficient	-
ΔP	Pressure drop	mmHg
$\Delta\pi$	Oncotic pressure	mmHg
[]	Concentration	mmol/L

Subscripts

b	Blood
d	Dialysis fluid/Dialysate
f	Filtrate
m	Membrane
p	Plasma
i/in	inlet
o/out	outlet

Abbreviations

ABL	Blood gas analyzer, ABL77 (Radiometer)
ABS	Apparent Bicarbonate Space
BG	Bicarbonate gain
BVM	Blood Volume Monitor
CA	Carbonic anhydrase
CV	Coefficient of variation
ESRD	End stage renal disease
F	Female
FMC	Fresenius Medical Care
HD	Hemodialysis
HDF	Hemodiafiltration
M	Male
MW	Molecular weight
PBS	Phosphate Buffer Solution
RBC	Red Blood Cell
SD	Standard Deviation
EPO	Erythropoietin

Introduction

Hemodiafiltration (HDF) is a dialysis technique proposed as an alternative to hemodialysis (HD) since the beginning of 1970 to end stage renal disease (ESRD) patients. This technique combines the usual diffusive transfer of hemodialysis with the convective transfer created by hemofiltration. The high ultrafiltration (UF) rate leads to the removal of a significant volume of plasma water which needs to be compensated by the reinjection of a liquid of the same composition as the dialysis fluid. Excellent clearances are obtained for both low and high molecular weight solutes, and this technique provides in addition a better cardiovascular stability for the dialysis patients. With the development of online production of reinjection fluid from dialysis fluid (called 'online hemodiafiltration') HDF has become less expensive and is thus potentially more widely applicable. In France this therapy represents 10% of dialysis treatments in 2009.

The potential benefits of this technique for acid-base balance of dialysis patients have not been thoroughly studied. Blood acidosis (the most frequent acid-base disturbance) needs to be corrected in ESRD patients as it affects several metabolic processes in the body and could lead to malnutrition. This correction can be achieved by including a buffer such as bicarbonate (HCO_3^-) in dialysis fluid. The buffer gain should be adjusted so that patients' plasma is maintained close to the physiological bicarbonate range. In HDF, a significant loss of HCO_3^- is expected from blood through the hemodialyzer membrane due to the high UF rate. This loss should be corrected by the reinjection fluid. Dialysis manufacturers such as Fresenius Medical Care (FMC) wish to promote online HDF for more patients, and thus need to collect more data on this aspect. The effects of online HDF parameters (operating conditions) in terms of pH, gas (pO_2 and pCO_2) and bicarbonate balance should be investigated. This is the subject of this PhD thesis.

A large number of parameters govern acid-base states in HDF, such as blood, UF and dialysis fluid flow rates, HCO_3^- concentration, pCO_2, pO_2, or pH. Associated with the necessity for collecting many blood samples, a complete study of the effects of these parameters is difficult to carry out in dialysis patients. Therefore we choose to carry out three approaches in parallel, as described in the following Figure.

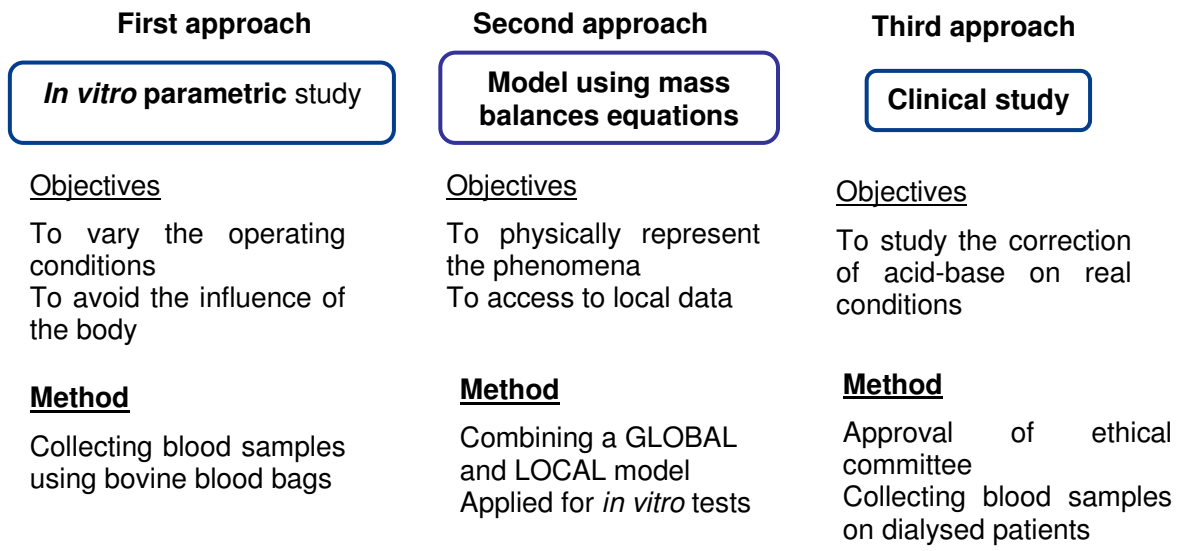

Figure 1 Methodology of the PhD thesis

As biomedical researcher, it is thus legitimate to check whether an *in vitro* HDF approach using fresh bovine blood could provide useful information for clinicians. This *in vitro* study excludes the gas exchanges at the lung levels and all the metabolic functions (including bicarbonate metabolism) of cells are avoided.

This parametric approach has been combined with the development of a kinetic model to physically represent the phemomena of mass transfers in patient and hemodialyzer compartment. Such kinetic model can be a convenient tool to compare efficiencies of various HDF strategies or various hemodialyzers. The aim is to model solute blood concentration time variation. The development of this kinetic modeling used mass balance equations for the *in vitro* patient and a description of the local mass transfer in the hemodialyzer.

After this simplified approach, we had the opportunity to perform an *in vivo* study to adress the question of acid-base parameters in online HDF postdilution under clinical situation. This study has been conducted at Amiens hospital in the Nephrology department under the supervision of the head of the hemodialysis unit, Dr Philippe Morinière. All acid-base balance parameters (pH, pCO_2, pO_2, HCO_3^- concentration) have been monitored during the dialysis sessions by taking periodically blood samples and comparisons of bicarbonate mass transfer in HD and online postdilution HDF sessions have been studied. This report contains the preliminary clinical study where 6 patients have been included and 23 dialysis sessions monitored.

HCO_3^- concentration, pO_2, pCO_2 and pH have been analysed during the *in vitro* and *in vivo* dialysis sessions and constituted data bases of operating conditions of the dialysis sessions.

In this report, the first chapter is dedicated to a general introduction to the renal functions and hemodialysis techniques, with special attention to solute and fluid transport mechanisms. Then gas

(CO_2 and O_2) exchanges are detailed in order to understand the acid-base balance in the body and its restoration mechanisms in dialysis patients. Finally an overview of the mathematical models in hemodialysis is proposed.

In the second chapter, we present the *in vitro* and *in vivo* methods. Because analysis methods can be a source of many errors, the measurements techniques to analyse acid-base parameters, dialysis machine parameters, hematocrit and pressures measurements have been described in details and studied. This chapter also gives an analysis of the *in vitro* tests repeatability. Since bicarbonate concentration and hematocrit have been obtained from various devices (using various analysis methods), it was thus legitimate to compare these measurements between each other. It is the subject of the last section of the second chapter.

The third chapter presents the kinetic modeling of the extracorporeal circuit applied for *in vitro* experiments. After the description of the global approach for the '*in vitro*' patient and the local model for the hemodialyzer, the equations and solving procedures are presented. The various parameters useful for the model are all described and assessed using the *in vitro* tests. Then the kinetic model is validated using the *in vitro* experiments. The last section of this chapter reports experimental time variations of blood and dialysis fluid pressure measurements. These pressures changes are interpreted using a mathematical analysis in terms of blood clotting of hemodialyser fibres during dialysis sessions.

In the fourth chapter we present the preliminary results of the *in vivo* study and a methodology to analyse them. After an overview of the 23 monitored dialysis sessions, the acid-base parameters time variations are evaluated using statistical analysis and a case study for HD sessions. This chapter ends with a synthesis of the effects of the acid-base parameters along the hemodialyzer in order to explain how their transfers take place inside the hemodialyzer.

The fifth chapter is dedicated to a deeper analysis of bicarbonate mass transfers during *in vitro* tests compared to results obtained by the kinetic model and during *in vivo* tests. Since clearance or dialysance is an important indicator of dialysis session efficiency for physicians, bicarbonate dialysances have also been calculated. Other indicators of the quantification of the dialysis sessions are proposed: experimental predictions of the increase of HCO_3^- plasma concentration and of the final HCO_3^- plasma concentration as a function of the initial one. Finally plasma HCO_3^- gains by the patients measured in the *in vitro* and *in vivo* studies during dialysis are compared with predictions by our models.

Major conclusions of this *in vitro*, modeling and *in vivo* studies, perspectives and possible extensions of this work are summurised in the last chapter.

Chapter I Bibliography

Résumé du Chapitre I

Dans un premier temps, les fonctions rénales et les méthodes d'épuration extrarénale, et plus particulièrement la technique d'hémodiafiltration (HDF) en ligne sont introduites.

Les principes physiques (diffusion et convection) permettant l'élimination des solutés et de l'eau en excès chez le patient en dialyse sont ensuite présentés.

L'équilibre acide-base de l'organisme, qui peut être contrôlé par le pH du sang, y est aussi décrit. Il est vital de maintenir cet équilibre, qui est fortement perturbé chez le patient en insuffisance rénale chronique. Ce chapitre aborde ces perturbations et explique comment ces déséquilibres peuvent être corrigés par les techniques de dialyse.

Enfin, ce chapitre donne aussi un aperçu des modèles mathématiques développés en dialyse. Deux types de modèle sont généralement décrits. Les premiers concernent les modèles cinétiques dont le système représente l'ensemble du système patient + hémodialyseur et où le but est de décrire l'évolution de la concentration d'un soluté au cours d'une séance de dialyse. Le second type de modèle concerne les modèles de transferts de masse, décrivant localement les transferts entre le sang et le liquide de dialyse au sein de l'hémodialyseur.

After a general introduction to the renal function and hemodiaysis, the solute and fluid transport mechanisms in hemodialysis are discussed with a brief description of the membrane characteristics. Then, a description of the acid-base balance in the body is given. As kidney failure cause disturbance in the acid-base balance, its restoration is also presented. The 4th section of this chapter is dedicated to a concise review of mathematical models of hemodialysis: kinetic model and mass transport models.

1. Introduction to renal functions and hemodialysis

1.1. Functions of the healthy kidneys

The urinary system consists of two kidneys which filter blood and deliver the produced urine into the two ureters. Through the ureters, the urine is passed to the urinary bladder, which is drained via the urethra during urination. The kidneys are bean-shaped organs of about 11 cm long, 4 to 5 cm wide and 2 to 3 cm thick, and are localised in the posterior part of the abdomen.

The major function of the kidneys is to remove toxic by-products of the metabolism and other molecules smaller than 69000 Da (molecular weight of albumin) by filtration of the blood flowing through the glomerulus. They also regulate body fluid composition and volume: they contribute to the regulation of blood pressure, and acid-base balance of the body.
Additionally, kidneys have an endocrine function: they produce the hormones renin, erythropoietin (EPO) and prostaglandines (derivatives of essential fatty acids to maintain homeostasis) and help in converting vitamin D to dihydroxycholecalciferol, a substance which controls calcium transport by increasing calcium reabsorption in kidneys and calcium absorption in intestine.

The functional units of the kidney are the nephrons (Figure I.1). They are composed of glomerulus and renal tubules. There are approximately 1 to 1.3 million nephrons in each kidney. Three processes occur in the nephron: filtration, reabsorption and secretion. The sum of these three processes is called excretion. Filtration takes place in the glomerulus: fluid is transported out of the artery into the cavity of the Bowman's capsule. The filtrate (primary urine) has nearly the same composition as plasma (water, glucose, urea, calcium, potassium, sodium and chloride ions) and contains a considerable amount of bicarbonate (HCO_3^-) which must not be wasted. This primary urine is produced at the rate of 7.5 L per hour (or 180 L in one day). The filtering pressure is the glomerular blood pressure reduced by the osmotic counter pressure and the pressure in the Bowman's capsule. The efficiency of this transport process is dependent on blood pressure regulation. Around 1% of the primary urine is excreted and 99% is reabsorbed. The reabsorption process forms concentrated urine. Reabsorption and secretion take place in the renal tubules: in the proximal tubule, in the loops of Henle, the distal tubule

and collecting duct. Water, nutrients, glucose, amino acids, calcium, magnesium, sodium chloride and bicarbonate ions return to the blood whereas phosphate and H+ ions are secreted into the urine. The pH of blood is then regulated at a constant value of 7.4 and the physiological bicarbonate level in blood of 24 – 27 mmol/L is restored. As a consequence of the ability of kidneys to excrete sufficient sodium chloride to maintain normal sodium balance, extracellular fluid volume, and blood volume, the blood pressure is also regulated.

Finally, urine flows through the collecting duct system, and is drained into the bladder via the ureters. The main function of the collecting duct system is to remove more water from the urine if necessary. Normal urine consists of water, in which waste products such as urea and salts such as sodium chloride are dissolved (Bray et al. 1999). The yellow colour in urine is due to chemicals called urobilins or urochromes. These are the breakdown products of the bile pigment bilirubin. Bilirubin is itself a breakdown product of the heme part of hemoglobin, a principal component of red blood cells. Most bilirubin is partly broken down in the liver, stored in the gall bladder, but some remains in the bloodstream to be extracted by the kidneys where, converted to urobilins, it gives urine that familiar yellow colour.

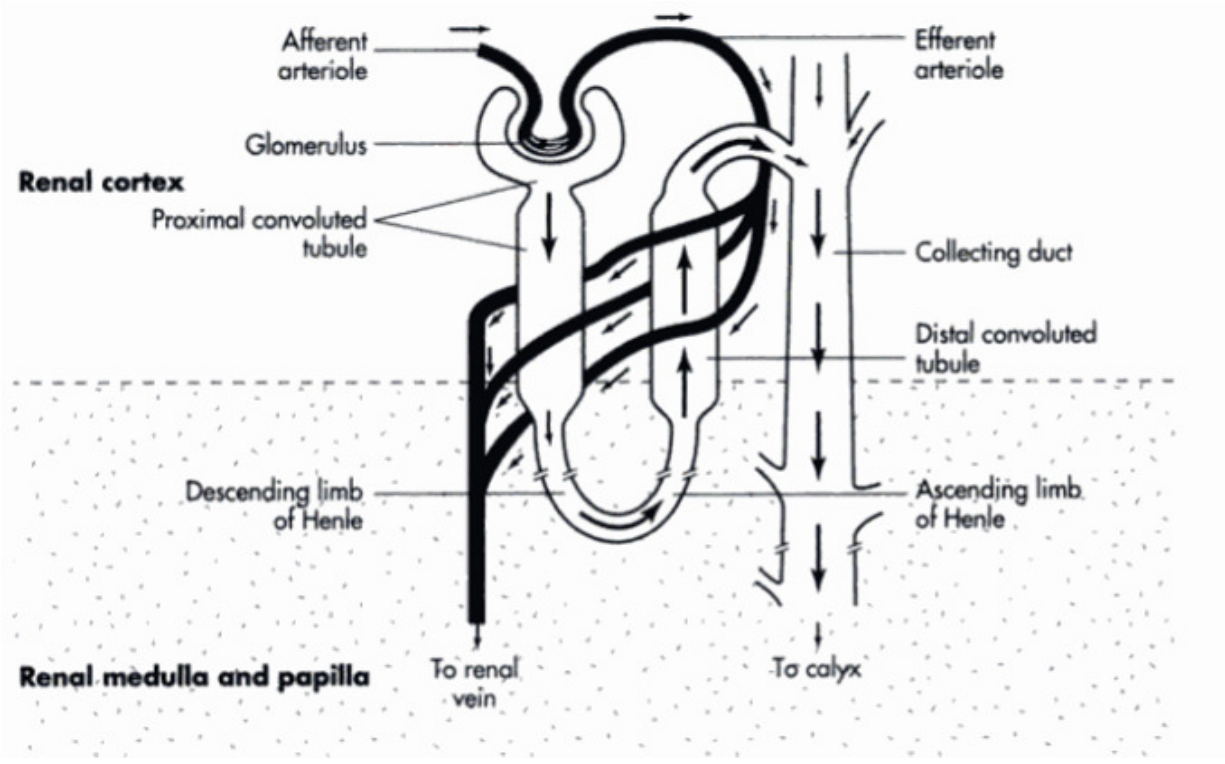

Figure I. 1 Diagram of a nephron with glomerulus, renal tubules and collecting duct (Kallenbach et al. 2005)

1.2. The uremic syndrome

Generally, humans can live with reduced kidney function or even with a single kidney. However, several diseases can threaten the health of a person as a result of dramatically diminished kidney function. Renal insufficiency can be subdivided into three categories according to the duration of functional loss: acute (hours to days), subacute (months) and chronic renal failure (CRF) (years). In contrast with the subacute and chronic forms, acute renal failure is often reversible. The uremic syndrome is the result of the retention of compounds, normally cleared by healthy kidneys, and of a disorder in the hormonal and enzymatic homeostasis. As renal failure progresses, glomerular filtration rate, as well as the amount of nephrons decrease. After years of suffering from CRF, the glomerula filtration rate of the kidney finally drops below 15% of normal rate, leading to end-stage renal disease (ESRD). The main causes of ESRD are diabetes and hypertension, while the most important symptoms are found in the cardiovascular, neurological, hematological and immunological status. When ESRD is reached, renal replacement therapy, like renal transplantation or dialysis technique is necessary. At the beginning of 2003, 30 882 patients in France (BEH n°37-38, 2005) have been treated by a dialysis technique, due to the shortage of kidneys donors.

1.3. Renal replacement therapies

As renal replacement therapy, two treatment modalities are available: a natural one (kidney transplantation from cadaver or living donors), and an artificial one (dialysis).
Dialysis allows removal of waste products (uremic toxins) and excess fluid from the blood of the patient. Two dialysis methods are currently available: peritoneal dialysis and hemodialysis (HD). HD is the most frequent renal replacement therapy and constitutes 85% of treatments worldwide. In France, peritoneal dialysis is only applied to 7% of dialysis patients (Merlo et al. 2007).

1.3.1. Kidney transplantation

Renal transplantation is the preferred therapy in case of ESRD. A donor kidney, from a living or a dead donor, is implanted in the iliac fossa because it is simple, can easily be observed and is easy accessible for biopsies. Donor and patient must have genetic compatibility for a successful transplantation. The patient has to take immunosuppressives to avoid rejection of the transplanted kidney. The advantages for the patient are: no limitation concerning water intake, a less restricted diet compared to the dialysis diet, a normalization of the bone metabolism and the return to an active life with a social and professional reintegration. However, kidney transplantation can not be proposed to all patients. Only a small number of patients are on the waiting list (in France in 2008, 6509 persons have been in the waiting list for a kidney donor), and only a small number of patients on the waiting

list are actually transplanted due to organ shortage (2937 persons have been kidney transplanted in 2008) (Agence de Biomédecine, France). Not every patient is transplanted; for those patients not suitable for transplantation, and for those awaiting transplantation, dialysis is a useful tool to maintain survival and quality of life.

1.3.2. Hemodialysis

During a HD session, the patient's blood is pumped into an extracorporeal circuit through an artificial kidney (hemodialyzer) where it is purified from waste products mainly by diffusion (concentration driven) and from the excess of water accumulated in the body by ultrafiltration or convection (pressure driven). Diffusion and convection will be extensively described in the next section of this chapter. The duration and the frequency of the sessions depend on the patient's needs, and HD is generally performed three times a week during 3 to 5 hours. Hemodialysis can be applied in the hospital, at home or in a low-care unit (self dialysis).

The arterial blood is generally pumped from the arteriovenous fistula (vascular access) of a patient to the blood compartment of the hemodialyzer, which contains around 5 000 to 10 000 hollow fibres with semi-permeable membranes. In the hemodialyzer, on the other side of the membranes, a dialysis fluid is pumped at counter-current to the blood allowing the diffusion of waste products from blood into dialysis fluid. In order to enhance toxin transfer through the membrane, blood is pumped at 250 - 400 mL/min while the dialysis fluid flows at the rate of 500-800 mL/min. The semi-permeable membrane contains pores large enough to allow water and uremic toxins to pass across. After flowing through the hemodialyzer the dialysate is discharged, while the cleansed blood is recirculated into the body.

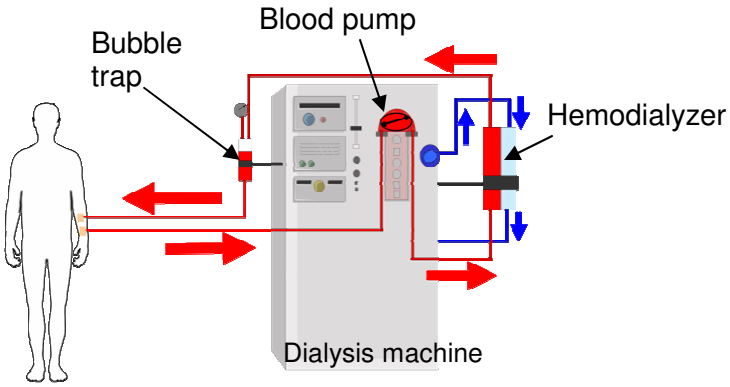

Figure I. 2 The extracorporeal blood circuit

In addition to hemodialysis, two other treatment modalities exist: hemofiltration (HF) and hemodiafiltration (HDF). Whereas in hemodialysis, mass transfers inside the hemodialyzer are mainly diffusive, in hemofiltration mass transfers are exclusively convective and in hemodiafiltration, both diffusive and convective. HF and HDF are thus called 'convective' therapies.

Dialysis fluid management

The dialysis fluid can be considered as a temporary extension of the patient's extracellular fluid because of the bi-directional transport process when blood and dialysis fluid are flowing through the hemodialyzer. For this reason, the composition of dialysis fluid is critical in achieving the desired blood purification and body fluid and electrolyte homeostasis. It contains water purified by reverse osmosis, different electrolytes like calcium, magnesium, potassium and sodium chloride and sodium acetate and/or bicarbonate. Acetate and/or bicarbonate fulfill the function of dialysis fluid buffer, responsible for the correction of metabolic acidosis in uremic patients. Bicarbonate is now used as buffer in the dialysis fluid; in the past acetate has been used, introduced by Mion et al. (1964) as dialysis fluid buffer but has been associated with hemodynamic instability and hypoxia.

The physical and microbiological characteristics are also important because toxic and pyrogenic substances can move from the dialysate towards the blood resulting in febrile reactions. The dialysis fluid is directly prepared by the dialysis machine by diluting dialysis fluid concentrate with purified water (approximately 120 L of treated water are required for each dialysis session). Proportioning systems are required for the mixing of the concentrates with water to produce a dialysis fluid of the desired composition. Two concentrates are necessary for the production of bicarbonate dialysis fluid in order to avoid the precipitation of carbonate with calcium and magnesium: the A component (acidified concentrate, with low pH and electrolytes) and the B component (basic bicarbonate concentrate, with pH around 7.7/7.9, and contains sodium bicarbonate) (Grassman et al. 2000).

In bicarbonate dialysis, a small acetate transfers are also performed due to the 2-7 mmol/L acetate usually present in bicarbonate dialysis fluids. Recent dialysis machines permit to vary HCO_3^- concentration over a wide range from 24 (-8) to 40 (+8) mmol/L, the level 0 being 32 mmol/L. Therefore it is possible to prescribe an individual HCO_3^- concentration to obtain the desired final plasma HCO_3^- concentration. But many physicians use a standard HCO_3^- concentration of 32/35 mmol/L for all patients, arguing that this concentration is suitable for all patients (Locatelli et al. 2004).

1.3.3. Hemodiafiltration

HD can be considered as the reference for all dialysis technique because it can keep patients without kidney function for up to 20-30 years. But up to now, the quality of life for many HD patients is still unsatisfactory (Ledebo 1998). That is why there is a growing interest in a more recent therapy, hemodiafiltration (HDF). At this time, in Europe, less than 10% of dialysis patients receive an online convective therapy.

HDF aims at improving patient outcomes in term of morbidity, quality of life and mortality (Canaud et al. 1998). This technique, first proposed by Leber et al. in 1978 in Europe, combines the diffusive toxin removal of HD with a convective transfer at a higher ultrafiltration flow rate. This ultrafiltration

is compensated by a substitution fluid containing ions and bicarbonate (HCO_3^-) buffer into the venous line of the extracorporeal circuit. In online HDF, this substitution fluid is directly prepared by the dialysis machine from a standard dialysis fluid. This online production of the substitution fluid results in cost savings for purchase and storage of commercial fluid bags. If the substitution fluid is added before the hemodialyzer, the technique is called predilution HDF; if the substitution fluid is added after the hemodialyzer, it is called postdilution HDF.

Technical aspects

In HDF as ultrafiltration exceeds the desired weight loss, it is compensated by the reinjection of a physiological solution which should be sterile and nonpyrogenic. This replacement solution is reinjected directly in the blood line in postdilution (after the hemodialyzer) or predilution (before the hemodialyzer) and can be provided either in bags, or by and integrated filtration of the dialysis fluid (online).

Postdilution HDF increases the clearance (defined in the next section) for small and large uremic toxins compared to HD. But this mode is limited by the hemoconcentration at the outlet of the hemodialyzer: a total ultrafiltration rate (total ultrafiltration rate = substitution flow rate (Qr) + weight loss rate (Qw)) of 30% of the blood flow can cause an increase of hematocrit from 35% to 50%. With increasing hematocrit, blood viscosity also increases, which results in an increase of the transmembrane pressure and also a higher possibility of fibres clotting. Therefore, in postdilution HDF, the ultrafiltration should not exceed 30% of the blood flow rate (Passlick-Deetjen et al. 2002).

The disadvantage of the predilution HDF is the dilution of the uremic toxins: the clearance of the small uremic toxins will be below that of HD with same hemodialyzer and flow rate even if this technique ensures better rheological conditions (Wizemann 2001). The combined use of the pre- and postdilution mode (mixed - dilution HDF) was proposed to optimise online HDF therapies (Pedrini et al. 2000).

Role of ultrapure water

Ultrapure water is needed when using online production of substitution fluid. The bacteriological quality of this ultrapure water should always be controlled because the substitution fluid is directly injected in the patient blood. Contaminated fluid introduced into the patient cause inflammatory reactions, which should be avoided because they can induce complications such as vascular disease or malnutrition (Van Laecke S et al. 2006).

In France, HDF is controlled by ‘une circulaire ministérielle’ on June 7, 2000 (Circulaire 2000) which defined the water quality: the rate of endotoxin has to be less than 0.25 UI/mL and for the reinjection fluid it has to be below 0.05 UI/mL. This control needs to be achieved each month.

Removal of uremic toxins

A number of complications and side-effects experienced by hemodialysis patients are associated with an accumulation of large uremic toxins that are difficult to remove. Therefore high-convection therapies, as HDF are recommended in this case (Maduell 2005). The uremic toxins can be divided into three categories according to the European work group, EUTox (European Uremic Toxin): small water-soluble solutes with a molecular weight (MW) lower than 500 Da, middle molecules with a MW higher than 500 Da, and protein-bound compounds (Vanholder et al. 2003). An important issue in HDF is that this technique increases the dialysis efficiency by removing not only small (as in HD) but also middle and large molecular weight solutes as β2-microglobuline (β2m, 11 800 Da) (Ronco et al. 1988).

Clinical effects of HDF

HDF also appears to provide greater hemodynamic stability than HD. HDF improves the clinical tolerance of sessions and the quality of life, and treatment biocompatibility by combining the use of high flux membranes and ultrapure dialysis fluid (Canaud et al. HI, 2006). High-efficiency HDF (with a reinjection volume of 15-25L per session) patients have a 35% lower mortality rate than low-flux HD patients. These results from DOOPS (Dialysis Outcomes and Practice Patterns Study) suggest that HDF may improve patient survival independently of its higher dialysis dose (Canaud et al. KI, 2006) but this study observational and not controlled.

Sato and Koga (1998) observed a decrease in joint pain and significant improvements in the range of upper arm adduction and abduction movements when six patients receiving hemodialysis were changed to online hemodiafiltration.

Locatelli et al. (1999) reviewed 6440 patients and found that the relative risk of carpal tunnel syndrome surgery is 44% lower in patients treated with convection therapies (Maduell 2005).

Renal anemia is a common feature of HD patients, requiring the use of EPO in 80% to 100% of patients. Although still controversial, it has been shown that anemia is improved and EPO needs reduced in patients treated by high-efficiency HDF (Maduell et al. 1999).

1.4. Body fluid and blood composition

Due to the loss of their normal kidney function, ESRD patient's body fluid composition is disturbed and needs to be restored during dialysis. This section describes normal body fluid compartments repartition and their electrolyte compositions and gives a non exhaustive list of normal range values for human blood.

1.4.1. Normal body fluid compartments and their electrolyte compositions

About 60% of an adult body weight consists of water distributed between two fluid compartments: 3/5 of this fluid (35-40% of the body weight) is located in the intracellular compartment (IC), and 2/5 (25% of the body weight) in the extracellular space (EC).

The EC space consists of plasma water (4.5 % of the body weight), interstitial fluid (19% of the body weight) and transcellular fluid (cerebrospinal fluid, fluid in the eyes, synovial fluid…) (1.5 % of the body weight).

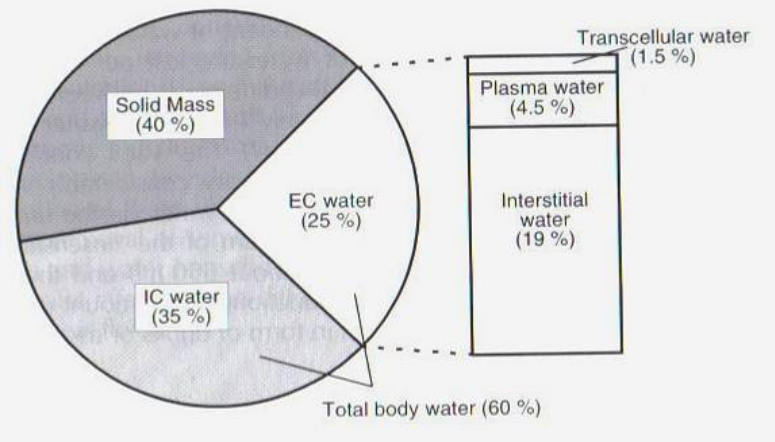

Figure I. 3 Fluid compartments and water distribution as percentage of the body weight in healthy subjects. EC = extracellular and IC = intracellular (Grassmann et al. 2000)

The IC and EC fluids differ in their electrolytes, protein and non-ionic substances content due to the different permeabilities of cell membrane for the various electrolytes, as seen in Table I.1.

Ions	Plasma		Interstitial fluid		Intracellular fluid	
Cations (mmol/l)						
Na^+	143		144		10	
K^+	4		4		155	
Ca^{2+}	2.5	(5)	1.25	(2.5)	0.001	
Mg^{2+}	1.0	(2)	0.75	(1.5)	15	(30)
Sum	150.5	(154)	150	(152)	180	(195)
Anions (mmol/l)						
Cl^-	103		114		2	
HCO_3^-	27		30		10	
HPO_4^{2-}	1	(2)	1	(2)	50	(100)
SO_4^{2-}	0.5	(1)	0.5	(1)	10	(20)
Organic acids	5		5		≈ 0	
Proteins	16		*		63	
Sum	152.5	(154)	150.5	(152)	135	(195)
Osmolality (mosmol/kg)	290		290		290	

Table I. 1 Example of ion distributions (total concentrations) in the different body fluid compartments. Values in brackets are concentration multiplied by the electric charge. Protein concentration in interstitial fluid * is low and varies in different organ tissues. (Grassmann et al. 2000)

It can be seen that sodium is the main cation in EC space, and chloride and bicarbonate, the main anions. Potassium is the main cation in IC space, whereas proteins and phosphates the main anions.

Dialysis patient accumulates fluid (approximately 1 to 4 liters of water), electrolytes and toxins during the interdialytic period (= between two dialysis sessions). An increase in the total body water primarily results in an expansion of the EC space and of the interstitial compartment (Grassmann et al. 2000).

The human body can be considered as a biological system, consisting of different compartments, which are separated by semi-permeable membranes. Transport between the different compartments can happen passively by free diffusion of non-charged particles (as water, oxygen, urea) or charged particles (ions), and by forced diffusion via channels. The transport can also occur as an active process where the energy is supplied by the ATP (adenosine triphosphate) hydrolysis ATPase, or as a secondary active transport according to an electrochemical gradient.

1.4.2. Human blood characteristics

An average adult has a total blood volume of about 5L, which is approximately 7% of total body weight. Blood is a dark red, viscous, slightly alkaline suspension (pH = 7.4) of cells - erythrocytes (red

blood cells), leukocytes (white blood cells) and thrombocytes (platelets) - suspended in a fluid, the plasma. The volume percentage of red blood cells is called hematocrit (H).

Table I.2 gives the normal range values for human blood.

	Human normal range values
pH	7.35 - 7.45
H^+	35 – 45 nmol/L
Hematocrit (H)	33 – 43 % (F) 39 – 49 % (M)
O_2 partial pressure: pO_2	75 – 105 mmHg (Arterial) 40 mmHg in tissue and venous
CO_2 partial pressure: pCO_2	35 – 45 mmHg (Arterial and venous)
HCO_3^- concentration in plasma: HCO_3^- (P)	22 – 28 mmol/L
O_2 saturation: sO_2	92-99 %
Hemoglobin concentration: tHb	12– 15 g/dL (F) 13.6– 17.2 g/dL (M)

Table I. 2 Human blood characteristics (F for female and M for male). Adapted from Moline (1992)

The main functions of blood include transportation of nutrients from the gastrointestinal system to all cells of the body and subsequently delivering waste products of these cells to organs for elimination. Oxygen (O_2) is carried from the lungs to all cells of the organism mainly by the hemoglobin in the erythrocytes, whereas carbon dioxide (CO_2) is transported back to the lungs for elimination both by the hemoglobin and the plasma. This point is explained in details in the third section of this Chapter.
Besides nutrients, numerous other metabolites, cellular products, and electrolytes are transported by the bloodstream. Additionally, blood also regulates body temperature and maintains the acid-base and osmotic balance of body fluids.

Plasma consists of water (90%), proteins (9%) and inorganic salts, ions, nitrogens, nutrients and gases (1%). There are several plasma proteins with different origin and function, for example, albumin (69 000 Da), α- and β-globulins, γ-globulins, clotting proteins, complement proteins (C1 to C9) and plasma lipoproteins (Bray et al. 1999).

1.4.3. ESRD patient blood

As it will be seen later (Section 3), metabolic acidosis is present in most patients receiving renal replacement therapy for ESRD. On average, serum [HCO_3^-] is reduced by 6 mmol/L in patients with moderate renal insufficiency. Even if hemodialysis or peritoneal dialysis therapy can correct this acid-base balance disturbance, most patients have a persistent metabolic acidosis.

Cardiac function is affected by metabolic acidosis and ESRD patients have a high incidence of cardiovascular disease: hypertension is a major risk factor contributing to the high cardiovascular morbidity and mortality in uremic patient. A lower pH and HCO_3^- during dialysis session are correlated with the number and severity of cardiac arrhythmias (Gennari and Feriani 2000).

High blood pressure is the second most leading cause of kidney failure, and ESRD. Extra fluid in the body increases the amount of fluid in blood vessels and makes blood pressure higher. Narrow, stiff, or clogged blood vessels also raise blood pressure.

2. Solute and fluid transport mechanisms in hemodialysis

In dialysis therapy, the hemodialyzer permits to purify the blood and to remove excess water by diffusion and convection, which determine the dialysis efficiency. As transport takes place between the blood and dialysis fluid compartments through a semi-permeable membrane, membrane properties, fluid transport and solutes transport have been considered in this section.

2.1. Membrane properties

Currently a wide spectrum of hemodialyzers combined with different membranes is available. Hemodialysis membranes vary in chemical compositional structure, transport properties and biocompatibility. Generally, membranes can be produced from two families of polymers: synthetic or cellulosic. They can be subdivided into high-flux membranes (large pores) or low-flux membranes (small pores). High flux membranes allow higher water flux and removal of middle and high molecular weight uremic solutes (> 500 Daltons) than low flux membranes.

The membrane polymer determines the physical, chemical and biological properties of a dialysis membrane. Ideally a membrane is highly biocompatible, adsorbs dialysate impurities from the dialysis fluid, allows the transfer of middle molecules and is resistant to all chemical and sterilising agents used in HD procedures (Boure 2004). Synthetic membranes perform better than cellulosic membranes in most of these properties - especially in biocompatibility – and their use is increasing despite their high cost (Vienken 2002).

Cuprophan®, for example, is a hydrophilic regenerated cellulose membrane and has been used for over 35 years. This membrane had good performance for small solute removal, but was not appropriate for HDF due to its small hydraulic membrane permeability. Most of all, this membrane had poor biocompatibility due to the presence of a large percentage of hydroxyl groups within the cellobiose structure and is not produced anymore.

Polysulphone (PS) is a membrane prepared from synthetic engineered thermoplastics and is hydrophobic, asymmetric and anisotropic with solid structures and open void spaces. This membrane is also characterised by a thin skin layer, and high hydraulic membrane permeability. Recently, the PS family has been enriched by the development of a new membrane, Helixone®, from Fresenius Medical Care (FX series). The inner fibre diameter (185 μm) and the wall thickness (35 μm) of Helixone® have been reduced, increasing the internal filtration and decreasing diffusion resistance.

The consequence of these structural refinements is an improvement of β2m removal capability of the membrane without incurring any loss of larger molecules (Ronco et al. 2004).

Among synthetic membranes, there are also poly(aryl)ethersulfone membranes, as PEPA® produced by Nikkiso, Polyamix™ by Gambro, DIAPES® by Membrana and Arylane® by Hospal.

Asahi and Hospal are producers of polyacrylonitrile (PAN) membranes: AN69® developed by Hospal has been a success since its introduction but today severe clinical limitations of this membrane have led to the development of AN69ST (Uhlenbusch-Körwer et al. 2004). ST stands for surface treated and the aim of this AN69ST is to introduce positive surface charges in order to improve the biocompatibility.

Figure I.4 lists the synthetic membrane for hemodialysis.

PAN (polyacrylonitrile) (Pan-DX Asahi, PAN AN 69 Hospal, SPAN Akzo)
PS (polysulfone) (Asahi, Fresenius, Helbio, Minntech, Toray)
PEPA (polyester polymer alloy) (Nikkiso)
Arylane® (polyarylethersulfone) (Gambro-Hospal)
Diapes® (polyethersulfone) (Membrana)
PA (polyamide) (Gambro)
PMMA (polymethylmethacrylate) (Toray)
EVAL (ethylene vinyl-alcohol copolymer) (Kuraray)
PPC Gambrane® (polycarbonate polyether copolymer) (Gambro)

Figure I. 4 List of synthetic membranes for hemodialysis (Ronco et al. 2004)

2.2. Fluid and solute transport across dialysis membranes

In a hemodialyzer, blood and dialysis fluid compartments are separated by a semi permeable membrane. Blood and dialysis fluid move in counter-current flow.

As for any membrane process, fluid transport is achieved by convection (pressure driven). Solute transfers can be achieved by diffusion or convection. This section explains both mechanisms (Zeman LJ and Zydney AL 1996).

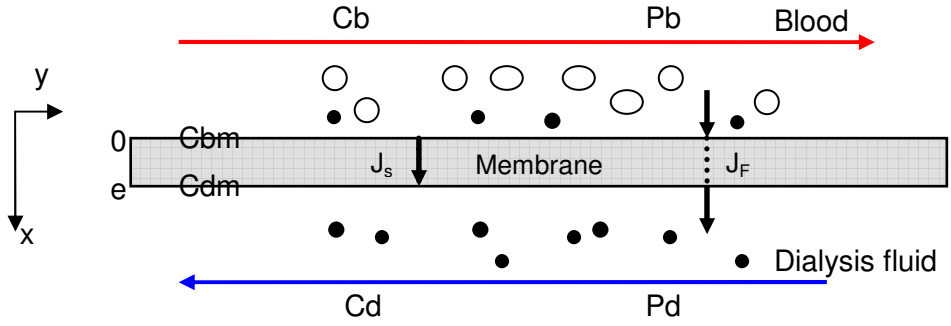

Figure I. 5 Local representation of ultrafiltration flux of water (J_F) and solute flux (Js) through an hemodialyzer membrane. e is the membrane thickness, Cb and Cd, blood and dialysis fluid concentration respectively, Cbm and Cdm, the blood and dialysis fluid concentration at the membrane and Pb and Pd, blood and dialysis fluid pressure

2.2.1. Fluid transport

Ultrafiltration is performed to remove water accumulated either by ingestion of fluid or by metabolism of food between 2 dialysis sessions. A patient being dialysed thrice weekly gains 1 to 4 kg of weight between treatments (most of it is water), which needs to be removed during 3 to 4 hours of dialysis session. Thus, the clinical range of ultrafiltration is usually from 0.5 to 1.5 L/h or 8.33 to 25 mL/min. This ultrafiltration of water due to weight loss is also called weight loss rate (Qw).

Ultrafiltration or convection

This form of transport implies a movement of fluid across the membrane as a consequence of a local transmembrane pressure gradient.

The J_F volumetric flux of water (mL/m²/h) per unit of area is given by:

$$J_F(y) = Lp \times (Pb(y) - Pd(y) - \Delta\Pi(y)) \qquad \textbf{I. 1}$$

Where Lp is the membrane hydraulic permeability (mL/h/m²/mmHg), Pb and Pd the local blood and dialysis fluid pressure (mmHg) and ΔΠ the oncotic pressure (mmHg) exerted by the proteins present at the hemodialyzer blood side.

Hagen-Poiseuille law

The relationship between flow and pressure in a horizontal tube is governed by the Hagen-Poiseuille low.

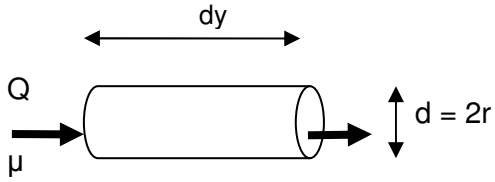

Figure I. 6 Schematic representation of flow and pressure in a tube. dy the tube's length, d the tube's diameter, μ the fluid viscosity and Q the input flow rate

The Hagen-Poiseuille law is used for laminar flow when Reynolds number is < 2000 and applies to viscous Newtonian flow through a tube of constant circular cross-section. These conditions are observed under clinical operating conditions for hemodialyzers.

The Hagen-Poiseuille equation in a circular tube, gives the relation between dP, the pressure drop along a length dy of the circular tube and the flow rate Q:

$$\frac{dP}{dy} = \frac{8\mu}{\pi \times r^4} Q \qquad \textbf{I. 2}$$

Where μ is the fluid viscosity (Pa.s) and r the tube radius (m)

This relation permits the calculation of the local pressure all over the fibre length.

This law corresponds to Ohm's law for electrical circuits (U=RI), where the pressure drop is analogous to the voltage U and flow rate is analogous to the current. The resistance of one fibre of the hemodialyzer can be defined as:

$$Rf(\mu) = \frac{8L}{\pi \times r^4}\mu \qquad \textbf{I. 3}$$

Where L is the fibre length (m). μ is the blood viscosity (Pa.s), r the fibre radius (m) and L the length fibre (m). This resistance Rf only depends on the blood viscosity for a given fibre in the hemodialyzer.

Hemodialyzer is composed of many circular fibres placed in parallel. Therefore the blood pressure drop, ΔP along the hemodialyzer (for N fibres in the hemodialyzer) is given by:

$$\Delta P = Pbi - Pbo = \frac{8\mu L}{\pi \times r^4 \times N}Qb \qquad \textbf{I. 4}$$

Where Pbi and Pbo are respectively hemodialyzer inlet and outlet pressure,

This relationship is critically dependent on the blood pathway dimensions. For example, the pressure depends on the fourth power of the fibre diameter (a 10% decrease in fibre diameter will result in a 52 % decrease in ΔP for the same blood flow through the fibres).

2.2.2. Solute transport across dialysis membranes

Diffusion and convection simultaneously occurs in dialysis practice for solute transport across dialysis membrane.

Diffusion

Diffusion refers to the transport of solutes from blood to dialysis fluid, across a membrane, due to the solute concentration difference in the two compartments. This passive transport is mainly used to remove solute as toxins (urea), but can also be used to maintain or enhance the concentration of various solutes in the patient's blood.

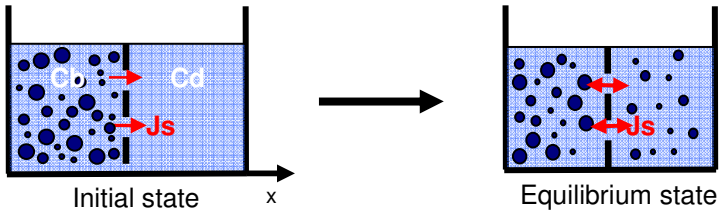

Figure I. 7 Diffusion process. Cb represents blood concentration of a solute and Cd its dialysis fluid concentration. x indicates the direction of diffusion

Ddiffusion transport through the membrane is governed by the first Fick's law (in one dimension, x) in a porous solid:

$$Js_d = -Ds \times \frac{dC}{dx} \qquad \textbf{I. 5}$$

Where Js_d is the net solute flux by diffusion (mmol/cm²/min), Ds the effective diffusivity (cm²/min) of the solute at a specific temperature, C the concentration of the solute, and dC/dx the gradient of concentration within the membrane. The minus sign means that solutes move from the region of high concentration to that of low concentration so that concentration will decrease in the direction of flux ($dC/dx < 0$).

In writing Equation I.5 we assume that longitudinal diffusion along the membrane is negligible, which is acceptable since, due to the very small thickness to length ratio and fluid films in a hemodialyzer, longitudinal gradients are much smaller than transverse ones (Jaffrin et al. 1990).
The diffusion process is influenced by the size and the charge of the solute, the protein concentration (the Donnan effect), the physicochemical and the temperature gradient properties of the hemodialyzer membrane, and the flow characteristics of the blood and dialysis fluid.

The diffusion of solute takes place through the 3 compartments: blood, membrane and dialysis fluid.
For membrane compartment, integration of equation I.5 gives:

$$Js_{d\_membrane} = \frac{Ds}{e} \times (Cbm - Cdm) = \frac{1}{R_M} \times (Cbm - Cdm) \qquad \textbf{I. 6}$$

Where R_M ($e/Ds = R_M$) in min/cm is the membrane diffusion resistance which depends on membrane thickness (e) as well as diffusivity in the membrane (Ds), varying with its chemical composition.
Cbm and Cdm (Figure I.5) represent concentration at the membrane surface in contact respectively with blood and dialysis fluid.

Donnan effect

The Gibbs-Donnan, or Donnan effect, is based on the preservation of electroneutrality in the two compartments, blood and dialysis fluid. Blood proteins are negatively charged and tend to accumulate at the membrane surface during the dialysis session. Cations (mostly sodium) must be retained in blood to ensure electroneutrality. This results in ion exchange across the hemodialyzer membrane. The asymmetry transport of ions induced by proteins is called the Donnan effect (Grassmann, 2000). The Donnan factor (α), defined as the ration of ionic concentration in dialysate and blood at equilibrium, is smaller than 1 for cations, and is higher than 1 for anions as bicarbonate, since the negatively charged proteins in blood exert a driving force on the negatively charged ions like bicarbonate in addition to the diffusive driving force.

Convection

The convective transport of solutes across the hemodialyzer membrane results from a movement of water due to the pressure gradient (ultrafiltration), as seen in section 2.2.1. The water is accompanied by small solutes which pass through the hemodialyzer membrane.

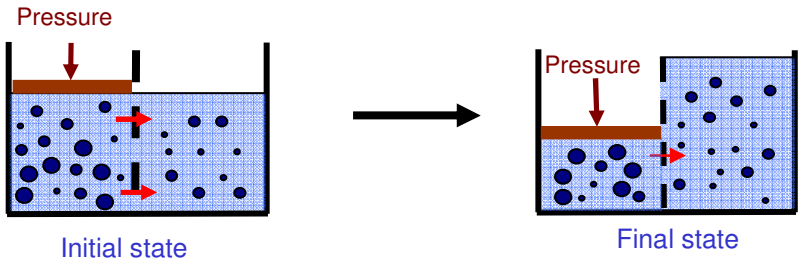

Figure I. 8 Convection process

The solute mass removal rate due to convection per unit of area Js_c (mmol/m²/h) is a function of J_F (defined in Equation I.1), solute concentration in plasma (Cp) and the sieving coefficient of the membrane or transmittance (S):

$$Js_c = J_F \times Cp \times S \qquad \textbf{I. 7}$$

S corresponds to the ratio between the concentration of a solute in the filtrate (Cf) divided by its concentration on blood side ((Cpi + Cpo) /2). If there is no restriction for the solute by the membrane (for example for urea, electrolytes and other small molecules) S = 1, if the solute is completely retained by the membrane (as for proteins) S = 0.

S can also be written using the rejection coefficient of the membrane R, according to:

$$S = 1 - R \qquad \textbf{I. 8}$$

This rejection coefficient R is closely related to, but different from the Staverman's reflection coefficient, σ, introduced by Van't Hoff. σ represents the intrinsic property of the membrane/solute pair and remains a constant number over a wide range of operating conditions, whereas R is a phenomenologic coefficient that takes into account rate of flow of the solution through the membrane, or the pore structure of the membrane. (Henderson 1989)

2.3. Mass transfers in hemodialyzer

In this section mass transfers by diffusion and convection are presented for the hemodialyzer.

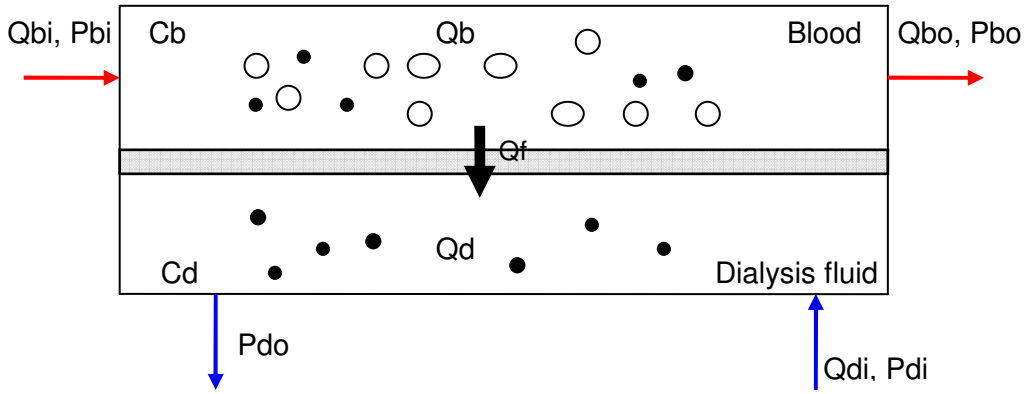

Figure I. 9 Mass transfer across hemodialyzer

2.3.1. Diffusive mass transfer

The diffusion of solute takes place through the 3 compartments: blood, membrane and dialysis fluid. Equation I.5 can be written as:

$$Qs_d = K_0 \times A \times (Cb - Cd) \qquad \textbf{I. 9}$$

Where Qs_d (mmol/min) is the mass transfer of a solute by diffusion in the entire surface of hemodialyzer, A the membrane surface area or hemodialyuser area (cm²), Cb and Cd the blood and dialysis fluid concentration (mmol/L). This mass transfer is positive for toxins when the transfer of solute goes from blood to dialysate (Cb>Cd), as the aim is to eliminate the toxins from blood.

The total mass transfer coefficient K_0 (cm/min) in hemodialyzer for a particular solute includes resistance to diffusion in blood (R_b), membrane (R_M) and dialysis fluid (R_d).

$$R_0 = \frac{1}{K_0} = R_M + R_b + R_d \qquad \textbf{I. 10}$$

Therefore, hemodialyzer efficiency can be increased by reducing each of these resistances.

The membrane surface area (A, m²) of a hollow fibre hemodialyzer is given by:

$$A = 2\pi \times r \times L \times N \qquad \textbf{I. 11}$$

Where r the fibre radius (m), L the fibre length (m) and N the number of fibres.

2.3.2. Convective mass transfer

As K_0, for diffusion, we define the ultrafiltration coefficient K_{UF} (mL/h/mmHg) which is the parameter to characterise the water permeability of a hemodialyzer and is given by:

$$K_{UF} = \frac{Qf}{TMP} \qquad \textbf{I. 12}$$

Where Qf is the ultrafiltration flow rate (mL/h), and TMP the transmembrane pressure.
In HD, Qf = Qw where Qw is the weight loss rate.
K_{UF} is unique for each hemodialyzer and is usually determined by *in vitro* experiments. K_{UF} is expressed as mL/h of fluid removed for each mmHg.

The mean transmembrane pressure is defined by the difference between hydrostatic pressure and oncotic pressure ($\Delta\pi$). The hydrostatic pressure equals the mean blood pressure (average of inlet and outlet pressures) minus the mean dialysis fluid pressure:

$$TMP = \frac{Pbi + Pbo}{2} - \frac{Pdi + Pdo}{2} - \Delta\pi \qquad \textbf{I. 13}$$

Where Pbi, Pbo are the blood pressures (mmHg), respectively at the hemodialyzer inlet and outlet, Pdi, Pdo, the dialysis fluid pressures (mmHg).

The relationship between ultrafiltration flow rate (Qf) and TMP is linear at relatively low TMP values for all membrane, whereas a plateau in Qf occurs at relatively high TMP values, due to protein and fibrin deposit on the membrane surface. K_{UF} is defined as the slope of the linear portion of Qf plotted in function of TMP.
The TMP reflects both positive and negative pressures in the hemodialyzer. Positive pressure is applied to the blood side of the hemodialyzer which pushes the plasma fluid out whereas negative pressure is applied to the dialysate compartment.

Following Equation I.7, the mass transfer of a solute by convection, Qs_c (mmol/h) is given by:

$$Qs_c = A \times Js_c = Qf \times Cp \times S \qquad \textbf{I. 14}$$

Where A is the area of the membrane (m²) and Cp the solute plasma concentration.

2.3.3. Clearance

The clearance characterizes the renal excretion capability of the hemodialyzer or of the patient. The clearance represents the amount of blood which is cleared of a particular substance per minute. The clearance of each solute decreases with increasing molecular weight.

In hemodialysis, the clearance CL (mL/min) is defined as the amount of solute removed from the blood per unit of time (M = QbiCbi – QboCbo), divided by its inlet blood concentration (Cbi):

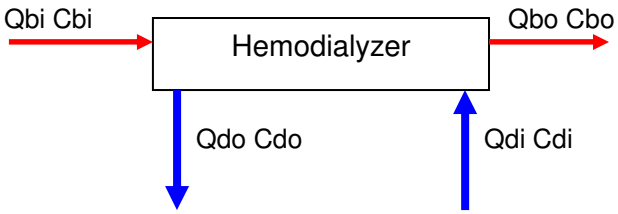

Figure I. 10 Schematic representation of flows and concentrations for a hemodialyzer in HD

$$CL = \frac{M}{Cbi} = \frac{QbiCbi - QboCbo}{Cbi} = \frac{QdoCdo - QdiCdi}{Cbi} \qquad \textbf{I. 15}$$

Where Qb and Qd refer to blood and dialysis fluid flow rates, respectively; Cb and Cd refer to blood and dialysis fluid concentrations, respectively; subscripts i and o refers for fluids flowing into and out the hemodialyzer, respectively.

In the absence of ultrafiltration (Qf = 0, and Qbi = Qbo), the clearance becomes CLd:

$$CL = CLd = \frac{Qbi(Cbi - Cbo)}{Cbi} = Qbi(1 - \frac{Cbo}{Cbi}) \qquad \textbf{I. 16}$$

When ultrafiltration is present:

$$Qf = Qbi - Qbo \qquad \textbf{I. 17}$$

The general definition of the clearance CL can also be written as:

$$CL = \frac{QbiCbi - (Qbi - Qf)Cbo}{Cbi} = CLd + Qf\frac{Cbo}{Cbi} \qquad \textbf{I. 18}$$

CLd is the solute clearance by diffusion (in the absence of ultrafiltration) whereas the term Qf(Qbo/Cbi) represents the convective part of the solute transport.

Clearance of a hemodialyzer for a particular solute is generally characterized by its diffusive clearance values. The clearances are generally measured *in vitro* for urea (60 Da), creatinine (113 Da), phosphate (134 Da) and vitamin B12 (1355 Da).

2.3.4. Dialysance

The dialysance D (mL/min) replaces the clearance CL, when the concentration of the solute in the dialysis fluid entering the hemodialyzer (Cdi) is different from zero. The dialysance is defined as, for non-charged solute:

$$D = \frac{QbiCbi - QboCbo}{Cbi - Cdi} = \frac{QdoCdo - QdiCdi}{Cbi - Cdi} \qquad \textbf{I. 19}$$

For dialysance of ions, the concentration driving force (Cbi – Cdi) becomes (αCbi –Cdi) where α represents the Donnan factor. Thus, the dialysance of charged solutes becomes:

$$D = \frac{QbiCbi - QboCbo}{\alpha Cbi - Cdi} \qquad \textbf{I. 20}$$

The term of dialysance can also be found in new technologies for online dialysis control. This technology is explained in Chapter II, section 3.3.

2.4 Mass transfers for the patient

In conventional hemodialysis, hemodialyzer clearance and patient clearance are the same, as no reinjection takes place in the patient lines.

During HDF postdilution (online or not), the substitution fluid is reinjected (at a reinjection flow rate, Qr) directly in the blood line after its passage through the hemodialyzer.

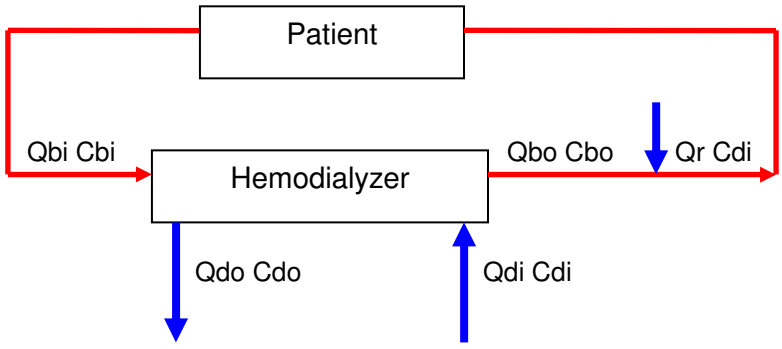

Figure I. 11 Schematic representation of flows and concentrations for a hemodialyzer in postdilution HDF where the patient is represented by one compartment

Thus the mass flow rate returning to the patient is QboCbo + QrCdi, so that the patient dialysance, Dp which is the clinically significant one, is given by:

$$Dp = \frac{M - Qr \times Cdi}{Cbi - Cdi} \quad \textbf{I. 21}$$

Where M is the solute mass lost by blood per time unit (mmol/min) inside the hemodialyzer:

$$M = Qbi \times Cbi - Qbo \times Cbo \quad \textbf{I. 22}$$

The weight loss rate Qw in HDF, (mL/min) is equal to:

$$Qw = Qf - Qr \quad \textbf{I. 23}$$

In HD, with the absence of reinjection (Qr = 0), comparison between Equations I. 20 and I. 21 shows that Dp = D, the hemodialyzer clearance.

NOTE: All these definitions involve blood concentrations and blood flows. But for the majority of solutes, due to the analysis methods, concentrations can only be measured in plasma, although they are also present in red cells. The solute is distributed in plasma and red cells according to:

$$C_{RBC} = K \times Cp \quad \textbf{I. 24}$$

where Cp and C_{RBC} denote concentrations in plasma and in red blood cells (RBC) respectively. K represents the partition coefficient K between plasma and RBC for a particular solute (K = C_{RBC}/Cplasma).
In that case, blood and plasma concentrations are related by, from mass flux conservation:

$$QbCb = H \times Qb \times C_{RBC} + (1 - H) \times Qb \times Cp \quad \textbf{I. 25}$$

where H denotes the local hematocrit
Therefore the blood concentration is related to plasma concentration by:

$$Cb = (1 - H + HK) \times Cp \quad \textbf{I. 26}$$

Therefore in all previous equations, the blood concentration (Cb) can be replaced by Equation I.26.

3. Acid-base balance in the body

The acids are formed during metabolism and are regulated by various buffer systems, as bicarbonate (HCO_3^-) which is the most important. To maintain the buffering capacity of the body, bicarbonate (base) needs to be reabsorbed and this phenomenon takes place in the kidneys, as we have seen in the first section of this chapter.

In patients with renal failure, acid accumulates in blood and plasma bicarbonate decreases below the physiological level. An excess of acid in blood is called acidemia (pH of the blood plasma < 7.35) and an excess of base in blood is called alkalemia (pH > 7.45). Acidosis and alkalosis refer to the processes that cause pH to change. Acidosis is much more common than alkalosis in renal patients. As many ESRD patients are in a state of constant metabolic acidosis, one of the goals of treatment is to improve the acid-base status of the patient by an adequate choice of bicarbonate and electrolyte concentrations in the dialysis fluid.

In next section, gas exchanges (O_2 and CO_2) in the body are described in order to understand the acid-base balance in the body and its restoration in dialysis patients.

3.1. Partial pressure

The partial pressure is the driving element of the gas transport in the body. All gases diffuse from areas of high pressure to areas of lower pressure.

In a mixture of ideal gases, each gas has a partial pressure which is the pressure which the gas would have if it alone occupied the volume. The total pressure of a gas mixture is the sum of the partial pressures of each individual gas in the mixture (Dalton's law).

At a constant temperature, the amount of a given gas dissolved in a given type and volume of liquid is directly proportional to the partial pressure of that gas in equilibrium with that liquid (Henry's law).

For example, for O_2:

$$cO_2 = \alpha O_2 \times pO_2 \qquad \textbf{I. 27}$$

Where cO_2 is the O_2 concentration, αO_2, the O_2 solubility constant and pO_2, the partial pressure of O_2.

3.2. Oxygen and carbon dioxide exchange in tissues and lung

The respiratory system consists in the airways, the lungs, and the respiratory muscles that mediate the movement of air into and out of the body. With the alveolar system of the lungs, molecules of oxygen (O_2) and carbon dioxide (CO_2) are passively exchanged, by diffusion, between the gaseous

environment and the blood. Thus, the respiratory system facilitates oxygenation of the blood to maintain the acid-base balance of the body through the efficient removal of CO_2 from the blood (Maton 1995).

Figure I.12 shows the exchange between blood and atmosphere and the release or the capture of CO_2 and O_2. Upon inhalation, gas exchange occurs at the alveoli, the tiny sacs which are the basic functional component of the lungs. The alveolar membranes are extremely thin (approx. 0.2 micrometres) and are permeable to gases. The alveoli are in contact with pulmonary capillaries with walls thin enough to permit gas exchange. O_2 diffuses from the alveoli into the blood and CO_2 from the blood into the alveoli. Diffusion requires a concentration gradient. So, the concentration (or pressure) of O_2 in the alveoli must be kept at a higher level than in the blood and the concentration (or pressure) of CO_2 in the alveoli must be kept at a lower lever than in the blood. This is done by breathing, continuously bringing fresh air (with much O_2 and little CO_2) into the lungs and the alveoli. The CO_2 fundamentally has a great capacity for diffusion, because of its good solubility in water. A property which, combined with the short distance of diffusion through the alveoli hair membrane, is responsible for the rapid passage in the lung. (CO_2 is 20 times more soluble in plasma and alveolar fluid than O_2). In order to bring oxygen into the cells, the opposite transfer is created at the cells level.

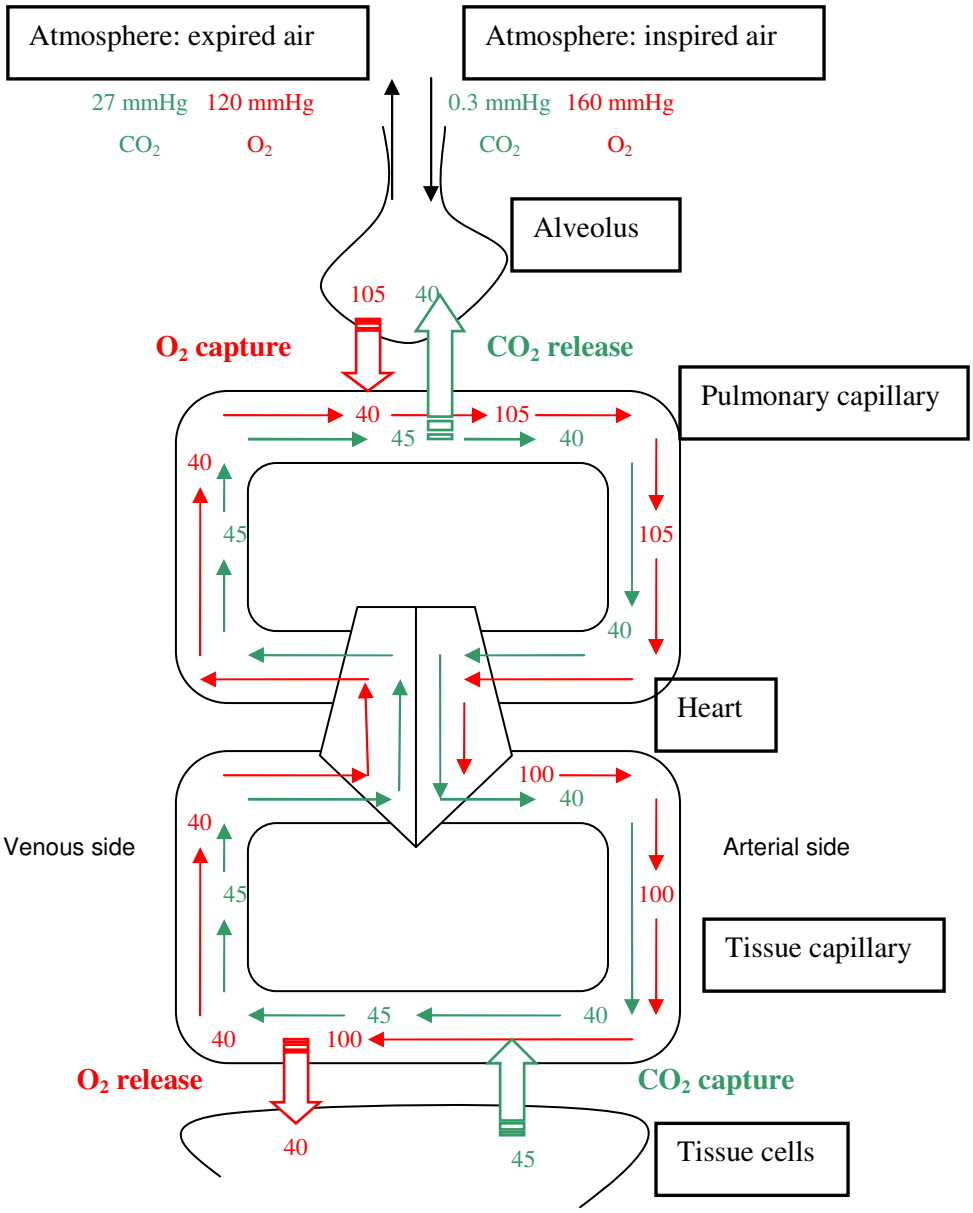

Figure I. 12 Partial pressure O_2 and CO_2 (in mmHg) from atmosphere until body tissue cells. At the top: gradients promoting O_2 and CO_2 exchange across the respiratory membrane in the lungs. At the bottom: gradients promoting gas movements across systemic capillary membranes in body tissues. The pO_2 small decrease in pulmonary venous blood is due to partial dilution of pulmonary capillary blood with less oxygenated blood. Adapted from Marieb 2007

3.2.1. How are O_2 and CO_2 transported in the blood?

O_2 is carried in blood:

1. Bound to haemoglobin (Hb) (98.5% of all oxygen in the blood)
2. Dissolved in the plasma (1.5%)

Because almost all oxygen in the blood is transported by Hb, the relationship between the pO_2 and sO_2 (the % of Hb molecules carrying O_2) is important. This relationship is called oxygen-haemoglobin

dissociation (saturation) curve. At pO_2 about 40 mmHg, sO_2 is between 75 and 80%. If pO_2 decreases, sO_2 also declines. This means that the blood 'unloads' O_2 to cells that need more O_2.

At rest, the CO_2 production is around 300 mL/minute, while during an important physical activity, it can reach 1500 mL. Storage is only temporarily allowed, but a rapid and total elimination is essential. The CO_2 is transported in the blood under 3 forms:

1. Dissolved in the plasma (about 7 to 10%)
2. Combined with Hb, carbaminohemoglobin (about 20%)
3. Bicarbonates in plasma (about 70%), formed when CO_2 (released by cells) combines with H_2O (due to the presence of enzyme in red blood cells called carbonic anhydrase = CA), carbonic acid H_2CO_3 which is unstable and quickly dissociates to H^+ and HCO_3^- as seen in Equation I.28

$$CO_2 + H_2O \xrightarrow[CA]{} \underset{\text{Carbonic acid}}{H_2CO_3} \rightarrow H^+ + HCO_3^- \qquad \textbf{I. 28}$$

The intake of CO_2 at the tissue and its rejection by the lungs are conditioned by the partial pressure of CO_2.

3.2.2. Gas exchanges inside the red blood cells

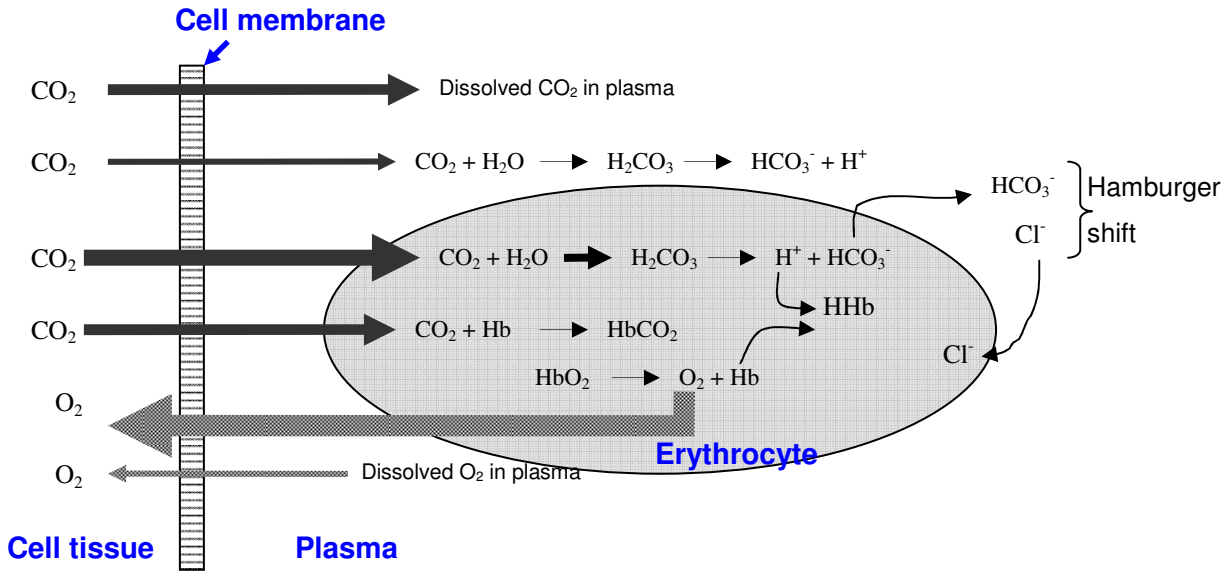

Figure I. 13 Scheme of the uptake of CO_2 and liberation of O_2 in systemic capillaries. Exactly opposite events occur in the pulmonary capillaries. In the tissues, dissolved CO_2 passes into the red blood cell where it combines with water to form H_2CO_3. This reaction is catalysed by the enzyme carbonic anhydrase. H_2CO_3 then dissociates into HCO_3^- and H+ ions. H+ ions bind to reduced haemoglobin to form HHb. HCO_3^- ions generated by this process pass back into the plasma in exchange for chloride ions (Cl^-). This ensures that there is no net loss or gain of negative ions by the red cell. In the tissues, oxygen detaches from iron and the resulting deoxyhemoglobin becomes dark red. The released oxygen diffuses from the blood into the tissue cells.

When CO_2 is leaving the cells of tissues and penetrates into red blood cells (RBC), the consequence is the dissociation of O_2 and Hb; this phenomenon is called Bohr effect (Figure I.13). Thus, a small part of CO_2 is combined with Hb and the rest is combined with H_2O; carbonic acid (H_2CO_3) is then formed due to the enzyme CA and is dissociated into bicarbonate (HCO_3^-) ions and acidic (H+) protons (Equation I.28)

Certain amounts of HCO_3^-, which accumulate in RBC, diffuse towards the plasma. In exchange, chloride ions diffuse from plasma inside the red blood cells. This exchange maintains the electrical balance between plasma and RBC and is called the Hamburger shift or chloride shift. Through the mechanism of H^+ formation, haemoglobin acts as a buffer, binding and neutralising the H+ and thus preventing any significant acidification of the blood.

When blood enters the lungs, where pCO_2 is lower, the H+ and bicarbonate ions join to form carbonic acid, which then dissociates into CO_2 and H_2O, as seen in Equation I.29.

$$H^+ + HCO_3^- \rightarrow \underset{\text{Carbonic acid}}{H_2CO_3} \rightarrow CO_2 + H_2O \qquad \textbf{I. 29}$$

The CO_2 that is thus re-formed, can enter the alveoli and be exhalted.

3.3. Regulation of acid-base balance

There are three ways to regulate the pH. The first regulation system is the buffer system as the function of a buffer is to prevent large changes in pH. Then, as gas exchange occurs, the acid-base balance of the body is also maintained by both the lungs and the kidneys, but these regulations are slower than the buffer system.

3.3.1. Buffers in body

Introducing a buffer in a solution stabilises its pH when amount of acid or base is added to it. Body buffers are mainly used to counterbalance acid production.

The body contains several different buffer systems as protein and phosphate, most active in intracellular water, and bicarbonate in extracellular water (Figure I.14). The bicarbonate buffer is the most important buffer in plasma. It consists of two pairs: carbonic acid / bicarbonate ion (H_2CO_3/ HCO_3^-) and bicarbonate ion / carbonate ion (HCO_3^-/CO_3^{2-}).

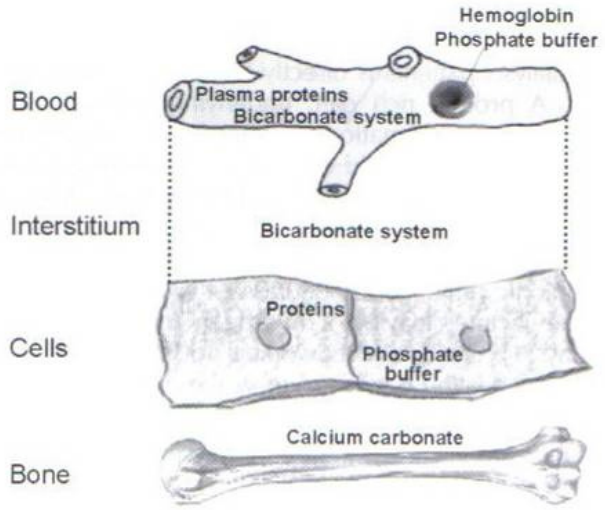

Figure I. 14 Main buffer systems in the body. Bicarbonate is the most important buffer in EC (blood and interstitium). (Grassmann et al. 2000)

Buffers in body are often separated between bicarbonate and non-bicarbonate buffer system which include all other buffers than bicarbonate buffers.

When acid is produced by the metabolism, the H^+ production is neutralised by bicarbonate. This reaction, as already described, produces water and CO_2 which is eliminated by respiration through the lungs, as seen in Equation I.28 (Equilibrium deplaced to the right).

3.3.2. Henderson-Hasselbalch equation

The ratio of HCO_3^- to H_2CO_3 at a physiological pH can be calculated using the Henderson-Hasselbalch relationship, which was developped independently by the American biological chemist L. J. Henderson and the Swedish physiologist K.A. Hasselbalch.

$$\underset{\text{Dissolved in the aqeous phase}}{CO_2 + H_2O} \overset{Ka}{\longleftrightarrow} \underset{\text{Carbonic acid}}{H_2CO_3} \overset{Kb}{\longleftrightarrow} H^+ + HCO_3^- \qquad \textbf{I. 30}$$

Equation I.30 defines the bicarbonate formation where Ka is the equilibrium constant of the first equilibrium for the carbonic acid formation, and Kb is the equilibrium constant of the buffer pair of the weak acid, carbonic acid / and its conjugate base, bicarbonate ion (H_2CO_3/ HCO_3^-).

$$Kb = \frac{[HCO_3^-][H^+]}{[H_2CO_3]} \qquad \textbf{I. 31}$$

CO_2 (dissolved in plasma) concentration is proportional to pCO_2 in the blood via:

$$[CO_2]_{dissolved} = [CO_2]_d = \alpha \times pCO_2 \quad \textbf{I. 32}$$

Where α represents the CO_2 solubility. For normal plasma at 37°C, α = 0.0307 mmol of dissolved CO_2 per liter of plasma per mmHg of pCO_2.

As most of the carbonic acid is dissolved CO_2 (which is present in plasma in an amount greater than 100 times the quantity of undissociated H_2CO_3) (Ravel et al. 1995), therefore Kb becomes K':

$$K' = \frac{[HCO_3^-] \times [H^+]}{[CO_2]_d} = \frac{[HCO_3^-] \times [H^+]}{\alpha \times pCO_2} \quad \textbf{I. 33}$$

Using logarithm function:

$$\log K' = \log[H^+] + \log \frac{[HCO_3^-]}{\alpha \times pCO_2} \quad \textbf{I. 34}$$

Or $$-\log[H^+] = -\log K' + \log \frac{[HCO_3^-]}{\alpha \times pCO_2} \quad \textbf{I. 35}$$

Then $$pH = pK' + \log \frac{[HCO_3^-]}{\alpha \times pCO_2} \quad \textbf{I. 36}$$

In this equation, and for human blood, the pK' is the apparent H_2CO_3 dissociation constant and is 6.1. This value is essentially constant under physiologic conditions (37°C).

The true value of H_2CO_3 pK (in aqueous solution and at 25 °C) is 3.8. The reason for the difference with pK' values is that only 0.5% of the dissolved CO_2 combines with water to form H_2CO_3. In physiology, it has been customary to consider that all CO_2 is in form of H_2CO_3. If to the true value pK for H_2CO_3 (3.8), we add the negative log of the hydration constant (-log 0.005 = 2.3), the sum is 6.1, which is the apparent pK' for H_2CO_3 as used in physiology (Schmidt-Nielsen 1997).

At a blood pH of 7.4, the predominant form is the bicarbonate ion, because its concentration is 20 times higher than the carbonic acid (H_2CO_3).

This can be explained using the Henderson Hasselbach, in Equation I.36:

$7.4 = 6.1 + \log \frac{[HCO_3^-]}{\alpha \times pCO_2}$ and as most of the H_2CO_3 is dissolved CO_2, then $\frac{[HCO_3^-]}{[H_2CO_3]} = 20$.

(Bhavagan 1992)

The Henderson-Hasselbalch is used in blood gas analyzers to calculate the HCO_3^- plasma concentration, knowing pH and pCO_2 of the whole blood.

Note:

The Henderson Hasselbalch is more generally given between an acid and base at equilibrium under the form:

$$pH = pK_A + \log\frac{[A^-]}{[AH]} \qquad \textbf{I. 37}$$

Where pK_A is the acid dissociation constant, $[A^-]$ the base concentration and [AH] the acid concentration.

3.3.3. Acid-base balance disorders

Acid-base balance disorders are changes in arterial pCO_2, plasma HCO_3^- concentration, and pH.

There are 4 primary types of acid-base balance disorder. Table I.3 summarises these disorders.

Disorder	**pH**	$[HCO_3^-]$	pCO_2
Metabolic acidosis	Down	Down	Down
Respiratory acidosis	Down	Up	Up
Metabolic alkalosis	Up	Up	Up
Respiratory alkalosis	Up	Down	Down

Table I. 3 Four acid-base balance disorders. Down and up indicate direction of change from normal

The normal values for pH, pCO_2, and HCO_3^- concentration are 7.40, 40 mmHg and 24 mmol/L, respectively.

If pH and pCO_2 are both increased or decreased outside the range of normal values, then the disorder is metabolic (= renal). If pH decreases and CO_2 increases or vice versa, the disorder is respiratory origin.

Determining if the disorder is acidosis or alkalosis depends upon the pH of the blood which is normally regulated between pH of 7.35 and 7.45: if pH is above 7.45, an alkalemia is present, this indicates the presence of alkalosis. If pH is below 7.35, then an acidemia is present, this indicates the presence of acidosis (Bhagavan 1999).

The evaluation of acid-base balance disorder can be made by blood gas analysis using a blood gas analyzer which analyses pH, pCO_2, pO_2 and HCO_3^- plasma concentration.

Dialysis patients with renal failure are often suffering of one or two acid-base disturbances which need to be corrected. The most common disorder in dialysis patient is metabolic acidosis: in a study of Feriani et al. (1998), 60% of patients had varying degrees of metabolic acidosis; 25% of patients had a bicarbonate level < 19.9 mmol/L and 10% of patients had a metabolic alkalosis. Only 25 % of the patients had a normal acid-base status (bicarbonate normal range 23.5-26.1 mmol/L. Therefore, the

function of the dialysis fluid is to correct the chemical composition of blood patient in order to reestablish normal physiological blood values for pH, pCO_2 and HCO_3^- concentration.

3.4. Correction of acidosis in hemodialysis

This correction is always a challenge in clinical practice because it has been shown to affect several metabolic processes in the body. One of the goals of treatment is to improve the acid-base status of the patient by an adequate choice of HCO_3^- and electrolyte concentrations in the dialysis fluid.

3.4.1 Bicarbonate dialysis

Dialysis is not able to perform base regeneration in the same way than normal kidney function because the elimination of free H^+ is insignificant. The correction of acidosis by hemodialysis takes place in a way inverse to the normal: it is not the excretion of H^+ that restore HCO_3^- but the uptake of HCO_3^- that cause the removal of H^+ from the organism.

$$H^+ + HCO_3^- \rightarrow H_2CO_3 \rightarrow CO_2 + H_2O \qquad \textbf{I. 38}$$

Equation I.38 gives the neutralization of H^+ by HCO_3^- in blood to form CO_2 which will be eliminated by the lungs.

When HCO_3^- is used as buffer in dialysis fluid, the patient plasma starts to be refilled in HCO_3^- from the beginning of the treatment. The target for acid-base correction is to maintain patients as close as possible to the physiological plasma HCO_3^- range (Ledebo 2000). In HD treatment, HCO_3^- in the dialysis fluid passes in blood across the hemodialyzer membrane due to its concentration gradient. In hemodiafiltration (HDF), with higher ultrafiltration (UF) rate than standard hemodialysis (HD), there must be a significant loss in HCO_3^- from blood through the hemodialyzer membrane. This loss can be corrected by including bicarbonate buffer in the reinjection fluid, which, in online HDF, has the same composition as dialysis fluid.
Bicarbonate dialysis fluid also contains a small amount of acid (2 to 7 mmol/L of acetate) which is necessary for the adjustment of the pH and the stability of HCO_3^- solution in respect to the escape of CO_2.

Acid-base balance is achieved in HCO_3^- dialysis when the base gain during dialysis compensates the loss of organic anions plus the inter- and intradialytic hydrogen production (Figure I.15). Organic anions are mainly lactate, β-hydroxybutyrate and intermediates of the Krebs cycle. With loss of these anions into dialysis fluid, oxidation to CO_2 and water can not be completed and the corresponding H^+ remains in the blood (Grassmann et al. 2000).

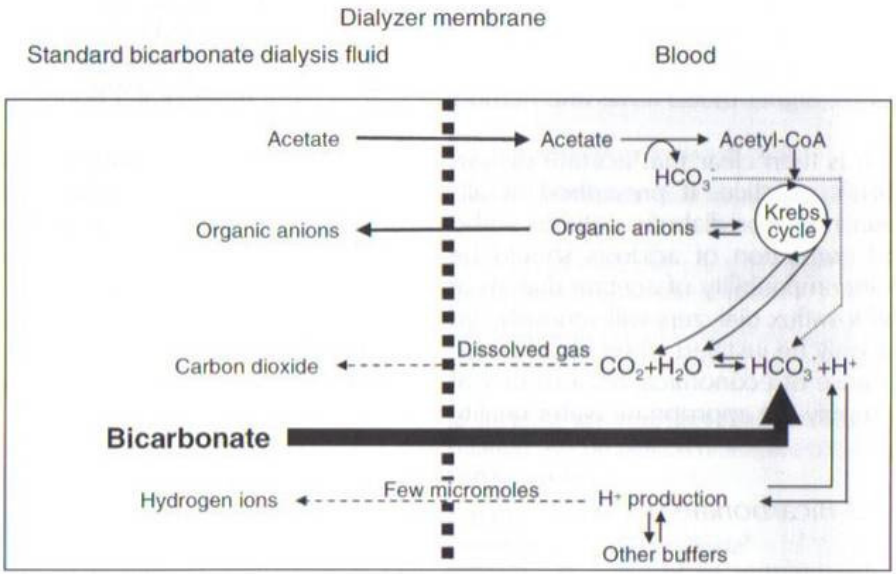

Figure I. 15 Buffer balance in bicarbonate dialysis (without ultrafiltration). (Grassmann et al. 2000).
Buffer balance: $[HCO_3^- + \text{acetate}]_{influx} + [H^+]_{lost} = [\text{organ anions}]_{lost} + [H^+ \text{ generation}]_{interdia}$

An example of the acid-base balance is the following: about 300 mmol of HCO_3^- has to be gained during one dialysis session if 140 mmol of H^+ are generated from metabolism in the interdialytic period, 100 mmol of anions are lost during dialysis, leaving the same amount of H^+ in the body and 60 mmol of buffer are lost with the ultrafiltrate (Grassmann et al. 2000).

3.4.2. Bicarbonate dialysis in HD and HDF modes in the literature

Sepandj at al. (1996) have observed in high efficiency hemodialysis, factors affecting intradialytic bicarbonate gain over 70 patients. They concluded that the diffusive gradient is the most important determinant of bicarbonate gain and they found a linear relationship between the predialysis plasma HCO_3^- concentration ($[HCO_3^-]$) and the increase in plasma $[HCO_3^-]$. They also observed that the predialysis plasma $[HCO_3^-]$ is the most important determinant of HCO_3^- gain because acidotic patients, with low predialysis HCO_3^- plasma concentration (less than 21 mmol/L) have a higher percent increase in HCO_3^- during HD than 'normal' patient.

Sombolos et al. (2005) investigated the pCO_2 and pO_2 increments observed in blood after its passage through the hemodialyzer in 14 hemodialysis patients. They measured a blood pCO_2 increase from 38.3 ± 4.3 to 62.8 ± 4.8 mmHg after 5 min of high flux dialysis, while dialysate pCO_2 fell from 79.8 ± 5.9 to 53.3 ± 2.6 mmHg. Blood pO_2 also rose from 86.8 ± 10.6 to 100.6 ± 12.3 mmHg while dialysate pO_2 dropped from 134 ± 8.8 to 125.8 ± 9.9 mmHg. They concluded that gas transfers from dialysate space into blood were responsible for these changes and measured mean dialysances for CO_2, O_2 and HCO_3^- of 0.45, 0.12 and 0.134 L/min respectively.

The kinetics of bicarbonate transfers in HDF has been investigated by Pedrini et al. (2002) for different infusion modes, pre, post and mixed dilution. They observed that, in HDF, blood always lost HCO_3^-, which was compensated by reinjection and that the HCO_3^- patient gain was larger in post-dilution than in pre-dilution (142 versus 99 mmol/session). They also computed the instantaneous net HCO_3^- mass flux to the patient and found that it decreased from 1.8 mmol/min to 0.4 mmol/min after 175 min in HDF post dilution. They concluded that using HCO_3^- in the fluid reinjected is the only way to obtain an adequate end [HCO_3^-] in online HDF.

Ahrenholz et al. (1998) also studied the impact of infusion mode (pre and postdilution in online HDF) on the acid-base status and concluded that acidosis was effectively corrected without excessive compensation by the buffer. They found that, in fact, the patient [HCO_3^-] increase during dialysis was larger when its initial concentration was low, so that the final HCO_3^- concentration remained generally between 28.3 and 29 mmol/L. They also proposed to use pCO_2 (between 40 and 60 mmHg) and pH (between 7.3 and 7.5) of the dialysis fluid rather than the [HCO_3^-] value, because this concentration is calculated from the Henderson-Hasselbalch equation with constant values valid for blood and not for an aqueous solution. They also found a linear relationship between the start plasma HCO_3^- concentration and the increase HCO_3^- concentration in dialysis session and that there are no significant differences in the pre/post acid-base parameters in pre and postdilution compared with HD.

Canaud et al. (1998) published a 12-month study on 56 patients treated with online HDF. Mean plasma HCO_3^- concentrations were 22.8 mmol/L pre-dialysis and 29.9 mmol/L post- dialysis. To avoid overcompensation resulting in post-dialysis alkalosis, dialysate HCO_3^- concentration had to be reduced from 39 to 35 mmol/L after a six months period.

4. The place of mathematical models in hemodialysis

In order to replace the function of the kidney, hemodialysis therapies rely on a complex exchange system between body fluids (plasma, interstitial and intracellular) and dialysis fluid for water, toxins and electrolytes. Mathematical model of these exchange processes have been developed to predict solute kinetics, osmolarity changes, plasma volume, acid-base balance….. Hopefully, model simulations may be used to find the best choice of operating conditions of the dialysis session. To develop a relevant model, it is necessary to analyse the physiological and chemical interactions between body fluids compartments. The choice is open between single pool and multi pools models to establish adequate equations for mass and water distribution between compartments. In general, there is a continuous search for balance between: (1) simplicity of the model, which is related to the often limited amount of available measurements and (2) its physiological precision and the need for providing more detailed information (Waniewski 2006).

Mathematical models can therefore help physicians and bioengineers to match dialysis therapy to the individual needs of the patient. They can combine the general physiological knowledge with information about individual patients yielded by clinical measurements. Many of these models (urea model, sodium model, models of peritoneal transport) have been presented to the community of clinical nephrologists in the form of computer programs. In Waniewski's (2006) brief review, current approaches to model transport processes in dialysis, including alternative and complementary versions, are described and discussed. This section gives examples and explanations about two categories of mathematical models in hemodialysis: solute kinetic modeling during hemodialysis and solute transport through the semi-permeable membrane.

4.1. Kinetic modeling

The purpose of a kinetic model, incorporating fluid mechanics and mass transport, is to represent the entire patient-hemodialyzer system. In general, kinetics describes the variation in time of a physical entity (mass, concentration) according to a driving force. Most of these models are restricted to a few compartments for the representation if the patient and few solutes (one or two). Each compartment is characterized by an internal solute concentration (C) and a volume (V). Different transport processes can change the solute concentration and volume: input and output amount of the solute, solute generation and/or its elimination. These models make it possible to analyse the course of treatment and to predict the effect of dialysis procedures.

For one compartment of solute distribution, in fixed total body water V, the mathematical description of mass balance of this total solute mass is (Waniewski 2006):

$$\frac{d(VC)}{dt} = G - CL \times C \qquad \textbf{I. 39}$$

Where a solution is:

$$C(t) = C_o e^{-CL \times t/V} + \frac{G}{CL}(1 - e^{-CL \times t/V}) \qquad \textbf{I. 40}$$

Where CL is the solute clearance, C_0 the initial solute concentration and G the rate of solute generation.

Wolf et al. (1951) were the first who described dialysis kinetics and hemodialyzer clearance. The application of modeling to renal replacement therapy was proposed in 1965 by Bell, Curtis and Babb which have developed a simulation to describe patient/hemodialyzer interactions. Before this time period, research about dialysis principally aimed at the patient survival. When patient survival was reached, it was necessary to improve dialysis conditions. Renkin (1956) was also a pioneer in the mathematical description of dialysis, while Sargent and Gotch (1978 and 1980) introduced the one-compartmental model to clinical practice in the late seventies directly applied for patient care. The benefits and risks of this model application have been described and discussed in many clinical and theoretical articles.

The concept of urea kinetic modeling pioneered by Gotch in the mid-1970 has then also been investigated by many authors; among them: (Ahrenholz et al. 1988), (Depner, 1994), (Daugirdas and Depner, 1994). These studies introduced the concept of urea distribution volume, assimilated to the total body water volume and the protein catabolism rate. All current indices of dialysis dose are based on urea measurements, and thus urea removal is still considered as the major goal of hemodialysis.

Sodium kinetic modeling has also been well documented by many authors, because the most serious side effects (as muscle cramps, symptomatic hypotension, or thirst…) induced by hemodialysis therapy are caused by changes in sodium concentration and water shift between intra- and extra-cellular space. Therefore the aim of sodium modeling is the improvement or dialysis therapy to prevent these side effects in dialysis patients (Pedrini et al. 1991), (Ursino et al. 1996), (Coli et al. 1998), (Mann and Stiller 2000).

Even if in the literature, most mathematical models have been developed with one or two compartments, few other authors have chosen to develop numerical mathematical models that described together acid-base and electrolyte balance, and water distribution: attempts have been undertaken to model and monitor several solutes and body compartments concomitantly (Thews 1990 and 1991; Ursino et al. 1999 and 2000; Ziolko et al. 2000; Prakash et al. 2002).

Figure I.16 gives an example of a two compartment model for a solute.

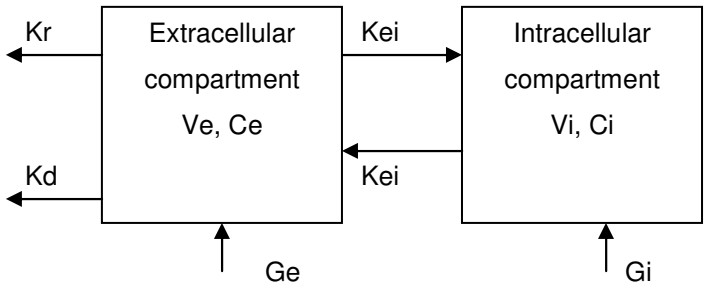

Figure I. 16 Two compartment model. Kei is the clearance between EC and IC, Ge and Gi the extra and intra cellular generation, Kr the residual clearance and Kd the hemodialyzer clearance.

Among them, Thews (Thews and Hutten, 1990, 1992) and Ursino et al. (1999 and 2000) and developed mathematical models with multi pools which require the knowledge of various parameters for these compartments.

Thews and Hutten model has been validated by comparing the results of computer simulations and measurements of arterial oxygenation, acid-base state, electrolyte concentrations and hematocrit during 190 haemodialysis sessions from 36 patients. The acid-base state is simulated by a 24-pool model, as CO_2, HCO_3^- and pH were simulated each by 8 compartments which describe dynamic exchange process during dialysis (chemical reactions, diffusion and convective transport). Using this model, the authors give the possibility to individualise the prescription of the dialysis fluid HCO_3^- concentration for each dialysis session. The most important factor for the quality of this model (among patient specific information) is the measurement of the acid-base status of the patient at the beginning of the hemodialysis. If this initial value is wrong, the prediction given by the model will be incorrect. The result of the model concerning the arterial HCO_3^- concentration is less than 2.4% of the measured value which is sufficient to valid the model for the prediction of the course of acid-base state during hemodialysis therapy. The large pools number is the most important difference to other models of the acid-base state (Thews 1992).

Ursino et al. developed a mathematical model of solute kinetics that included a two compartments model (intra/extra cellular space) for K^+, Na^+, Cl^-, Urea, HCO_3^-, H^+, a three compartments model for body fluids (plasma, interstitial and intracellular) and acid-base equilibrium through the two buffers systems (bicarbonate and non bicarbonate system). The model can be individually assigned a priori, on the basis of body weight and plasma concentrations measured before beginning the session. Model predictions have been compared with clinical data obtained during 11 various hemodialysis sessions performed on 6 patients. Analysis of results confirms that the validated model is able to predict intradialytic kinetic of solutes with a good approximation. The time pattern of plasma HCO_3^- concentration and pH always increase monotonically during HCO_3^- hemodialysis reflecting the buffer effect of bicarbonate. They found in average for HCO_3^- concentration, 3.82 % standard deviations

between model prediction and *in vivo* data. They observed in few cases that during *in vivo* treatments, pH or CO_2 concentration had significant variations which can not be reproduced by the model. These variations could be linked to a biological phenomenon, as a pulmonary leukocyte sequestration.

Even if the intradialytic kinetic of acid-base state in almost impossible to predict exactly, due of many influencing factors of internal acid-base exchanges processes, Heineken et al. (1988) have used a model for individual prescription of the dialysis fluid HCO_3^- concentration. They have demonstrated that individual prescribing of this dialysis fluid HCO_3^- concentration has a strong beneficial effect towards a more normal acid-base state for patients. Dialysis fluid HCO_3^- concentrations for their 9 patients ranged from 29 to 38 mmol/L. After a 30 weeks study period, they concluded that individually prescribed HCO_3^- concentrations resulted in a more normal acid-base status. They used a rearrangement of the equation of Sargent and Gotch (1989):

$$Cdi = \frac{J + Q_{UF} Cb}{D(1 - \frac{Q_{UF}}{Qb})} + Cb \qquad \textbf{I. 41}$$

Where Cdi is the dialysate bicarbonate concentration into hemodialyzer, J the desired flux of bicarbonate (mmol/min to the patient) assuming that the mmol of H+ generated per day is approximately equal to the g/day of protein catabolized, D the hemodialyzer dialysance for bicarbonate (assuming that mass transfer coefficient of HCO_3^- is 80% of the mass transfer coefficient for urea), Qf the average ultrafiltration rate (mL/min), Qb the blood flow rate (mL/min), Cb the targeted plasma bicarbonate concentration of 25 mmol/L. In this model, HCO_3^- is assumed to be distributed in a single pool corresponding to about 40 % of the body weight (Grassmann at al. 2000). Moreover, if this model allowed calculating the bicarbonate concentration needed for the dialysis session, it did not predict the exact course of the acid-base state during hemodialysis (Thews, 1992).

4.2. Mass transport through membranes of hemodialyzer

Over the past 30 years, efforts have also been made to develop models aimed at describing transport phenomena in hemodialyzer (Kunimoto et al. 1977), (Jaffrin et al. 1981, 1990, 1995), (Mineshima et al. 1987), (Werynski et al. 1995), (Wüpper 1996), (Ahrenholz et al. 1997).

Most models have been based on simplifying assumptions, which have sometimes made it possible to obtain analytical solutions to conservation equations: the water ultrafiltration flux Jf was often assumed constant; accumulation of partially rejected solutes at the membrane wall was also generally neglected. Solute transport from the blood bulk to the membrane, across the membrane wall and from the membrane to the dialysate bulk was generally described in terms of a lumped overall mass transfer

coefficient, whose value was assumed equal to membrane diffusive permeability or is estimated for a given solute in a given hemodialyzer under given operating conditions from the experimental clearance of that solute. As a result, mass transfer coefficient was often dealt with as an adjustable parameter and models were rather used to establish semi-empirical correlations for the hemodialyzer clearance of a solute under varying operating conditions.

Some authors provided a more detailed description of how solute transfer across the membrane occured and was related to module geometry, membrane properties and operating conditions. However, they neither accounted for the effective Jf profile that established along the module length, as a result of the hydrostatic and the osmotic pressure profiles in the blood and dialysate compartment, nor did they account for the change of the mass transport coefficient on either side of the membrane along the module length with the actual flow conditions.
Besides, such models were not validated experimentally (Sigdell 1982) or their predictions were proven satisfactory only for low molecular weight solutes, such as urea (Jaffrin et al. 1981).
Legallais et al. (2000) reported on the development of a model that predicts the performance of hemodialyzers based on module geometry, membrane transport and separation properties and the actual operating conditions. The model accounts for solute transport across the membrane by both a diffusive and convective mechanism; for concentration polarization of partially or totally rejected species at the membrane wall; for the change of the mass transport coefficient on either side of the membrane and of the water filtration flux along the module length with the actual flow conditions. The model computes concentration, flow rate and pressure profiles in both compartments of a hemodialyzer. Model predictions were validated with respect to experimental clearances of low and high molecular weight solutes reported in literature at increasing net overall filtration flow rates and blood flow rates. The predicted clearance enhancements were also compared to the best-fit values of other, non-predictive models.
This model for solute transport has been developed under following assumptions:

- steady state conditions in counter current mode are reached (the membrane characteristics do not change with time)
- axial diffusion is negligible compared to axial convection
- fluids in the blood and dialysate compartment are considered as Newtonian
- solute adsorption on the membrane is not considered
- solute partition coefficient between membrane and surrounding fluids is equal to 1
- flow rates, concentrations and pressures are uniformly distributed over the module cross-section and vary only along the module length
- uniform distribution of fibres in the module
- plasma proteins are completely rejected by the membrane

5. Conclusions

This chapter was dedicated to the presentation of the scientific context of the PhD work.

Renal functions and hemodialysis therapies have been detailed. Calculation methods of solute and fluid transport by diffusion and convection between blood and dialysis fluid inside the hemodialyzer have been presented. As acid-base balance and its restoration are one of the major goals of the dialysis therapies, this chapter has also presented this fundamental subject. We have seen that our body must maintain a balance between acid and base which is associated with the regulation of the hydrogen ion concentration (pH) in body fluids. Disturbances in acid-base balance have numerous significant physiologic consequences that affect ESRD patients. Previous authors have detailed the correction of these disturbances by hemodialysis techniques and our objectives are to deepen their conclusions and to propose a more complete approach.

Finally, the place of the mathematical models in dialysis is then discussed in order to have a view of existing kinetic and local (inside the hemodialyser) models. The Legallais et al. model has been detailed as it will be used in this thesis.

Chapter II Materials and methods

Résumé du Chapitre II

Ce chapitre aborde les matériels et les méthodes utilisés dans ce travail de thèse pour les essais *in vitro* et *in vivo*.

Le protocole expérimental des tests *in vitro* est d'abord présenté. Les tests, les conditions opératoires ainsi que la démarche qualité mise en place pour la réalisation de ces tests sont décrits. Nous avons choisi de travailler avec 2L de sang bovin hépariné, des hémodialyseurs de faible surface membranaire (0.6 m^2), des débits sanguins et de réinjection diminués et le temps des séances de dialyse *in vitro* est écourté (60 minutes). Cette étude *in vitro* est une étude paramétrique car certains paramètres (débit de réinjection et concentration en bicarbonate dans le liquide de dialyse) ont été modifiés afin de déterminer leur impact sur le déroulement des séances de dialyse.

Nous présentons ensuite le protocole mis en place pour la réalisation des essais cliniques (*in vivo*) au CHU d'Amiens. Cette étude a été réalisée en incluant 6 patients et 23 séances de dialyse ont été suivies en hémodialyse (HD) et en HDF en ligne. Les conditions opératoires identiques pour chaque séance sont présentées. La méthodologie de l'étude statistique concernant l'analyse des résultats préliminaires est également décrite.

Puis les matériels (l'analyseur des gaz du sang, l'automate de biochimie, les principaux capteurs des générateurs d'hémodialyse, l'appareil de mesure de l'hématocrite, les capteurs de pression et la microcentrifugeuse) utilisés pour les tests expérimentaux sont détaillés afin de permettre une meilleure compréhension des résultats obtenus.

Une autre section présente la bonne répétabilité des tests *in vitro* ainsi que les coefficients de variation des paramètres acide-base déduits de cette étude. Les caractéristiques du liquide de dialyse des tests *in vitro* et *in vivo* sont détaillées, permettant d'observer la bonne cohérence des concentrations, du pH et des gaz (pCO_2 et pO_2) pour les générateurs d'hémodialyse entre eux et pour les caractéristiques théoriques du dialysat.

Enfin, la dernière section de ce chapitre aborde des comparaisons pour la concentration en bicarbonate et pour l'hématocrite entre les différentes méthodes d'analyse. Il est intéressant de constater que pour l'hématocrite, les valeurs sont fortement dépendantes de l'appareil utilisé et de sa technique.

This chapter concerns the materials and methods used in the research project. First we present the *in vitro* and the *in vivo* experimental set-up and conditions. Then we describe the measurements techniques, the blood gas analyzer, the colorimetric clinical chemistry analyzer, sensors in the dialysis machine, the hematocrit monitoring, the pressure sensors and the microcentrifuge.
Another section consists in the presentation of the *in vitro* and *in vivo* tests characteristics: a repeatability analysis and inlet dialysis fluid characteristics.
The last section of this chapter compares measurements of bicarbonate concentration and hematocrit by various analysis methods corresponding to various devices, during the *in vitro* and *in vivo* tests.

1. *In vitro* tests

1.1. Procedure

1.1.1. Blood collection

The patient is represented by a 2-L plastic bag of heparinised bovine blood. Blood is collected at the Laon slaughterhouse (France) into tanks containing the anticoagulant solution: one volume of anticoagulant (1L of PBS + 5 mL of heparin at 5 000U.L./mL) is used for eight volumes of blood. PBS solution (Phosphate Buffer Solution) has been prepared with NaCl (8g/L), KCl (0.2g/L), Na_2HPO_4 (1.136g/L), and KH_2PO_4 (0.2g/L) to obtain a pH of 7.45. The anticoagulated blood is then inserted in plastic bags by the means of a pump at the slaughterhouse.

1.1.2. Dialysis equipment

In vitro experiments are carried out using a 4008H hemodialysis machine (Fresenius Medical Care, Bad Homburg, Germany). FX40 (FMC) hemodialyzers with a membrane area of 0.6 m² are selected because of the small blood volume. The FX40 parameters are L = 25.5 cm, 4588 fibres of 185 µm inner diameter, a 35 µm membrane thickness and a membrane hydraulic permeability of 34 mL/h/mmHg/m².
The 4008H hemodialysis machine allows HD, HF, HDF or online HDF treatment (due to the reinjection pomp = ONLINEplus™ option) using bicarbonate (with BiBag®), or acetate in uni- or biponction. This hemodialysis machine can vary concentrations for sodium and bicarbonate, and includes ultrafiltration control, UF and sodium profiles, dialysis fluid filtration (DIASAFE®plus), heparin pomp and a disinfection program.
For all *in vitro* tests, no sodium and UF profiles are applied. The prescribed sodium is always fixed to 140 mmol/L, and the dialysis fluid temperature is set to 37°C. The parameters that have been changed are bicarbonate concentration, blood and reinjection flow rate.

The exact same equipment as used in the dialysis centres (as hemodialyzer, pressure monitors, dialysis machine…) has been employed and as an *in vitro* study permits to add other equipments, pressure sensors and sampling site in dialysate line have been added.

1.1.3. Quality control

Blood dialysis lines and hemodialyzers have only been used for one test corresponding to one dialysis session (single use).

The protocol of bovine blood collecting at the slaughterhouse and its use in the laboratory UMR6600 of the University of Technology of Compiègne (UTC) has been validated by the Direction Départementale des Services Vétérinaires de l'Aisne (DDSV), by the UTC security engineer (Comité d'hygiène et sécurité de l'UTC) and by the Director of UMR6600.

At the end of each test, as the bovine blood circulates in closed loop in the plastic bag, the bovine blood bag has been frozen and discarded according to the local procedure for dead animals for lab experimentation.

In vitro measurements have first been realised using 2L of saline solution (PBS + urea) in plastic bag to represent our *in vitro* patient. This pre-study has allowed us to take the control of all devices (dialysis machine, analysis devices, pressures control, sampling frequency…) for the development of the *in vitro* tests using bovine blood.

1.2. Tests description

1.2.1. Experimental set-up

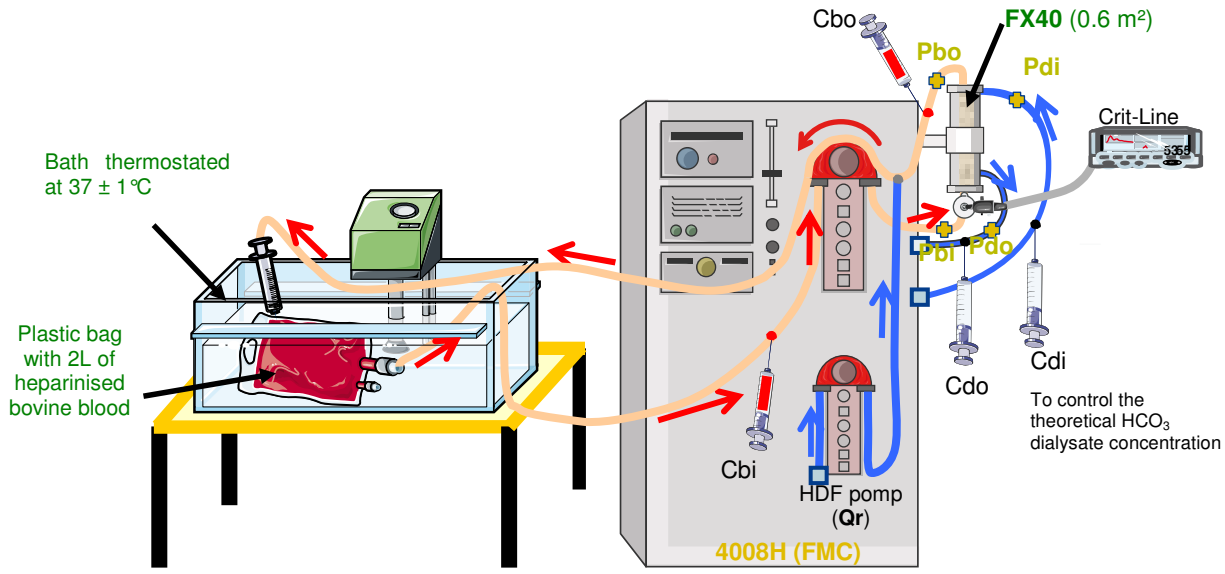

Figure II. 1 *In vitro* tests schematic representation

This experimental set-up summarises the *in vitro* tests experimental conditions and procedures:

1. The bath containing water is thermostated to 37 ± 1 °C in order to continuously heat the blood bag
2. The venous line is pumped back into the plastic bag by a syringe in order mix 'arterial' and 'venous' blood
3. The dialysis sessions are carried out in HD or in online postdilution HDF mode with the reinjection pump which delivers a reinjection flow rate, Qr of 0, 30 or 50 mL/min
4. Hematocrit measurements are carried out by adding a measuring cell (linked to the Crit-Line) before the hemodialyzer in arterial line
5. Pressures measurements are obtained by adding 4 pressures sensors (linked to acquisition box and computer) in the 4 hemodialyzer inputs/outputs
6. 4 samples sites (Cbi, Cbo, Cdi, Cdo) are used to analyse the blood and dialysate characteristics. Sampling site at the dialysis fluid line outlet has been added by us.

1.2.2. Tests parameters

Nine tests have been carried out in duplicate at an inlet blood flow (Qbi) of 200 mL/min, a dialysate inlet flow rate (Qdi) of 500 mL/min and a weight loss rate (Qw) of 0 mL/min.

Three tests are carried out in HD, three in online HDF with postdilution and a reinjection rate (Qr) of 30 mL/min, and three in online HDF with postdilution and Qr of 50 mL/min.

For one operating condition (Table II.1), three theoretical dialysis fluid HCO_3^- concentrations are programmed in the dialysis machine: 28 mmol/L, 32 mmol/L and 40 mmol/L.

The duration of each test is about 1 hour.

Dialysis fluid HCO_3^- concentration (mmol/L) →	28		32		40	
	HD	HDF	HD	HDF	HD	HDF
Qr = 0	28 HD		32 HD		40 HD	
Qr = 30 mL/min		28 HDF 30		32 HDF 30		40 HDF 30
Qr = 50 mL/min		28 HDF 50		32 HDF 50		40 HDF 50

Table II. 1 Nomenclature for the 9 *in vitro* tests realised in duplicate

The initial blood and plasma characteristics (pH, hematocrit, pCO_2, pO_2, HCO_3^- plasma concentration, urea and total protein plasma concentration) of the 18 bovine blood tests are given in Table II.2. Urea and TProt are obtained using the automated clinical analyzer, Konelab (Thermo Fisher Scientific), the other values are given by the blood gas analyzer, ABL (Radiometer). ABL and Konelab are two chemistry devices presented in section 3 of this chapter. Each test has been repeated (except 28 HDF 50) under same conditions using a second blood bag from the same animal, in order to check the repeatability of the tests. The 1st blood bag is used 24h after collection at the slaughterhouse and the 2nd blood bag at 48h for tests 32 HD, 32 HDF 30 and 32 HDF 50. For other tests, the 1st blood bag is

used 7h after collection at the slaughterhouse and the 2nd blood bag at 24h. Tests using the 2nd blood bag are indicated by '(2)'. Blood bags have been transported in an ice box and have been refrigerated (4°C) before their use.

	pH	H (%)	pCO_2 (mmHg)	pO_2 (mmHg)	HCO_3^- (P) (mmol/L)	Urea (mmol/L)	TProt (g/L)
40 HD	7.28	28	48	26	21.8	3.89	60.51
40 HD (2)	7.25	25	50	28	21.2	3.78	61.18
32 HD	7.17	34	35	53	12.3	na	65.66
32 HD (2)	7.10	46	47	50	13.9	na	68.22
28 HD	7.28	29	46	28	20.9	5.77	59.50
28 HD (2)	7.26	30	49	29	21.2	5.78	59.56
40 HDF 30	7.28	24	38	35	17.3	7.19	53.81
40 HDF 30 (2)	7.27	23	38	35	16.9	7.25	53.59
32 HDF 30	7.26	34	45	30	19.5	5.3	57.42
32 HDF 30 (2)	7.2	35	57	20	21.4	5.5	59.34
28 HDF 30	7.32	27	38	34	19	5.94	56.4
28 HDF 30 (2)	7.27	23	43	34	19.1	5.92	54.89
40 HDF 50	7.31	33	47	21	23	4.28	64.62
40 HDF 50 (2)	7.28	35	50	22	22.7	4.39	64.75
32 HDF 50	7.24	31	46	35	19	5.71	55.07
32 HDF 50 (2)	7.14	30	56	39	18.3	6	55.23
28 HDF 50	7.26	27	38	29	16.5	5.93	65.06
28 HDF 50 (2)	7.25	26	42	29	17	5.94	65.2
Mean ± SD (all)	7.25 ± 0.059	30.24 ± 5.75	45.35 ± 6.36	32.23 ± 9.02	19.06 ± 2.98	5.51 ± 1.04	59.69 ± 4.63

Table II. 2 Blood and plasma initial characteristic for the *in vitro* tests (na = not available). HCO_3^-, urea and TProt (total protein) are plasma concentration. H = hematocrit

Table II.2 shows that even if blood is taken from various animals, the standard deviations (SD) of these seven parameters are low; this indicates a low variability between the tests.

It can also be seen that hematocrit (H), pCO_2 are comparable to those of dialysed patients, but that values of pO_2, pH and bicarbonate concentration are lower than for *in vivo* arterial blood, as expected since blood has been collected from a vein and due to contact with air in the slaughterhouse.

Even if initial characteristics for 28 HDF 50 (2) are included in Table II.2, this test has not been retained due to errors in the *in vitro* protocol.

1.2.3. Blood samples collection

Three 1-mL samples in the extracorporeal circuit are collected simultaneously at blood inlet and outlet of hemodialyzer and at dialysate outlet, every 5 min in the first 30 min and then every 10 min. One or two samples in the dialysis fluid inlet are taken during the dialysis session in order to check bicarbonate concentration.

Blood samples are immediately analysed by the ABL.

Plasma samples of 0.3 mL obtained after centrifugation, are also analysed by the clinical chemistry analyzer, Konelab (presented in section 3 of this chapter), together with dialysate samples. All Konelab measurements are done in triplicate and average values and SD are recorded.

1.2.4. Dialysis fluid management

Table II.3 gives the theoretical dialysis fluid composition used in the *in vitro* tests.

Substances	Na^+	K^+	Ca^{2+}	Mg^+	Bicarbonate (HCO_3^-)	Glucose	Cl-	Acétate
A component : 472 A (mmol/L)	107	3	1.75	0.5	0	1 g/L	114.5	3
B component: BiBag (mmol/L)	35	0	0	0	35	0	0	0
Dialysis fluid	**142**	**3**	**1.75**	**0.5**	**32**	**1 g/L**	**114.5**	**3**

Table II. 3 Theoretical dialysis fluid composition for *in vitro* tests

As there is 35 mmol/L of bicarbonate in the B component and 3 mmol/L of acetate in the A component, the final dialysis fluid HCO_3^- concentration should be 32 mmol/L (at the level 0).

2. *In vivo* tests

Clinical trials have been carried out at the Amiens University Hospital in the nephrology department under the supervision of the head of the dialysis unit, Dr Philippe Morinière. The first task has consisted in the redaction of the *in vivo* protocol in order to receive the approval of the local ethics committee (Comité de Protection des Personnes, CPP Nord-Ouest II). The set-up of the protocol has taken 9 months (information, redaction, corrections…) and has been finally approved by this ethics committee (N° ID-RCB: n° 2009 - A00394-53). All dialysis patients have been informed by the physician before their enrolment in the study.

2.1. Procedure

2.1.1. Patients

The number of patients to be included in the clinical study was based on the following calculation.

Estimation of the sample size for a comparison between two groups

The power analysis is commonly used in the field of design of experiments in order to plan experiments and to decide how much samples are necessary (Mason et al. 2003).

Sample size may be determined on either precision analysis or power analysis. Precision analysis and power analysis for sample size determination are usually performed by controlling type I error and type II error, respectively. The probability of making type I and type II errors are given by: α = p (type error I) = p (reject Ho when Ho is true) and β = p (type error II) = p (fail to reject Ho when Ho is false). Therefore power = 1- β = p (reject Ho when Ho is false) where Ho is the null hypothesis. The null hypothesis proposes no difference or relationship between the variables of interest. For example we can have Ho: $\mu_1 = \mu_2$ where μ_1 and μ_2 are respectively mean of group 1 and 2.

To estimate the required sample size of each group, it is necessary to specify the significance level (Type I error, α), the power (1- β) and the anticipated difference that may be expected between the groups. The two-tailed Type I error rate of 5% is usually taken as standard for a superiority trial. It is then recommended that the power of the trial should be 90% with 80% the minimum.

Therefore, the sample size needed to achieve power 1- β can be obtained by solving (Aday et al. 2006, p168 and Laplanche et al. 1989) with the hypothesis of two groups comparison, Ho: $\mu_1 = \mu_2$ and Ha: $\mu_1 \neq \mu_2$ (alternative hypothesis):

$$n = (Z_{1-\frac{\alpha}{2}} + Z_{1-\beta})^2 \times \frac{2\sigma^2}{|\mu_1 - \mu_2|^2} \text{ with } \sigma = \sqrt{\frac{\sigma_1 + \sigma_2}{2}} \qquad \textbf{II. 1}$$

Where n is the number of measurement, σ the estimated standard deviation (assumed to be equal for the two groups), μ_1 estimated mean (larger), and μ_2 estimated mean (smaller). $Z_{1-\alpha/2}$ (standard error associated with confidence interval of 95%) and $Z_{1-\beta}$ (standard error associated with power of 90%) can be read in Normal distribution tables and are respectively equal to 1.96 and 1.282.
As we want to detect differences in HD and HDF treatments, the parameter of comparison which has been taken is the initial or the final plasma bicarbonate concentration. Therefore the estimated standard deviation for the two groups (σ) has been taken at 2 mmol/L (from literature and our *in vitro* tests) and the estimated difference between the smaller and larger mean ($|\mu_1 - \mu_2|$) has been taken as 2 mmol/L (corresponding to the 7% error measurements on the bicarbonate plasma concentration). With Equation II.1, we find n = 21.
Therefore the number of patients estimated to reach a power of 90% with a standard deviation of 2 mmol/L and a difference of 2 mmol/L is approximately 21.

This number of patients has been proposed for the approval by the ethical commity but the members of this committee asked us to increase this number of patient until 30. Therefore 30 patients with renal failure requiring dialysis will be included and each patient will follow 3 HD sessions and 3 online HDF postdilution sessions (paired and cross-over design). The participants of the study are recruited from the patients of the Amiens University Hospital according to inclusion and exclusion criteria. Among them, patients who had been stable on thrice weekly hemodialysis and who had a permanent blood access (arteriovenous fistula) capable of delivering a blood flow rate of at least 350 mL/min are eligible for inclusion in the study. Therefore, a total of 180 hemodialysis treatments (over a period of 18 months) using bicarbonate dialysis fluid are forecasted using 5008 dialysis machine (Fresenius Medical Care, Bad Homburg, Germany)

2.1.2. Sampling protocol

Samples of patients blood (0.7 mL) are collected periodically during the dialysis session from the arterial and venous line simultaneously of the extracorporeal circuit at the times : +3 min, +13 min, +23 min, +33 min, +43 min, +53 min, +63 min, +90 min, +120 min, +150 min, +180 min, +210 min, +237 min, in order to measure acid-base parameters (pH, pCO_2 and pO_2), and electrolytes (Ca^{2+}, Na^+, Cl^- and K^+) concentrations. These micro-samples are collected in heparin syringes (Pico50, Radiometer) and are immediately analysed by a blood gas analyzer, ABL, taken on site (the same as for *in vitro* study) in the dialysis unit.

Inlet dialysis fluid samples are also analysed with ABL in order to compare the theoretical dialysis fluid HCO_3^- concentration set on the dialysis machine, with the measured HCO_3^- concentration.

2.1.3. Data collection

In addition to blood samples, blood, dialysis fluid ultrafiltration and reinjection flow rate, arterial and venous pressure, TMP, urea clearance, hematocrit and haemoglobin are recorded periodically along the dialysis session. All technical problems, clinical adverse effects as well as clotting episodes are recorded if encountered. Using 5008 dialysis machine, mean or characteristic data of the dialysis session are recorded in the internal memory of the machine. These values are recorded by hand in the patient book (to register the specifications of the dialysis session) at the end of the dialysis session. They include the duration of the session (treatment time), the weight loss rate, the mean dialysis fluid temperature, the blood flow rate, the urea clearance, the mean reinjection rate (in HDF), the recirculation percentage, initial and final hematocrit and haemoglobin.

All laboratory and technical data are registered into Excel file protected by a password, to ensure full confidentiality.

2.1.4. Statistical analysis

We have used descriptive statistics to numerically describe the data by calculating the mean, the standard deviation (SD), the coefficient of variation (CV), and the range or the measure of spread.

Then in order to judge how 'significant' these trends are, we have used probability tests for the comparison of two populations (two groups). The methodology consists in two steps: first, the comparison of variances and secondly the comparison of means between the two groups. The preliminary test for comparison of variances (F value, Fisher test) indicates that the variances of the two groups (for example for the comparison between HD and HDF groups) are significantly different under a significance level of 5% if F value is situated inside the critical region. Then, two-tailed t-tests (Student t-test) are performed to compare means of the two groups. If the two groups are dependent, the paired t-test will be used but if the two groups are independent, the t-test will be used knowing the results of the F-test. p value < 0.05 of the t-test is considered statistically significant (under a significance level of 5%). These two tests are based on the assumption that data come from the normal distribution.

Linear regressions are also employed to compare parameters between the two techniques (HD and HDF).

2.2. *In vivo* dialysis sessions realised

Due to the late start the study, (from May to July 2009), only 6 patients have been included in this pre study (3 men and 3 women) and 23 dialysis sessions have been recorded. All the 6 patients have an arteriovenous fistula and have been informed by the physician before their enrolment in the study. The

in vivo study is gloing to continue from January 2010 in Amiens Hospital in collaboration with the nephrology department to reach the number of 30 included patients.

2.2.1. Patients included

The patient characteristics and the repartition of the HD or online postdilution HDF sessions are given in Table II.4. Patients are usually in HD sessions and have been followed HDF sessions for the *in vivo* protocol.

The HD or HDF sessions are not always consecutive. 12 HD sessions and 11 online postdilution HDF sessions (or total of 23 dialysis sessions) have been recorded.

The dry body weight is defined as the state where there is no excess extracellular fluid volume and has to correspond to the postdialysis weight.

Patient	Gender (M/F)	Age (year)	Dry body weight (kg)	Height (cm)	Number of dialysis sessions recorded	Dialysis fluid ("acid" component)
PC01	M	53	66.5	162	3 HD + 2 HDF	SW 139
MA02	F	85	87.25	160	3 HD + 3 HDF	SW 139
SG03	F	77	76	147	1 HD + 2 HDF	SW 649
LC04	F	56	40	170	1 HD + 3 HDF	SW 139
GV05	M	19	51.5	166	3 HD	SW 139
LR06	M	87	83.5	170	1HD + 1 HDF	SW 139
Mean ± SD **Men**		53 ± 34	67.17 ± 16.01	166 ± 4		
Mean ± SD **Women**		72.67 ± 14.98	67.75 ± 24.68	159 ± 11.53		
Mean ± SD **All**		62.83 ± 25.85	67.46 ± 18.61	162.5 ±8.62		

Table II. 4 Mean ± SD patients characteristics. M is for male and F for female

Table II.5 gives dialysis sessions operating conditions which are kept constant during all the sessions.

Treatment duration (min)	4 hours
Blood flow rate Qb (mL/min)	350
Dialysis fluid flow rate Qd (mL/min)	500
HCO_3^- dialysis fluid concentration (mmol/L)	38

Table II. 5 Dialysis sessions operating conditions

2.2.2. Materials and dialysis fluid composition

All HD and online postdilution HDF sessions are performed using 5008 dialysis machines and polysulfone hollow fibre hemodialyzers FX 80 (FMC, 1.8 m² and 59 mL/h/mmHg).

Dialysis fluid is produced by dialysis machine from the 'acid' component (SW 139 and SW 649, from BBraun, according to patient needs) and from the 'base' component (B component), BiBag (from FMC).

Substances concentration in mmol/L	Na^+	K^+	Ca^{2+}	Mg^+	Bicarbonate (HCO_3^-)	Glucose (g/L)	Cl^-	Acetic acid
A component: SW 139	103	2	1.75	0.5	0	1	109.5	3
A component: SW 649	103	2	1.5	0.375	0	1	108.75	3
B component: BiBag	35				35			

Table II. 6 Theoretical dialysis fluid composition for *in vivo* tests

As seen in Table II.6, only small differences exist between the two 'acid bath' SW 139 and SW 649 on Ca^{2+}, Mg^+ and Cl^- concentration.

2.2.3. Online*plus*™ technology for online HDF sessions

As seen previously, the term 'online' means that the replacement solution is directly produced from dialysis fluid solution. This technology can be used in HDF, in HF for the rinsing of blood lines, for the restitution of blood at the end of the dialysis session and for the administration of a bolus in case of hypotension. The dialysis fluid produced composition is identical to the dialysis fluid circulating inside the hemodialyzer.

There are various strategies for the determination of the reinjection flow rate, Qr.

The usual theory (Henderson 1989) uses the following equation:

$$Qr = 0.5 \times Qpw \qquad \textbf{II. 2}$$

Where Qpw (mL/min) is the water plasma flow given by Colton's equation:

$$Qpw = Qb \times (1 - \frac{H}{100}) \times (1 - 0.00107 \times T\,\mathrm{Pr}\,ot) \qquad \textbf{II. 3}$$

Where Qb is the real blood flow rate (mL/min), H the hematocrit (%), and TProt the total protein concentration (g/L). σ =0.00107 L/g represents the protocrit or the volume occupied by the proteins in the plasma (Colton et al. 1970).

In the 4008H, the reinjection flow rate (Qr) must be manually recorded. In practice, we used in HDF postdilution:

$$Qr = \frac{1}{3} \times Qb \qquad \textbf{II. 4}$$

But this equation does not take into account the individual variations of hematocrit and protein concentration.

The option 'autosubstitution' in 5008 dialysis machine allows the automatic adaptation of the reinjection flow rate (Qr) using:

$$Qr = Qb \times (1 - \frac{H}{100}) \times (1 - \frac{7 \times T\,\mathrm{Pr}\,ot}{1000}) \qquad \textbf{II. 5}$$

This equation gives more importance to the protein concentration than Equation II.3 (Potier 2008).
For example, with Qb = 350 mL/min, H = 35% and TProt =82 g/L, Equation II.2 gives Qr = 103.77 mL/min, while Equation II.4 gives Qr = 116.67 mL/min and Equation II.5, Qr = 96.92 mL/min.

3. Measurements techniques

3.1. Blood gas analyzer

3.1.1. Measured and calculated parameters

The device, ABL77 (Radiometer, Denmark) pH, blood gas and electrolyte analysis system has been employed. It is a portable, automated analyzer that measures in whole blood parameters detailed in Table II.7. It is designed for use with human arterial, venous, and capillary whole blood and requires a minimum sample volume of 70 µL. The ABL77 analyzer has not been tested with animal blood. Some components in animal blood might differ from those in human blood. We will use the name ABL in the rest of the study (ABL means "Acid Base Laboratory", a trademark of Radiometer since 1973).

The following parameters can be measured:

Type	Parameters Symbol	Description	Units
pH	pH	Acidity or alkalinity	
Blood gases	pCO_2	Carbon dioxide pressure	mmHg
	pO_2	Oxygen pressure	mmHg
Electrolytes	Ca^{2+}	Ionized calcium ion concentration in plasma	mmol/L
	Cl^-	Chloride ion concentration in plasma	mmol/L
	K^+	Potassium ion concentration in plasma	mmol/L
	Na^+	Sodium ion concentration in plasma	mmol/L
Hematocrit	H	Volume fraction of erythrocytes in blood	%

Table II. 7 Parameters measured by ABL

The ABL also calculates other parameters; Table II.8 lists the most important calculated parameters used in this study (acid-base and oxygen parameters).

Parameters Symbol	Description	Units
HCO_3^- (P)	Concentration of hydrogen carbonate ion (bicarbonate) in plasma	mmol/L
tCO_2 (B)	Concentration of total carbon dioxide in blood (CO_2 content)	mmol/L
tCO_2 (P)	Concentration of total carbon dioxide in plasma (CO_2 content)	mmol/L
tHb	Concentration of the total hemoglobin in blood	g/dl
tO_2(B)	Concentration of total oxygen in blood	mmol/L
sO_2	Oxygen saturation of hemoglobin in blood.	%

Table II. 8 Main calculated parameters by ABL

The ABL system consists of the analyzer, a multi-use, disposable sensor cassette and a calibration solution pack (cal pack). The temperature of the sensor cassette measuring chamber is maintained at 37.0 ± 0.2 °C during sample analysis and calibration.

Calibration of the system is accomplished using the cal pack that contains two levels of precision tonometered electrolyte solutions packaged in gas tight disposable bags.

3.1.2. Sensors

The ABL sensor system incorporates micro-electrodes technology for the measurement of the blood parameters listed Table II.7. These sensors are located in the cassette. The sensor methodologies are analogous to traditional electrodes for the measurement of blood gases and electrolytes. Adams and Hahn (1982) have described the principles of blood gas analysis and electrodes for the measurement of pH, pCO_2 and pO_2.

Three various measuring principles are employed for sensors in the ABL.

1) Potentiometry: the potential of a sensor chain is recorded using a voltmeter, and related to the concentration of the sample (by the Nernst equation II.6). The potentiometric measuring principle is applied for the pH, pCO_2, and electrolytes sensors (Na^+, K^+, Ca^{2+}, Cl^-).

The Nernst equation gives the potential of the sample:

$$E_{sample} = E_0 + \frac{RT}{nF} \times \ln a_{\times} \qquad \textbf{II. 6}$$

Where:

E_0 =	Standard potential of the electrode chain
R =	Gas constant (8.3143 J/°K-mole)
T =	Absolute temperature (°K)
n =	Charge on the species x
F =	Faraday constant (96487 C/mole)
a_x =	Activity of the species x

2) Amperometry: the magnitude of an electrical current flowing through a sensor chain is proportional to the concentration of the substance being oxidized or reduced at an electrode in the chain. The amperometric measuring principle is applied for the pO_2 sensor.

3) Conductimetry: specific impedance between two conducting electrodes held at a constant voltage (frequency of 10 kHz) is directly proportional to the conductive properties of that sample. The conductimetric measuring principle is applied for the hematocrit electrode.

Due to the presence of ions in the plasma phase, blood is conductive. The cells present in blood are generally non-conductive; therefore a measurement of the conductivity of blood is inversely proportional to the number and size of erythrocytes present in the blood. This measurement, therefore, can be related to the volume % of red blood cells or hematocrit of a blood sample. The electrolyte, protein, and osmotic concentrations in a whole blood sample will affect the hematocrit measurement. Sodium is the primary electrolyte in plasma. The concentration of sodium has a direct effect on the

conductivity of the blood sample because it is a charged ion. Measurement of the sodium concentration in each sample is performed and the results used to correct the conductivity value for the effects of the sodium concentration. Plasma proteins are non-conducting structures that can occupy 1 to 7% of the plasma volume. The protein concentration is assumed constant for all patients. This assumption holds true in most cases but can cause an error for hematocrit.

3.1.3. ABL equations for calculating physiologic parameters

The ABL uses the method of Siggaard-Andersen (1974 and 1988), with the following equations described in the ABL operating guide.

Equation for HCO_3^- (P)

The HCO_3^- concentration in plasma is calculated from the Henderson-Hasselbalch equation

$$pH = pK' + \log(\frac{[HCO_3^-]}{[CO_2]}) = pK' + \log(\frac{[HCO_3^-]}{\alpha CO_2 \times pCO_2}) \quad \textbf{II. 7}$$

where pK' value is an empirical "constant" which takes into account the various forms of bound CO_2. Equation II.7 becomes:

$$HCO_3^-(P) = \alpha CO_2 \times pCO_2 \times 10^{(pH - pK')} \quad \textbf{II. 8}$$

with $pK' = 6.125 - \log[1 + 10^{(pH-8.7)}]$ **II. 9**

where αCO_2 = 0.23 mmol/L/kPa (or 0.0307 mmol/L/mmHg), HCO_3^- in mmol/L and pCO_2 in kPa or in mmHg.

For many purposes a constant pK' of 6.1 may be used. But pK' value changed during dialysis in the majority of patients. (Santoro et al. 1987). Calculating HCO_3^- from pH and pCO_2 using the Henderson-Hasselbalch equation is equivalent to use a bicarbonate selective electrode. HCO_3^-(P) includes ions of hydrogen carbonate, carbonate and carbamate in the plasma

Equation for tCO_2 (P)

The tCO_2 concentration in plasma is the sum of all the CO_2 species including physically dissolved CO_2, and various forms of bound CO_2.

$$tCO_2(P) = \alpha CO_2 \times pCO_2 + HCO_3^-(P) \quad \textbf{II. 10}$$

Equation for tCO_2 (B)

The calculation is based on tCO_2(B) divided in 2 phases, plasma (P) and erythrocyte fluid (Ery):

$$tCO_2(B) = tCO_2(Ery) \times \varphi Ery(B) + tCO_2(P) \times (1 - \varphi Ery(B)) \quad \textbf{II. 11}$$

The volume fraction of erythrocyte is estimated from the hemoglobin concentration (tHb):

$$\varphi Ery(B) = \frac{tHb}{tHb(Ery)} \quad \textbf{II. 12}$$

with tHb(Ery) = 21 mmol/L (corresponding to the normal mean concentration of haemoglobin in the erythrocytes) and tHb in mmol/L

The concentration of tCO_2 in the erythrocyte fluid is calculated from the erythrocyte pH, the pCO_2 and the sO_2 with a modified Hendersen-Hasselbalch equation.

$$tCO_2(Ery) = \alpha CO_2(Ery) \times pCO_2 \times [1 + 10^{pHEry - pKEry)}] \quad \textbf{II. 13}$$

Where $pHEry = 7.19 + 0.77 \times (pH - 7.4) + 0.035 \times (1 - sO_2)$ **II. 14**

And $pKEry = 6.125 - \log(1 + 10^{pHEry - 7.84 - 0.06 \times sO_2})$ **II. 15**

This equation represents an adaptation to tCO_2 values calculated with the Singer&Hastings monogram. with αCO_2(Ery) = 0.195 mmol/L/kPa, sO_2 is in decimal fraction, and pO_2 in kPa.

Equation for tO_2 (B)

The tO_2 concentration in blood is calculated as the sum of free and bound oxygen:

$$tO_2 = \alpha O_2 \times pO_2 + HHb \times sO_2 \quad \textbf{II. 16}$$

Where αO_2 = 0.00983 mmol/L/kPa (with this solubility constant, we can observe that CO_2 is 24 times more soluble than O_2) and HHb may be termed the concentration of "functional hemoglobin".

$$HHb = tHb \times (1 - xHbCO - xHi) \quad \textbf{II. 17}$$

with xHbCO is the substance fraction of carboxyhemoglobin = 0.005 (a value of 0.002 to 0.005 is due to the endogenous carbon monoxide production) and xHi is the substance fraction of hemoglobin or methemoglobin = 0.005.

Equation for sO_2 (B)

The oxygen saturation is the fraction of the hemoglobin molecules in a blood sample that are saturated with oxygen at a given partial pressure of oxygen. The oxygen saturation proposed by Siggaard-Andersen can be calculated from pO_2 with the function representing the oxyhemoglobin dissociation curve (OCD).

The following equation is given by the manufacturer guideline.

$$sO_2 = \frac{(pO_2^{'})^3 + 150 \times pO_2^{'}}{(pO_2^{'})^3 + 150 \times pO_2^{'} + 23400} \times 100\% \quad \textbf{II. 18}$$

where $pO_2^{'} = pO_2 \times 10^{0.48 \times (pH - 7.4) - 0.0013 \times (HCO_3 - 25)}$ **II. 19**

Equation for tHb (B)

$$tHb = \frac{Hct/100 - 0.0083}{0.0485} \times 1.6114 \text{ in g/dl} \quad \textbf{II. 20}$$

The molar mass of the haemoglobin containing one iron atom is 16 114 g/mol.

3.2. Colorimetric clinical chemistry analyzer

3.2.1. Principles

The device, Konelab 20 (Thermo Fisher Scientific, Denmark) has been employed. It is a fully automated clinical chemistry analyzer. The Konelab 20 is an integrated system for routine clinical chemistry tests, electrolytes and special chemistries including specific proteins, and toxicology tests. It allows continuous loading of samples, cuvettes and system reagents and relies on to a fully graphical user interface.

The measurements are made following colorimetric and turbidimetric principles. Kinetic or end-point modes can be used. The light source is a halogen lamp with a linear absorbance (A) range of 0 to 2.5 A, resolution of 0.001 A and reproducibility of SD≤0.005 A at 2 A. Spectral range is between 340 and 800 nm.

The absorbance measures the capacity of a medium to absorb light passing through it. In spectroscopy, the absorbance A is defined as:

$$A_\lambda = \log(\frac{Io}{I}) \quad \textbf{II. 21}$$

where I is the intensity of light at a specified wavelength λ that has passed through a sample (transmitted light intensity) and I_0 is the intensity of the light before it enters the sample or incident light intensity. The absorbance is a positive value, without unity. The bigger A is, the lower the transmitted intensity is.

Absorbance measurements are often carried out in analytical chemistry, since the absorbance of a sample is proportional to the thickness of the sample and the concentration of the absorbing species in the sample. The Beer-Lambert relationship assumes that absorbance A_λ of a solution at a wavelength λ, is proportional to the concentration (c) of the absorbed specie of the solution, and the length (l) of optical path (distance over which the light passes through the solution).

$$A_\lambda = c \times l \times \varepsilon_\lambda \quad \text{II. 22}$$

Where ε_λ the coefficient of molar extinction of the specie. (Also know as molar absorptivity, a measurement of how chemical specie absorbs light at a given wavelength)

3.2.2. Concentrations analysis

Konelab has been used in our *in vitro* study to obtain urea, bicarbonate and total protein concentration. The calibrations for bicarbonate, total protein and urea are made before each test. Then the concentrations are automatically calculated by the Konelab analyzer using the calibrating curve. The chemical reactions are described in the Konelab operating guide.

Bicarbonate concentration ($kHCO_3^-$) in mmol/L

Bicarbonate concentration in plasma is measured by a colorimetric enzymatic method using the Konelab 20. The plasma CO_2 (in the form of bicarbonate ions) reacts with phosphoenolpyruvate (PEP) to form oxaloacetate and phosphate. This reaction is catalyzed by phosphoenolpyruvate carboxylase (PEPC). Malate dehydrogenase (MDH) then catalyzes the reduction of oxaloacetate to malate and the oxidation of NADH to NAD+.

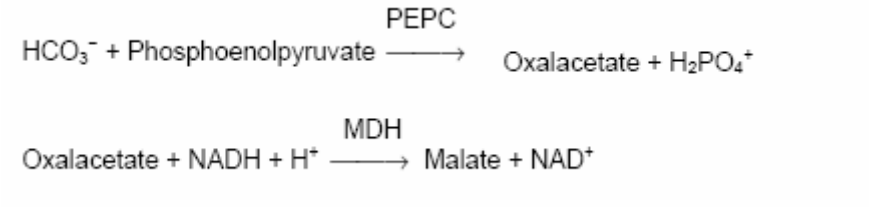

Figure II. 2 HCO_3^- reactions using Thermo kits

The resulting decrease in absorbance at 380 nm is proportional to the amount of bicarbonate present in sample (Norris et al. 1975). In the manufacturer's book, it is mentioned that concentrations in plasma are expected between 22 and 29 mmol/L, and the validity limit is 1 mmol/L.

Total protein concentration (TProt) in g/L

The human body contains thousands of various proteins. Many proteins are structural elements of cells or organised tissues. Other proteins are soluble and they are free molecules moving in extracellular or intercellular fluids. Proteins form a colored complex with cupric ions in alkaline solutions. (Doumas, 1975). The formation of the complex is measured at 540 nm. The method employs EDTA (ethylenediaminetetraacetic acid) as a chelating and stabilising agent for cupric ions. In the manufacturer's book, it is mentioned that concentrations in plasma are expected between 64 and 83 g/L and the validity limit is 1 g/L.

Urea concentration (Urea) in mmol/L

Urea is formed in the liver as a product terminal catabolism protein and more than 90% of urea is excreted through the kidneys. The content of the blood urea is directly related to the functioning kidney.

Urea is hydrolysed in the presence of water and urease to produce ammonia and CO_2. In the presence of glutamate dehydrogenase (GLDH) and reduced nicotanamide adenine dinucleotide (NADH), the ammonia combines with a-ketoglutarate (α-KG) to produce L-glutamate. The resulting decrease in absorbance at 340 nm, as NADH is converted to NAD proportional to the level of urea in the sample.

$$\text{Urea} + H_2O \xrightarrow{\text{Urease}} 2\,NH_3 + CO_2$$

$$NH_3 + \alpha\text{-CG} + \text{NADH} \xrightarrow{\text{GLDH}} \text{L-Glutamate} + \text{NAD}$$

Figure II. 3 Urea reactions Thermo kits

In the manufacturer's book, it is mentioned that values in plasma are expected between 2.2 and 7.2 mmol/L (or 13 and 43 mg/L) and the validity limit is 1.1 mmol/L.

3.3. Sensors in the dialysis machine

The modern machines for hemodialysis permit a complete manipulation of the dialysate composition, temperature, flows, and pressures in order to control and to optimise the extracorporeal treatment. With sensors added to the extracorporeal circulation it is possible to gain information by non invasive means. This part describes some blood line sensors methods of Fresenius Medical Care dialysis machine in 4008H (for *in vitro* study) and 5008 (for *in vivo* study).

3.3.1. Transmembrane pressure, TMP

In early HD dialysis machine, the ultrafiltration rate (Qf) could be directly controlled by TMP using Equation I.13 (Chapter I). But this method of ultrafiltration control is too inaccurate for high flux dialysis techniques. Thus the introduction of high flux dialysis leads to the development of new methods of ultrafiltration control, such as volumetric ultrafiltration control. The TMP evaluation plays only a minor role in these new technologies since it is Qf which is controlled by the action of an ultrafiltration pump in the dialysis fluid circuit incorporating balancing chambers for fresh and spent dialysis fluid (Grassmann et al. 2000). Now a negative TMP indicates a possibility of backfiltration during dialysis.

The TMP is defined by the difference between the mean blood pressure and mean dialysis fluid pressure. In practice some systems use only 2 or 3 pressure measurements to calculate the TMP.

Dialysis machine 4008H gives the measurement of the TMP, displayed on the dialysis machine screen. The TMP displayed (TMP_d) is defined by the Equation II.23 (operating guide from FMC) and uses only 2 pressures measurements (Pbo and Pdo) to calculate the TMP:

$$TMP_d = Pbo - Pdo + blood\ flow\ pressure\ drop \quad \textbf{II. 23}$$

Where the blood pressure drop (ΔP) inside the hemodialyzer is

$$\Delta P = Pbi - Pbo \quad \textbf{II. 24}$$

ΔP depends on the hemodialyzer used and is generally calculated from blood flow rate. For example, for FX 40 hemodialyzer, with Qb = 200 mL/min, ΔP = 136 mmHg (operating guide from FMC).

Now the 5008 dialysis machine uses 3 pressures measurements in the TMP measurement (operating guide):

$$TMP_d = Pbo - (Pdi + Pdo)/2 + \Delta P \quad \textbf{II. 25}$$

It is still not correct because ΔP is not measured.

For our *in vitro* trials, we have developed our own TMP measurements with 4 pressure sensors (see in paragraph 3.5.). The pressures and TMP are recorded in order to assess membrane hydraulic permeability and pressure loss in hemodialyser.

3.3.2. Blood Volume Monitor (BVM)

The change of hematocrit can be monitored over the course of an entire dialysis treatment to track hemoconcentration caused by unbalance between ultrafiltration and vascular refilling.

This approach can be realised using the Blood Volume Monitor (BVM). The BVM is based on measurement of sound velocity in blood. The time of flight of short ultrasonic pulses transmitted across the blood sample is measured and corrected for temperature effects. The measurement is done in a special measuring cell inserted in the pre-pump segment of the arterial line. From a change in hemoconcentration measured with a maximum sampling period of 1.2 seconds, the relative change in blood volume is determined assuming a single blood volume compartment (Schneditz 2005).

3.3.3. Blood Temperature Monitor (BTM)

Blood recirculation can be detected using the Blood Temperature Monitor (BTM). Two temperature heads measure the blood temperature in the arterial and venous lines of the extracorporeal circuit. A bolus of “cold” blood is generated for several minutes by cooling the dialysis fluid temperature by several degrees. This temperature bolus is monitored by the venous head before the bolus passes into the patient. Fractions of the temperature bolus which are recirculated through the patient are monitored by the arterial head for a period of 5 to 8 minutes. The BTM measures the total recirculation which is

the sum of the cardiopulmonary and access recirculations. The reproducibility of the BTM *in vitro* is ± 3 to 5 %. (Chamney 2001)

Recirculation rate is calculated from the change in arterial temperature (ΔA) caused by a change in venous line temperature (ΔV) (Schneditz 2005):

$$R = \frac{\Delta A}{\Delta V} \qquad \textbf{II. 26}$$

3.3.4. Online clearance monitor (OCM)

The Online Clearance Monitor (OCM) from FMC estimated the effective urea clearance from the direct correlation with electrolyte (sodium) dialysance by measuring conductivity differences between dialysate inlet and outlet of the hemodialyzer for two different dialysis fluid inlet concentrations (Polaschegg 1993).

OCM allows the determination and the variation during dialysis session of urea clearance CL, of the index for quantification of the hemodialysis dose (CL*t/V) and of plasma sodium concentration. CL*t/V is a dimension-less parameter where t the duration of the dialysis session and V the distribution volume of urea in the body. The minimum CL*t/V recommended for all patients is 1.2.

V can be calculated in 5008 dialysis machine using weight, age, sex and height of the dialysis patient using Watson et al. (1980) correlation.

For most authors, the conductivity measurements provide a value of 'ionic dialysance' (Petitclerc 2006).

3.4. Hematocrit monitoring

The Crit-Line instrument (In-Line Diagnostics Corporation, Utah, USA) offers the opportunity to measure non-invasively the hematocrit and saturation of blood oxygen continuously by optical trans-illumination method. This device works with a measuring sterile disposable cell that is placed on the arterial line of extracorporeal circuit at the entrance to the hemodialyzer. The manufacturer claims that the accuracy is about 1% for a hematocrit between 5% and 60%.

The Crit-Line can be used with any type of hemodialysis machine. The sensor consists of a transmitter and red light receiver that can evaluate the absorption and diffusion of the light transmitted through the blood flowing in the blood room or measuring cell. The Crit-Line is calibrated to standard hemodialysis patient's blood with a mean cell volume (MCV) of 91μm^3.

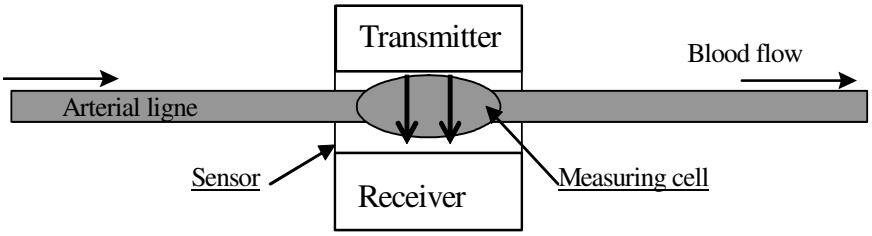

Figure II. 4 Crit-Line principles

The Crit-Line has been used in 7 *in vitro* tests and the measuring cell has been added in the arterial line at the hemodialyzer inlet. In some *in vitro* tests, the Crit-Line is used to compare various measurements of hematocrit.

3.5. Pressures sensors

In order to measure the pressures in the blood and dialysis lines, pressures sensors have been added and used in some tests. Before *in vitro* dialysis session, blood and dialysis lines are cut, in order to insert the 4 pressures sensors in branch corresponding to the 4 input/output of the hemodialyzer. The pressures sensors are connected to a data acquisition box which is linked to the computer equipped with software developed by the UTC electronics department.

These pressures sensors are similar to the pressures sensors inserted in the dialysis machine (HOSPAL Reference: 501079002).

Figure II.5 gives an example of one sensor position.

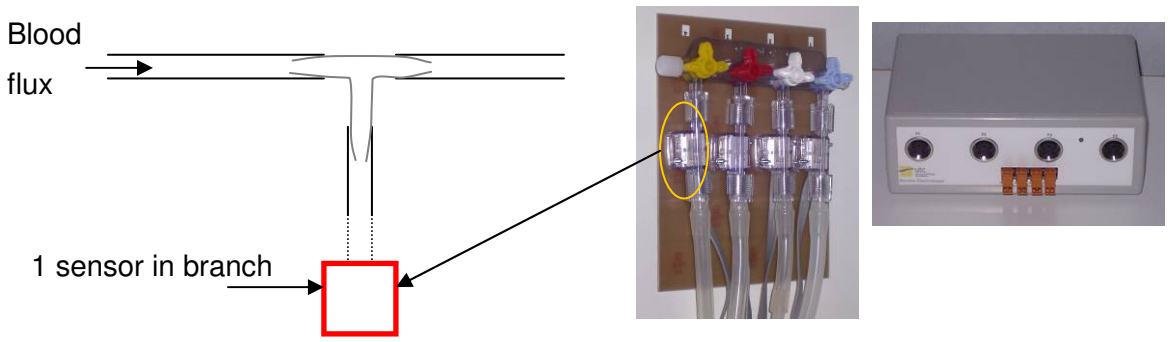

Figure II. 5 Pressure sensors position and devices

The pressures sensors are calibrated at the beginning of each *in vitro* experiment with an electronic manometer.

3.6. Microcentrifuge

Centrifugation with Sigma (201 M) using capillary tubes is the standard method for hematocrit measurement. This method needs small blood samples as blood is introduced by capillarity in 75 µL glass microtubes where one of its extremities is closed.

The value of hematocrit is then read by positioning the microtube under a special rule and by measuring the height occupied by cells.

4. *In vitro* and *in vivo* tests characteristics

4.1. *In vitro* tests repeatability

Parameters repeatability

In order to add error bars in all measured parameters, coefficients of variation (CV) have been determined. A coefficient of variation is a normalised measure of dispersion of a probability distribution. It is defined as the ratio of standard deviation (SD) to mean value.

The ABL coefficients of variation are obtained from a study realised by Braconnier at al. (2003) for pH, pCO_2, pO_2, Na^+, Cl^-, K^+, and Ca^{2+}. As HCO_3^- concentration is a calculated parameter, its coefficient of variation has been estimated from the errors calculations.

Since all Konelab measurements are done in triplicate, coefficients of variation for Konelab are deduced from one reference test. Then for each Konelab characteristics measured, average values and SD are recorded.

Device	ABL								Konelab		
Parameters	pH	pCO_2	pO_2	Na^+	K^+	Ca^{2+}	Cl^-	HCO_3^-	$kHCO_3^-$	TProt	Urea
CV (%)	0.135	4.65	3	0.4	0.94	1.01	1.06	**7**	**1.34**	**0.61**	**2.98**

Table II. 9 Coefficients Variation (CV) in % for ABL and Konelab parameters. $kHCO_3^-$ is the HCO_3^- plasma concentration obtained by Konelab. TProt represents the plasma total protein concentration.

It can be seen that coefficient of variation is very low for pH (0.135%) and high for pCO_2 (4.65%) and pO_2 (3%).

Test repeatability

Each test has been performed in duplicate using two blood bags from the same animal, in order to check the repeatability of the tests. The 1st blood bag has been used 6h to 24h after collection at the slaughterhouse and the 2nd blood bag, 24 to 48h after the 1st one, after storage at 4°C.

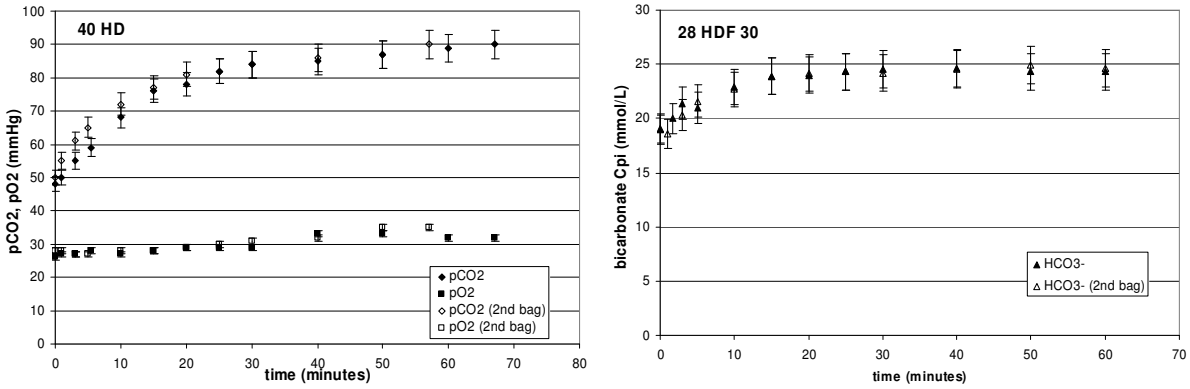

Figures II. 6 Example: repeatability of pCO_2 and pO_2 in 40 HD test and HCO_3^- plasma concentration in 28 HDF30 test measured by ABL for the 1st and 2nd blood bag

Figures II.6 shows good repeatability for pCO_2, pO_2 and HCO_3^- concentration measurements obtained with same blood and under the same experimental conditions. If small differences exist, it may due to blood quality which tends to deteriorate in the 2nd blood bag.

4.2. *In vitro* inlet dialysis fluid characteristics measured by ABL

As inlet dialysis fluid samples are taken during *in vitro* tests, comparisons are made between the theoretical (programmed by the dialysis machine) and measured composition of the dialysis fluid.

During tests, one inlet dialysis fluid sample have been taken in order to analyse by ABL their pH, pO_2, pCO_2, HCO_3^- and other electrolytes concentrations after 10 minutes of *in vitro* dialysis session. The mean ± SD have been calculated and summarised in Table II.10, as function of the theoretical HCO_3^- concentration programmed by the dialysis machine.

Theoretical HCO_3^- concentration = Cdi_b (mmol/L)	ABL parameters (mmol/L for concentrations and mmHg for partial pressures)			
	HCO_3^-	pH	pCO_2	pO_2
28 (n = 5)	**26.8 ±0.71**	7.22 ±0.04	68.8 ±6.82	107.85 ±13.2
32 (n = 4)	**30.14 ±0.9**	7.35 ±0.077	57.0 ±10.12	111.8 ±11.26
40 (n = 5)	**39.2 ±0.99**	7.42 ±0.017	62.3 ±3.04	109.0 ±8.46

Table II. 10 Inlet dialysis fluid characteristics measured by ABL for various HCO3- dialysis fluid concentration (Cdi_b). n refer to the number of independent experiments

When Cdi_b is set to 32 mmol/L in the dialysis machine, Cdi_b measured values ranged from 29.1 to 31.3 mmol/L, with a mean value of 30.14 mmol/L. The more common volumetric proportioning system of

water and dialysis fluid concentrates is the water metering based on volume measurements (Grassmann et al. 2000): fixed amounts of concentrates are added to fixed amounts of water. This system is controlled by measuring the conductivity of the final dialysis fluid. The use of volume and conductivity parameters should offer protection against mixing errors.

Dialysis fluid pCO_2 is higher than normal blood (arterial blood pCO_2 is between 35 and 45 mmHg) whereas dialysis fluid pO_2 is similar to normal blood values (arterial blood pO_2 is between 75 and 105 mmHg).

Ahrenholz et al. (1998) proposed that a correct calibration of the bicarbonate delivery system is when dialysis fluid pH is between 7.3 and 7.5 and pCO_2 ranges between 40 and 60 mmHg. Dialysis fluid pH and pCO_2 should be used rather than HCO_3^- concentration, because HCO_3^- concentration is calculated from the Henderson-Hasselbalch equation which uses constants established for blood and not for aqueous solutions.

4.3. *In vivo* inlet dialysis fluid characteristics measured by ABL

Inlet dialysis fluid samples are collected for each dialysis session (4 to 5 per dialysis session) and analysed by ABL. Outlet dialysis fluid samples could not be taken because dialysis FMC 5008 machines are not equipped with a special sampling site.

The 23 dialysis sessions have been performed using 4 various 5008 dialysis machines. For the study, each patient has been dialysed using the same dialysis machine (number from 1 to 4).

Table II.11 presents the mean ± SD results of inlet dialysis fluid characteristics.

Acid bath	Dialysis machine number	pH	pCO_2 (mmHg)	pO_2 (mmHg)	Na (mmol/L)	K+ (mmol/L)	Ca2+ (mmol/L)	Cl- (mmol/L)	HCO_3^- (mmol/L)
SW 139	**1** (n = 15) Patient: PC01	7.39 ± 0.09	63.00 ± 11.14	152.53 ± 5.25	148.87 ± 9.93	1.95 ± 0.11	1.48 ± 0.03	111.53 ± 6.2	36.75 ± 1.47
	CV (%)	1.2	17.7	3.4	6.7	5.6	2	5.6	4
	2 (n = 28) Patients: MA02, and LR06	7.34 ± 0.05	69.89 ± 6.95	147.86 ± 2.37	145.18 ± 5.74	1.91 ± 0.1	1.49 ± 0.09	109.4 ± 6.23	36.85 ± 1.19
	CV (%)	0.7	9.9	1.6	3.9	5.2	6	5.7	3.2
	3 (n = 13) Patient: LC04	7.40 ± 0.09	61.23 ± 11.61	150.54 ± 6.44	144.92 ± 5.62	1.91 ± 0.12	1.44 ± 0.10	107.7 ± 5.03	36.12 ± 1.03
	CV (%)	1.2	18	4.3	3.9	6.3	6.9	4.7	2.9
	4 (n = 14) Patient: GV05	7.41 ± 0.04	61.36 ± 5.21	146.50 ± 4.49	149.36 ± 3.99	1.99 ± 0.08	1.45 ± 0.15	111.86 ± 3.94	38.14 ± 0.85
	CV (%)	0.5	8.5	3.1	2.7	4	10	3.5	2.2
SW 649	**2** (n = 10) Patient: SG03	7.40 ± 0.06	63.1 ± 7.05	148.0 ± 4.69	150.1 ± 5.20	2.02 ± 0.12	1.28 ± 0.03	113.9 ± 6.13	37.8 ± 1.35
	CV(%)	0.8	11.2	3.2	3.5	5.9	2.3	5.4	3.6

Table II. 11 Mean ± SD inlet dialysis fluid characteristics (analysed by ABL) for the 4 dialysis machines used in this study. The number n represents the number of dialysis fluid samples. CV represents the coefficient of variations

It can be seen that concentration values are close between dialysis machines. The higher variations concern pCO_2 values (with a mean CV of 13.1 %) and the smaller variations, the pH (with mean CV of 0.9 %). Mean HCO_3^- concentration variations is 3.2 % .
These inlet dialysis fluid characteristics have been pooled together because the same acid baths have been used.

Distinctions have been made between dialysis fluid constituted with 2 'acid baths' (SW 139 and SW 649) depending of the patient's need. The theoretical composition of these 'acid baths' has been given in Chapter II (Table II.6). The differences between the two baths can be seen in the Ca^{2+} concentration: theoretically, SW 139 contains 1.75 mmol/L and SW 649, 1.5 mmol/L. We also find a lower Ca^{2+} concentration in SW 649. Concerning the other parameters, the variations are similar.

As seen in Chapter I, dialysis fluid is a mixture of 'acid bath' and bicarbonate solution (diluted to a HCO_3^- 41 mmol/L), made only seconds before its delivery to the hemodialyzer. A small amount of acetic acid (CH_3COOH), 3 mmol/L reacts with bicarbonate, when the two solutions are combined:

$$CH_3COOH + HCO_3^- \rightarrow CH_3COO^- + CO_2 \qquad \textbf{II. 27}$$

At equilibrium, these concentrations are respectively:

0 38 mmol/L 3 mmol/L 3 mmol/L

Acetate is necessary for the adjustment of pH and the stability of the bicarbonate solution concerning CO_2 escape (Grassmann et al. 2000). Therefore, the dialysis fluid provides a new CO_2 concentration of 3 mmol/L, an acetate concentration of 3 mmol/L and HCO_3^- of 38 mmol/L in the final bath solution. The 3 mmol/L of CO_2 produces at 37 °C a pCO_2 of 100 mmHg, insuring an almost neutral pH in the mixture (Feriani et al. 2004).
But CO_2 dialysis fluid also depends on CO_2 infusion in the closed system (la Greca et al. 1989). Therefore we only find a mean pCO_2 of 63.7 mmHg in the inlet dialysis fluid which gives a CO_2 concentration of 1.91 mmol/L.

As only small differences have been observed between dialysis machines for pCO_2, pO_2 and HCO_3^- concentration, Table II.12 sums up the mean ± SD of these parameters which will be taken in the following as reference:

Acid-base parameters	pH	pCO_2 (mmHg)	pO_2 (mmHg)	HCO_3^- (mmol/L)
Mean ± SD	7.39 ± 0.03	63.7 ± 3.56	149.09 ± 2.42	37.13 ± 0.82
CV (%)	0.9	13.6	3.12	3.2

Table II. 12 Mean ± SD of acid-base parameters for inlet dialysis fluid

Symreng et al. (1992) also measured inlet dialysis fluid using a Gambro dialysis machine and they found a pH of 7.36 ± 0.07, pCO_2 of 62.3 ± 11.1 mmHg, pO_2 of 127.5 ± 6 mmHg and HCO_3^- concentration of 34.8 ± 0.6 mmol/L (for 35 mmol/L of HCO_3^-). Except for our high pO_2 as compared to values of Symreng, the 3 others parameters are in the same range.

4.4. *In vitro* evaluation of the membrane permeability

In this study, the hydraulic permeability (Lp) of FX 40 (A = 0.6 m² and K_{UF} = 20 mL/h/mmHg) has been investigated using our *in vitro* set-up. We propose to calculate Lp from experimental tests and to compare the results with theoretical values.

As seen in Chapter I, the ultrafiltration coefficient K_{UF} (mL/h/mmHg) is calculated as the ratio of ultrafiltration flow rate (Q_{UF}) and transmembrane pressure (TMP) measurements.
Therefore the hydraulic membrane permeability, Lp (mL/h/m²/mmHg) can be calculated by:

$$Lp = \frac{J_F}{TMP} = \frac{K_{UF}}{A} = \frac{Qf}{A \times TMP} \qquad \textbf{II. 28}$$

Where J_F is the volumetric flux of water (mL/h/m²), A is the hemodialyzer membrane (m²), and TMP the transmembrane pressure (mmHg).

The ultrafiltration flow of pure water through a membrane increases linearly with the average transmembrane pressure. After exposure to proteins, the blood diffusive transport as well as the hydraulic permeability of the membrane decrease significantly due to protein adsorption. Moreover, these plasma proteins exert an osmotic pressure of 20-30 mmHg opposing the applied hydrostatic pressure (Henderson 1996). Finally, the ultrafiltration flow deviates from linearity for high TMP values due to concentration polarization of high molecular weight substances (such as proteins and cells) in the blood which are not freely filtrated through the membrane pores. Because blood cells are 2000 times larger than pores of a high flux polysulphone membrane, one single blood cell may block several pores, reducing the effective membrane area and ultrafiltration flow. Individual variations in the hematocrit, plasma protein concentration and coagulation may lead to significant variation in the ultrafiltration flow at a given TMP.

The Lp coefficients have been calculated for 4 tests. As pressure measurements can vary during dialysis session, mean ± SD TMP have been calculated using Equation I.13 (without ΔΠ) and taking mean of the 4 pressure measurements during the five first minutes of the session (where TMP is stable). Osmotic pressures (ΔΠ) have been calculated using the Landis and Pappenheimer's semi empirical correlation (Equation 20 of the Legallais et al's paper presented in Annexe A). This equation

uses the concentration of total protein (which is presented in Chapter III, section 3.2.1) and has been applied at the hemodialyser inlet and outlet.

Tests	40 HDF30	40 HDF50	28HDF30	32 HDF50
TMP mean (mmHg)	60.43 ± 1.94	153.42 ± 4.72	53.56 ± 2.85	163.78 ± 3.48
ΔΠ mean (mmHg)	20.82	24.34	21.19	25.28
Qf = Qr (mL/min)	30	50	30	50
J_F = Qf / A (mL/h/m²)	3000	5000	3000	5000
Lp (mL/h/m²/mmHg)	49.64	32.6	56.01	30.53

Table II. 13 TMP, ΔΠ , Qf, J_F and Lp calculated in 4 *in vitro* tests. Qw = 0 as no weight loss rate is programmed

Experimental J_F has been represented for each test as function of TMP - ΔΠ in Figure II.7.

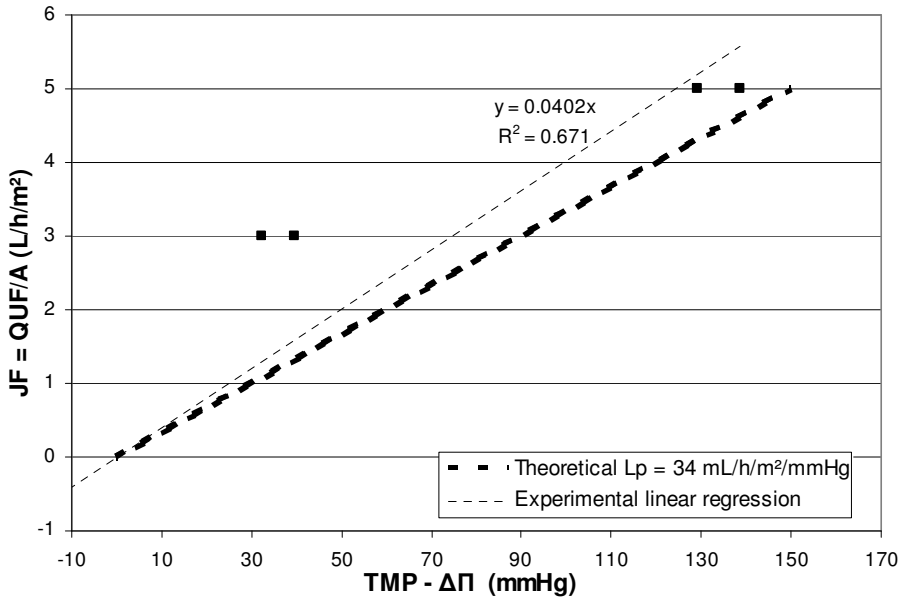

Figure II. 7 Representation of the volumetric flux of water J_F as function of the transmembrane pressure TMP. Experimental Lp is the slope of the linear regression between the 6 tests.

As TMP is low, we can assume the linear relationship between TMP and J_F.

Manufacturer data for FX 40 hemodialyzer give A = 0.6 m² and K_{UF} = 20 mL/h/mmHg. Therefore Lp should be equal to 34 mL/h/m²/mmHg.

It can be seen that there is a good agreement between theoretical Lp of 34 mL/h/m²/mmHg and the mean result found by the 4 tests (40.2 mL/h/m²/mmHg).

In the following the theoretical Lp value for the FX40 has been used rather than the experimental one. This calculation is indicative and would need another *in vitro* test to be more precise.

5. Comparison of measurements methods

This section is dedicated to metrology in order to be aware and conscious about measurement errors. Bicarbonate and hematocrit have been compared using various analysis methods using *in vitro* and *in vivo* tests.

5.1. Bicarbonate concentration

5.1.1. Methods description

Bicarbonate (HCO_3^-) concentration can be measured with methods based on different principles. (Métais 1980)

1. In titrimetric analysis, the titrant solution is volumetrically delivered using a burette, to a recipient containing the solution for analysis. Delivery of the titrant is called a titration. The titration is complete when sufficient titrant has been added to react with all the substances in the solution. An indicator (methyl orange, for example) is often added to the recipient to signal when all of the substances have reacted.

2. Volumetric methods (at constant pressures) as Van Slyke method or Astrup's extrapolation (also called equilibration technique) method can be used to measure a gas volume released by the plasma. With the equilibration technique, three pH measurements of the solution are made (directly and after the samples are equilibrated with 4% and 8% CO_2 in a microtonometer). The values are plotted on the Siggaard-Anderson nomogram for pH and pCO_2. The position of the slope allows graphically determination of HCO_3^- concentration.

3. Manometric methods (at constant volume) use Van Slyke or Natelson apparatus. These methods are accurate but take time and money. Therefore these methods can not be used in clinical practice.

4. Enzymatic method as described for the Konelab can be used to determine the amount of bicarbonate present in the sample.

5. Blood gas analyzers only need small blood quantity (due to the development of microelectrodes and microanalyses), measure the pH, pCO_2 and pO_2 and calculate the plasma HCO_3^- concentration with algorithms and constants derived from healthy persons.

5.1.2. Previous comparisons

Engelhardt et al. (1988) have compared acid-base parameters in blood and dialysate by 3 techniques: titrimetric method, equilibration technique (ET) and blood gas analyzer. For blood, an acceptable agreement is obtained for pH, pCO_2 and HCO_3^- between the blood gas analyzer and ET, but for dialysate HCO_3^-, values obtained by titrimetric method are 3-4 mmol/L higher than those determined by the gas analyzer and ET. This difference may be due to the choice of constants (CO_2 solubility and pK') in Henderson-Hasselbalch equation.

Story et al. (2000 and 2001) have compared bicarbonate concentration by using a blood gas analyzer with Henderson-Hasselbalch equation method and by using the spectrophotometric enzymatic method. They found that the difference between the two techniques (enzymatic – calculated by Henderson-Hasselbalch equation) gives a bias of -1.6 mmol/L. They explained that this difference may be due to the amount of CO_2 lost during processing for enzymatic assay because the duration of exposure to the atmosphere is not standardised. Another reason is that the manufacturer of enzymatic method describes this assay as a bicarbonate assay although it is a total CO_2 assay, because all CO_2 is converted to bicarbonate. As dissolved CO_2 is lost in the atmosphere at a rate about 6 mmol/L, measured total CO_2 is closer to the initial bicarbonate concentration than the initial total CO_2 content.

5.1.3. Our *in vitro* comparisons

In our *in vitro* study, HCO_3^- concentrations are measured by enzymatic method (Konelab) and are also calculated by blood gas analyzer (ABL) for each sample of the nine tests.

The mean difference between the 2 techniques for 99 values (11 samples by tests) is found to be 0.269 ± 1.999. The following graph gives the linear regression between the two techniques.

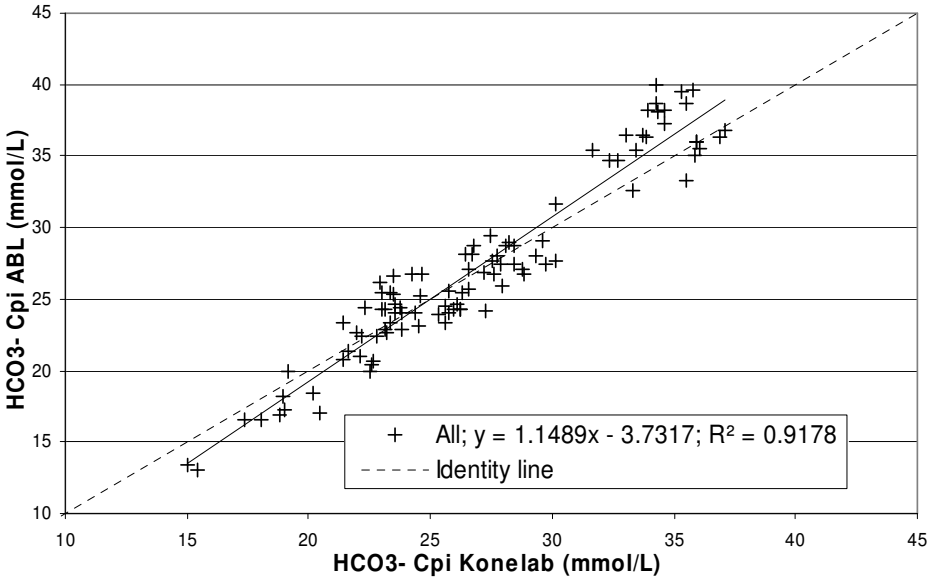

Figure II. 8 Bicarbonate plasma concentration comparison between ABL and Konelab devices

Mean HCO_3^- plasma concentration are found 27.15 ± 6.4 mmol/L with ABL and 26.88 ± 5.34 mmol/L with Konelab.

Fisher F-test and Student t-test applied for comparison between the two techniques give that differences are not statistically significant as p> 0.05 for the 2 statistical tests.

Agreement between the two techniques is also assessed using Bland-Altman analysis. The plasma bicarbonate concentration difference between ABL and Konelab is plotted in function of the one average (ABL + Konelab)/2. The full lines are the limits of agreement (between -3.73 and 4.27 mmol/L) and the dashed line is the bias.

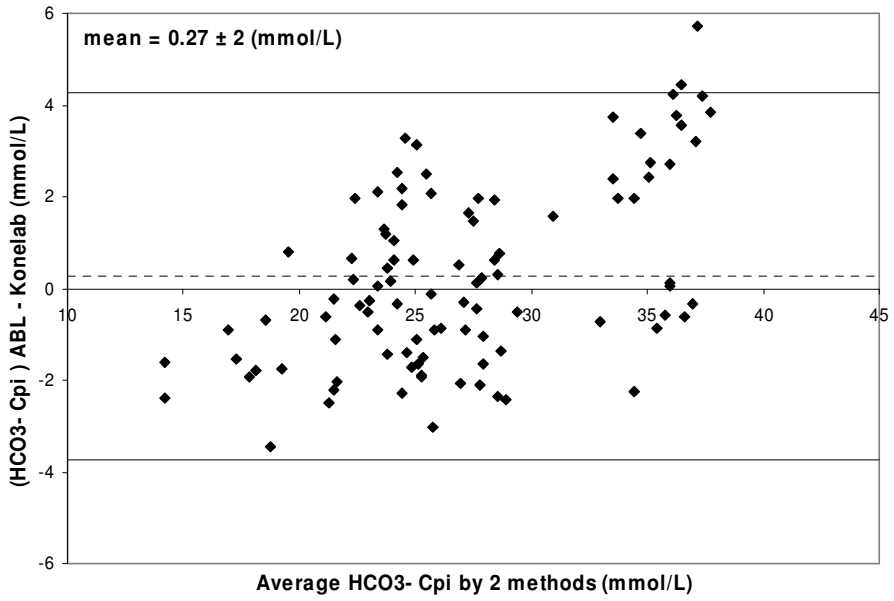

Figure II. 9 Bland-Altman plot of the difference between the two bicarbonate concentration determinations

For the *in vitro* study, even if the bias we find between the two techniques is smaller than the one determined by Story et al., we consider that ABL give more consistent results than the Konelab. In addition the ABL is more versatile, as it also measures blood gases, total CO_2 etc, and most authors (Pedrini et al. 2000, Ahrenholz et al. 1998) use blood gas analyzers to measure HCO_3^- concentration. Therefore in order to present our results we have made the choice to only use ABL values for the *in vitro* study.

5.2. Hematocrit monitoring

5.2.1. Methods description

Hematocrit can be measured by various methods. The following paragraph gives the most commonly used techniques for measuring hematocrit.

1. Hematocrit can be determined by centrifuging heparinised whole blood in a capillary tube (microhematocrit tube) at 10 000 RPM (revolution per minute) for five minutes. This separates the blood into layers. Then with a special ruler, the volume of red blood cells is read and the hematocrit is determined. This manual method is considered to be the reference method for most authors even if it takes time in clinical practice. Studies have shown that spun hematocrit gives values approx. 1.5-3.0 % too high due to plasma trapped in the red blood cells layer.

2. In hematology laboratories, automatic cell count analyzers measuring multiple parameters are the most commonly used. The hematocrit is determined indirectly from the average size and number of red blood cells, using the coulter impedance principle (Coulter 1956). The whole blood sample is diluted automatically with an isotonic solution prior to analysis and the coulter principle is applied to count and size the various cells that make up whole blood. This principle states that particles pulled through an orifice, in presence of an electric current, produce a change in impedance that is proportional to the size of the particle traversing the orifice.

3. Blood gas analyzers determine hematocrit by a conductivity measurement which is corrected for the concentrations of conducting ions (mostly sodium) in the sample. Due to the presence of ions in the plasma phase, blood is conductive. The cells present in blood are generally non-conductive, therefore a measurement of the conductivity of blood is inversely proportional to the number and size of erythrocytes present in the blood. This measurement, therefore, can be related to the volume % of red cells or hematocrit of a blood sample. The electrolyte, protein, and osmotic concentrations in a whole blood sample will affect the hematocrit measurement as explain in the Chapter I. This method can underestimate hematocrit values as corrected algorithms used constant based on healthy persons.

4. Hematocrit can also be measured by ultrasound using the BVM sensor included in dialysis machine (explained in section 3.3.2 of this Chapter)

5.2.2. Our *in vitro* comparison

In our *in vitro* study, hematocrit is measured by conductivity method (ABL), by centrifugation (Sigma) and by optical method (Crit-Line).
As hematocrit is determined at the beginning of the dialysis session (t=0) by ABL and Sigma, a first comparison has been made between the two corresponding methods. Then another hematocrit comparison is made between ABL and Crit-Line (at same sampling time), since hematocrit by ABL is determined for each blood samples at various time.

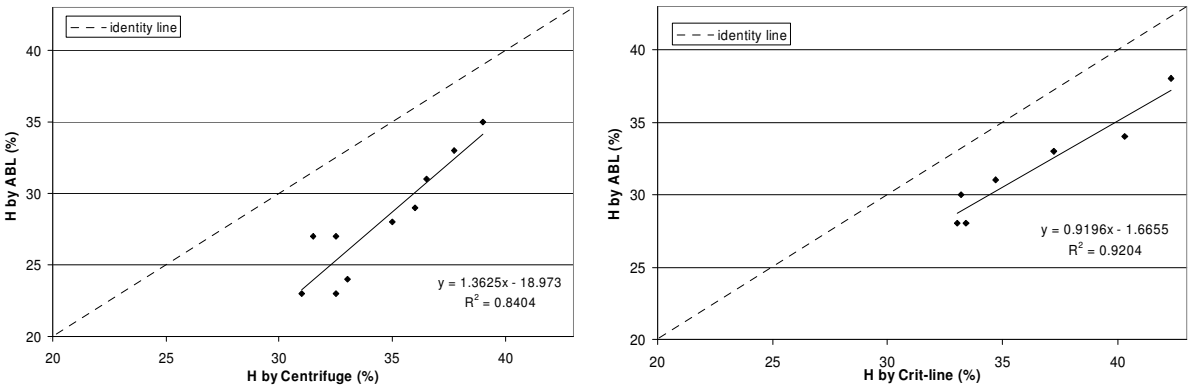

Figures II. 10 *In vitro* hematocrit comparisons between ABL and Centrifuge and between ABL and Crit-Line

Figure II.10 shows that ABL underestimates hematocrit as compared to hematocrit underestimations by Sigma and Crit-Line. These results can be explained by the reasons detailed above but also by the fact that bovine blood is analysed on devices normally used for human blood.

Student t-test applied for hematocrit between ABL and centrifuge and between ABL and Crit-line gives differences statistically significance with $p< 0.05$.

To calculate blood concentration from plasma concentration, we have decided to use hematocrit given by ABL.

5.2.3. Our *in vivo* comparison

In our *in vivo* study, hematocrit is measured by conductivity method (ABL), and by ultrasound method (BVM) on human blood during the 23 *in vivo* dialysis sessions.

Figure II.11 gives the comparison of these two techniques.

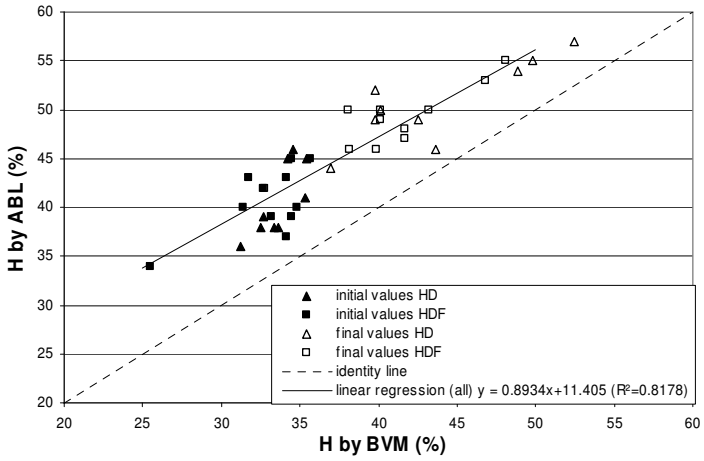

Figure II. 11 Hematocrit comparisons between ABL and BVM for the 23 *in vivo* dialysis sessions. Initial values are taken at the beginning of the dialysis session and final values at the end. The linear regression is given without distinctions between initial and final values and without distinctions between HD and HDF mode

It can be seen that hematocrit measured by ABL is overestimated compared to hematocrit measured by BVM. This difference is due to the two various methods for hematocrit monitoring.
The conductivity measured by ABL is affected by electrolyte, protein, and osmotic concentrations. These parameters based on healthy persons are introduced in an equation to calculate the hematocrit.
Nevertheless the two devices measure a higher hematocrit at the end of the dialysis session (240 minutes) than at the beginning. This observation confirms the hemoconcentration at the end of the dialysis session. Mean ± SD initial hematocrit is 33.26 ± 2.25 % for BVM and 40.65 ± 3.45 % for ABL whereas final hematocrit is 42.24 ± 4.85 % for BVM and 49.6 ± 3.9 % for ABL.
The FMC 5008 manufacturer claims that the accuracy of the BVM is about 2.9 % for a hematocrit between 20% and 55%. Our data suggest a mean difference between BVM and ABL of 7.4 ± 2.5 %.
Student t-test applied for initial or final hematocrit between BVM and ABL gives differences statistically significant as $p< 0.05$. Student t-test applied for BVM or ABL hematocrit between HD and HDF sessions gives $p> 0.05$ which means that there are no differences in hematocrit between HD and HDF initial and final values for one technique (BVM or ABL).

5.2.4. Hematocrit monitoring in literature

Steuer et al. (1993) have compared the hematocrit measured by Crit-Line and centrifuge on 15 dialysis treatment. The bland-Altman revealed that the 95% confidence interval is ± 2.32%
The BVM has been evaluated by Johner et al. (1998). They have compared the relative blood volume obtained by the BVM and by the reference methods, involving calculation of relative blood volume from serial measurements of hemoglobin. They found a very good agreement between the two methods. They also compared hematocrit value derived indirectly by BVM with the centrifuge method and this comparison revealed a mean deviation in H of -0.5% and SD of 2.9 %.

6. Conclusions

This chapter has presented the *in vitro* and the *in vivo* protocol by the description of the tests and their operating conditions. The devices (blood gas analyzer, chemistry analyzer, sensors in dialysis machine, hematocrit device, pressures sensors and microcentrifuge) have been discussed in details in order to allow a better understanding of the results. The repeatability of acid-base parameters for the *in vitro* tests is very good when using the same blood under the same experimental conditions. The analysis of the inlet dialysis fluid for the *in vitro* and *in vivo* tests by our blood gas analyzer (ABL) shows that the standard deviation and the coefficient of variations are very low between tests and between dialysis machines. This important result confirms the consistency of our data and the confidence about the dialysis fluid composition delivered by dialysis machines. Our investigation of measurements reveals that, very different results can be obtained to measure the same parameter, especially for hematocrit, when using different methods. We have made the choice to use bicarbonate concentration and hematocrit measurements from ABL device because this method is rapid, widely spread and available at the patient's bedside.

Chapter III *In vitro* study: kinetic modeling and experimental results

Résumé du Chapitre III

Dans un premier temps, ce chapitre aborde la présentation et la validation du modèle cinétique. Ce modèle est appliqué aux essais *in vitro* et permet d'obtenir la variation de la concentration d'un soluté (ici le bicarbonate et l'urée) au cours d'une séance de dialyse.

Le système modélisé se compose du patient, du circuit extracorporel d'hémodialyse (les pompes et les lignes) et de l'hémodialyseur. Les équations de bilan de masse global et spécifique à un soluté sont appliquées au patient qui est représenté par un seul compartiment (la poche de sang bovin). L'hémodialyseur est représenté par un modèle local développé par Legallais et al. (2000). Ce modèle prédit les performances de l'hémodialyseur fondées sur la géométrie de l'hémodialyseur, les conditions opératoires, et les propriétés de transport à travers les membranes de l'hémodialyseur (diffusion et convection) et a été modifié et utilisé selon nos spécifications.

Le modèle cinétique prend en compte un certain nombre de paramètres qui sont déterminés dans ce chapitre : les conditions initiales, les conditions opératoires des essais *in vitro*, les paramètres physiques relevés dans la littérature et les paramètres déduits du modèle local (concentration de sortie de l'hémodialyseur). Par ailleurs, le coefficient d'ultrafiltration (Qf) a été vérifié en utilisant la concentration des protéines totales, et le coefficient de perméabilité membranaire (Pm) a été calculé en utilisant les mesures de pression. Le modèle est enfin validé en utilisant les résultats expérimentaux *in vitro* : on a observé un bon accord entre les résultats expérimentaux et les résultats du modèle avec une petite différence qui reste inférieure à l'erreur de mesure.

Dans un second temps, ce chapitre aborde l'étude des mesures de pressions du sang et du dialysat à l'entrée et à la sortie de l'hémodialyseur : dans certains essais *in vitro*, on a obtenu une augmentation de la pression sanguine à l'entrée de l'hémodialyseur. Une analyse mathématique simplifiée est alors proposée pour expliquer cette augmentation. On a montré que l'utilisation de capteurs de pressions pouvait aider à détecter la présence de fibres bouchées qui peuvent considérablement réduire les performances de l'hémodialyseur.

This chapter presents the kinetic modeling of the extracorporeal circuit applied on the *in vitro* experiments. The extracorporeal circuit is composed of the blood tank ('*in vitro*' patient), the pumps and the hemodialyzer. The aim is the modeling of solute plasma concentration time variations in *in vitro* tests. Another section is dedicated to the determination of the model parameters. Then, the kinetic model is validated using the *in vitro* tests and a sensitivity analysis is presented.
Finally, in the last section of this chapter, we report experimental time variations of blood and dialysis fluid pressure measurement. The mathematical analysis of these variations could lead to useful tools for analysing blood clotting during dialysis sessions.

1. Description of the kinetic modeling

In order to investigate the efficiency of hemodialysis, a kinetic model, incorporating mass transport inside the hemodialyzer has been set-up to describe the entire '*in vitro*' patient-hemodialyzer system. Kinetics describe the variation with time of solutes mass. Such model may consist of a single pool, two pools or even more compartments. Each compartment is characterised by an internal solute concentration (C) and a volume (V). Different transport processes can change the solute concentration and volume: input and output, and solute generation and/or elimination.

As seen in the literature model overview of Chapter I, solutes kinetic models often use many constant parameters to characterise transport between compartments. Based on the analysis of these methods, we propose to adopt an alternative strategy based on two choices:

(1) Our first choice is to reduce the number of constant parameters by reducing the number of patient's compartments. The '*in vitro*' patient is thus represented by a single compartment and the equations for the model have been derived from mass balance on the complete extra-corporeal circuit.

(2) Our second choice is to use a local approach to represent the hemodialyzer: local transfers between blood and dialysis fluid inside hemodialyzer using the Legallais et al. (2000) model, also called 'local' model. Instead of using clearance or dialysance (given the efficiency of the hemodialyzer as seen in chapter I) to describe transfers inside the hemodialyzer, this choice has been done, first because electrolytes dialysances are mostly unknown (for example for bicarbonate, some values can be found in the literature, but are dependant of the hemodialyzer and dialysis machine parameters) and secondly, because transfers are more precisely represented using a local model based on hemodialyzer geometry, membrane transport and operating conditions.

This model could also be of help for physicians but also dialysis therapy engineers to compare various HDF strategies such as pre dilution, post dilution or mixed mode or various hemodialyzers as alternative methods to animal or patients experimentations.

The online hemodiafiltration with postdilution (HDF) extracorporeal circuit is represented in Figure III.1. The hemodialysis (HD) case is obtained in the absence of reinjection flow rate (Qr = 0). The '*in vitro*' patient is represented by a one-compartment where the analysed solute is characterised by its concentration (Cb) and its distribution volume (Vb). This compartment is the sum of all body fluids containing the substance and in the case of *in vitro* experiments represents the blood bag.

The circuit describes the entire patient-hemodialyzer system. In our *in vitro* experiments, the patient is represented by a 2L blood tank.

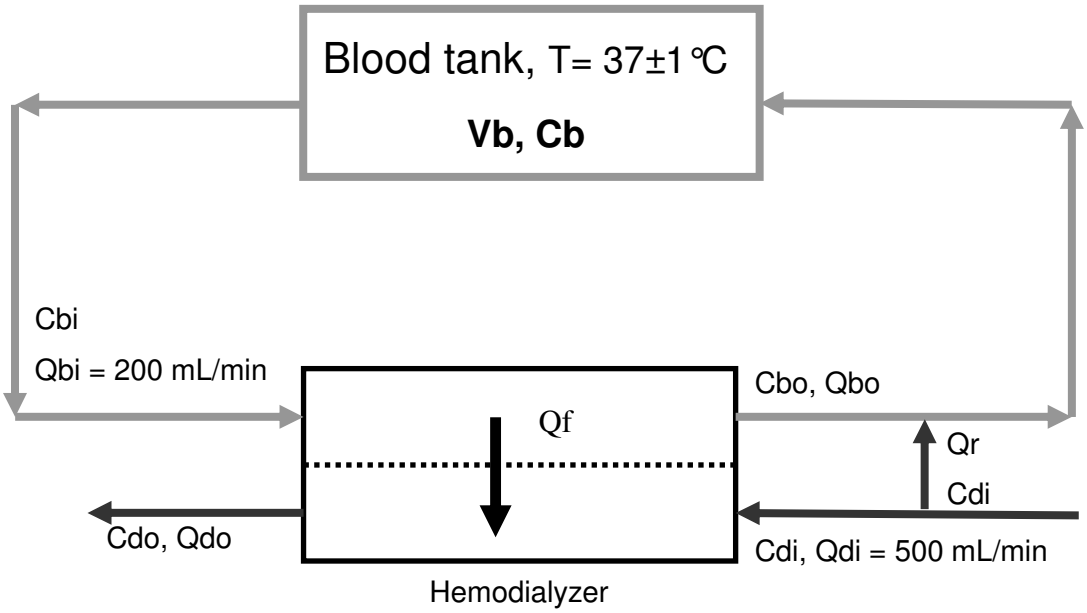

Figure III. 1 Schematic of one compartment model for the 'patient', extracorporeal circuit and hemodialyzer in HDF with postdilution

The following concentrations have to be considered:

- inlet blood concentration Cbi of a solute: concentration of the solute within the body and in the arterial line between the body and the inlet of the hemodialyzer
- outlet blood concentration Cbo of a solute: concentration of the solute in the venous line between the hemodialyzer outlet and the vascular access
- inlet dialysis fluid concentration Cdi of a solute: delivered by the dialysis machine
- outlet dialysate concentration Cdo of a solute

The following flow rates have to be considered:

- weight loss rate Qw
- reinjection flow rate Qr (Qr = 0 in HD)
- ultrafiltration flow rate Qf: Qf = Qw in HD and Qf = Qw + Qr in HDF
- inlet blood flow rate Qbi: blood flow rate at the hemodialyzer inlet (programmed by the dialysis machine)
- outlet blood flow rate Qbo: blood flow rate at the hemodialyzer outlet. Qbo = Qbi - Qf
- inlet dialysis fluid flow rate Qdi: dialysis fluid flow rate at the hemodialyzer inlet (programmed by the dialysis machine)
- outlet dialysis fluid flow rate Qdo: dialysis fluid flow rate at the hemodialyzer outlet. Qdo = Qdi + Qf

Choice of representative elements

Since toxins but also electrolytes transfers are studied, the representative elements have been chosen:

- Urea for waste solute (low molecular weight)
- Bicarbonate for electrolytes and acid-base balance

These solutes are chosen because of their similar molecular weight, 60 and 61 Da respectively. Moreover in HD and HDF their transfers are in opposite direction, from blood to dialysate for urea, and from dialysate to blood for HCO_3^-. However urea is only present in blood whereas bicarbonate is contained both in blood and dialysis fluid.

Urea is also chosen because urea removal remains a valuable parameter with impact on patient survival. Urea is widely used as a marker of adequate dialysis by many clinicians. As urea is normally eliminated by the native kidneys, the efficiency of a hemodialyzer and of the dialysis session are generally characterized by its urea clearance.

2. Mass balance equations

2.1. Mass balance of the *in vitro* "patient"

2.1.1. Assumptions

The kinetic modeling has been developed under the following assumptions:

- The single 'patient' compartment represents the blood volume of the blood bag
- Transfers of solute between plasma and red blood cells have been described by K, the partition coefficient (Chapter I, Equation I.26) is supposed constant during dialysis session
- Solute generation and elimination have not been taken into account
- Chemical reactions have not been taken into account
- Mass balance law is applied: accumulation = input to system – output to system
- Cdi of a solute (bicarbonate) is constant during dialysis session
- Qw, Qr, Qbi and Qdi are constant during dialysis session

2.1.2. Equations

According to Figure III.1 the specific mass balance applied to a solute in blood in the total extracorporeal circuit writes, if Vb denotes the total patient blood volume:

$$\frac{dVbCb}{dt} = QboCbo + QrCdi - QbiCbi \qquad \textbf{III. 1}$$

The global mass balance of extracorporeal circuit is written using the constant blood density along dialysis time and the hypothesis of the ideal volumes (volume conservation):

$$\frac{dVb}{dt} = -Qbi + Qbo + Qr = -Qf + Qr = -Qw \qquad \textbf{III. 2}$$

leading to

$$Vb = -Qw \times t + Vbin \qquad \textbf{III. 3}$$

Where Vbin is the 'patient' initial blood volume. Since during our *in vitro* tests, no weight loss rate has been applied (Qw = 0), therefore Vb stays constant and Equation III.3 becomes Vb = Vbin.

Using Equations III.1 and III.2, and the relation between plasma and blood concentration (given in Chapter I, Equation I.26), Equation III.1 becomes

$$Vbin \times (1 - Hi + HiK) \frac{dCpi}{dt} =$$

$$QboCpo \times (1 - Ho + HoK) + QrCdi - (Qbi) \times Cpi \times (1 - Hi + HiK) \quad \textbf{III. 4}$$

with

$$Ho = Hi \frac{Qbi}{Qbo} = Hi \frac{Qbi}{Qbi - Qf} \quad \textbf{III. 5}$$

Where Ho and Hi are hematocrit at the hemodialyzer inlet and outlet, respectively. As Qw = 0, Hi and Ho are constant over time.

By solving Equation III.4, we will obtain Cpi (inlet plasma hemodialyzer concentration and concentration within the body) variations with time. Plasma concentration is taken instead of blood concentration as analysis method always determines solute concentration in plasma.

2.1.3. Solving procedure

To solve Equation III.4, we need to know Vbin, Hi, Qw, K, Cpo, Qr, Cdi, Qbi. Among these parameters there are:

- Initial conditions: Vbin, Hi and Cpin, the initial plasma solute concentration. These initial conditions are known from the *in vitro* experiments.
- Operating conditions: Qbi, Cdi, Qr and Qw. These parameters are known as they are set in the dialysis machine at the beginning of the *in vitro* tests.
- Physical parameter: K. This parameter is unknown but it has been determined using the literature data.
- Cpo, the outlet hemodialyzer solute plasma concentration. This parameter is unknown but it has been determined using the local model of the hemodialyzer (Legallais et al. 2000).

The following diagram describes the procedure for solving Equation III.4.

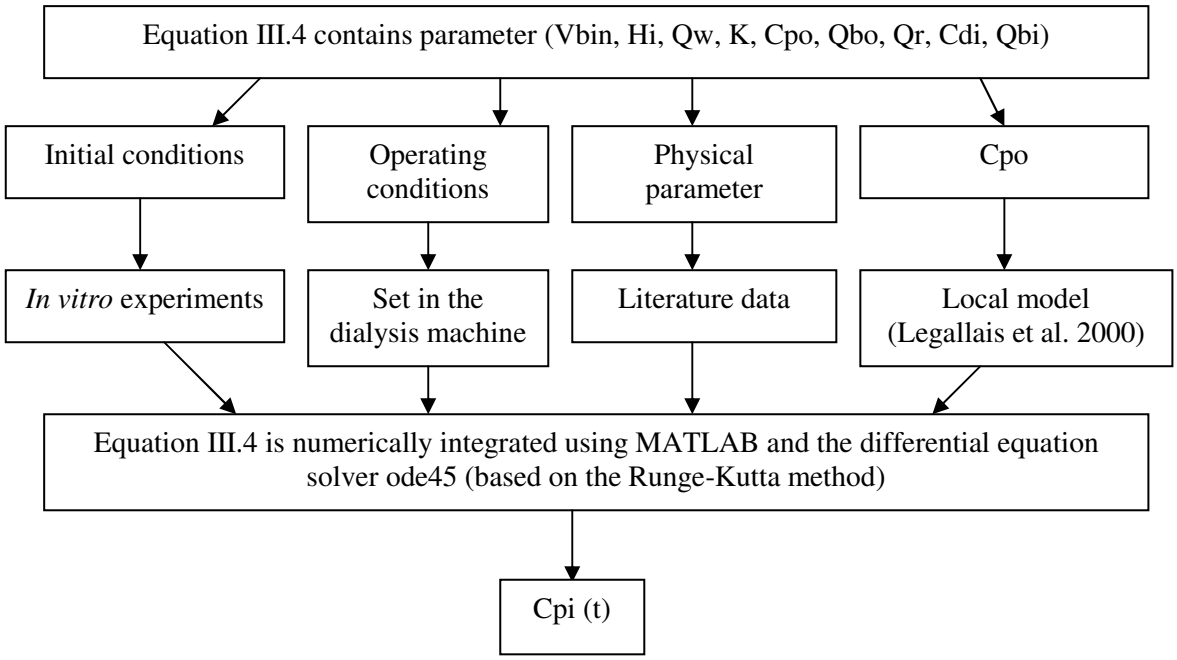

Figure III. 2 Schematic representation of parameters determination of the kinetic modeling to obtain Cpi(t)

Physical parameter: Partition coefficient K

The partition coefficient (K) is defined by the ratio of the solute concentration in the RBC by the solute concentration in plasma, as seen in Chapter I and depends on the molecule size. According to Colton, (1970) all molecules larger than sucrose (343 D) are not present into RBC: for example, K = 0 for vitamin B12 and for β2m. In literature, we have found various values for HCO_3^- partition coefficient, but all are between 0.4 and 0.6. For example, Wieth et al. (1982) reported a value of 0.4.

In our study, as only urea and bicarbonate are considered, their partition coefficients are taken as 0.86 (Colton and Lowrie 1983) and 0.57 (Pellet 1977), respectively.

2.2. Modeling of the hemodialyzer: local model

2.2.1. Assumptions and description

- Assumptions of the Legallais et al. model are given in Chapter 1.
- Membrane permeability (Pm) and free diffusivity in water (D) are the same for urea and bicarbonate
- Sieving coefficient for urea and bicarbonate are taken equal to 1

The Legallais et al. one-dimensional model predicts the performance of hemodialyzers based on its geometry, membrane characteristics and the actual operating conditions.

The model accounts for solute transport across the membrane by both a diffusive and convective mechanism for various kinds of fluids: water, plasma, dextran solution and blood. The model

computes concentration, flow rate and pressure profiles in both blood and dialysate compartment of a hemodialyzer.

The model is based on conservation equations (continuity equations, mass balance of permeating species, mass balance for rejected species and momentum conservation) and boundary conditions. All equations are presented in Annexe A in the paper of Legallais et al. (2000).

Figure III.3 shows the Legallais et al. model parameters.

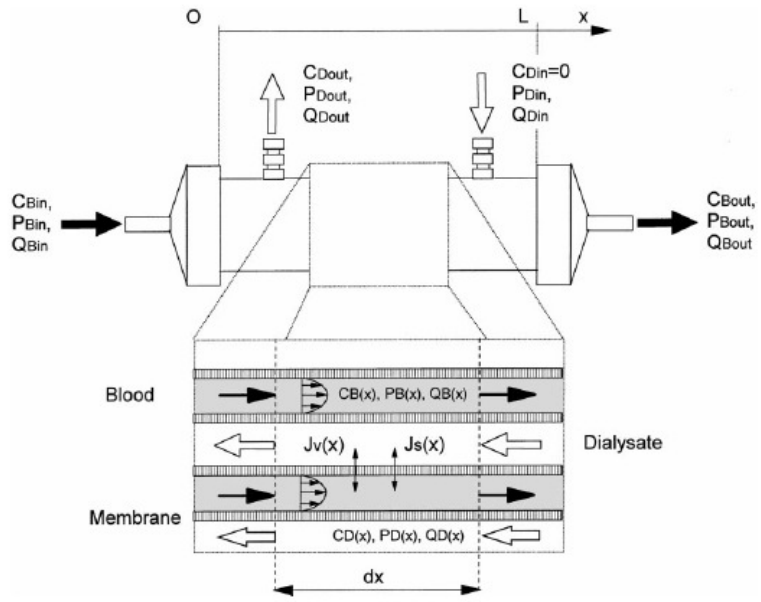

Figure III. 3 Hemodialyzer schematic representation for the one-dimensional Legallais et al. model

L is the length of the hemodialyzer. Js and Jv, the permeable solute filtration flux and the water filtration flux, respectively have been expressed according to mathematical relations found in the literature (Blatt et al. 1969, Zydney 1993 and Villaroel et al. 1977). Blood and plasma viscosity has been assumed to depend on the protein concentration according to Pallone et al. equation and oncotic pressure is expressed according to Landis and Pappenheimer's semi-empirical correlation.

The Legallais et al. model has first been developed for toxins which are not present in the dialysis fluid (Cdin = 0). The flow chart (Figure III.4) describes the procedure for diffusive and convective mass transport of the model.

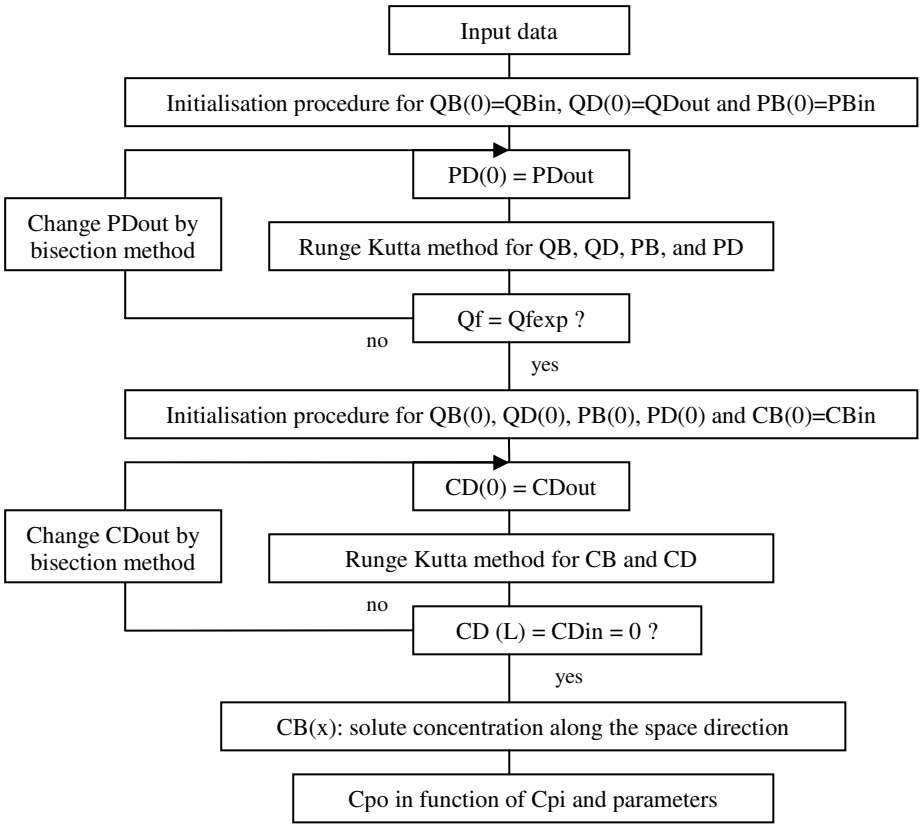

Figure III. 4 General flow chart of the model for diffusive and convective transport. Two-step numerical code was written to integrate the equations toghether with the boundary condations using the 4th order Runge Kutta procedure.

Even if the local model is developed for blood concentration, only plasma concentration is considered. Our aim is to obtain the Cpo concentration in function if the initial and operating parameters and in function of the geometry of hemodialyzer.

2.2.2. Adaptation of the local model

As we want to study electrolyte (bicarbonate) kinetics (bicarbonate is present in the dialysis fluid), the local model has been modified by introducing a concentration at hemodialyzer inlet in dialysis fluid side ($CDin \neq 0$) in order to use it for bicarbonate at any inlet dialysis fluid HCO_3^- concentration.

2.2.3. Input data

Boundary conditions, hemodialyzer geometry, solutes data and blood parameters are adapted to our specifications.

The boundary conditions are:

Boundary conditions	Values
Cbi (inlet blood concentration) for x = 0	Adapted to experimental tests conditions
Cdi (inlet dialysis fluid concentration) for x = L	0 for toxins; 26.8, 30 or 39 mmol/L for bicarbonate (measured values)
Qbi (inlet blood flow rate) for x = 0	200 mL/min
Qdi (inlet dialysate flow rate) for x = L	500 mL/min
Pbi (inlet blood pressure) for x = 0	300 mmHg
Qf = Qr (reinjection flow rate)	0, 30 or 50 mL/min
TProt (Total inlet protein concentration) for x = 0	60 g/L

Table III. 1 Local model boundary conditions

The parameters of the hemodialyzer geometry, the solutes data and blood characteristics are:

Parameters	Values
HEMODIALYSEUR GEOMETRY for FX40	
L (fibre length) including potting	25.5 cm
La (active fibre length)	22.5 cm
d (internal fibre diameter)	185 µm
e (fibre thickness)	35 µm
N (fibres number)	4 588 (average)
Casing diameter	2.3 cm
Lp (hydraulic membrane permeability)	34 mL/h/mmHg/m²
SOLUTES DATA: physical parameters	
D (free diffusivity in water)	1.81 10^{-5} cm²/s (same for urea and bicarbonate)
Pm (membrane permeability)	34 10^{-2} cm/min (same for urea and bicarbonate)
K (partition coefficient)	0.86 (urea) 0.57 (HCO_3^-)
BLOOD	
Hi (hematocrit)	28, 33 or 29 % (adapted to experimental tests conditions)
Inlet oncotic pressure	20 mmHg

Table III. 2 Local model parameters. Hemodialyzer geometry for FX40 are obtained from manufacturer data

The manufacturer specifications used for the adaptation of Pm (for FX40) are given for urea clearance in HD mode at Qf = 0 mL/min: CL = 170 mL/min. (Under specifications: H = 32%, total protein concentration = 6 g/L, Qd = 500 mL/min, temperature = 37°C and Qb = 200 mL/min).

Pm (membrane permeability) has been adjusted in order to obtain a calculated clearance of 170 mL/min in HD mode with manufacturer specifications.

3. Parameters determination

This section presents the used parameters for the implementation of the kinetic modeling presented in Figure III.2.

First the initial conditions and operating conditions of the *in vitro* tests are given. In the second section, as Qr and Qw are set on the dialysis machine and that Qf = Qw + Qr and Qbo = Qbi – Qf, Qf, the ultrafiltration rate is verified using the total protein concentration of the *in vitro* tests.

In a 3rd section, Lp the hydraulic membrane permeability (local model parameters) has been obtained from the *in vitro* tests.

The 4th section contains the Cpo determination (for bicarbonate and urea) using the local model.

3.1. Initial conditions and operating conditions

The three following tables sum up the bovine blood characteristics between before (predialysis) and after (postdialysis) one hour dialysis session. Each table corresponds to one HCO_3^- dialysis fluid concentration (28 mmol/L, 32 mmol/L or 40 mmol/L).

Data of three last lines (urea, TProt, and kHCO_3^- concentrations) are obtained by Konelab; the other data are obtained by ABL.

TESTS	Pre	Postdialysis	Pre	Postdialysis	Pre	Postdialysis
	28 HD		28 HDF 30		28 HDF 50	
Mode	HD		HDF		HDF	
Qb (mL/min)	200		200		200	
Qf (mL/min)	0		30		50	
pH	**7.28**	**7.14**	**7.32**	**7.06**	**7.26**	**7.13**
pCO_2 (mmHg)	**46**	**88**	**38**	**91**	**38**	**79**
pO_2 (mmHg)	**28**	**34**	**34**	**48**	**29**	**43**
H (%)	29	32	27	27	27	29
Na (mmol/L)	142	140	143	140	149	142
K (mmol/L)	4.2	3.1	4.5	3.2	4.2	3.2
Ca (mmol/L)	0.869	1.68	0.88	1.72	0.81	1.73
Cl (mmol/L)	113	111	116	112	121	111
HCO_3^- (P) (mmol/L)	**20.9**	**26.1**	**19**	**24.6**	**16.5**	**25.2**
tCO_2 (P) (mmol/L)	22.3	28.8	20.2	27.4	17.7	27.6
tCO_2 (B) (mmol/L)	20.3	26.3	18.4	25.4	16.2	25.3
tO_2 (B) (mmol/L)	2.6	2.9	3.3	3.5	2.5	3.7
sO_2 (%)	44.8	46.5	61	63.6	46.5	61.4
tHb (g/dl)	9.4	10.4	8.7	8.7	8.7	9.4
Urea (mmol/L)	5.77	0.28	5.94	0.19	5.93	0.1
TProt (g/L)	59.5	58.68	56.4	55.24	65.06	68.31
k HCO_3^- (mmol/L)	20.09	26.22	20.26	27.34	18.49	22.94

Table III. 3 Pre/postdialysis blood characteristics for HCO_3^- dialysis fluid concentration (Cdi_b) of 28 mmol/L. k HCO_3^- represents the HCO_3^- concentration given by Konelab. Bold data represent the acid-base parameters (pH, pCO_2, pO_2 and HCO_3^- plasma concentration)

TESTS	Pre	Postdialysis	Pre	Postdialysis	Pre	Postdialysis
	32 HD		32 HDF30		32 HDF50	
Mode	HD		HDF		HDF	
Qb (mL/min)	200		200		200	
Qf (mL/min)	0		30		50	
pH	**7.17**	**7.12**	**7.26**	**7.14**	**7.24**	**7.15**
pCO_2 (mmHg)	**35**	**91**	**45**	**88**	**46**	**85**
pO_2 (mmHg)	**53**	**58**	**30**	**40**	**35**	**45**
H (%)	34	35	34	36	31	33
Na (mmol/L)	146	139	143	139	147	140
K (mmol/L)	4.9	2.9	5.2	2.9	4.1	2.9
Ca (mmol/L)	0.89	1.55	0.95	1.6	0.97	1.62
Cl (mmol/L)	113	106	111	106	119	108
HCO_3^- (P) (mmol/L)	**12.3**	**28.3**	**19.5**	**28.7**	**19**	**28.4**
tCO_2 (P) (mmol/L)	13.4	31.1	20.9	31.4	20.4	31
tCO_2 (B) (mmol/L)	12	27.7	18.7	27.9	18.4	28
tO_2 (B) (mmol/L)	5.4	5.8	3.3	4.5	3.6	4.4
sO_2 (%)	78.3	77.6	48.2	56.7	57.1	65.1
tHb (g/dl)	11	12	11	12.7	10	10.7
Urea (mmol/L)	na	na	5.3	0	5.71	0.18
TProt (g/L)	65.66	66.69	57.42	56.9	55.07	54.8
k HCO_3^- (mmol/L)	14.59	30.5	19.73	28.99	20.02	27.54

Table III. 4 Pre/postdialysis blood characteristics for HCO_3^- dialysis fluid concentration (Cdi_b) of 32 mmol/L (na = not available). Bold data represent the acid-base parameters (pH, pCO_2, pO_2 and HCO_3^- plasma concentration)

TESTS	Pre	Postdialysis	Pre	Postdialysis	Pre	Postdialysis
	40 HD		40 HDF30		40 HDF50	
Mode	HD		HDF		HDF	
Qb (mL/min)	200		200		200	
Qf (mL/min)	0		30		50	
pH	**7.28**	**7.26**	**7.28**	**7.28**	**7.31**	**7.25**
pCO_2 (mmHg)	**48**	**89**	**38**	**82**	**47**	**90**
pO_2 (mmHg)	**26**	**34**	**35**	**38**	**21**	**42**
H (%)	28	31	24	27	33	36
Na (mmol/L)	146	136	148	137	141	136
K (mmol/L)	4	2.6	4.2	2.6	4.9	2.6
Ca (mmol/L)	0.85	1.38	0.83	1.38	0.95	1.39
Cl (mmol/L)	117	98	121	100	113	100
HCO_3^- (P) (mmol/L)	**21.8**	**38.6**	**17.3**	**37.3**	**23**	**38.1**
tCO_2 (P) (mmol/L)	23.3	41.3	18.5	39.8	24.4	40.9
tCO_2 (B) (mmol/L)	21.3	37.3	17	36.3	21.9	36.1
tO_2 (B) (mmol/L)	2.3	3.3	2.9	3.4	2	4.8
sO_2 (%)	40	49.1	60.3	61.8	29.7	65.9
tHb (g/dl)	9	10	7.7	8.7	10.7	11.7
Urea (mmol/L)	3.89	0.02	7.19	0.29	4.28	0.34
TProt (g/L)	60.51	62.52	53.81	54.73	64.62	65.87
k HCO_3^- (mmol/L)	21.62	35.46	18.21	38.41	20.23	35.12

Table III. 5 Pre/postdialysis blood characteristics for HCO_3^- dialysis fluid concentration (Cdi_b) of 40 mmol/L. Bold data represent the acid-base parameters (pH, pCO_2, pO_2 and HCO_3^- plasma concentration)

The initial HCO_3^- concentration in 32 HD test (Table III.4) is unrealistically low, but it is interesting to observe that the final value is similar to those in other tests. Another difference with real conditions is the pCO_2 final values for all tests: this is due to the fact that the CO_2 transfer from the dialysate described by Sombolos et al. (2005) is confined into 2L of blood, which is much less than *in vivo* under breathing conditions: even if dialysis fluid pCO_2 has a mean value of 60/70 mmHg (Chapter II, Table II.10), the blood pCO_2 reaches 80/90 mmHg, because CO_2 can not be eliminated and accumulates during the dialysis session in the plastic bag (blood circulates in closed loop).
The pO_2 also increases postdialysis, but less than pCO_2, due to the smaller pO_2 in dialysate.
Unlike the *in vivo* case, the pH does not increase as expected after *in vitro* dialysis, due to absence of breathing, which would have reduced CO_2.

Electrolytes concentrations (Ca^{2+}, K^+, Cl^-, Na^+ and HCO_3^-) have reached a final concentration corresponding to their theoretical concentrations programmed by the dialysis machine (Table II.10). Differences in HCO_3^- concentration between Konelab and ABL have been investigated in the last section of Chapter II. As expected, urea final concentration is close to zero, as urea has been eliminated from blood.

3.2. Estimation of real ultrafiltration flow rate using total protein concentration measurements

Total protein concentrations (TProt) in plasma have been measured with Konelab in each sample collected during *in vitro* tests. In bovine blood, normal values for TProt are between 60 and 80 g/L.
In this section, we propose to use these data to determine if a protein loss appears during *in vitro* tests and secondly to control the ultrafiltration flow rate (Qf).

3.2.1. Protein loss

In hemodialysis the dialysate protein loss is negligible and is often ignored (the sieving coefficient for albumin is 0.001). While in peritoneal dialysis, protein loss can be important and constitutes one of the parameters of the peritoneal dialysis adequacy. The usual way to determine the protein loss in a dialysis session is to collect the overall dialysate (after the passage of dialysis fluid inside the hemodialyzer) over 1 hour or more of the dialysis session and then to measure the total protein concentration in the total dialysate volume.

Total protein concentrations have been measured in each blood samples but also in dialysate at the same sampling time than blood samples. Values of total protein concentrations in dialysate are found around 0.4 g/L and are below the validity limit of Konelab for total protein concentration (1g/L).

Therefore it is difficult to take into account these concentrations in dialysate and the calculation of protein loss has been made using total protein concentrations in plasma.

Figure III.5 represents the TProt plasma concentration Cpo in function of TProt plasma concentration Cpi for three HD tests and three HDF 30 tests.

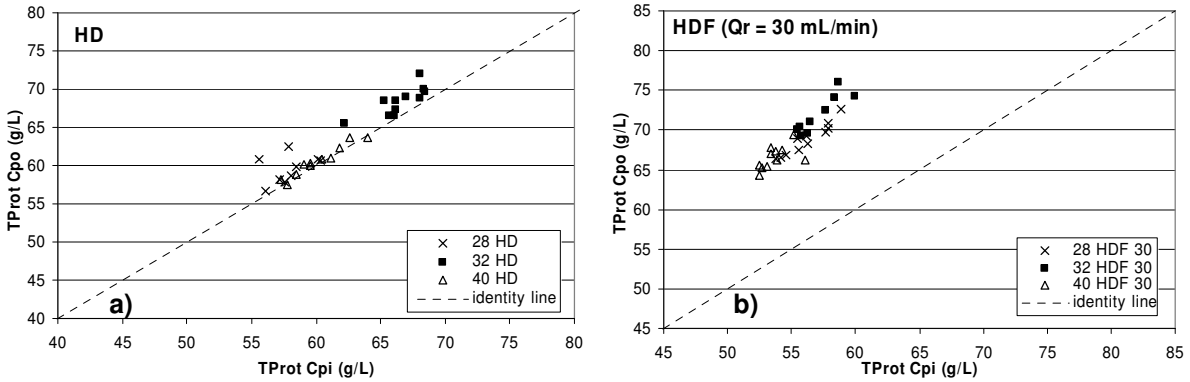

Figure III. 5 TProt plasma concentration Cpo (at the hemodialyzer outlet before the reinjection site) in function of Cpi (at the inlet) for HD tests (a)) and for HDF 30 tests (b))

These results show that ultrafiltration has an influence on plasma protein concentration: in HD tests, TProt Cpo values are little higher than TProt Cpi (+1.6%). In HDF tests, due to ultrafiltration of water (Qr = Qf = 30 mL/min), TProt Cpo values are much higher than TProt Cpi (+24.2%). Due to ultrafiltration, plasma water volume decreases between the inlet and outlet of the hemodialyzer, and total protein concentration in plasma is higher after its passage inside the hemodialyzer as seen in Figure III.5. These results show the hemoconcentration.

Moreover we can observe that values are consistent even if bovine blood is different between tests.

Using initial and final (at 60 minutes) plasma TProt concentrations, hematocrit and volumes (bovine blood bags are weighted before and after the dialysis sessions), initial and final plasma TProt masses have been determined. The mean difference between final and initial plasma TProt mass is about 3g. This calculation could not be made accurately due to many uncertainties in the experimental set-up: reinjection volume, blood volume lost in blood line due to pressure measurements, bovine blood quality…

In the literature, Santoro et al. (2004) have found in hemofiltration an albumin loss lower than 3 g per treatment (found in the ultrafiltrate) and they concluded that convective treatments that use high exchange volume can be performed with no risk of significant albumin loss. Combarnous et al. (2002) have investigated the kinetics of albumin in online predilution HDF. They found that the total albumin loss was 3.99 ± 1.81 g with no significant decrease of the albumin concentration in plasma during predilution HDF sessions.

Our result using the *in vitro* tests shows that we can consider that no protein loss occurs.

3.2.2. Effect of ultrafiltration on total protein concentration

The aim of this section is to compare the theoretical rate of total protein concentrations (TProt) in plasma on both sides the hemodialyzer to the measured one (using *in vitro* tests).

Mean experimental total protein concentration ratio PR_{exp} have been calculated using around 10 plasma samples for each *in vitro* test:

$$PR_{\exp} = \frac{Cpo}{Cpi} \quad \textbf{III. 6}$$

Where Cpi is the TProt plasma concentration at the hemodialyzer inlet and Cpo its concentration at the outlet.

This ratio has been compared to a theoretical one (PR_{theo}) using mass balance equation applied for TProt:

$$Qbi \times Cbi + Qdi \times Cdi = Qdo \times Cdo + Qbo \times Cbo \quad \textbf{III. 7}$$

For TProt, since dialysis fluid does not contain protein, Cdi = 0 and Cdo = 0 (as no protein loss has been found).

Therefore Equation III.7 becomes:

$$Qbi \times Cbi = Qbo \times Cbo \quad \textbf{III. 8}$$

Using relations between blood concentration and plasma concentration applied for protein (Equation I.26), Equation III.8 becomes:

$$Qbi \times Cpi(1 - Hi) = Qbo \times Cpo(1 - Ho) \quad \textbf{III. 9}$$

Where Hi is the decimal hematocrit of the inlet sample (hemodialyzer inlet) and Ho, the outlet hematocrit.

Therefore PR_{exp} should be equal to PR_{theo}, with

$$PR_{theo} = \frac{Qbi \times (1 - Hi)}{(Qbi - Qf) \times (1 - Ho)} \quad \textbf{III. 10}$$

Hi is used from experimental values from ABL and Ho is estimated using red blood cell conservation:

$$Qbi \times Hi = Qbo \times Ho \quad \textbf{III. 11}$$

Therefore PR_{theo} becomes:

$$PR_{theo} = \frac{Qbi \times (1 - Hi)}{(Qbi - Qf) \times (1 - Hi \times {Qbi}/{Qbo})} \quad \textbf{III. 12}$$

PR_{exp} and PR_{theo} (Equations III.6 and 12) have been calculated for each of the 17 *in vitro* tests and results are given in Tables III.6/7/8.

- In HD mode, Qbi = Qbo = 200 mL/min, Qf = 0

	32 HD	32 HD (2)	40 HD	40 HD (2)	28 HD	28 HD (2)	**Mean ± SD**
PR_{exp}	1.03 ± 0.018	1.013 ± 0.015	1.002 ±0.02	1.013 ±0.016	1.022 ± 0.029	1.008 ± 0.008	1.015 ± 0.009
PR_{theo}	1	1	1	1	1	1	1

Table III. 6 Comparison between PR_{exp} and PR_{theo} for HD tests. (2) means tests using the 2nd blood bag (same animal blood and same dialysis machine parameters). Coefficient of variation on TProt is 0.61% (see Table II. 9)

- In HDF mode, Qbo = Qbi – Qf with Qf = Qr (Qw = 0)

Qb = 200 mL/min and Qf = 30 mL/min

	32 HDF 30	32 HDF 30 (2)	40 HDF 30	40 HDF 30 (2)	28 HDF 30	28 HDF 30 (2)	**Mean ± SD**
PR_{exp}	1.258 ± 0.019	1.263 ± 0.024	1.24 ± 0.025	1.244 ± 0.015	1.226 ± 0.0104	1.236 ± 0.055	1.245 ± 0.014
PR_{theo}	1.29	1.29	1.24	1.24	1.26	1.24	1.26 ± 0.025

Table III. 7 Comparison between PR_{exp} and PR_{theo} for HDF tests (Qr = 30 mL/min)

Qb = 200 mL/min and Qf = 50 mL/min

	32 HDF 50	32 HDF 50 (2)	40 HDF 50	40 HDF 50 (2)	28 HDF 50	**Mean ± SD**
PR_{exp}	1.55 ± 0.018	1.541 ± 0.062	1.556 ± 0.055	1.530 ± 0.038	1.491 ± 0.102	1.534 ± 0.026
PR_{theo}	1.56	1.56	1.58	1.61	1.51	1.564 ± 0.036

Table III. 8 Comparison between PR_{exp} and PR_{theo} for HDF tests (Qr = 50 mL/min)

It can be seen that experimental and theoretical values PR_{exp} and PR_{theo} are very close. The small differences can be attributed to errors in pump flow rate or in hematocrit measurements.

Even if the ultrafiltration flow rate (Qf) is not directly set on the dialysis machine but comes from Qw and Qr (set on the dialysis machine) since Qf = Qw + Qr, this section shows that we have verified the real ultrafiltration flow rate (Qf) using the total protein concentration measurements.

3.3. Determination of Cpo by the local model

3.3.1. Use of the local model to determine Cpo for bicarbonate

For HCO_3^- solute, mathematical relations which link Cpi and Cpo, depend on the inlet dialysis fluid HCO_3^- concentration Cdi_b and on the dialysis mode. For consistency with experimental tests, measured mean values of Cdi_b have been taken rather than theoretical values.

From Figure III.6 and using an inlet dialysis fluid HCO_3^- concentration of 30 mmol/L, it seems that a linear relation exits between Cpi and Cpo for each dialysis mode (Qf = 0, 30 and 50 mL/min).

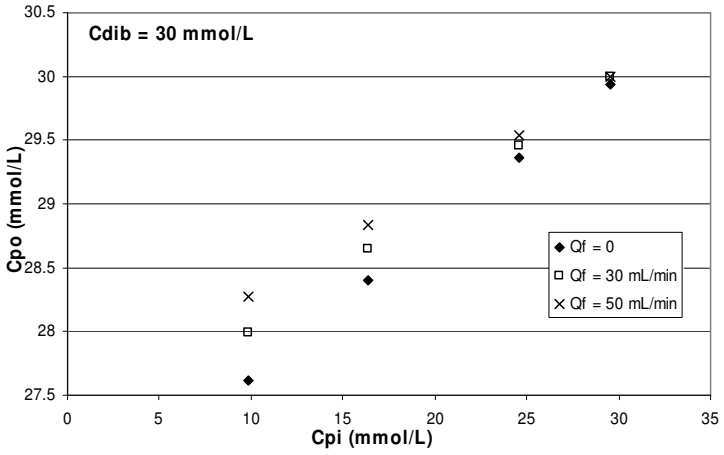

Figure III. 6 Relation between Cpi and Cpo for inlet dialysis fluid HCO_3^- concentration of 30 mmol/L and for 3 various ultrafiltration rate. The points are obtained from the modified local model for FX 40 and initial conditions of the *in vitro* tests

Table III.9 lists the relations between Cpi and Cpo determined with the local model. The boundary conditions have been detailed in Table III.1 (Qbi = 200 mL/min and Qdi = 500 mL/min) and the geometry hemodialyzer parameters in Table III.2 (FX40 hemodialyzer).

Measured Cdi_b (mmol/L)	HD with Qf = 0 (mmol/L)	HDF with Qf = Qr = 30 mL/min (mmol/L)	HDF with Qf = Qr = 50 mL/min (mmol/L)
26.8	Cpo = 0.1256 Cpi + 23.44	Cpo = 0.1075 Cpi + 23.92	Cpo = 0.0935 Cpi + 24.30
30	Cpo = 0.1179 Cpi +26.46	Cpo = 0.1015 Cpi +26.99	Cpo = 0.0871Cpi + 27.41
39.2	Cpo = 0.1248 Cpi + 34.14	Cpo = 0.1059 Cpi + 34.87	Cpo = 0.0919 Cpi + 35.42

Table III. 9 Relations between HCO_3^- Cpi and Cpo for Qb=200 mL/min andQd= 500 mL/min and Qw=0.

Using an Excel tool (Analysis ToolPak) allowing determination of linear empirical relations between many parameters, we find a simplified generalisation (Equation III.13) of these 9 equations presented in Table III.10.

$$Cpo = 0.11\ Cpi + 0.008\ Qf + 0.88\ Cdi_b + 0.26 \qquad \textbf{III. 13}$$

Where Cpi, Cpo and Cdi_b are in mmol/L and Qf in mL/min.

This equation is only available for the boundary conditions presented in Table III.1 and the geometric parameters in Table III.2.

As expected, it can be seen that Cpo HCO_3^- concentrations are always higher than Cpi concentrations.

The ultrafiltration rate Qf and the constant (0.26) have a very small influence on Cpo concentration and could be neglected on Equation III.13. Therefore we can propose the following simplified empirical linear relation:

$$Cpo = 0.11\ Cpi + 0.88\ Cdi_b \qquad \textbf{III. 14}$$

Therefore we can observe that Cdi_b concentration accounts for 88 % in the outlet hemodialyzer HCO_3^- concentration and Cpi for 11%. This relation is then used to solve Equation III.4 of the kinetic model.

3.4.2. Use of the local model to determine Cpo for urea

As inlet dialysis fluid does not contain any toxins, initial urea concentration in dialysis fluid is always zero. For urea concentration, the local model developed by Legallais et al. has been used without any modifications.

Table III.10 gives the 3 linear relations between Cpi and Cpo determined with the local model. As for bicarbonate, these linear relations depend on the boundary conditions and geometric hemodialyzer parameters presented in Tables III.1 and III.2.

HD with Qf = 0 (mmol/L)	HDF with Qf = Qr = 30 mL/min (mmol /L)	HDF with Qf = Qr = 50 mL/min (mmol /L)
Cpo = 0.1495 Cpi	Cpo = 0.1318 Cpi	Cpo = 0.1178 Cpi

Table III. 10 Linear mathematical relations between urea Cpi and Cpo for Qb = 200 mL/min andQd = 500 mL/min and Qw = 0

As expected urea Cpo concentration is smaller than Cpi concentration as dialysis eliminates urea.

It can be seen that outlet Cpo urea concentration is smaller with high ultrafiltration rate. This means that the hemodialyzer lose more urea at higher ultrafiltration but the difference is small: for Cpi of 15 mmol/L, Cpo is 12% smaller in HDF 30 (HDF with Qr = 30 mL/min) mode and 21% in HDF 50 than in HD mode.

4. Validation of the kinetic model

In what follows, we have investigated the time variation of urea and bicarbonate by experimental *in vitro* tests and using the kinetic model.

4.1. Dialysis equivalent time

The test duration is 1 hour for all *in vitro* tests.

A normal duration t for a dialysis run is such that the ratio CL*t/V is around 1.4. Assuming a urea clearance of around CL = 160 mL/min (see Figure D.3 in Annexe D) and V = 2 L (because the bovine blood bags contain about 2L of blood), gives a time duration t of 17 min.

In the following, the equivalent dialysis duration is defined for 20 minutes, and final parameters (partial pressure, pH or concentrations) are taken at 20 minutes.

4.2. Urea time variation

Figure III.7 gives the urea plasma time variation for 2 tests in HD and in HDF 30 mode (with a reinjection rate of 30 mL/min). The figure compares the urea concentration calculated with the kinetic model and obtained by *in vitro* tests. Urea concentration time variations for other *in vitro* tests (under other initial conditions) are similar.

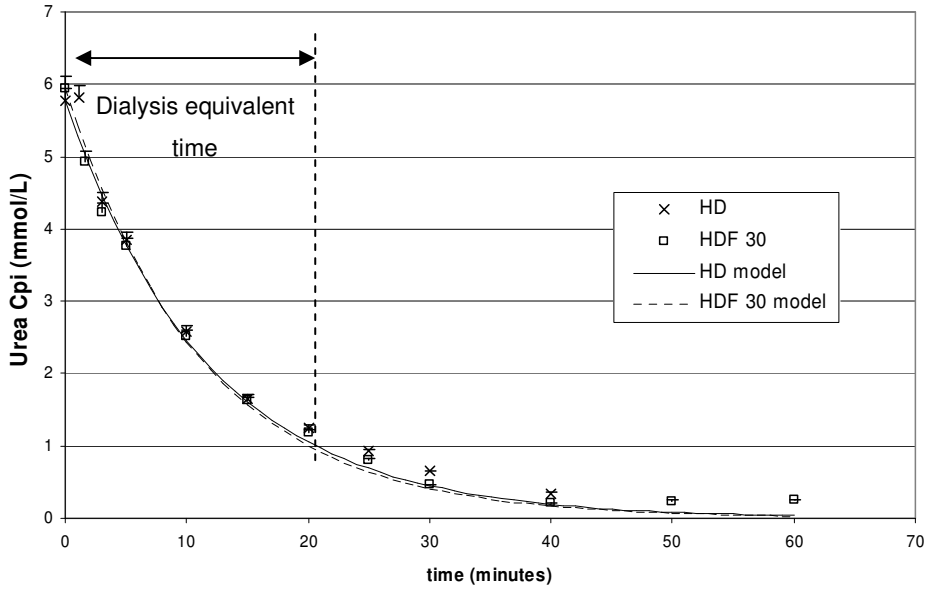

Figure III. 7 Urea plasma concentration in tests 28 HD and 28 HDF30: experimental and theoretical comparison

It can be seen that urea plasma concentration reaches zero at 60 minutes. This means that the urea has been totally eliminated by dialysis. Little differences between dialysis modes can be observed: the

urea elimination is slightly quicker in HDF 30 than in HD for experimental and theoretical data. At 20 minutes, data calculated from kinetic model show differences of 9% between HD and HDF 30 mode, with an initial concentration difference of 3%.

Agreements between theoretical and experimental data are very good for the two tests until 20 minutes, and then the model slightly underestimates the urea concentration. This may be due to the analysis method: the detection limit of Konelab for urea is 1.1 mmol/L. After 20 minutes, as the urea concentration becomes smaller than 1.1 mmol/L, the value can not be reliable.

4.3. Influence of dialysis fluid HCO_3^- concentration on bicarbonate time variation

The effect of various inlet dialysis fluid HCO_3^- concentrations (Cdi_b) on plasma HCO_3^- concentration time variation (Cpi in hemodialyzer inlet samples) has been studied. The tests have been labelled by their theoretical values of Cdi_b 28, 32 and 40 mmol/L.

Figure III.8 represents the HCO_3^- concentrations time variation according to experiments and kinetic model data in HD tests.

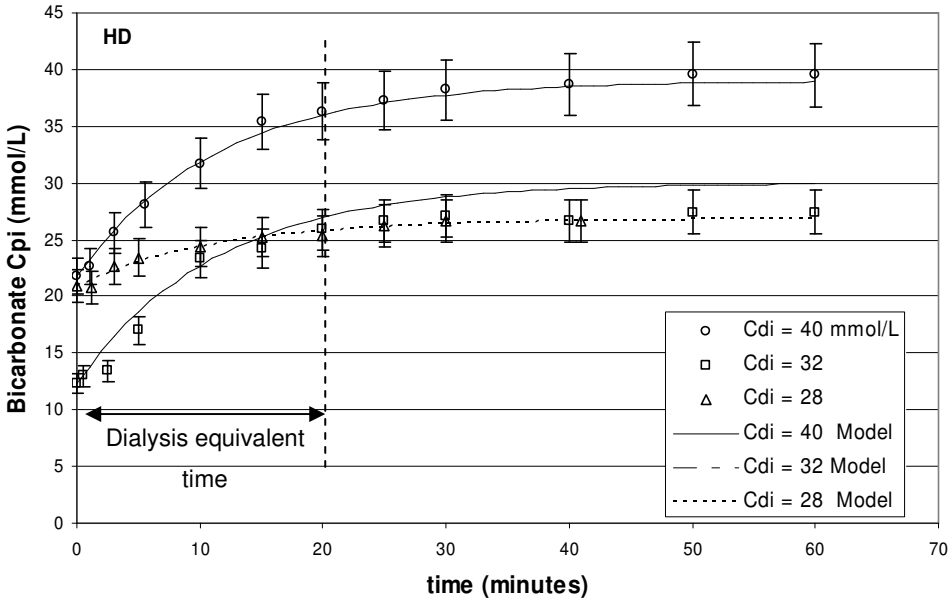

Figure III. 8 HCO_3^- plasma concentrations (Cpi) variation with time in HD tests for 3 various HCO_3^- dialysis fluid concentration (Cdib)

If we compare 28 HD and 40 HD tests with similar initial inlet plasma HCO_3^- concentration (19 mmol/L), the rise in Cpi during the test is smaller for Cdi_b = 28 mmol/L, as expected since it has the smallest difference blood-dialysis fluid concentration. However, the 32 HD test which has the smallest unrealistic initial Cpi (12.3 mmol/L) gives a HCO_3^- concentration increase comparable to that of 40 HD test.

Agreements between experimental and theoretical data are very good for 28 HD and 40 HD tests at all times, whereas for 32 HD test, the model slightly overestimates the HCO_3^- plasma concentration after 20 minutes.

Figure III.9 represents a similar comparison for the HCO_3^- concentrations time variation for experimental and theoretical data, but in postdilution HDF (with a reinjection rate Qr, of 30 mL/min).

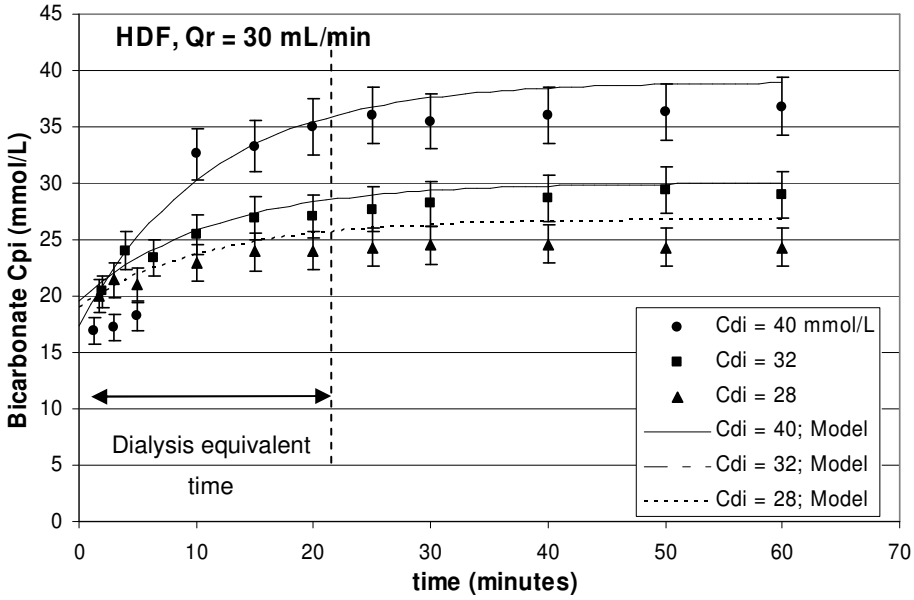

Figure III. 9 HCO_3^- plasma concentrations (Cpi) variation with time in HDF 30 tests

These tests have similar initial HCO_3^- Cpi, ranging from 17.3 and 19.5 mmol/L. It can be seen that rises in Cpi increase with values of HCO_3^- Cdi and reach equilibrium from 30/40 minutes. The kinetic model overestimates HCO_3^- Cpi for all tests, while the best fit is observed for 32 HDF 30 test.

4.4. Conclusions

Analysis of results confirms that our kinetic model is able to predict the *in vitro* intradialytic time (during dialysis session) of urea and HCO_3^- concentration with a good approximation.

It can be seen that HCO_3^- Cpi calculated by the kinetic model reaches the HCO_3^- dialysis fluid concentration, whereas the experimental HCO_3^- plasma concentration always stays slightly below. But this difference is smaller than the 7% errors deduced from experimental data, and blood gas analyzer accuracy. With urea, the kinetic model results fit well with the experimental results.

Since our *in vitro* study differs from a patient in several respects, smaller blood volume and absence of extracellular and intracellular water other than in blood as well as of O_2 transfer from the lungs, it is important to verify if and how our results differ from those of clinical studies.

We first compare variations of plasma HCO_3^- concentrations with time with those given by Pedrini et al. (2002) in their Figure 1. For a blood flow (Qbi) of 400 mL/min, a reinjection rate (Qr) of 120 mL/min and a dialysate HCO_3^- concentration of 28.9 mmol/L, these authors found, for postdilution HDF, a HCO_3^- concentration rising from 19.6 mmol/L to 24.3 after 60 min and to 26.6 after 175 min (end of run). In our test tests (Figure III.8 and III.9), with Qbi = 200 mL/min, Qr = 0, 50 and 30 mL/min plasma HCO_3^- concentration increase from around 19.5 to 28.7 mmol/L for a dialysis fluid HCO_3^- concentration of 32 mmol/L at the end of test (60 min). The mean HCO_3^- concentration rise in our tests (using dialysis fluid HCO_3^- concentration of 32 mmol/L) was 9.2 mmol /L against 7.2 for those of Pedrini et al.

Ursino et al. have also investigated HCO_3^- kinetics in HD mode using a three-compartment model and they compared it with clinical data. They reported rises in HCO_3^- from 20 to 25 mmol/L in one patient (for a HCO_3^- Cdi_b of 30 mmol/L) and from 20 to 29 mmol/L in another (for a HCO_3^- Cdi_b of 39 mmol/L). They also found higher final plasma HCO_3^- concentration when the dialysis fluid has a higher HCO_3^- concentration. They found a mean deviation between model prediction and *in vivo* data of 1.46 mmol/L and they concluded to an acceptable agreement. We obtained similar rises in HCO_3^- concentration from initial concentrations of about 20 mmol/L.

These data also show that our choice of scaled down blood volumes (2L), blood flow rates (Qb = 200 mL/min) and membrane (FX40) area leads to HCO_3^- and urea time variations close to that observed *in vivo* with of course, a reduced time scale of about 20 minutes for a dialysis run.

Nevertheless the small overestimation by the kinetic modeling for HCO_3^- (and not for urea) observed in Figures III.8 and III.9 can be due to the fact that the local model does not take into account physiological considerations but only diffusive and convective HCO_3^- amount transported between blood and dialysis fluid. For HCO_3^-, chemical reactions or other unknown phenomena can appear leading to a diminution of the HCO_3^- amount measured. We are going to discuss these phenomena in the 5th section of Chapter V.

5. Sensitivity analysis

A sensitivity analysis on kinetic modeling has been performed to identify input parameters which have an effect on the result using FX40 (0.6 m², FMC) hemodialyzer characteristics. As an input parameter can be subject to many sources of uncertainty, for example errors of measurement, or absence of information, it is necessary to understand how the model reacts with input parameter changes. This sensitivity analysis is based on a method developed by Ursino et al. (2000).

The output parameter (or result) taken to test the sensitivity analysis of the kinetic modeling is the hemodialyzer inlet Cpi plasma concentration at 20 minutes of the dialysis session for urea and bicarbonate. Using basal values (Table III.11), the reference output parameter is found to be 29.1 mmol/L for Cpi HCO_3^- concentration and 0.92 mmol/L for urea concentration at 20 minutes of dialysis session.

Each input parameters change is accomplished by maintaining all the other parameters at their normal value. As input parameters, we have selected initial parameters of the kinetic modeling. The parameter variations (minimum and maximum values) are written in Table III.11.

Basal values for initial volume, blood flow or ultrafiltration flow rate can be considered too small when compared to physiological values. Since the aim is to validate the kinetic mathematical modeling with *in vitro* tests using plastic bags of 2L of bovine blood and small surface hemodialyzer (FX 40, 0.6m²), these basal values are selected accordingly.

Parameters	Vbin (L)	HCO_3^- Cpin (mmol/L) at t = 0	Urea Cpin (mmol/L) at t = 0	H (%)	K HCO_3^-	K Urea	Qf (mL/min)
Basal values	2	**25**	**5**	40	0.57	0.86	30
Max value	5	25	7.5	60	1	1	50
Min value	2	12.5	2.5	20	0	0	0

Parameters	Qb (mL/min)	Qd (mL/min)	TProt (g/L)
Basal values	200	500	60
Max value	200	800	78
Min value	100	300	42

Table III. 11 Basal parameters and their variations for the sensibility analysis. K is the partition coefficient and Cpin the initial plasma concentration

After a variation of a single input data, the output data (plasma concentration of urea and bicarbonate at 20 minutes of the dialysis session) is compared to the reference output data. Values in Table III.12

represent these minimum and maximum percentage changes in the output data compared to the reference output data.

		Vbin	Cpin HCO_3^-/urea	H	K HCO_3^-/urea	Qf	Qb	Qd	TProt
HCO_3^- output	Max (%)	5.5		-0.2	0.3	-0.1		-0.1	-0.2
	Min (%)		7.7	0.2	-0.3	0.2	4	0.2	-0.2
Urea output	Max (%)	-176.4	-50	2.7	-3.3	4.4		3.8	0.2
	Min (%)		50	-2.0	15.6	-7.4	-111.4	-7.8	0.2

Table III. 12 Sensitivity analysis on the effect of initial parameters changes. Negative percentage represents higher output concentration than the reference concentration

Sensitivity on urea concentration

It can be seen that a change in blood volume has a high influence on urea elimination: instead of reaching 0.92 mmol/L at 20 minutes, urea concentration decreases from 5 to 2.5 mmol/L by increasing the blood volume from 2 to 5L.

The smallest influences on urea concentration are seen for the total protein concentration (0.2%) and hematocrit (about 2%).

Decreasing the blood flow rate, the dialysis flow rate or the ultrafiltration flow rate leads to worse urea elimination by hemodialysis: the increase of urea concentration is 7.4 % for Qf, 111.4% for Qb, and 7.8% for Qd.

Urea partition coefficient K = 0 has a higher influence (15.6%) on urea concentration than K = 1 (-3.3%). K = 0 means that urea is not present into the RBC, whereas K = 1 means that there is the same concentration of urea in plasma and in RBC. This results show that if we consider that urea is only present in plasma, the urea elimination has be improved of 15.6% since there will be no influence of the urea in RBC.

Sensitivity on HCO_3^- concentration

Results indicate that total protein concentration, hematocrit, dialysis fluid and ultrafiltration flow rate and partition coefficient K have a negligible effect on the HCO_3^- concentration at 20 minutes.

It can be seen that an increase in blood volume (from 2 to 5L) has an impact on the final HCO_3^- concentration: instead to be 29.1 mmol/L after 20 minutes, final HCO_3^- concentration will only reach 27.5 mmol/L. As expected, increasing the blood volume also increases the dialysis time necessary for HCO_3^- to reach equilibrium in blood compartment. Decreasing the blood flow rate or the initial HCO_3^- plasma concentration leads to a smaller gain of HCO_3^- by the patient.

6. *In vitro* blood pressures analysis

Arterial and venous pressures are always continuously monitored by dialysis machine during dialysis session. The arterial pressure corresponds to the negative pressure created by the blood pump and venous pressure measured the resistance of the blood returning to the patient via the venous needle. If the arterial or venous pressure alarm is activated (bubble trap or needle clotted or vascular access problem…), this means that there is an abnormal condition that needs to be corrected (Kallenbach et al. 2005). Therefore indications in blood pressures are very important in dialysis as they give details about the management of the dialysis session.

Local blood pressures are recorded in dialysis lines for some tests using 4 pressures transducers linked to an acquisition module (presented in details in Chapter II). These 4 local blood pressures measurements give indications of the blood pressure at the hemodialyzer inlet and outlet both in blood and dialysis fluid lines.
This section presents the *in vitro* experimental pressure time variations for two cases: one dialysis session represents a standard dialysis session pressures time variation whereas another dialysis session presents pressure time variation when problems occur. In the 2nd part, a modeling approach has been investigated in order to understand the cause of these phenomena.

6.1. *In vitro* experimental pressures time variations

Pbi and Pbo correspond to inlet hemodialyzer and outlet hemodialyzer blood pressures measurements respectively; Pdi and Pdo to inlet and outlet dialysis fluid pressures measurements respectively.
Hematocrit (H) has been measured using the blood gas analyzer (ABL).

6.1.1. Pressure time variations

In a standard dialysis session, Figure III.10 represents an example of these pressure measurements recorded during dialysis session using 40 HDF 30 *in vitro* test.

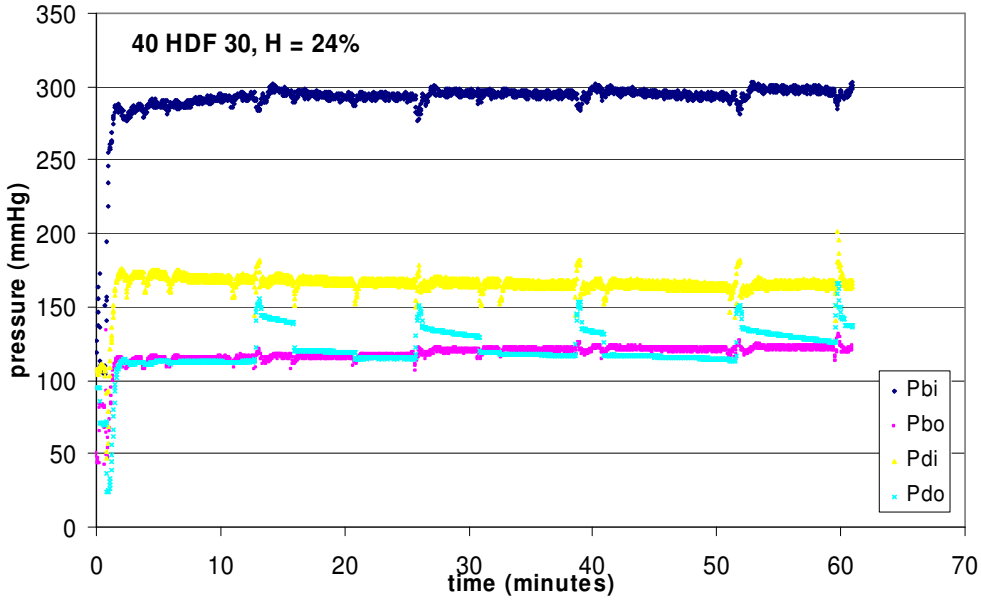

Figure III. 10 Time variation pressures in 40 HDF 30 test. Errors on pressure measurements are ± 7 mmHg (manufacturer book of pressure sensors)

For this test, it can be seen that measured pressures stay stable along the 60 minutes of the dialysis session.

Mean values of the 4 pressures are: Pbi = 295 mmHg, Pbo = 115 mmHg, Pdi = 165 mmHg and Pdo = 115 mmHg. The error measurements on pressure are ± 7 mmHg (manufacturer book). The real TMP (Transmembrane Pressure) is calculated, according to the Equation I.13 (Chapter I, with $\Delta\Pi = 0$) and is TMP = 65 mmHg.

The small variations in pressures correspond to the time where samples are taken from the blood and dialysis fluid compartment.

In some cases, we have observed some problems in pressure time variations as seen for example, using 28 HD test, where Pbi increases during dialysis session (Figure III.11).

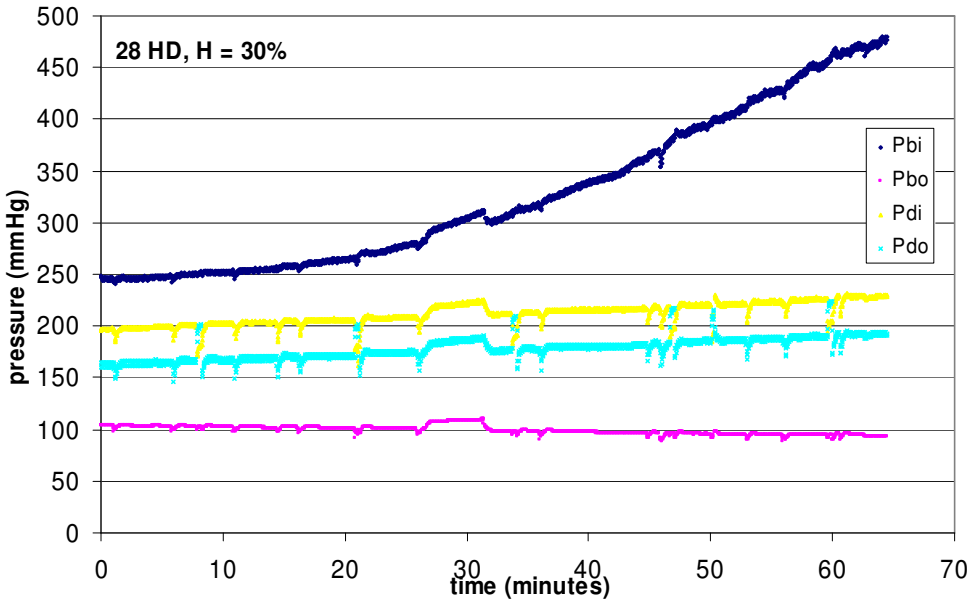

Figure III. 11 Time variation pressures in 28 HD test. Errors on pressure measurements are ± 7 mmHg (manufacturer book)

For this test, TMP is calculated at the beginning of the dialysis session (mean during the 5 first minutes where TMP is stable) from Pbi = 245 mmHg, Pbo = 110 mmHg, Pdi = 200 mmHg and Pdo = 160 mmHg. The TMP is closed to zero (TMP = -5 mmHg). As in HD test, there is no ultrafiltration rate (Qp = 0 and Qr = 0), it is correct to find a TPM close to zero.

At 40 minutes of the dialysis session, Pbi measurements are found around 340 mmHg (39% increase) whereas the three other pressure measurements (Pbo, Pdi, and Pdo) are stable. If we calculate a new value for the TMP at 40 minutes, it will be different from zero although the test is in HD mode. Based on TMP calculations, a positive Qf is expected, however this phenomenon does not occurred since the blood bag weight remains constant. Membrane plugging should be suspected.

6.1.2. Blood pressure drop

Blood pressure drop is calculated as the difference between inlet and outlet hemodialyzer blood pressure: $\Delta P = Pbi - Pbo$.

For 3 tests (40 HDF 50, 40 HDF 30 and 40 HD), blood pressure drops (ΔP) are calculated from experimental Pbi an Pbo pressures measurements and are represented as function of time on Figure III.12.

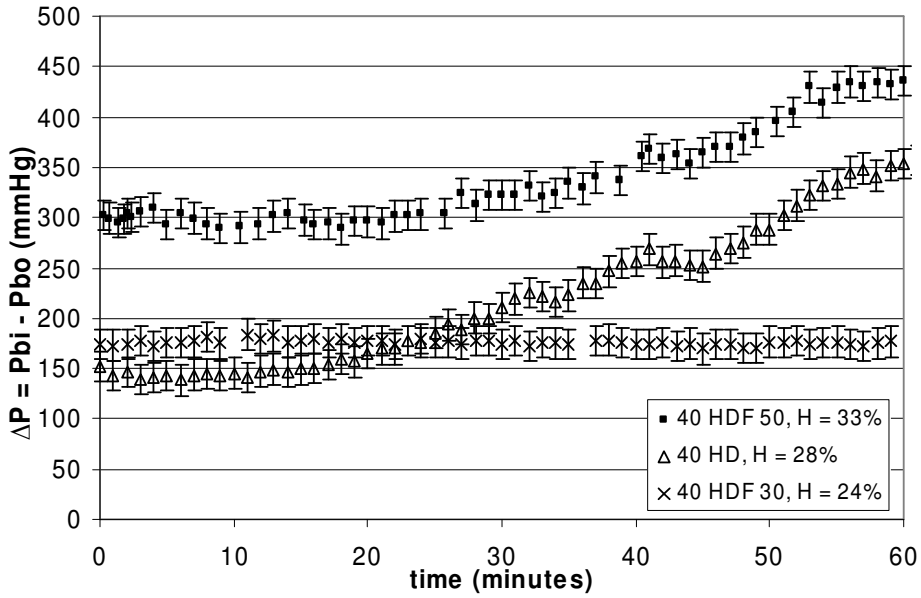

Figure III. 12 Blood pressure drop (ΔP) for 3 tests with errors bars (± 14 mmHg for ΔP). 40 HDF 50 means *in vitro* test using a HCO_3^- dialysis fluid concentration of 40 mmol/L and a reinjection flow rate of 50 mL/min

Between 0 and 10 minutes of the dialysis session, mean blood pressure drop are: 142 mmHg for 40 HD test, 174 mmHg for 40 HDF 30 test and 300 mmHg for 40 HDF 50. These values of ΔP are always higher than the value given by the manufacturer data: ΔP_{FMC} = 136 mmHg (for Qb = 200 mL/min, H = 32% and protein concentration at 60 g/L).

It can be seen that ΔP stays stable in 40 HDF 30 (as seen previously in Figure III.12) but linearly increases for 40 HDF 50 (+ 47 %) and 40 HD (+130 %) from 20/30 minutes of the dialysis session. Although hematocrit is different for the three tests, 40 HD and 40 HDF 30 tests have almost the same initial conditions whereas for 40 HDF 50 test, ΔP_0 (at t = 0) is very high. This may be due to bovine blood quality or to the differences in hematocrit or plasma protein concentrations which are (Table III.5) 60.51 g/L for 40 HD, 53.81 g/L for 40 HDF 30 and 64.62 g/L for 40 HDF 50, respectively.

The reason why the inlet blood pressure and the blood pressure drop increases during dialysis session (generally after 20/30 minutes) need to be investigated. Therefore we propose to use a modeling approach presented in the following section.

6.2. Interpretation of pressure changes

6.2.1. Model equations

As seen in Chapter 1, the pressure drop in a blood compartment can be calculated using the Hagen-Poiseuille law, assuming that blood is newtonien at this shear rate and laminar flow in a circular tube assuming a constant fluid viscosity and a constant fluid flow rate over the tube length:

Therefore the hemodialyzer blood pressure drop is given by:

$$\Delta P_{hemo} = \frac{8\mu L}{\pi r^4 N} Qb \qquad \textbf{III. 15}$$

Where μ is the blood viscosity (Pa.s), r the fibre radius (m), L the fibre length (m), Qb the blood flow rate (mL/min) and N the number of hemodialyzer fibres.

As pressures sensors have been added in blood and dialysis lines, the ΔP measured (ΔP_{meas}) is not directly equal to ΔP hemodialyzer (ΔP_{hemo}) because of lines portion (ΔP_{ext}):

$$\Delta P_{meas} = \Delta P_{ext} + \Delta P_{hemo} \qquad \textbf{III. 16}$$

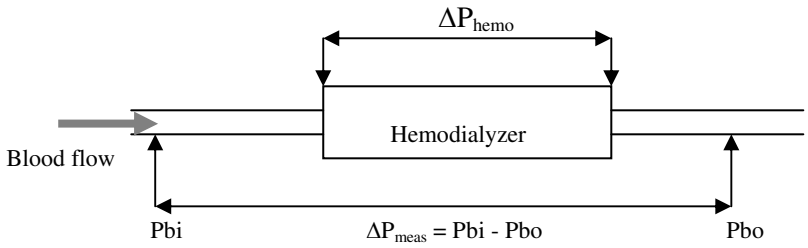

Figure III. 13 Dialysis circuit blood pressures

ΔP_{ext} can be estimated from blood lines properties (r = 5 mm and L = 20/50 cm), blood viscosity (μ = 2 /4 10^{-3} Pa.s) and blood flow rate (Qb = 200 mL/min). ΔP_{ext} is found to be between 0.04 and 0.2 mmHg. Therefore ΔP_{ext} can be neglected and ΔP_{meas} becomes

$$\Delta P_{meas} = \Delta P_{hemo} = \frac{8\mu L}{\pi r^4 N} Qb \qquad \textbf{III. 17}$$

This Hagen-Poiseuille equation applied for blood assumes a constant pressure drop over the length of the hemodialyzer during dialysis session if all parameters are supposed constant (μ, L, r, N, and Qb).

1. During HDF sessions, if we do the hypothesis that r, L, and N stay constant, therefore due to the ultrafiltration rate, Qb and μ will be affected and can contribute to a change in ΔP_{meas}.
2. During HD sessions (without ultrafiltration), if we do the hypothesis that r, L, Qb and μ stay stable over the hemodialyzer length, therefore the reason why ΔP_{meas} increases can be attributed to the decrease of N, the number of active fibres.
3. Another assumption could be that the fibre radius, r, can be reduced and lead to an increase of ΔP_{meas}. This assumption will be not described here because of its weak possibility in hemodialyser.

We propose to use the Hagen-Poiseuille law to investigate the ΔP_{meas} increase according to the two first assumptions. An example of the Hagen-Poiseuille law calculated for one *in vitro* test is also presented in Annexe B.
The theoretical number of fibres for the hemodialsyer FX40 used for the *in vitro* test is first calculated.

Theoretical number of fibres, N

Using FX40 hemodialyzer, the number of fibres N can be calculated by:

$$N = \frac{A}{2\pi \times r \times La} \qquad \textbf{III. 18}$$

Where A is the hemodialyzer surface (0.6 m²), r the fibre radius (92.5 µm), La the active fibre length (22.5 cm). The equation III.18 gives N = 4588 (± 1%).

6.2.2. Effect of ultrafiltration (increase of blood viscosity)

In this section, the effect of ultrafiltration on ΔP increase has been investigated. We have done the hypothesis that the number of fibres N stays constant (N = 4588) during dialysis session.

Due to ultrafiltration and among interest parameters to apply the Hagen-Poiseuille law, it has been seen that hematocrit, blood viscosity and total protein concentration increases along the hemodialyzer (between hemodialyzer inlet and outlet).

The total protein concentration has been studied in section 2.2 of this chapter and we have seen that even if total protein concentration increase through hemodialyzer, total protein concentration (Cpi) is not higher at the end of the dialysis session than at the beginning.

ΔP has been calculated using Hagen-Poiseuille law for 40 HD and 40 HDF 50 tests (tests where ΔP increase) by taking a mean blood flow rate (Qb) and a mean blood viscosity (mean of µim and µom) between inlet and outlet hemodialyzer. Blood viscosity has been calculated using Mockros equation (presented in Annexe B, equation B.2). Results are indicated in Table III.13.

Tests	Mean Qb (mL/min)	Hi (%)	Ho (%)	µim (Pa.s)	µom (Pa.s)	Viscosity increase	Calculated ΔP (mmHg)
40 HD	196	28	29	$2.51\ 10^{-3}$	$2.57\ 10^{-3}$	2.4%	121.85
40 HDF 50	175	33	44	$2.82\ 10^{-3}$	$3.66\ 10^{-3}$	23%	137.18

Table III. 13 40 HD and 40 HDF 50 tests characteristics for Hagen-Poiseuille law

It can be seen that the calculated values of ΔP always stay below measured values ΔP_{meas} (as seen in Figure III.12). Moreover by calculating ΔPi with values at hemodialyzer inlet (mean Qb and mean viscosity) and ΔPo at hemodialyzer outlet for 40 HDF 50 test, we obtain a decrease ΔP difference of 2.54%.

This result does not depend on the linear relationship between hematocrit and viscosity as the increase viscosity between hemodialyzer inlet and outlet will stay in the same range. This result shows that for our *in vitro* tests, the ultrafiltration has a negligible role on our ΔP measurements.

6.2.3. Effect of blocked fibres (decrease of active fibres number)

The ΔP increase can be interpreted by a decrease in the number of active (open) fibres N. In this section we do the hypothesis that blood viscosity, μ stays constant during dialysis sessions of 40 HD and 40 HDF 50 tests since the extracorporeal circuit is operated in closed loop.

At initial time (for t = 0), the initial blood pressure drop is (ΔP_0):

$$\Delta P_0 = \frac{8\mu L}{\pi r^4 N_0} Qb \qquad \textbf{III. 19}$$

Where N_0 corresponds to the initial number of hemodialyzer fibres (No = 4588).

At any time of the dialysis session, the blood pressure drop becomes a function of time (ΔP(t)):

$$\Delta P(t) = \frac{8\mu L}{\pi r^4 N(t)} Qb \qquad \textbf{III. 20}$$

Where N(t) depends on time and corresponds to the number of active fibres (where blood can circulate).

The ratio between Equations III.19 and 20 gives:

$$\frac{\Delta P(t)}{\Delta P_0} = \frac{N_0}{N(t)} \qquad \textbf{III. 21}$$

and $N(t) = N_0 \times f(t)$ **III. 22**

Where $f(t) = \frac{\Delta P_0}{\Delta P(t)}$ **III. 23**

Applying and calculating these relations to 40 HD and 40 HDF 50 tests, N(t)/No and N(t) are represented in Figures III.14.

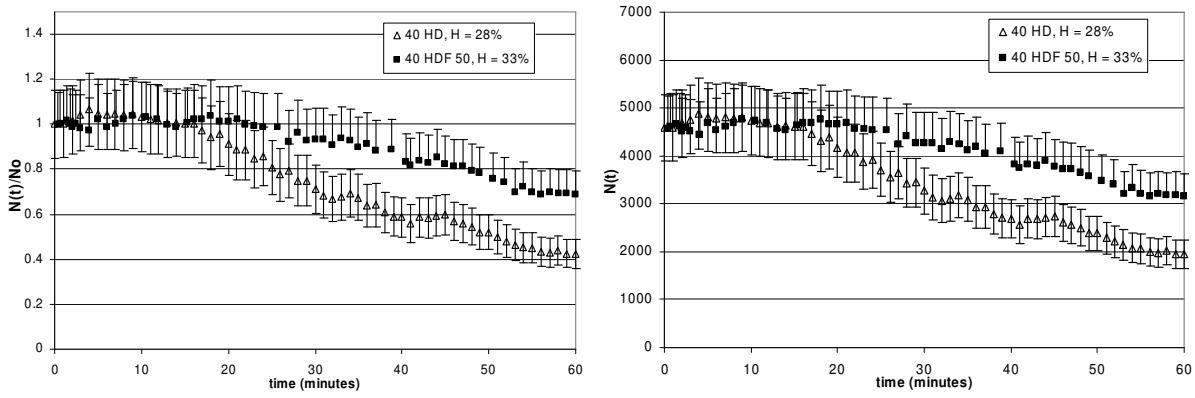

Figures III. 14 N(t) is number of available fibres during dialysis session for 40 HD and 40 HDF 50 tests. No is the initial number of fibres. Errors bars have been estimated to be 15%

It can be seen that after 15 or 20 minutes, N(t) decreases and the numbers of active fibres linearly decrease. Therefore we can also calculate the number of blocked fibres (Nb(t)):

$$Nb(t) = N_0 - N(t) \qquad \textbf{III. 24}$$

After applying Equation III.24 to 40 HD and 40 HDF 50 tests, it can be seen on Figure III.15 that Nb(t) linearly increases with time.

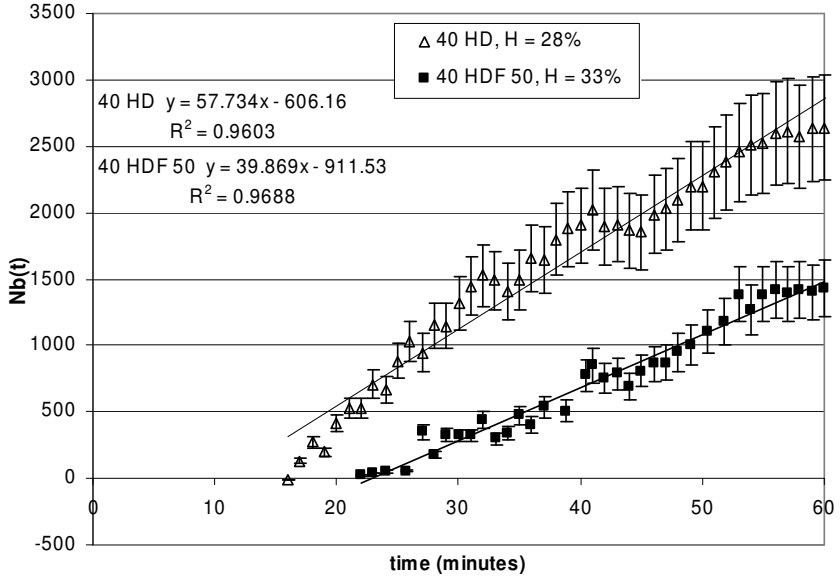

Figure III. 15 Nb(t), number of blocked fibres during dialysis session for 40 HD and 40 HDF 50 tests

At t = 20 minutes, it can be seen that around 10% of the fibres are blocked for 40 HD test and 0% for 40 HDF 50 test. This percentage linearly increases with time until 60 minutes where 54% of the fibres are blocked for 40 HD test and 33 % for 40 HDF 50 test.

6.3. Conclusions

In this section we have observed that pressure and pressure drop increase in some *in vitro* tests. We have tried to interpret these changes with the rise of blood viscosity due to the UF and with the calculation of blocked fibres. Our conclusion is that fibre clotting leads to the increase of blood pressure.

The equivalent duration of dialysis session for our *in vitro* experiments is between 20/30 minutes. Until 20 minutes we can consider that the number of active fibres stays constant and that the number of blocked fibres can be neglected. But from 20 until 60 minutes of our *in vitro* tests, the number of blocked fibres can not be neglected as it linearly increases with dialysis time.

This calculation depends on many parameters (ultrafiltration, hemodialyzer longer length, viscosity precision…) and could be improved by doing numerical simulations using for example the Legallais et al. model.

This simple analysis shows that the presence of pressure sensor between the blood pump and the hemodialyzer inlet would be of help to detect any trouble concerning blood clotting in the hemodialyzer. Potential reduction of dialysis efficiency due to the reduction of available membrane surface area could be easily implemented for the online estimation of clearance.

Urea clearance has been calculated using the local model and, and we can conclude that a decrease of the number of active fibres (due to blocked fibres) up to 20% does not have a significant impact on urea clearance (a decrease < 10%). This question has been detailed in Annexe D.

7. Conclusions

In a first part, this chapter deals with the implementation and the validation of the kinetic modeling applied to the *in vitro* tests. It has presented the comparisons of urea and bicarbonate concentrations time variations between *in vitro* tests and the kinetics model. The small overestimation by the kinetic modeling for HCO_3^- can be due to the fact that the local model does not take into account biochemical considerations but only diffusive and convective HCO_3^- transfers between blood and dialysis fluid. For HCO_3^-, chemical reactions or other unknown phenomena can lead to a diminution or generation of the HCO_3^- amount measured. We are going to discuss these phenomena in the Chapter V. We have also shown that our choice of scaled down blood volumes (2L), blood flow rates (Qb = 200 mL/min) and membrane (FX40, 0.6 m²) area leads to HCO_3^- and urea time variations close to that observed *in vivo* in the literature with a reduced time scale of about 20 minutes for a dialysis run.

In the second part, pressures in the *in vitro* extracorporeal circuit have been investigated. This simple analysis shows that the presence of pressure sensors would be helpful to detect blood clotting in the hemodialyzer.

This complete analysis has also shown its limits: the reduction of patient to his blood compartment reduces the complexity of the acid-base balance analysis. Therefore, we propose to prolong this work by the set-up of a clinical study, whose preliminary results are provided in the next chapter.

Chapter IV Clinical study: effect of HD/HDF on acid-base status

Résumé du Chapitre IV

Ce chapitre présente une méthodologie appliquée à l'étude préliminaire des résultats des essais cliniques (*in vivo*).

Après avoir réalisé une étude paramétrique *in vitro* et une modélisation des cinétiques du bicarbonate et de l'urée au cours d'une séance de dialyse (Chapitre 3), nous avons eu l'opportunité de réaliser des essais cliniques au service de néphrologie du CHU d'Amiens sous la direction du Dr Morinière. Un total de 6 patients ont été inclus et 23 séances de dialyse ont été suivies entre les mois de mai et juillet 2009.

Une première section décrit l'ensemble des 23 séances, réparties en 12 séances en HD et 11 séances en HDF postdilution. La clairance de l'urée et le pourcentage de recirculation sont détaillés. Une seconde section présente l'évaluation des paramètres acide-base (pH, pCO_2, pO_2 et la concentration en HCO_3^-) durant les séances de dialyse. Une étude statistique révèle des différences significatives entre l'état initial (au début de la séance de dialyse) et final (à 240 minutes) pour le pH et la concentration en HCO_3^-, mais aucune différence pour les gaz. De plus, cette étude ne montre aucune différence significative pour chacun de ces paramètres entre les modes HD et HDF pour les états finaux et initiaux de l'ensemble des patients. Pour le moment, nous pouvons donc conclure que la technique d'HDF ne semble pas créer de déséquilibre ionique par rapport à celle en HD. Toutefois d'autres séances et d'autres patients sont à inclure pour confirmer ces observations.

Une seconde section détaille les séances de dialyse pour un patient en particulier : les variations des paramètres acide-base au cours de ses séances de dialyse et les comparaisons des séances entre les modes HD et HDF sont analysées. Ces études révèlent que les résultats sont cohérents et reproductibles entre les séances d'un même patient et présentent des tendances intéressantes. Néanmoins, il reste quelques phénomènes difficiles à expliquer mais qui sont plutôt liés à l'état de chaque patient et à la petite taille de l'échantillon actuel.

After the *in vitro* and kinetic modeling analysis, we had the opportunity to perform an *in vivo* study to really address the question on dialysis patients. We could therefore compare the bicarbonate patient gain between online postdilution HDF and HD sessions. All acid-base balance parameters (pH, pCO_2, pO_2, HCO_3^- concentration) have been monitored during the dialysis sessions by periodically taking blood samples (as explained in Chapter II).

This chapter is dedicated to the presentation of *in vivo* results in 23 dialysis sessions for a total of 6 patients. The 6 patients' characteristics (PC, MA, SG, LC, GV and LR) have been presented in Table II.4 (Chapter II) together with the dialysis sessions operating conditions given in Table II.5.
As the clinical study has not yet completed, we present in this chapter a methodology to analyse the results. The 1st section presents the efficiency of the 23 *in vivo* dialysis sessions in terms of urea clearance and percentage of recirculation and a study case to describe the data obtained in HD sessions. In the 2nd section, acid-base parameters time variations are presented and compared between patients. In the 3rd section, HCO_3^- transfers inside the hemodialyzer have been investigated for a better understanding of transfers between blood and dialysis fluid.

1. Overview of the dialysis sessions

After listing the *in vivo* dialysis sessions characteristics, we presente a study case, GV05 patient in order to details the acid-base parameters time variation.

1.1. Dialysis sessions characteristics

The *in vivo* operating conditions are kept constant during dialysis sessions: the treatment duration is 4 hours, the blood flow rate Qb is 350 mL/min, and the dialysis fluid flow rate Qd is 500 mL/min (as seen in Table II.5). The patients are all dialysed using a FX 80 (1.8 m²) hemodialyzer.
Table IV.1 presents the 23 dialysis sessions characteristics of the 6 patients: the weight loss rate Qw, the reinjection flow rate Qr, the reinjection volume, the urea clearance given by OCM and the recirculation percentage. Mean ± SD are calculated for all sessions but also separately for the 12 HD sessions and for the 11 online postdilution HDF sessions.

Patients	Session order	HD/HDF	Qw (mL/min)	Qr (mL/min)	Qf = Qw + Qr (mL/min)	Reinjection volume (L)	Urea clearance CL (mL/min)	Recirculation (%)
PC01 HD1	1	HD	16.67		16.67		205	16
PC01 HD2	2	HD	13.33		13.33		197	12
PC01 HD3	3	HD	16.67		16.67		209	13
PC01 HDF1	4	HDF	10.83	99	109.83	22	215	12
PC01 HDF2	5	HDF	12.5	81	93.5	19.1	217	15
MA02 HD1	4	HD	13.33		13.33		194	na
MA02 HD3	5	HD	13.33		13.33		189	33
MA02 HD4	6	HD	11.25		11.25		188	13
MA02 HDF1	1	HDF	10.63	94	104.63	22.4	196	29
MA02 HDF2	2	HDF	10.43	100	110.43	22.7	na	18
MA02 HDF3	3	HDF	13.33	96	109.33	22.2	203	18
SG03 HD1	2	HD	7.5		7.5		211	11
SG03 HDF1	1	HDF	12.92	88	100.92	20.6	225	11
SG03 HDF2	3	HDF	13.33	93	106.33	21.2	227	12
LC04 HD1	1	HD	12.5		12.5		196	16
LC04 HDF1	2	HDF	8.75	102	110.75	24.1	222	15
LC04 HDF2	3	HDF	6.25	107	113.25	24.9	239	20
LC04 HDF3	4	HDF	7.92	104	111.92	24.2	237	8
GV05 HD1	1	HD	16.67		16.67		199	12
GV05 HD2	2	HD	16.25		16.25		210	11
GV05 HD3	3	HD	10		10		211	10
LR06 HD1	1	HD	13.75		13.75		201	14
LR06 HDF1	2	HDF	9.17	94	103.17	21.7	212	15
Mean ± SD **HD** (n = 11)		12	13.44 ± 2.89		13.44 ± 2.89		200.83 ± 8.35	14.64 ± 6.39
Mean ± SD **HDF** (n = 12)		11	10.55 ± 2.36	96.18 ± 7.43	106.73 ± 5.85	22.28 ± 1.69	219.3 ± 13.69	15.72 ± 5.62
Mean ± SD **All** (n = 23)		23	12.06 ± 2.98		58.06 ± 47.86		209.23 ± 14.33	15.18 ± 5.9

Table IV. 1 Weight loss rate (Qw), reinjection flow rate (Qr), ultrafiltration flow rate (Qf), urea clearance (mean 5008 data) and recirculation percentage (mean 5008 data) for 23 dialysis sessions. na = not available

The second column (session order) gives the chronological order of sessions for each patient.

Mean weight loss rate (Qw) for all sessions is 13.06 ± 2.93 mL/min. Postdilution HDF sessions have been performed with a reinjection flow rate Qr = 96.18 ± 7.43 mL/min and a reinjection volume of 22.28 ± 1.69 L.

The mean ultrafiltration flow rate (Qf) which is the sum of the reinjection and weight loss rates, is 13.44 mL/min for HD sessions and 106.73 mL/min for HDF sessions.

The effects of the dialysis mode (HD/HDF) on urea clearance and the recirculation have been commented in Annexe C in order to check that the dialysis sessions were efficient. Urea clearance is a measure of urea removal by the blood and is generally expressed in terms of CL*t/V which should be equal to at least 1.2 for each dialysis session (details are given in section 3.3.4 of Chapter II). Recirculation percentage refers to the performance of the vascular access (here all vascular access are fistula).

1.2. Study case, GV05 patient

The GV05 patient has been monitored during 3 HD dialysis sessions. Its weight loss rates are 16.67 mL/min for HD1, 16.25 mL/min for HD2 and 10 mL/min for HD3.

Blood samples have periodically been taken at hemodialyzer inlet (noted pi) and at hemodialyzer outlet (noted po) and data are represented in the same graph. Each graph provides information on both time variations of the parameters and variations along hemodialyzer. As explained previously, values of samples taken at hemodialyzer inlet reflects the status of the dialysis patient.

Error bars have been added in only one dialysis session (in order to improve the reading of the Figures) according to variation coefficients determined for each parameter (given in Chapter II).

1.2.1. pCO_2 time variations

Figure IV.1 gives pCO_2 time variations for GV05 patient.

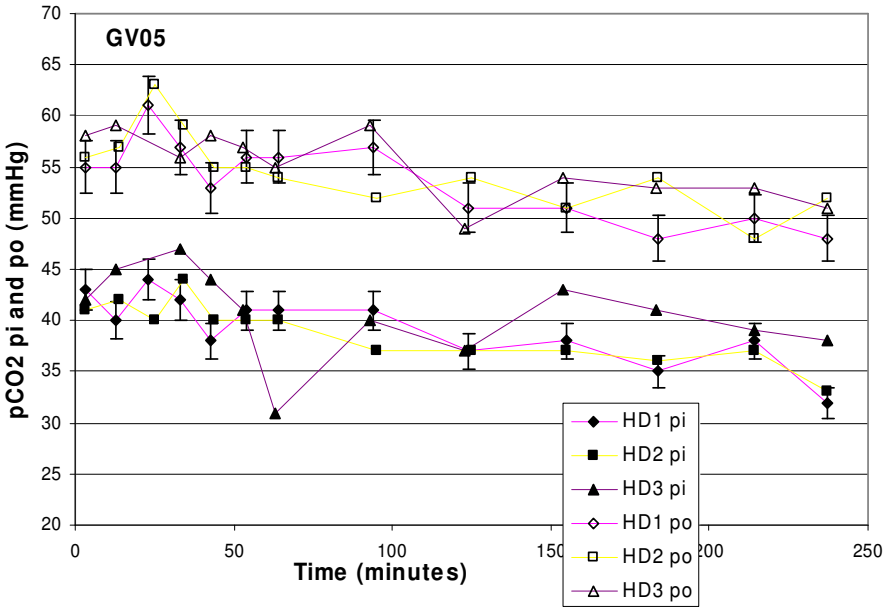

Figure IV. 1 pCO_2 pi and po time variations for GV05 patient. pi = plasma hemodialyzer inlet and po = plasma hemodialyzer outlet

pCO_2 variations along the hemodialyzer:

It can be seen that pCO_2 at hemodialyzer outlet (po) is higher than at the inlet (pi). This result is due to CO_2 transfer from the dialysis fluid to blood in the hemodialyzer (Sombolos et al. 2005).

As the relationship between CO_2 partial pressure and its concentration is $[CO_2] = 0.0307 * pCO_2$ (Equation II.7), the concentration of dissolved CO_2 increases from 1.29 mmol/L to 1.68 mmol/L after its passage through the hemodialyzer (+30 %). As seen in Chapter II (Table II.12), dialysis fluid provided a dissolved CO_2 concentration of 1.91 mmol/L at hemodialyzer inlet.

Moreover, we can observe that this difference along the hemodialyzer, seems to stay constant until the end of the dialysis session (with a mean increase of 30 % between pre and post hemodialyzer pCO_2).

Time variation of patient pCO_2:

For this patient, pCO_2 at hemodialyzer inlet presents a moderate decrease during the sessions: from 42/43 to 33/38 mmHg depending of the dialysis session. It can be seen that, even if the blood after its passage through the hemodialyzer, returns to the patient with a high pCO_2 (po samples), the pCO_2 will be lower in the next sample (pi samples), due to CO_2 elimination by lungs.

1.2.2. HCO_3^- concentration time variations

Figure IV.2 gives plasma HCO_3^- concentration time variations for GV05 patient.

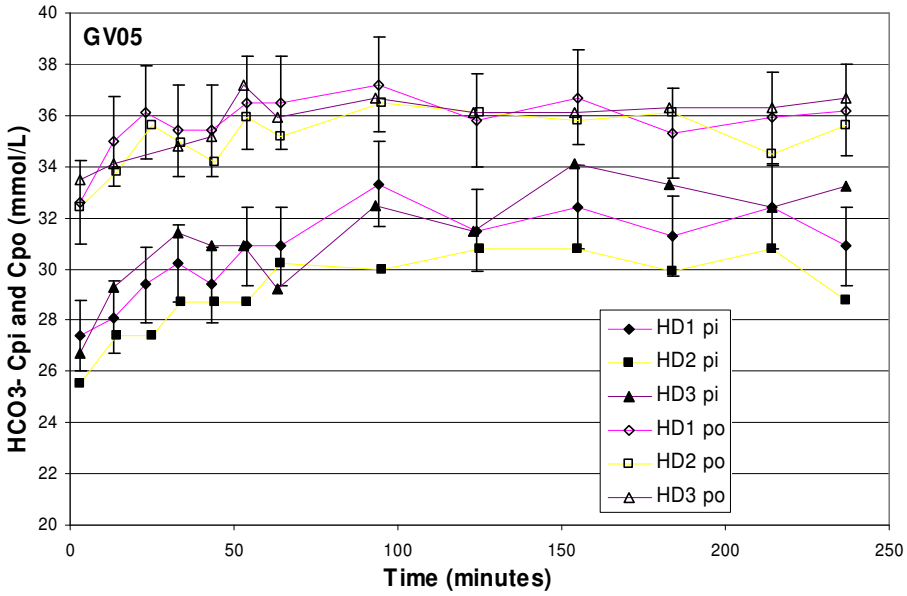

Figure IV. 2 Cpi and Cpo HCO_3^- time variation for GV05 patient

Plasma HCO_3^- concentration variations along the hemodialyzer:

Dialysis session with a delivered bicarbonate dialysis fluid concentration of 38 mmol/L (measured at 37.1 mmol/L) results in a rise of HCO_3^- concentration from 26/27 mmol/L in the arterial blood entering the hemodialyzer to 33 mmol/L in the venous blood returning to the patient at the start of dialysis.

The difference between inlet and outlet blood samples, represented by the HCO_3^- gradient along the hemodialyzer, is not constant throughout dialysis. This difference is larger at the beginning than at the end of the dialysis session. This is due to HCO_3^- retained in extracellular compartment which increases plasma HCO_3^- and reduces the transmembrane concentration gradient.

Moreover, even if arterial (pi) samples time variations are very different, venous samples (po) have lesser variations and they are more consistent.

Time variation of patient plasma HCO_3^- concentration:

HCO_3^- plasma concentration in arterial sample increases during the three HD sessions. It seems that this increase is constant during the first 100 minutes, and then remains quite stable, except for small variations between samples. As these small variations are included in the errors bars, they can be assimilated to measurement errors and are not physiological.

For this patient, final HCO_3^- concentration for HD1 and HD2 decreases whereas increases for HD3 between 213 and 237 minutes. For these two sessions, the HCO_3^- increases are 3.5 and 3.3 mmol/L respectively, whereas for HD3 session, the increase is 6.5 mmol/L, even if the initial HCO_3^- plasma concentration of HD3 is lower than HD1.

1.2.3. pH time variations

Figure IV.3 gives pH time variations for GV05 patient.

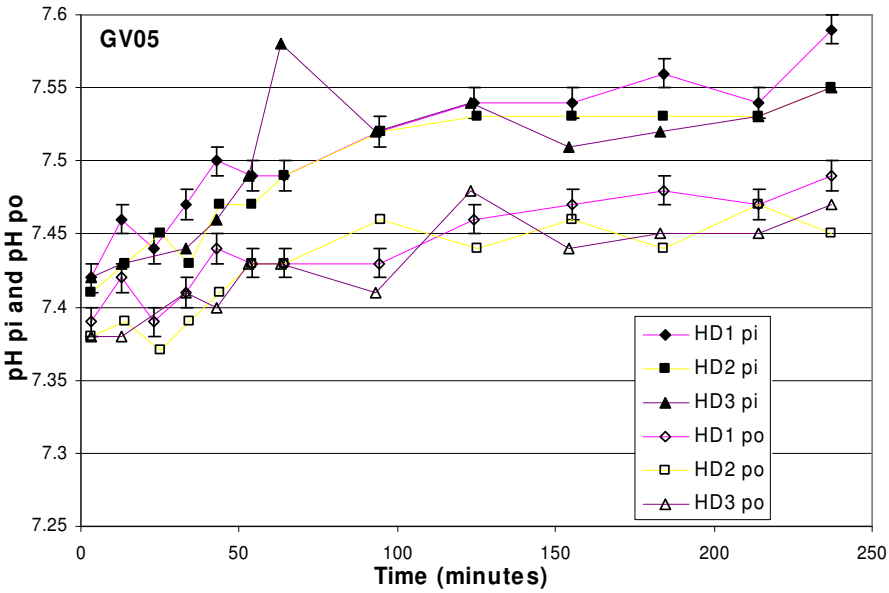

Figure IV. 3 pH pi and pH po time variation for GV05

pH variations along the hemodialyzer:

pH in samples at hemodialyzer outlet (pH po) is always lower than pH in samples from hemodialyzer inlet (pH pi). As pH = - log [H+], the H+ concentration is then higher in outlet samples than in inlet samples.

This can be explained by the CO_2 transfer from dialysis fluid to blood as seen in Figure IV.1. According to Henderson-Hasselbach equation, it can be seen that a rise of pCO_2 and a rise of HCO_3^- lead to a blood pH returning to the patient reduced to 7.42 (while the arterial pH is 7.46).

For example:

$$pH(pi) = 6.1 + \log\frac{28}{40 * 0.03} = 7.46 \qquad \textbf{IV. 1}$$

$$pH(po) = 6.1 + \log\frac{35}{55 * 0.03} = 7.42 \qquad \textbf{IV. 2}$$

Moreover it seems that differences between pH at hemodialyzer inlet and pH at hemodialyzer outlet are higher at the end of the dialysis sessions than at the beginning.

Time variation of patient pH:

Even if the blood pH po returning to the patient is lower after its passage into the hemodialyzer, pH pi increases during dialysis sessions. Excess blood CO_2 has been eliminated by the lungs, increasing the pH in the next arterial sample.

pH pi progressively increases throughout the dialysis session. For this patient, initial pH is the same for the three HD sessions (7.41) and at the end of the dialysis session, pH increases to 7.55 (+ 1.9 %) for HD2 and HD3 and to 7.59 (+ 2.4%) for HD1.

1.2.4. pO_2 time variations

Figure IV.4 gives pO_2 time variations for GV05 patient.

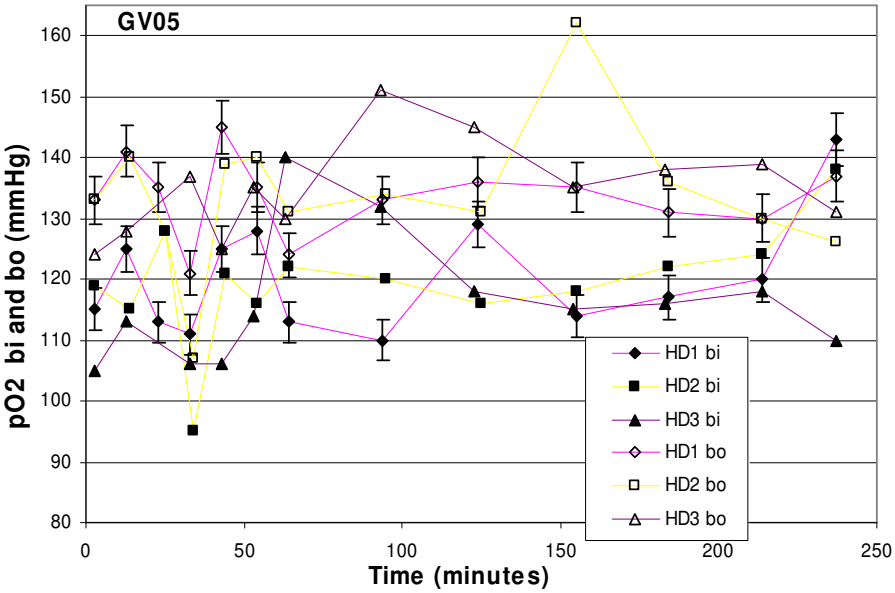

Figure IV. 4 pO_2 bi and bo time variation for GV05

pO_2 strongly fluctuates during dialysis session. No single mechanism is likely to be responsible for the observed variations in arterial pO_2 during hemodialysis due to sudden changes in the internal milieu (Abbott and Ward 2005). Some authors have observed hypoxemia during dialysis: hypoxemia is the pO_2 decrease in blood. This phenomenon has been the subject of numerous investigations which have compared hypoxemia in acetate and bicarbonate dialysis (De Broe et al. 1989) and is detailed in the following.

Despite the pO_2 variations, mean O_2 saturation remains at 98.9% for the 3 HD sessions in arterial and venous samples.

pO_2 variations along the hemodialyzer:

The hemodialyzer due to dialysis fluid pO_2 of 149 mmHg, seems to increase blood pO_2 between inlet and outlet samples. This may be due to O_2 transfer from dialysis fluid to blood but the differences stay small.

Time variations of patient pO_2:

For this patient pO_2 increases from the beginning of the session until the end. The increases are 24.3 % for HD1, 16 % for HD2 and 4.8 % for HD3. High or low increase for HD1 and HD3 are due to the final status of this patient (between 214 and 237 minutes) which sudden changes.

1.2.5. Synthesis and additional remarks

This section has presented acid-base parameters time variation for the GV05 patient. For the other patients (as presented in the next section) we have observed similar trends for acid-base parameters.
Therefore we can conclude that from this preliminary study, an encouraging result is that time variations of all various sessions are consistent for each parameter and are similar for different patients.

Our additional remarks concern two points.

Bicarbonate dialysis fluid concentration

The dialysis fluid HCO_3^- concentration of 38 mmol/L may be too high in comparison with other dialysis centres (mostly 35 mmol/L). Therefore pH of GV05 patient (as seen in Figure IV.3) at the end of the dialysis session is around 7.56. This value can be considered too high compared to the normal pH range body (between 7.35 and 7.45). We can wonder if this patient is in alkalosis at the end of its dialysis session. Mean HCO_3^- concentration at the end of the dialysis session, for this patient, is around 31 mmol/L.
Nevertheless, once the dialysis session is ended, there must be a rapid HCO_3^- concentration decrease. Symreng et al. (1992) have shown HCO_3^- concentration decrease in the several hours following hemodialysis. In their study, HCO_3^- concentration falls abruptly by over 2 mmol/L during the first hour after hemodialysis, but then increases again the second hour reaching a value only 1.2 mmol/L less than the HCO_3^- concentration at the end of the hemodialysis. After 2 hours after the end of the dialysis session, HCO_3^- concentration progressively decreases until the next dialysis session. Gennari (1996) supposed than the rapid fall in the first hour can not be only due to a simple equilibration with a larger distribution space, otherwise there will be no rebound. There must be a continued production of

organic acid when hemodialysis session is stopped, which are retained by bicarbonate. And their later metabolism could regenerate the bicarbonate titrated.

Ahrenholz et al. (1998) also show decrease of bicarbonate after HD, HDF predilution and HDF postdilution sessions. But as they studied patients during consecutive sessions, they did not give details on the bicarbonate decrease during hours after the sessions, but just link the last HCO_3^- concentration of previous session with the initial of the following session. The decrease of HCO_3^- concentration is found around 5 to 6 mmol/L between sessions (48h to 72h). This decrease also depends on each patient metabolism and on the uptake during sessions (which can lead to a more or less acid production).

Benefit of synthetic membrane

Contact of blood with cellulosic membrane (described in Chapter II) activates the alternative pathway of complement to generate C5a. White cells are then aggregate by C5a, leading to increase adherence of these cells to capillary endothelial surfaces in lungs. Therefore this results in pulmonary sequestration of white cells aggregates (Craddock et al. 1977) and a decrease of white cells occurs during the first 15 to 20 minutes of the dialysis session. This phenomenon is named leukopenia (or decrease in the number of white blood cells found in the blood) and is minimal with non cellulose membrane (Eschbach 1989). From an analysis of literature, authors have observed that acetate and bicarbonate dialysis is accompanied by a certain degree of hypoxemia: pO_2 starts to deteriorate soon after the start of the session. The main cause seems to be complement activation by the non-hemocompatible membranes (Ghezzi and Ronco 1999).

In our study, synthetic membranes are used (polysulfone, FX 40) and we observe small falling on our pO_2 curves as seen in Figure IV.4 around 30 minutes.

2. Evaluation of acid-base parameters

In this section acid-base parameters pH, pCO_2, pO_2 and HCO_3^- concentration are studied. Initial (at the beginning of the dialysis session) and final (at the end of the dialysis session) values of these parameters are first presented.
In a 2nd section, time variations of these parameters during dialysis sessions are compared between HD and HDF sessions for patients monitored during the two dialysis modes.

2.1. Initial versus final acid-base parameters

For each dialysis sessions, as seen in Chapter II, blood samples have been taken at the hemodialyzer inlet and at the hemodialyzer outlet at various sampling time. We have considered that the analysis of samples taken at the hemodialyzer inlet reflects the status of the dialysis patient whereas comparisons between inlet and outlet parameters indicate the parameters variations along the hemodialyzer.

2.1.1. Acid-base parameters data

All acid-base parameters recorded are presented in Table IV.2. Initial parameters (of blood samples at hemodialyzer inlet) have been registered after 3 minutes of the beginning of the dialysis session whereas final parameters, 3 minutes before the end (at 237 minutes). In the practice, it is difficult to shorten this time due to the interventions of nurses on patients and on dialysis machine screen.

Parameters	pH		pCO_2 (mmHg)		pO_2 (mmHg)		HCO_3^- (mmol/L)	
Patients	Initial pH	Final pH	Initial pCO_2	Final pCO_2	Initial pO_2	Final pO_2	Initial HCO_3^-	Final HCO_3^-
PC01 HD1	7.41	7.51	35	40	109	82	21.7	31.7
PC01 HD2	7.44	7.53*	41	37*	82	89*	27.4	30.8*
PC01 HD3	7.43	7.51	37	40	114	97	24.1	31.7
PC01 HDF1	7.45	7.5	39	40	107	88	26.7	30.9
PC01 HDF2	7.35	7.57	39	31	105	107	21	28.5
MA02 HD1	7.4	7.46	46	49	95	76	27.9	34.4
MA02 HD3	7.44	7.5	38	40	90	75	25.4	30.9
MA02 HD4	7.42	7.45	42	49	86	76	26.7	33.5
MA02 HDF1	7.42	7.45	41	51	98	86	26.1	34.9
MA02 HDF2	7.41	7.46	41	48	92	81	25.5	33.7
MA02 HDF3	7.37	7.47	45	45	129	82	25.4	32.3
SG03 HD1	7.45	7.53	38	38	71	69	26	31.6
SG03 HDF1	7.4	7.5	46	43	68	66	27.9	33.2
SG03 HDF2	7.47	7.52	40	37	78	70	28.7	31.7
LC04 HD1	7.46	7.52	37	41	137	100	26	33.3
LC04 HDF1	7.39	7.55	44	35	116	125	26.1	30.6
LC04 HDF2	7.39	7.5	47	41	98	129	27.8	31.7
LC04 HDF3	7.39	7.56	44	36	112	153	26.1	32.2
GV05 HD1	7.42	7.59	43	32	115	143	27.4	30.9
GV05 HD2	7.41	7.55	41	33	119	138	25.5	28.8
GV05 HD3	7.42	7.55	42	38	105	110	26.7	33.2
LR06 HD1	7.46	7.54	37	40	107	79	26	34.1
LR06 HDF1	7.41	7.49	44	45	76	82	27.3	34
Mean ± SD **HD (n =12)**	7.43 ± 0.02	7.52 ± 0.04	39.75 ±3.22	40 ± 5.33	102.5 ± 18.38	95 ± 25.75	25.9 ± 1.68	32.19 ± 1.68
Mean ± SD **HDF (n =11)**	7.4 ± 0.03	7.51 ± 0.04	42.72 ± 2.83	41.09 ± 6.02	98.09 ± 18.52	97.18 ± 27.64	26.24 ± 2.03	32.15 ± 1.79
Mean ± SD **All (n =23)**	7.42 ± 0.03	7.51 ± 0.04	41.17 ± 3.34	40.64 ± 5.53	100.39 ± 18.17	96.09 ± 26.09	26.06 ± 1.82	32.17 ± 1.7

Table IV. 2 Acid-base initial/final characteristics in blood samples taken at the hemodialyzer inlet. HCO_3^- concentration represents plasma concentration. * means final state at 185 minutes instead of 240 minutes

All patients have been dialysed using a HCO_3^- dialysis fluid concentration of 38 mmol/L, even during dialysis sessions where no samples are taken. It can be seen that, except for patient PC01, initial HCO_3^- concentrations are very close for all dialysis sessions: between 25.4 and 27.9 mmol/L. PC01 patient has been dialysed using HCO_3^- dialysis fluid concentration of 32 mmol/L in dialysis sessions where no samples are taken. That is why its initial HCO_3^- plasma concentration can be very low: 21 mmol/L for PC01 HDF2 or 21.4 mmol/L for PC01 HD1.

It can be seen that pH and HCO_3^- concentration clearly increase during dialysis session whereas pCO_2 and pO_2 seem to decrease. The differences between initial and final parameters and between HD and HDF sessions have been studied in the next section with a detailed statistical analysis.

It can also be seen that for pH, pCO_2 and pO_2, standard deviations (SD) for final state are always higher than initial ones as if dialysis sessions would have increased differences between individual values. SD for pO_2 are very high in HD and in HDF sessions (18.17 mmHg for initial and 26.06 mmHg for final state).

2.1.2. Statistical analysis

Even if the number of values is not high enough to allow an accurate statistical analysis, this section presents a preliminary statistical analysis study for the 11 HD sessions and 11 HDF sessions (PC01 HD2 session is eliminated due to the earlier final state).
We are aware that we should have the totality of the included patients to reach a power of 90%, nevertheless we presented the statistic approach on this small sample (22 dialysis sessions).

Three comparisons are made:
- Between initial and final states of parameters for the 22 tests (no distinctions between HD and HDF)
- Between initial and final states of parameters for the 11 HD tests and for the 11 HDF tests
- Between initial states in HD and HDF and between final states in HD and HDF for each parameter

The Fisher test is first applied under a significance level of 5%, to compare variances between the two groups and then the p value of the paired student t-test is determined under a significance level of 5% to compare mean of the two groups.

1) Comparison between initial and final values of parameters for the 22 tests:

- The critical region of the Fisher test (where the hypothesis of the equality of variances is rejected) under a significance level of 5% is $F < 0.42$ or $F > 2.41$
- The student t-test determines the p-value: if $p < 0.05$, the differences (between means values) are statistically significant under a significance level of 5%

	pH initial/final	pCO_2 initial/final	pO_2 initial/final	HCO_3^- initial/final
Statistical F value, F	0.57	0.38	0.48	1.18
Conclusion for F-test	NSS	SS	NSS	NSS
p value of the t-test	2.27 E-11	0.65	0.45	1.35 E-14
Conclusion for t-test	SS	NSS	NSS	SS

Table IV. 3 Comparison between initial/final states of the acid-base parameters for the 22 tests. NSS = not statistically significant under a significance level of 5%, SS = statistically significant

It can be seen that, except for the pCO_2, there are no differences for the variances between initial and final states (F test) under a significance level of 5% and that the difference for the means are significant for pH and HCO_3^- concentration.

This result is expected as pH and HCO_3^- significantly increase during dialysis session; their means are significantly different between initial and final state whereas their standard deviation are not. For the partial pressures (pCO_2 and pO_2) it can be seen that initial and final means values are not significantly different.

2) Comparison between initial and final states of parameters for HD (11 tests)

- The critical region of the Fisher test under a significance level of 5% is $F < 0.27$ or $F > 3.72$
- The student t-test is applied in same conditions as seen previously

	pH initial/final	pCO_2 initial/final	pO_2 initial/final	HCO_3^- initial/final
Statistical F value, F	0.26	0.4	0.49	1.02
Conclusion for F-test	SS	NSS	NSS	NSS
p value of the t-test	8.96 E-6	0.85	0.33	1.99 E-8
Conclusion for t-test	SS	NSS	NSS	SS

Table IV. 4 Comparison between initial/final states in HD mode of the acid-base parameters for the 11 tests. NSS = not statistically significant under a significance level of 5%, SS = statistically significant

Comparison between initial and final states of parameters for HDF (11 tests)

The conditions for F-test and t-test are the same as for HD as the number of samples is also 11.

	pH initial/final	pCO_2 initial/final	pO_2 initial/final	HCO_3^- initial/final
Statistical F value, F	0.71	0.22	0.45	1.28
Conclusion for F-test	NSS	SS	NSS	NSS
p value of the t-test	2.81 E-6	0.43	0.93	5.29 E-7
Conclusion for t-test	SS	NSS	NSS	SS

Table IV. 5 Comparison between initial/final states in HDF mode of the acid-base parameters for the 11 tests. NSS = not statistically significant under a significance level of 5%, SS = statistically significant

From Tables IV.4 and IV.5, it can be seen that the variannces are not statistically significant between initial and final states except for pH in HD and pCO_2 in HDF. In HD and in HDF mode, the results are the same concerning the difference for the mean values: as expected for pH and HCO_3^- concentration, the differences are statistically significant between initial and final state. For pCO_2 and pO_2 as their differences are not statistically significant between initial and final state, we can conclude that their increase or decrease during dialysis session is not significant.

3) Comparison between initial and between final states of parameters for HD and HDF tests

The conditions for F-test and t-test are the same as for HD as there are also 11 tests.

	pH **initial** HD/HDF	pH **final** HD/HDF	pCO_2 **initial** HD/HDF	pCO_2 **final** HD/HDF	pO_2 **initial** HD/HDF	pO_2 **final** HD/HDF	HCO_3^- **initial** HD/HDF	HCO_3^- **final** HD/HDF
Statistical F value, F	0.37	1.015	1.4	0.783	0.95	0.87	0.69	0.87
Conclusion for F-test	NSS	NSS	NSS	NSS	NSS	NSS	NSS	NSS
p value of the t-test	0.05	0.47	0.03	0.68	0.43	0.85	0.56	0.96
Conclusion for t-test	NSS	NSS	SS	NSS	NSS	NSS	NSS	NSS

Table IV. 6 Comparison between initial states of the acid-base parameters in HD/ HDF mode and comparison between final states of the acid-base parameters in HD/ HDF mode for the 11 tests. NSS = not statistically significant under a significance level of 5%, SS = statistically significant

Table IV.6 compares initial and final states parameters between HD and HDF. It can be seen that the differences for variances and for means are not statistically significant for the 4 acid-base parameters between HD and HDF tests (except for initial pCO_2 which is statistically significant between HD and HDF but not for its final state).

Figure IV.5 gives histograms of the mean and standard deviations for the 4 acid-base parameters in the 22 dialysis sessions. We have represented the results of the statistical analysis by only adding the significant differences (in mean with *).

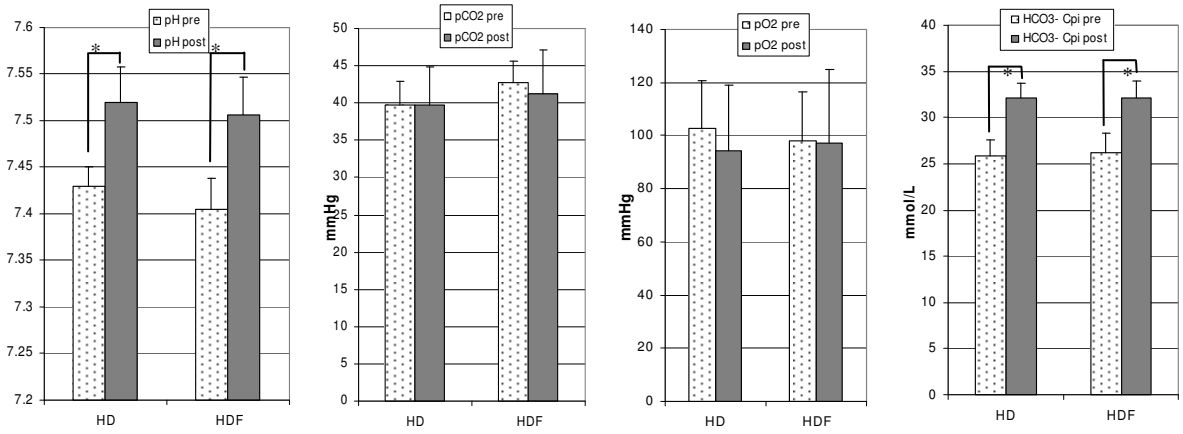

Figure IV. 5 pH, pCO_2, pO_2 and HCO_3^- concentration initial (pre) and final (post) mean values and standard deviation over the 22 dialysis sessions

On Figure IV.5, it can be seen that:

- The mean pH increases is the same in HD and HDF sessions

- While mean pCO_2 remains constant in HD, it slightly decreases in HDF. But this difference is not statistically significant. This may be due to the fact that means initial pCO_2 are higher in HDF sessions (42.72 mmHg) than in HD sessions (39.75 mmHg).

- Mean pO_2 decreases in HD but stays almost constant in HDF. As normal range values for arterial pO_2 are between 75 and 105 mmHg, it is quite difficult to interpret this result.
- There are no differences in mean HCO_3^- plasma concentration between HD and HDF

2.1.3. Differences between initial and final acid-base parameters

Table IV.7 gives mean ± SD of acid-base parameters differences between final and initial state for the 11 HD and 11 HDF dialysis sessions (except for PC01 HD2).

	ΔpH	ΔpCO_2 (mmHg)	ΔpO_2 (mmHg)	ΔHCO_3^- (mmol/L)
Mean ± SD **HD (n =11)**	0.09 ± 0.041	0.36 ± 5.66	-9.36 ± 20.17	6.43 ± 1.94
Mean ± SD **HDF (n =11)**	0.1 ± 0.059	-1.63 ± 6.2	-0.9 ± 23.78	5.91 ± 1.89

Table IV. 7 Mean ± SD of differences between final and initial values of Table IV.2

It can be seen that pH and HCO_3^- plasma concentrations always increase between initial and final state as their differences are clearly positive.
For pCO_2 and pO_2 the differences between initial and final state depend on patient states and on their dialysis sessions. Nevertheless, we can observe that the range of the differences is very high due to some patient particularity (agitation or wake up which can lead to hyperventilation): the standard deviation is around 20 mmHg for pO_2.

Figures IV.6 give another representation of the initial/ final pH, pCO_2, pO_2 and HCO_3^- concentration in HD and HDF sessions. This representation brings information about acid-base parameters behaviour for the 22 dialysis sessions.
For pH and plasma HCO_3^- concentration in all HD and HDF sessions, final (post-dialysis) values are always higher than initial (pre-dialysis) one. For pCO_2 and pO_2 it is not always the case and final values can be higher or smaller than initial status.

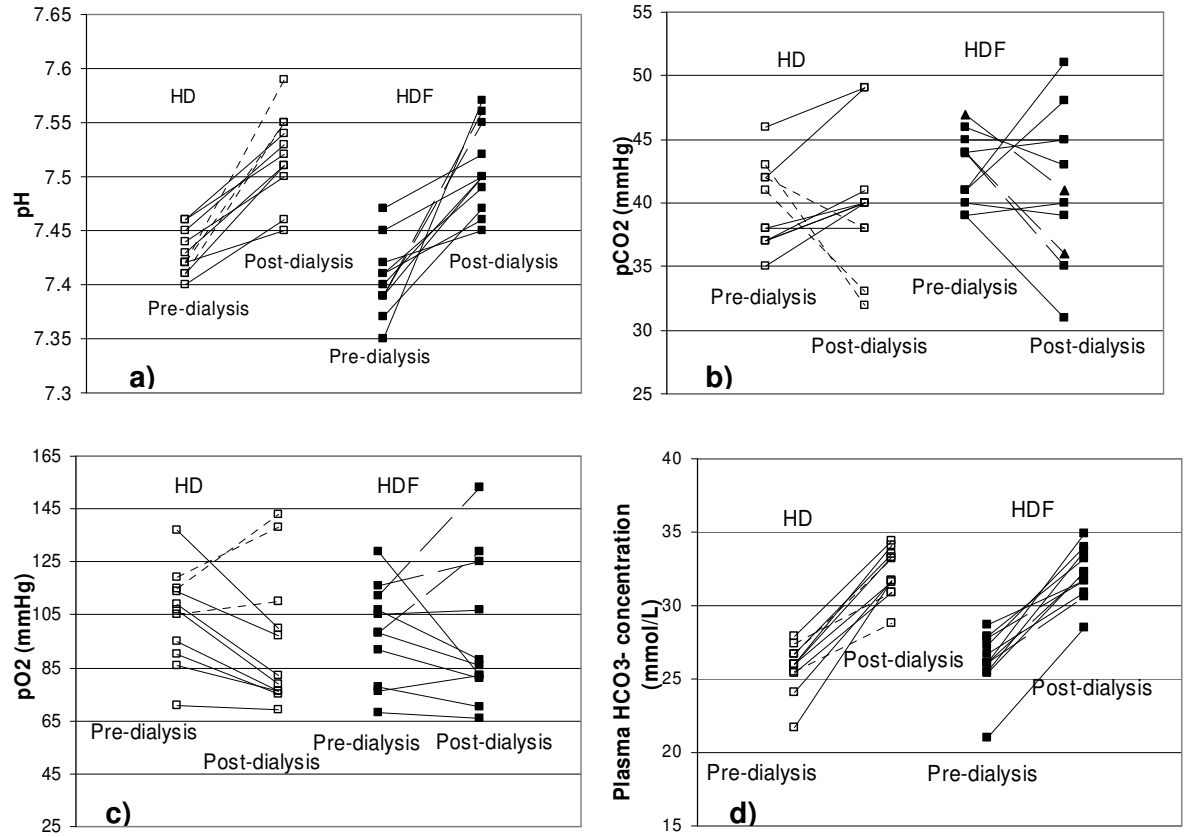

Figures IV. 6 Initial (pre-dialysis) and final (post dialysis) representation of the pH (a)), pCO_2 (b)), pO_2 (c)) and plasma HCO_3^- concentration (d)) in 11 HD and 11 HDF sessions. GV05 patient has been identified by small dotted lines and LC04 by large dotted lines

In order to analyse these differences, we have identified the corresponding patients.

As far as pCO_2 in HD sessions (Figure IV.6 (b)) is concerned, the only 3 sessions where pCO_2 decreases during dialysis, correspond to the 3 sessions of GV05 patient. Moreover this same patient has also the three high increase of pH (a) and the only three high increase of pO_2 (c).These trends are not issued from the final state of this patient, as increases or decreases are progressive during these dialysis sessions of this patient (as it will be seen the section 2.2.). Furthermore this GV05 patient has a normal recirculation percentage of 11 ± 1% for its three HD sessions (presented in Table IV.1).

As this patient has not been monitored during HDF sessions, it is not possible to compare if the same trends appear in his HDF sessions.

For pCO_2 in HDF sessions (Figure IV.6 (b)), there are three strong decreases of pCO_2 which correspond to the 3 HDF sessions of LC04 patient. For this same patient, pO_2 (c) and pH (a) highly increase. We find completely different acid-base status after 213 minutes of the dialysis session (corresponding to the penultimate samples and not the last sample as represented here). Therefore differences between initial and final state (at 213 minutes) give an increase of pCO_2 and a decrease of pO_2, as seen in the other dialysis sessions for other patients.

This LC04 patient has also been monitored during one HD session where we have observed that pCO_2 increase and pO_2 decrease between initial and final state. Moreover this patient had high recirculation percentage (up to 20% for its HDF2 sessions) but we did not see more differences for this HDF2 session than for the other two.

Plasma HCO_3^- concentrations are not commented from (d) because they follow the calculation of the Henderson-Hasselbach equation which depends on pH and pCO_2. Nevertheless, we can observe that the increases between initial and final state are similar for various sessions even if the initial concentration is very low (as seen in HDF sessions for PC01 patient in its HDF2).

It is not easy to interpret these data and a stronger analysis of the patient state would be mandatory. Apparently these trends are more related to the patient state and behaviour during dialysis sessions (excitement at session ending, wake up after a sleep phase…) than to the dialysis techniques (HD or HDF).

2.1.4. Synthesis and additional remarks

The statistical analysis of this preliminary study does not reveal any differences between HD and HDF sessions as far as initial and final states of the acid-base parameters are concerned. It can be suggested that HDF technique seems not likely to create ionic unbalances as compared to HD. For the moment we cannot conclude on the differences between HD and HDF sessions, due to the too small number of included patients.
A larger number of dialysis sessions in HD and HDF mode are requested in order to appreciate acid-base parameter evolution. When 3 HD and 3 HDF sessions will be monitored per patient, each patient will be his own control in the comparison HD/HDF.

A question appears about the definition of the final state of the dialysis session. As seen in Figures IV.6, the patient state can dramatically change between 213 and 237 minutes of its dialysis session. A question arises to which state matches the end of its dialysis session. An answer could be to prolong the dialysis session in order to observe if this trend stabilises.

2.2. Acid-base parameters time variations in other patients and comparison between HD and HDF mode

This section presents a review data of the three other patients: HD and HDF sessions are going to be compared in details.

The LC04 patient has been monitored during 3 HDF and 1 HD dialysis sessions. The ultrafiltration rates (weight loss rate + reinjection flow rate) are 12.5 mL/min for HD1, 110.75 mL/min for HDF1, 113.25 mL/min for HDF2 and 111.92 mL/min for HDF3.

The SG03 patient has been monitored during 2 HDF and 1 HD sessions. The ultrafiltration rates are 7.5 mL/min for HD1, 100.92 and 106.33 mL/min for HDF1 and HDF2, respectively.

The LR06 patient has been monitored during 1 HDF and 1 HD sessions. The ultrafiltration rates are 13.75 mL/min for HD1 and 103.17 mL/min for HDF1.

2.2.1. pCO_2, pH and HCO_3^- concentration time variations

Figures IV.7 show pCO_2 and pH time variations for dialysis sessions of LC04 patient.

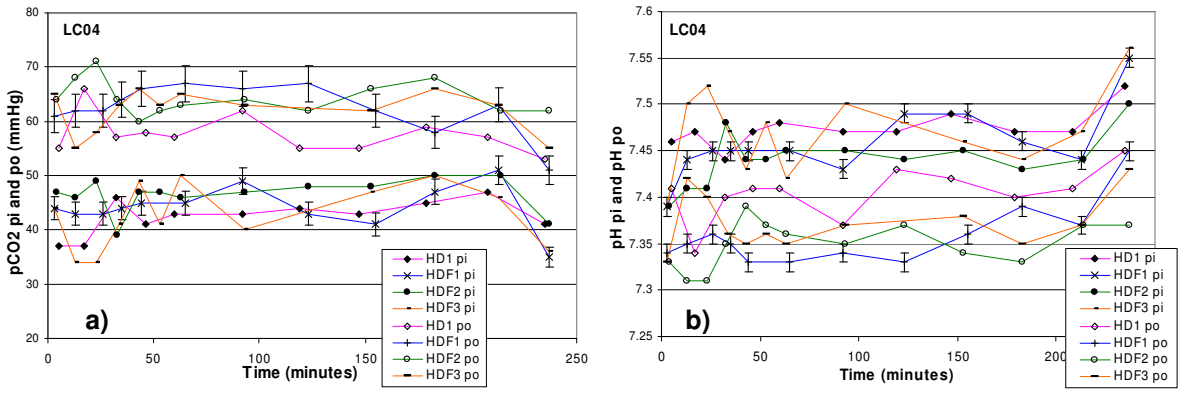

Figure IV. 7 pCO_2 (a)) and pH (b)) time variation at inlet and outlet of the hemodialyzer for patient LC04

It can be seen that pCO_2 and pH in blood after its passage through the hemodialyzer (outlet samples) seems to be higher and smaller respectively in HDF sessions than in HD session between about 40 and 150 minutes of the dialysis session (but not at the beginning and not at the end). This can also be found for the two other patients, SG03 and LR06. Figures IV.8 confirm the results.

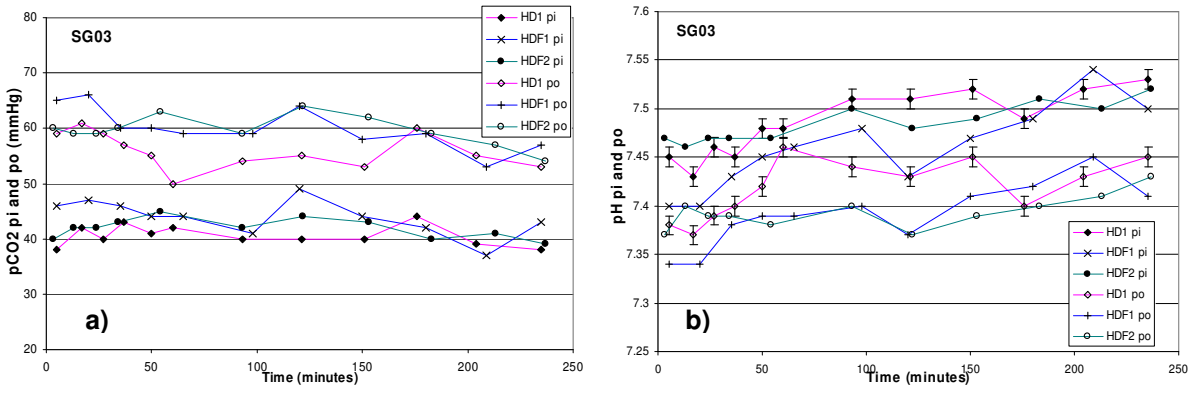

Figure IV. 8 pCO_2 (a)) and pH (b)) time variation at the inlet and outlet of the hemodialyzer for patient SG03

These differences in pCO_2 and pH occur during the passage of blood through the hemodialyzer and may be due to the difference between the dialysis mode (HD or HDF). We can observe that:

- Blood pCO_2 at the hemodialyzer outlet (po samples) is higher in HDF sessions between 30 and 170 minutes (approximately) than in HD session. This means that HDF mode transfers more CO_2 to blood than in HD sessions.
- Blood pH at the hemodialyzer outlet is lower in HDF sessions between 40 and 150 minutes than in HD sessions. This means that HDF mode transfers more H+ to blood than HD sessions.

These differences curiously only exist during the middle of the dialysis session. The only differences between HD and HDF sessions are the ultrafiltration flow rate which is 8 to 9 times more important in HDF than in HD.

We need to collect more data by including other patients and by following more dialysis sessions to confirm or not this phenomen.

Figures IV.9 show HCO_3^- plasma concentration time variations in patients LC04 and SG03.

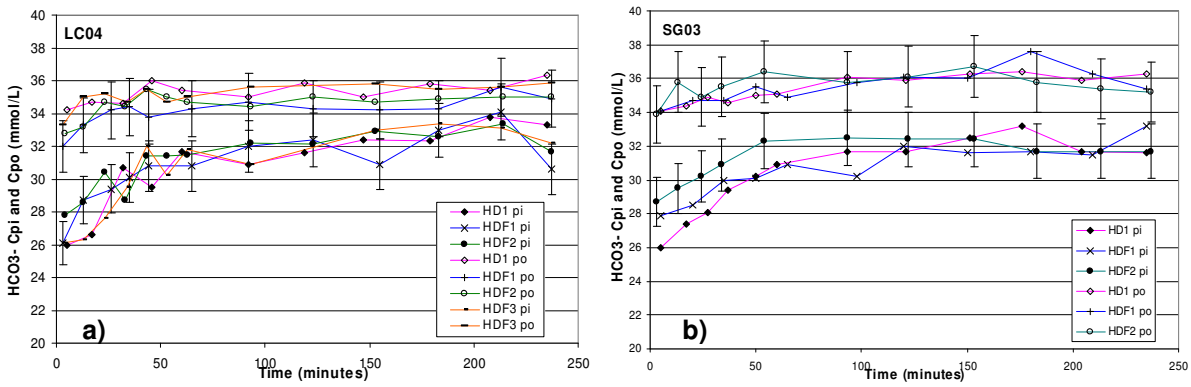

Figure IV. 9 HCO_3^- time variations in inlet and outlet samples for LC04 (a)) and SG03 (b))

As for the GV05 patient, HCO_3^- concentration (in inlet and outlet samples) seems to increase until 60-100 minutes, and then stays quite stable until the end of the dialysis session.

Contrary to pCO_2 and pH, no differences in HCO_3^- concentration can be observed at the hemodialyzer outlet between HD and HDF sessions. Even though HCO_3^- is lost from blood by ultrafiltration, this does not change its concentration as HCO_3^- is lost as the same rate as plasma rate as its transmission coefficient is equal to 1.

The change in the plasma volume in HDF has been observed from hematocrit measurements: in LC04 patient in HDF1 session, mean inlet hemodialyzer hematocrit is 45.7% whereas mean outlet is 79.6% (for Qf = 110.75 mL/min and Qb = 350 mL/min). This result corresponds to an increase of 74.2% between inlet and outlet hemodialyzer hematocrit. For the same patient, but during its HD1 session, mean inlet hemodialyzer hematocrit is 46.3% whereas mean outlet is 52.1% (for Qf = 12.5 mL/min). This result corresponds to an increase of 12% in HD session.

2.2.2. Oxygen partial pressure: pO_2

Figures IV.10 show pO_2 time variations for patient LC04 and SG03.

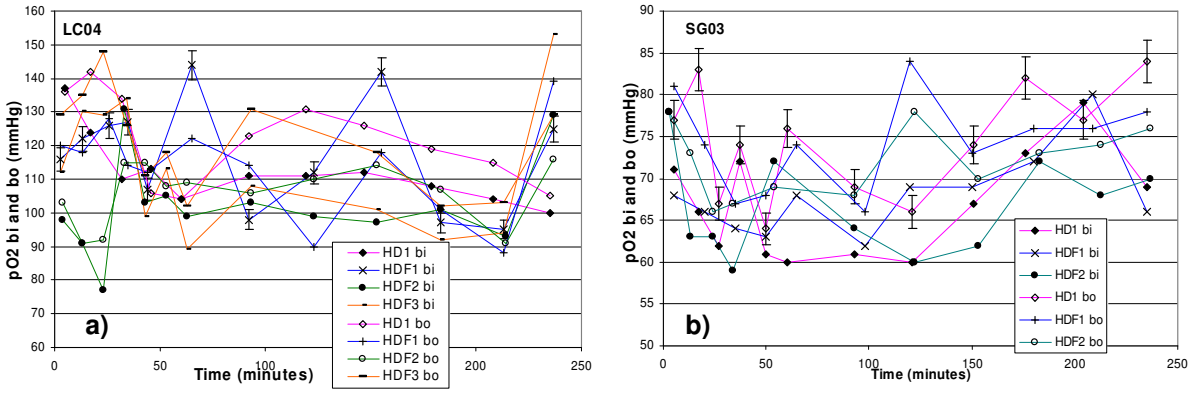

Figure IV. 10 pO_2 time variations for LC04 (a)) and SG03 (b)) patients

As for GV05 patient, pO_2 in outlet samples seems to be higher than in inlet samples due to O_2 transfer from dialysis fluid to blood. No distinctions can be made between HD and HDF sessions.

It can be seen that for LC04 patient (a), except in HD mode, its pO_2 at hemodialyzer inlet and outlet widely increase between 213 and 237 minutes of the dialysis session. This phenomenon is repeated for its three dialysis sessions (which are not consecutive) even if initial conditions are completely different. This phenomenon can be due to a large agitation of the patient which has been observed around the end of its dialysis treatment.

This result also confirms the difficult choice of the final state (as explained previously) as the parameters can strongly change between the penultimate and the last sample.

3. Synthesis on the effects of the hemodialyzer on blood acid-base parameters

O_2, CO_2 and HCO_3^- have low molecular weight (32, 44 and 61 Da respectively) and move across the hemodialyzer membrane by diffusion and convection. Dialysis fluid entering the hemodialyzer has higher pO_2, pCO_2 and HCO_3^- concentrations than blood.

Changes in acid-base status (influx of HCO_3^- and dissolved CO_2 into the blood) across the hemodialyzer membrane are expected whereas a change in pH is more surprising. As seen on previous figures, blood returning to the patient is more acidic than that entering the hemodialyzer. This can be explained by the higher mean increase of pCO_2 (32 % for patient LC04 and 38% for patient GV05 in HD sessions) than in mean HCO_3^- concentration (14% for patient LC04 and 17% for patient GV05 in HD sessions).
Symreng et al. (1992) also found these results and wrote that blood entering the extracorporeal circuit presents metabolic acidosis and returns to the patient with values reflecting a respiratory acidosis. Even if pH is high in blood outlet sample due to high pCO_2, the dissolved CO_2 administrated to the patient is considered as neutral as it does not interfere with acid-base balance, and the excess of CO_2 is removed by the lungs (la Greca et al. 1989).

In this section, we have tried to explain how the transfers take place inside the hemodialyzer.

3.1. Pre and post hemodialyzer acid-base parameters

This section gives graphical representations for acid-base parameters (pH, pCO_2, and HCO_3^- concentration) changes along hemodialyzer at different times during dialysis session for LC04 patient. pO_2 is not represented due to its too large fluctuations. This patient has been selected due to the monitoring of 3 HDF and 1 HD session.

Figure IV.11 represents changes in pH along hemodialyzer at different time during dialysis session for LC04 patient.

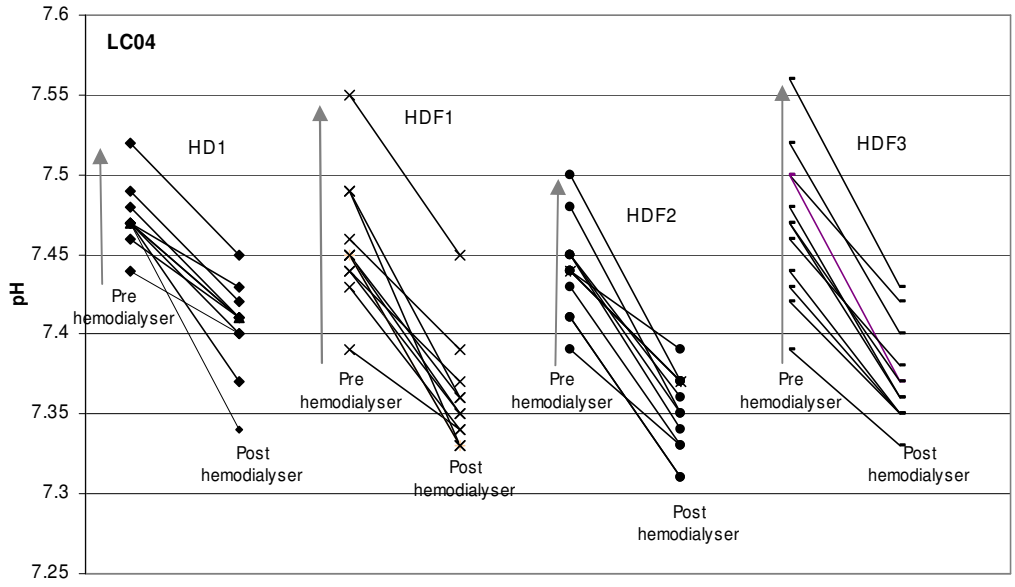

Figure IV. 11 Changes in pH along hemodialyzer in HD1, HDF1, HDF2, HDF3 of LC04 patient. The vertical arrows indicate the chronology of measurements

As seen previously, pH decreases in HD and in HDF sessions between pre and post hemodialyzer: the mean decreases are 0.92% for HD1, 1.33% for HDF1, 1.22% for HDF2 and 1.31% for HDF3.

Figure IV.12 represents changes in pCO_2 status along hemodialyzer at different time during dialysis session for LC04 patient.

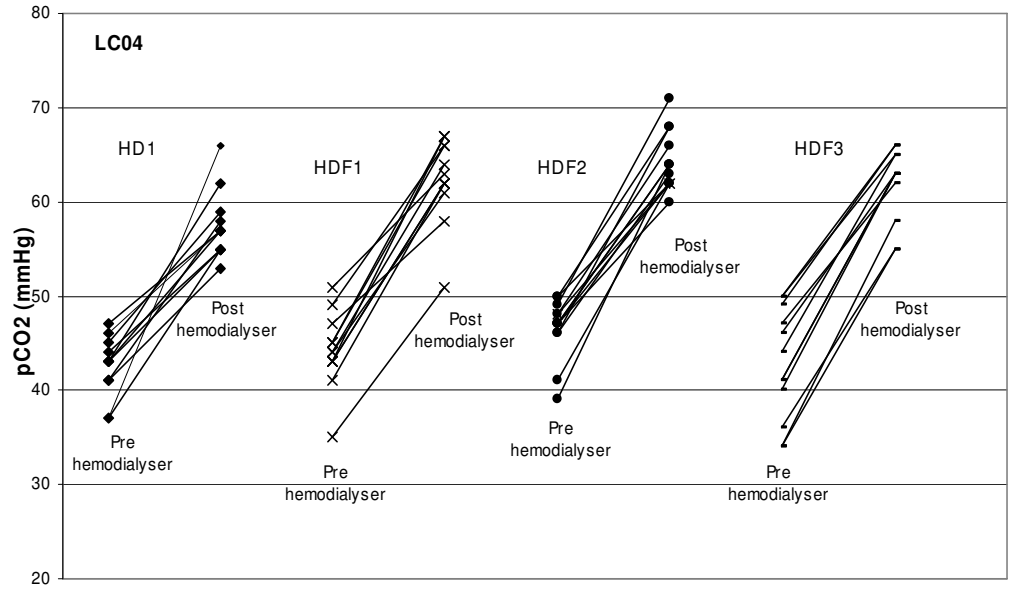

Figure IV. 12 Changes in pCO_2 along hemodialyzer in HD1, HDF1, HDF2, HDF3 of LC04 patient

As seen previously, pCO_2 increases in HD and in HDF session between pre and post hemodialyzer: the mean increases are 35.76% for HD1, 45.71% for HDF1, 38.18% for HDF2 and 45.31% for HDF3. For

pCO_2 it is not possible to indicate the time on Figure IV.12 due to pCO_2 variations during dialysis sessions between each pre-hemodialyzer samples.

Figure IV.13 represents changes in HCO_3^- plasma concentration status along hemodialyzer at different time during dialysis session for LC04 patient.

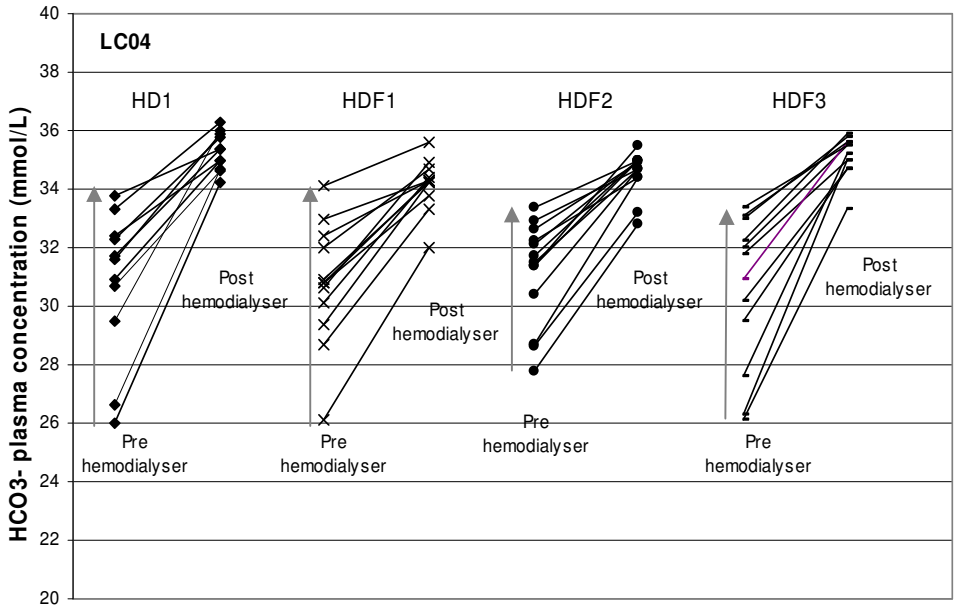

Figure IV. 13 Changes in HCO_3^- plasma concentration along hemodialyzer in HD1, HDF1, HDF2, HDF3 of LC04 patient. The vertical arrows indicate the chronology of measurements

As seen previously, HCO_3^- plasma concentration increases in HD and in HDF session between pre and post hemodialyzer: the mean increases are 14.61% for HD1, 14.05% for HDF1, 11.02% for HDF2 and 15.21% for HDF3.

These results about comparison between pre and post hemodialyzer on acid-base parameters can also be found for the three other patients and means that hemodialyzer membranes have a significant impact on acid-base parameters.

Moreover it can be seen that, while the rate (slope) of the increase through hemodialyzer for pH and pCO_2 stays constant during dialysis sessions, rate of increase HCO_3^- is higher at the beginning of the dialysis sessions than at the end. The final concentrations range is much smaller (about 2 mmol/L in HD mode) as compared to the initial one (about 8 mmol/L for HD1 and HDF1). As already seen previously, the HCO_3^- plasma concentration gradient through the hemodialyzer is higher at the beginning of the dialysis session than at the end.

We can also observe that there is a good reproducibility between sessions for the same patient which give confidence in our results.

3.2. How acid-base transfers take place inside the hemodialyzer?

In this section, we try to explain how acid-base transfers take place inside the hemodialyzer by considering first the HD mode.

HCO_3^- influx

Hemodialysis is not effective in removing large quantities of H^+ ions, due to their low concentration in blood (about 40 nmol/L at pH = 7.4). Therefore the removal of H+ during dialysis is considered negligible.

Dialysis fluid contains not only 38 mmol/L of HCO_3^- but also an additional source of alkali of 3 mmol/L of acetate. The acetate diffuses into the blood and is metabolised into various end-products (via Krebs cycle), and one HCO_3^- molecule is formed for each acetate molecule utilised. But this mechanism takes place in the liver, in the heart and muscle and does not interfere in acid-base transfer inside the hemodialyzer.

When treatment starts, HCO_3^- diffuses from dialysis fluid into the blood. This transfer is affected by the efficiency of the treatment (blood and dialysis fluid flow, surface area of the hemodialyzer…) and is highest at the beginning of the dialysis session (as seen in Figures IV.2 and IV.9). Plasma HCO_3^- is directly influenced by the dialysis fluid HCO_3^- concentration.

The rapid addition of HCO_3^- to the blood generates a buffer response (from non-bicarbonate buffer): the non-bicarbonate buffers in blood (hemoglobin, phosphate and plasma protein) are regenerated to their anionic form (Grassmann et al. 2000):

$$\underset{\text{Non bicarbonate buffer}}{AH} + HCO_3^- \rightarrow \underset{\text{Regenerated buffer}}{A^-} + H_2CO_3 \rightarrow H_2O + CO_2 \qquad \textbf{IV. 3}$$

This reaction consumes one HCO_3^- molecule to regenerate one of non-bicarbonate buffer.

There is also a metabolic production of organic acids (such as lactate or acetoacetate). These organic acids produce organic anions which are removed by dialysis and this loss of organic anions is equivalent to alkali loss (Feriani et al. 2004).

CO_2 influx

Because of differences in pCO_2 between plasma and dialysis fluid, some dissolved CO_2 diffuses to the patient during hemodialysis.

In summary, we should expect an alkalinization in the blood compartment, but transfers of CO_2 from dialysis fluid to blood may first occur, leading to a greater magnitude of change in pCO_2 than in HCO_3^- and to a further acidification of the patient's blood because as seen previously pH at hemodialyzer outlet is lower than pH at hemodialyzer inlet. These transfers are schematised in Figure IV.14 for HD mode.

In Figure IV.14 we have separated blood into plasma and red blood cells in order to try to understand the influx to HCO_3^- and CO_2 in blood inside the hemodialyser.

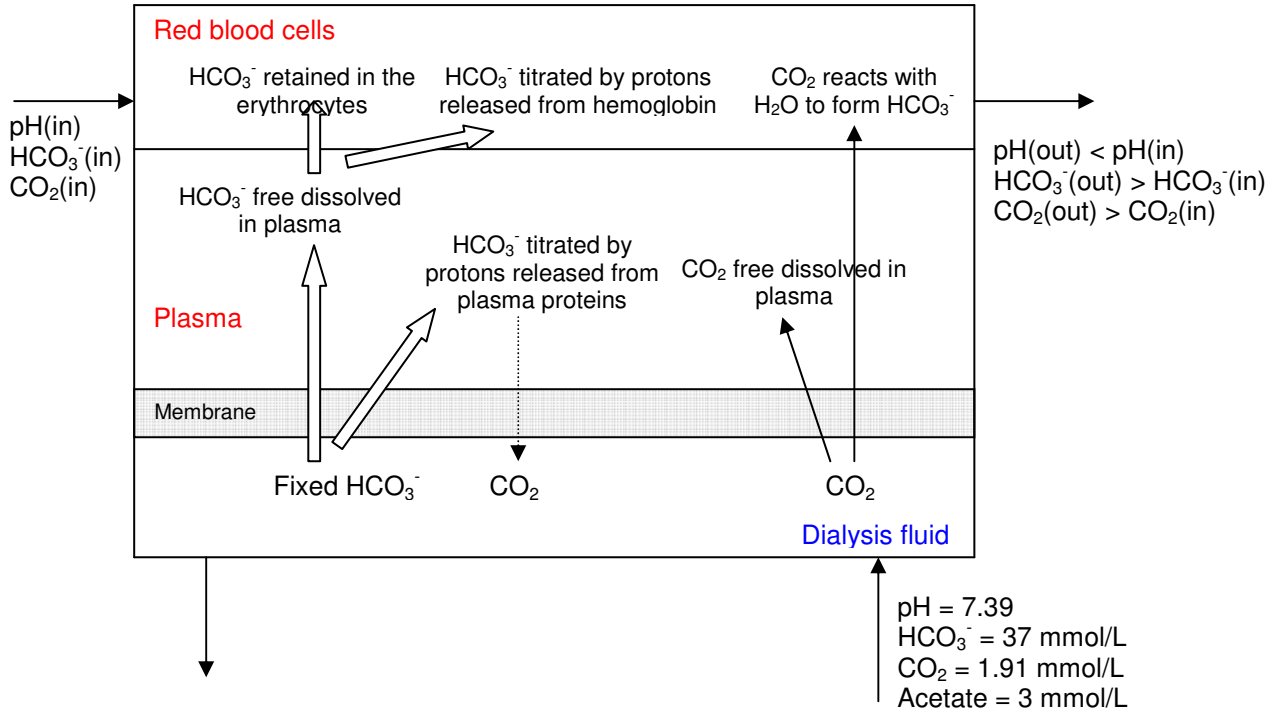

Figure IV. 14 Mechanism of HCO_3^- and CO_2 transfers inside the hemodialyzer in HD mode. *In vivo* dialysis fluid characteristics are taken from Table II.12

When blood enters in contact with dialysis fluid through hemodialyzer membranes, mechanisms of chemical reactions appears leading to consumption or reduction of HCO_3^-, CO_2 or H+ amount. As these three solutes are always linked between each other due to equilibrium equation (presented in Chapter II), it is not easy to isolate all phenomena and to take them separately.

Therefore we have presented the possible interactions of acid-base parameters between blood and dialysis fluid in Figure IV.14.

It can be observed that inside the red blood cells, chemical reactions are also present leading to variations of the HCO_3^- and CO_2 concentrations.

We can assume that HCO_3^- transfers from dialysis fluid to blood do not only help to restore the free HCO_3^- in plasma but also regenerate the non-bicarbonate buffer of plasma (plasma protein and hemoglobin). This means that the HCO_3^- amount measured at the outlet of the hemodialyzer could be

reduced contrary to the value that we could be obtained if these buffers are not present, and this could be due to the consumption of HCO_3^- by the non-bicarbonate buffer.

But what makes the problem still more complex is that base transfer can also be achieved by convection. During HD, weight loss is achieved by ultrafiltration of plasma water. This process leads to small HCO_3^- loss which continuously interferes with diffusion process.

Figure IV.14 can be seen close to Figure I.15 (Chapter 1) but represents the instantaneous transfers of HCO_3^- and CO_2 through the hemodialyser membrane.

In postdilution HDF

In HDF due to the high ultrafiltration, large amounts of HCO_3^- are lost in the dialysate and the reinjection of dialysis fluid after the hemodialyzer allows substitution of bases lost by ultrafiltration and increases of plasma HCO_3^- concentration (la Greca et al. 1989).

Therefore due to diffusion and convection process, various chemical reactions can take place inside the hemodialyzer in blood but also in dialysis fluid side. In this section, we try to identify all mechanisms that can appear but without giving a clarification of them. Nevertheless, investigation of these mechanisms will be extended in the following Chapter V where *in vitro* bicarbonate transfers in blood and in dialysis fluid are studied.

4. Conclusions

This chapter has presented an overview of the *in vivo* dialysis sessions performed up to now. The evaluation of the acid-base parameters shows that the initial (at beginning of dialysis) and the final (at the end) values of pH and HCO_3^- concentration are significantly different. Moreover, as statistical analysis of this preliminary study does not reveal any differences between HD and HDF sessions as far as initial and final states of the acid-base parameters are concerned, it can be concluded that HDF is not likely to create more ionic unbalances than HD. This chapter has also presented acid-base parameters time variations for GV05 patient as well as its variation along hemodialyzer. For the other patients similar trends have been observed. This study reveals that the results are consistent and reproducible between sessions of the same patient. However, there are some phenomena (for example, pO_2fluctuations) difficult to explain but which are probably related to the status of each patient and the small sample size. Finally, a synthesis of the hemodialyser transfers of the acid-base parameters has been investigated showing the possible interactions between HCO_3^- and CO_2 from blood and dialysis fluid through the hemodialyser membrane.

The following chapter is dedicated to the quantification of the *in vitro* and *in vivo* dialysis sessions regarding one of the acid-base parameters, the bicarbonate.

Chapter V Quantification of *in vitro* and *in vivo* dialysis sessions regarding bicarbonate

Résumé du Chapitre V

Ce chapitre porte sur l'analyse des sessions *in vitro* et *in vivo* appliquée à la restauration de l'équilibre acide-base. La concentration en bicarbonate a été utilisée comme paramètre représentatif de l'équilibre acide-base. La quantification de la séance de dialyse quant au bicarbonate, a porté sur l'étude des transferts de masse par unité de temps (hémodialyseur avec Mbh et Mdh et patient avec Mbp) et sur l'étude de la dialysance.

Après un rappel de la méthodologie et des équations employées pour les calculs de transferts instantanés de bicarbonate, l'étude des transferts de bicarbonate fait l'objet de la seconde section de ce chapitre. Les résultats *in vitro* et *in vivo* montrent un transfert (perdu par le sang) entre l'entrée et la sortie de l'hémodialyseur, négatif en HD et positif en HDF. Ce résultat signifie que, le long de l'hémodialyseur, en HD, le sang du patient « gagnerait » du bicarbonate alors qu'en HDF, il en perdrait. Lorsque l'on observe le transfert « patient », en tenant compte de la réinjection postdilution en HDF, il apparaît que les transferts en HD et en HDF sont similaires : en HDF, la réinjection a corrigé le déséquilibre causé par la forte ultrafiltration.

La troisième section est dédiée à l'observation des différences pour les transferts de bicarbonate calculés coté sang et coté dialysat : en effet, des effets chimiques tels que des réactions du bicarbonate pour régénérer les tampons non-bicarbonate ou encore le piège de bicarbonate dans les membranes de l'hémodialyseur peuvent se produire, ce qui modifierait la valeur réelle du transfert de bicarbonate au travers des membranes de l'hémodialyseur. Lorsque l'on calcule la dialysance du bicarbonate, qui utilise cette notion de transferts de masse coté sang, on constate qu'elle décroît lors des essais *in vitro* et *in vivo*. Ce résultat est inattendu car la dialysance, comme la clairance devrait être indépendante de la concentration du soluté et rester constante durant la session de dialyse. Ce résultat suggère que pour le bicarbonate, la dialysance ne serait pas un paramètre représentatif de la quantité de bicarbonate « rechargée » pour le patient.

Ce chapitre termine par la présentation de deux notions qui permettent aussi de quantifier la « recharge » en bicarbonate du patient : l'une d'elle porte sur la détermination expérimentale de la concentration de bicarbonate en fin de dialyse et l'autre traite du calcul du gain plasmatique de bicarbonate au cours des séances *in vitro* et *in vivo*.

In this chapter, we are interested in describing the quantification of the dialysis session regarding the acid-base balance. Bicarbonate (HCO_3^-) concentration has been taken as the parameter representing the acid-base balance as ESRD patients mostly suffer of metabolic acidosis which needs to be corrected during dialysis sessions. The bicarbonate correction along the dialysis sessions is quantified using mass flow rates (mass transfer per unit of time) along the hemodialyzer membrane and HCO_3^- dialysance. The two last sections of this chapter are dedicated to the other two parameters of evaluation of the dialysis sessions about HCO_3^-: final plasma HCO_3^- concentration estimated from the initial one and plasma HCO_3^- gain during *in vitro*, modeling and *in vivo* dialysis sessions.

1. Transfer equations

In this section, mathematical relations are derived to determine the amount of bicarbonate transferred to blood through the hemodialyzer or for the patient.

The principle of mass balance is applied for the establishment of equations involving blood and dialysis fluid input and output concentrations and flow rates. Figure V.1 represents the extracorporel dialysis circuit. Mbh, Mdh and Mbp described in the following by their equations have been represented on Figure V.1.

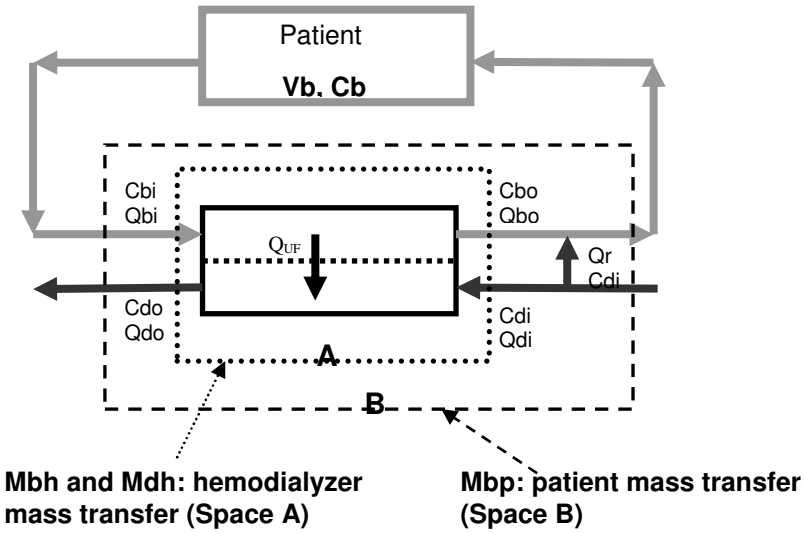

Figure V. 1 Extracorporeal dialysis circuit representation in HDF postdilution and representation of the hemodialyzer mass transfer (Mbh and Mdh) and of the patient mass transfer (Mbp)

The solute mass transfer per unit time, Mbh (mmol/min) from blood to dialysate through the hemodialyzer membrane is given by

$$Mbh = QbiCbi - QboCbo \qquad \textbf{V. 1}$$

This mass transfer can also be calculated in the dialysate by

$$Mdh = QdoCdo - QdiCdi \qquad \textbf{V. 2}$$

If the amount lost by blood reaches the dialysis fluid, we should find Mbh = Mdh. This equation will be used to check the consistency and the validity of our data.

In HD, QboCbo is equal to the mass flow rate returning to the patient. But in postdilution HDF with a reinjection flow rate Qr, the mass flow rate returning to the patient is QboCbo + QrCdi.
Thus in postdilution HDF, the net mass transfer gained by the patient per unit time (Mbp) is

$$Mbp = QboCbo + QrCdi - QbiCbi = QrCdi - Mbh \qquad \textbf{V. 3}$$

This representation of Mbp has been taken in order to obtain a positive Mbp (as blood is refilled of HCO_3^-) and to compare our *in vitro* transfers to clinical data from the literature.
Mbh, Mdh and Mbp represent the mass flow rate of the solute in mmol/min.

As seen, Mbh and Mdh reflect the mass flow rate of the solute along the hemodialyzer whereas Mbp reflects the mass flow rate of the solute for the patient (by taking into account the reinjection). Table V.1 gives the meaning of these transfers if they are positive or negative.

Mbh, Mdh or Mbp	Definition of the solute state
Mbh > 0	the solute is lost by blood (in space A)
Mbh < 0	the solute is gained in blood (in space A)
Mdh > 0	the solute is gained in dialysis fluid (in space A)
Mdh < 0	the solute is lost by dialysis fluid (in space A)
Mbp < 0	the solute is lost by blood (in space B)
Mbp > 0	the solute is gained in blood (in space B)

Table V. 1 Definition of Mbh, Mdh et Mbp for a solute. Space A and B refer to the Figure V.1

All these equations involve blood concentrations and blood flow rates. Since solutes are generally measured in plasma, as seen in Chapter I, blood concentration (Cb) relates to plasma (Cp) concentration by:

$$Cb = (1 - H + HK) \times Cp \qquad \textbf{V. 4}$$

Where H is the hematocrit and K the partition coefficient of a solute between plasma and red blood cells ($K = C_{RBC}/Cplasma$).

These mass flow rate equations have been used with experimental results (*in vitro* and *in vivo* data) and with theoretical results determined by the kinetic model for Cpi and Cpo.

2. Bicarbonate instantaneous transfers

This section presents HCO_3^- hemodialyzer (Mbh) and patient (Mbp) transfers variation with time applied to bicarbonate during *in vitro* and *in vivo* dialysis sessions.

HCO_3^- concentrations have been analysed by ABL. As laboratory HCO_3^- concentrations are measured in plasma, they need to be multiplied by (1- H + HK) with K = 0.57 for HCO_3^- to obtain blood concentrations.

2.1. *In vitro* study

For the *in vitro* study, operating conditions are Qb = 200 mL/min, Qd = 500 mL/min and no weight loss rate (Qw = 0) is applied.

In this section, experimental transfers are compared with theoretical transfers calculated using Cpi from the kinetic modeling and Cpo from Equation III.14.

2.1.1. Influence of the dialysis mode on transfers in the hemodialyzer

Figures V.2 show Mbh differences between dialysis mode for HD, HDF with Qr = 30 mL/min and HDF with Qr = 50 mL/min and for 2 various HCO_3^-dialysis fluid concentrations (Cdi_b of 32 and 40 mmol/L, respectively).

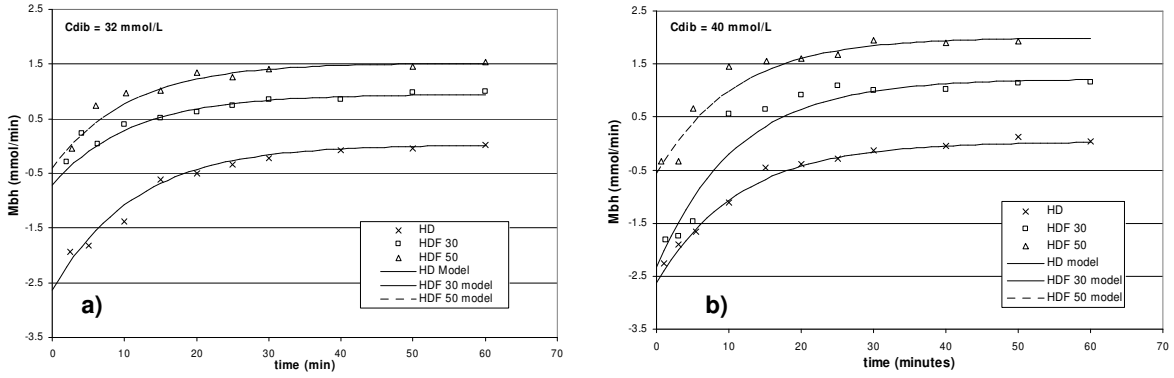

Figures V. 2 HCO_3^- Mbh for 3 tests using HCO_3^- dialysis fluid concentration of 32 mmol/L(a)) and 40 mmol/L (b))

HCO_3^- Mbh transfers through the hemodialyzer depends on the dialysis mode and seems to reach equilibrium after 30-40 minutes of the *in vitro* dialysis session.

In HD mode, this transfer remains negative since, in contrast to urea, HCO_3^- is gained by the *in vitro* patient only by diffusion (no ultrafiltration) from dialysis fluid. In HDF the transfer is negative at the beginning of the dialysis session since HCO_3^- concentration gradient is high enough to 'refill' the

patient's blood. Then this transfer becomes positive after 6-12 minutes when the plasma loss of HCO_3^- by ultrafiltration exceeds the diffusive transfer from dialysis fluid.

Figures V.2 also shows differences between the two various reinjection rates (Qr), 30 and 50 mL/min: the mass transfer is higher and the blood lose a higher amount of HCO_3^- at higher ultrafiltration flow rate.

We can also observe that this transfer depends on the initial HCO_3^- plasma concentration: the larger the difference between HCO_3^- plasma and dialysis fluid concentrations, the longer lasts the HCO_3^- plasma gain from dialysis fluid.

Agreement between theoretical and experimental data is very good for the 6 tests presented.

Analysis of these instantaneous HCO_3^- transfers across the hemodialyzer membrane during HD and online HDF postdilution can help to understand the mechanisms of HCO_3^- transfer: in HDF once Mbh becomes positive, blood is loosing HCO_3^-. Therefore the gain of HCO_3^- by the patient can be achieved by the reinjection fluid, as it will be seen in section 2.1.3 with patient transfers.

2.1.2. Influence of HCO_3^- dialysis fluid concentration on transfers in the hemodialyzer

In this section instantaneous mass transfers across hemodialyzer (Mbh) have been compared for the three various HCO_3^- dialysis fluid concentrations (28, 32 and 40 mmol/L) in two dialysis modes: HD and HDF 30.

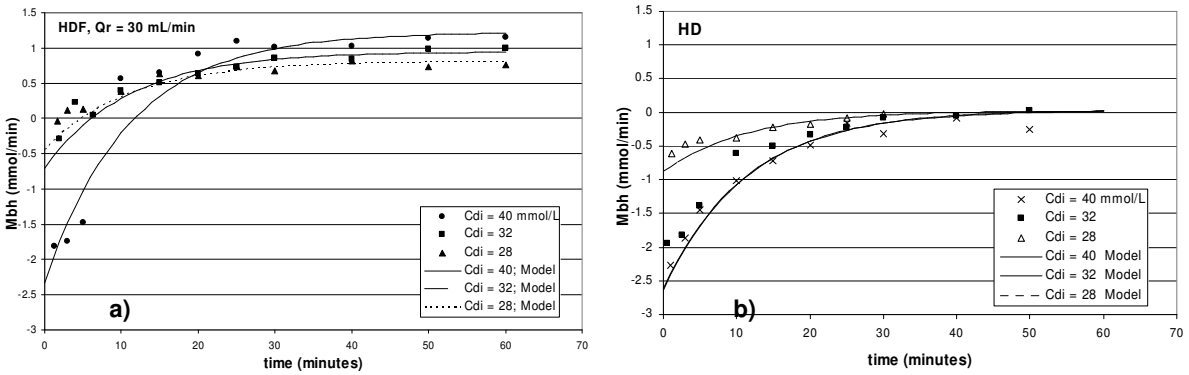

Figures V. 3 HCO_3^- Mbh for 3 various HCO_3^- dialysis fluid concentrations and 2 dialysis modes (HDF with Qr = 30 mL/min (a)) and HD (b)))

Figures V.3 show that Mbh transfers reach equilibrium after 40 minutes whereas the equivalent dialysis session time is 20 minutes. This suggests that in a real dialysis session, this transfer would never reach equilibrium.

In HD without ultrafiltration, the Mbh transfers reach zero as the HCO_3^- amount entering the hemodialyzer becomes equal to the HCO_3^- amount leaving the hemodialyzer: the *in vitro* 'patient' plasma concentration reaches the HCO_3^- dialysis fluid concentration.

Mass transfers for HD 32 and HD 40 tests are almost equal (Figure V.3 (b)) since the difference between initial plasma value and equilibrium value (given by Cdi) is almost the same.

In HDF with a reinjection flow rate of 30 mL/min the HCO_3^- amount entering the hemodialyzer is not equal to the amount leaving the hemodialyzer, due to ultrafiltration; but the Mbh transfer reaches equilibrium as the *in vitro* 'patient' HCO_3^- plasma concentration reaches the inlet HCO_3^- dialysis fluid concentration.
As for the previous section, agreement between theoretical and experimental data is very good for the 6 tests presented.

2.1.3. HCO_3^- mass transfers for the 'patient'

The variations of Mbp, the HCO_3^- mass transfer gained by the *in vitro* patient calculated by the model are represented in Figure V.4 for HDF 30 test (Qr = 30 mL/min).

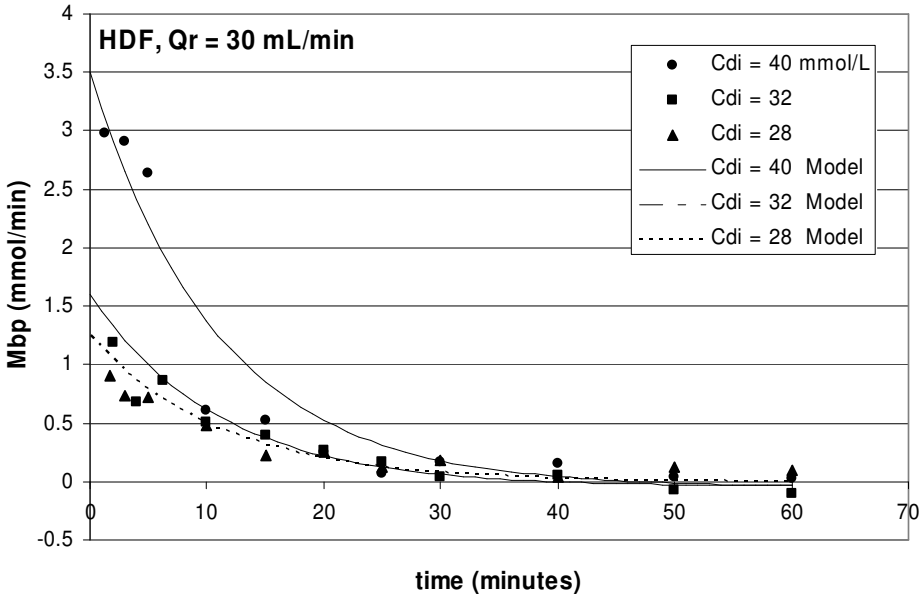

Figure V. 4 Patient mass transfer, Mbp (mmol/min) in HDF tests and Qr = 30 mL/min

Mbp mass transfers to the patient decay with time towards zero more or less slowly depending on initial plasma concentration because no further HCO_3^- amount from dialysis fluid occurs when plasma HCO_3^- concentration reaches HCO_3^- dialysis fluid concentration.
For the 32 HDF 30 test, Mbp decreases from 1.2 mmol/min at 3 minutes, until 0 at 30 minutes of the dialysis session. For 40 HDF 30, Mbp decreases from 3 mmol/min at 3 minutes, until 0.1 at 30 minutes. The agreement with the model is good in all tests even if the model always slightly overestimate experimental results.
In HD mode, as there is no reinjection flow rate, Mbp = -Mbh. That is why Mbp in HD sessions is not represented as Mbp is given by the opposite of Mbh in Figure V.3 (b).

2.2. *In vivo* study

For the *in vivo* study, operating conditions are Qb = 350 mL/min and Qd = 500 mL/min. The dialysis fluid HCO_3^- concentration is 38 mmol/L and a weight loss rate has been programmed for each patient as presented in Table IV.1 (Chapter IV). As the mean weight loss rate is around 12 mL/min (around 3.5% of Qb), ultrafiltration in HD sessions can be considered negligible.

As the kinetic model is not applied for the *in vivo* data, this section only describes the *in vivo* results about HCO_3^- mass transfers.

2.2.1. Hemodialyzer transfers

Figures V.5 give two examples of time changes of HCO_3^- transfers for SG03 and LC04 patients.

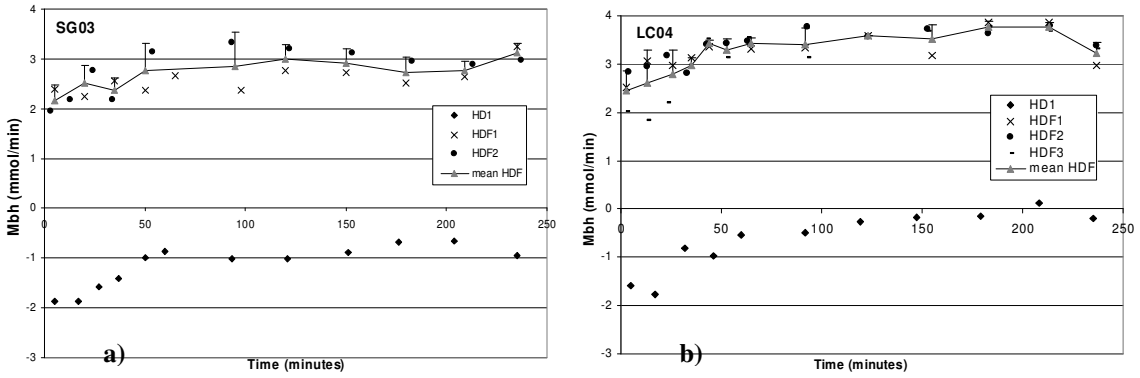

Figures V. 5 HCO_3^- hemodialyzer Mbh transfers for SG03 (a)) and LC04 (b)) patients. Experimental linked marks in grey show mean values of the HDF sessions

As two (for SG03) or three (for LC04) HDF sessions are carried out, mean ± SD is calculated (in grey on Figures V.5). The Mbh of HDF dialysis sessions have been compared and are found not significantly different under a significance level of 5%, as p value of the t-test is > 0.05. Even if physiologic differences can be very high from a patient to another, their transfers in HDF are nearly similar. This may be due to dialysis machine parameters (Qb, Qd, HCO_3^- concentration in dialysis fluid) which are identical in all sessions. Small differences are due to weight loss rate (Qw) and to reinjection flow rate (Qr) which can slightly change between patients.

For both cases, Mbh remains negative in HD sessions, as HCO_3^- is gained by the blood. On the opposite, Mbh is positive in all over HDF sessions. The Mbh transfers slightly increase during dialysis session: from -2 to -0.5-0 mmol/min in HD sessions and from 2 to 3-3.5 mmol/min for HDF sessions.

2.2.2. Transfers for the patient

Figures V.6 give HCO_3^- patient mass transfer (gained by the patient) for the same patients as in Figure V.5.

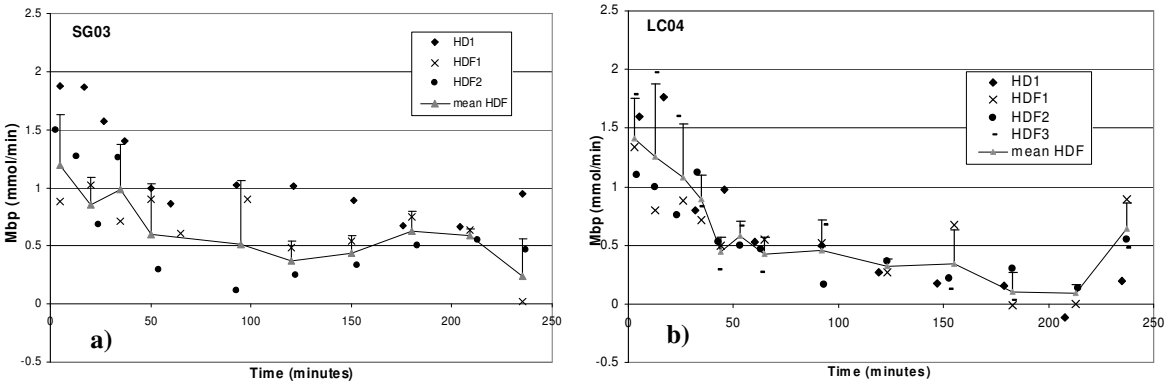

Figures V. 6 HCO_3^- patient Mbp transfers for SG 03 (a)) and LC04 (b)) patients

It can be seen that these transfers are positive and decay towards zero: from 2-1.5 until 0.5-0 mmol/min after 237 minutes. Pedrini et al. (2002) also calculated HCO_3^- instantaneous flux across the hemodialyzer in postdilution HDF and found transfer decay from 1.8 to 0.5 mmol/min at 175 minutes. This transfer depends on the initial HCO_3^- concentration: the lower the initial HCO_3^- plasma concentration, the higher the transfer of HCO_3^- from dialysis fluid to blood. For example, for SG03 patient, among its HD1, HDF1 and HDF2 sessions, HD1 has the lower initial HCO_3^- plasma concentration (26 mmol/L, against 28 mmol/L for HDF1 and 28.7 mmol/L for HDF2). Therefore at the beginning of the dialysis session, HD1 transfer is higher than that of HDF1 and HDF2.

HCO_3^- Mbp transfers are compared between HD and HDF sessions. For SG03 patient, HD1 transfer is statistically significant from those of HDF1 and HDF2 ($p = 0.004$ and 0.0012) whereas comparisons between HDF sessions are not statistically significant. For LC04 patient, Mbp transfers in HD1 are not statistically significant ($p = 0.8$ for the 3 comparisons) from those of the 3 HDF sessions. This may be due to initial HCO_3^- plasma concentrations which are very different in sessions for SG03 patient whereas for LC04 patient, initial HCO_3^- plasma concentrations are closer (as seen in Table IV.2).

2.3. Conclusion

Comparisons between *in vitro* and *in vivo* HCO_3^- transfers show that we obtain the same trends for these transfers. The HD transfers Mbh remain negative during dialysis sessions and tend toward zero whereas HDF Mbh transfers are positive and increase until equilibrium is reached (about 1.5 mmol/min for *in vitro* tests and 3 mmol/min for *in vivo* tests) in Figures V.3 and V.5.

Mbp mass flow rates decrease towards zero in HD and HDF mode in both *in vitro* and *in vivo* studies (Figures V.4 and V.6).

The differences between measured values are due to differences in hemodialyzer surface used for the *in vitro* (FX40, 0.6 m²) and the *in vivo* study (FX80, 1.8 m²) and from differences in the operating conditions (blood flow rate and reinjection flow rate).

3. Mass balance analysis Mbh/Mdh for bicarbonate

As samples are taken in blood side and also in dialysate side during the *in vitro* tests, it is wise to check the agreement between blood (Mbh) and dialysate (Mdh) mass flow rate.

For urea we have observed a good agreement between blood and dialysis fluid mass flow rate Mbh and Mdh. This result can be observed in the Annexe D (1st section, Figure D.1).

3.1. *In vitro* Mbh and Mdh: comparison for bicarbonate

For the determination of Mdh, experimental HCO_3^- inlet dialysis fluid concentrations (Cdi_b) analysed for each test have been used.

Experimental results for 2 tests (28 HD and 28 HDF with Qr = 30 mL/min) are given in Figure V.7.

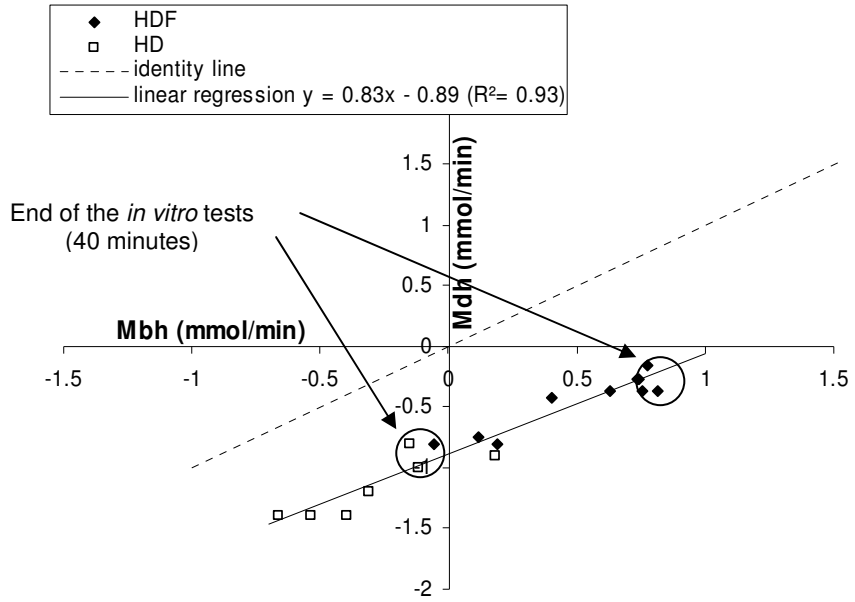

Figure V. 7 HCO_3^- Mdh in function of Mbh (mmol/min)

In contrast to urea transfers, Figure V.7 shows differences between Mdh and Mbh transfers for HCO_3^-.

In HD session, we observe that Mdh is negative, that is to say that dialysis fluid losses HCO_3^-. Mbh is also negative, that is to say that the blood gains HCO_3^- as expected. It can be seen that in absolute value, |Mbh| < |Mdh|: for example when the dialysate loses 1.5 mmol/min of HCO_3^-, the blood seems to gain only 0.5 mmol/min of HCO_3^-.

If the mass balance is correct from the dialysis fluid side, the transfer of HCO_3^- through the hemodialyzer membrane is 1.5 mmol/min. From the blood side, among these 1.5 mmol/min, 1 mmol/min 'disappears' and only 0.5 mmol/min is accounted for HCO_3^-.

If we now consider the HDF session, the only difference with HD is that 30 mL/min of plasma containing about 25 mmol/L of HCO_3^- are filtered through the hemodialyzer membrane, that is to say that blood lost about 0.75 mmol/min (25*0.03) of HCO_3^-. Under these conditions, the gain of HCO_3^- in blood side which is about 0 to 0.5 mmol/min in HD decreases of 0.75 mmol/min and becomes a loss of HCO_3^- between 0.25 and 0.75 mmol/min, that is to say a positive Mbh between 0.25 and 0.75 mmol/min, as seen in Figure V.7.
Similarly, the 0.75 mmol/min of filtered bicarbonate appears in the dialysis fluid. Instead of having a loss of HCO_3^- in the dialysate between 1 and 1.5 mmol/min, this loss is reduced by 0.75 mmol/min and then becomes between 0.25 and 0.75 mmol/min as also seen in Figure V.7.
Even if the two transfers (diffusion and convection) interfere but can not be added, we have shown a logical understanding of these transfers.

Moreover at the end of the dialysis session in HD mode, it can be seen that Mbh is close to zero whereas Mdh is about -1 mmol/min. This means that even if plasma does not seem to gain HCO_3^-, dialysis fluid continues to lose about 1 mmol/L of HCO_3^-. In HDF mode, Mbh is close to 0.75 mmol/min whereas Mdh is about -0.25 mmol/L.

Finally, the slope of the linear regression for HCO_3^- transfers (0.83) is very close to the one for urea transfers (0.82) as seen in Annexe D, whereas the intercept point at the origin is 0.89 mmol/min (close to 1), instead to be close to zero in the case where Mbh = Mdh.
This means that the same mass flow rate (of about 1 mmol/min) is 'lost' in the transfer between blood and dialysate.

The case in HDF mode seems impossible: we observe that Mdh < 0 and Mbh > 0. HCO_3^- amount can not be both lost from blood and lost from dialysis fluid. Nevertheless, it is what the data suggests in Figure V.7. In the following sections we try to understand this contradiction.

3.2. Correction in HCO_3^- blood transfers

In this section we do the hypothesis that no interactions of bicarbonate solute with other dialysis fluid components are possible. We consider that Mdh is correct and represents the real mass flow rate of HCO_3^- through the hemodialyzer membrane.

As explained for the HD mode, among 1.5 mmol/min of HCO_3^- transferred to blood, about 1 mmol/min disappears. Taking 0.9 mmol/min of HCO_3^- which disappears and correcting the Mbh mass

flow rates in 28 HD and 28 HDF 30 tests by subtracting 0.9 mmol/min, it can be find that Mbh becomes negative in 28 HDF 30. This means that the transfer of HCO_3^- is diffusive even in HDF mode.

Figure V.8 shows the good linearity between Mbh mass flow rate corrected by 0.9 mmol/min and Mdh transfers for the same *in vitro* tests as already seen (28 HD and 28 HDF 30 tests).

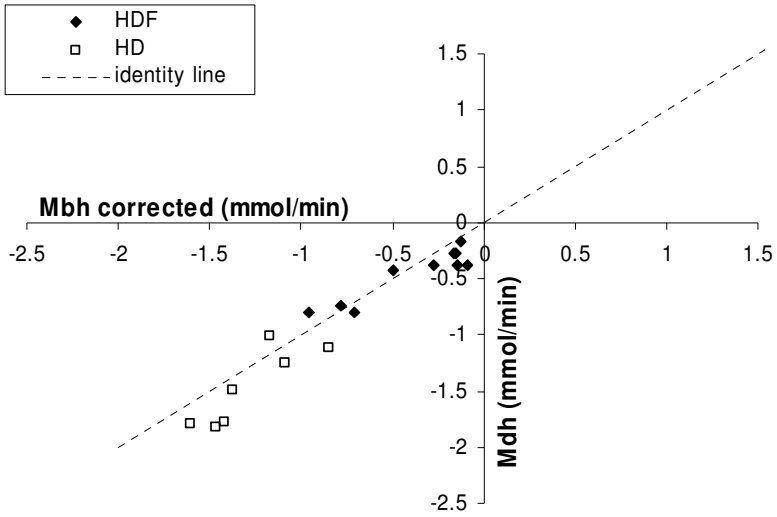

Figure V. 8 HCO_3^- Mdh in function of the Mbh corrected by 0.9 mmol/min in 28 HD and 28 HDF 30 tests

It can be seen that in HD mode, the gain of HCO_3^- in blood is between 1.7 and 1 mmol/L. As in HDF the blood lost about 0.75 mmol/L of HCO_3^- (see section 2.3.1. for more details), the gain of HCO_3^- in HDF mode becomes between 0.95 and 0.25 mmol/L as seen in Figure V.8.

In Figure V.9 the opposite of the HCO_3^- Mbp mass flow rate has also been represented using:

$$-Mbp = Mbh\ (corrected) - QrCdi = QbiCbi - QboCbo - 0.9 - QrCdi \qquad \textbf{V. 5}$$

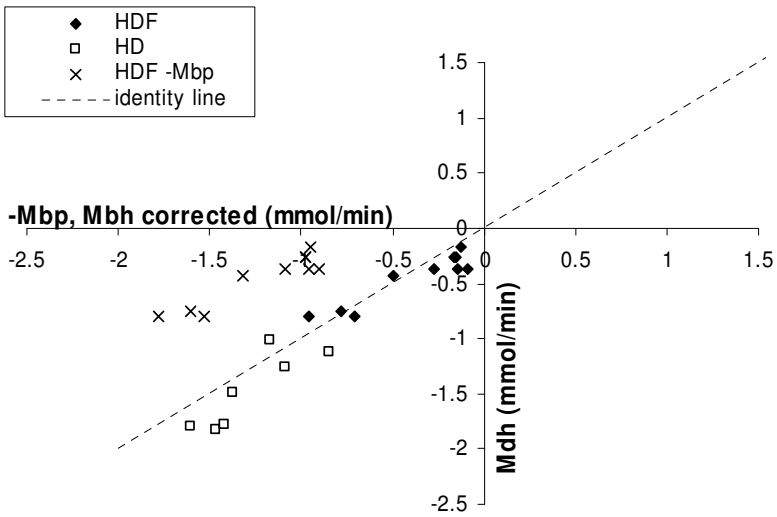

Figure V. 9 HCO_3^- Mdh in function of the Mbh corrected by 0.9 mmol/min for 28 HD and 28 HDF 30 tests and – HCO_3^- Mbp calculated with Mbh corrected for 28 HDF 30 test

It can be seen that -Mbp are more negative than Mbh. Moreover HD and HDF tests have the same range of –Mbp (in HD mode, Mbh = -Mbp as Qr = 0).
This correction is only applicable for our *in vitro* tests due to the small blood volume and the closed blood bag (no interaction with oxygen). Nevertheless we can wonder if we would also obtain the same difference between blood and dialysis fluid mass flow rates in dialysed patients.
Symreng et al. (1992) observed differences in these transfers analysed in blood and dialysis fluid compartments: at 60 minutes of dialysis sessions, mean HCO_3^- gain in blood is 0.319 ± 0.534 mmol/min whereas HCO_3^- gain in dialysis fluid is -0.660 ± 1.223 mmol/min. They did not comment these differences probably to the higher standard deviations than the means values which mean the high disparities of values and the difficulties to interpret these transfers.

3.3. How to explain these differences in HCO_3^- transfer?

It can be seen that these results for the *in vitro* HCO_3^- mass flow rates are consistent but are different from what we expect. They mean that instead of measuring HCO_3^- concentration in plasma, we should also measure it in the dialysis fluid. In practice, it is not always possible as dialysis machines are not equipped with a sampling site in the dialysis fluid line at hemodialyzer outlet (as seen in Chapter II, for our *in vitro* tests, special sampling sites have been added by us).

In this section, we try to understand these differences in HCO_3^- blood and dialysis fluid transfers by proposing different physiological hypotheses which are probably not distinct but can interfere: the HCO_3^- amount could be trapped by the non-bicarbonate buffers in blood or could be trapped inside the membrane.

In the previous section, we have corrected in the HCO_3^- blood transfers by 0.9 mmol/min. This disappearance of HCO_3^- blood transfers may be used to regenerate the non-bicarbonate buffers. The non-bicarbonate buffers (plasma proteins or hemoglobin) are not present in dialysis fluid, but only in plasma. These non bicarbonate buffers have also been presented in Chapter I (Figure I.14). As explained at the end of the Chapter IV, HCO_3^- solute can be found free dissolved in plasma but can also be titrated by protons released from plasma proteins. HCO_3^- can also be retained in erythrocytes in order to regenerate the hemoglobin buffers.

HCO_3^- could also be captured inside the membrane. Synthetic membranes as the Helixone® dialysis membrane (FX40 for *in vitro* tests and FX80 for *in vivo* tests) are asymmetric with two layers with different porosities: a thin layer named ‘skin layer’ of 1µm and a thick layer of 34 µm with larger pore. Immediately after contact of blood with synthetic membrane surface, plasma proteins (negatively

charged at pH = 7.4) begin to adsorb at the interface forming a thin layer during a low ultrafiltration of blood. Then blood cells (platelet and leukocytes) can adhere to the protein layer which may lead to activation of the blood coagulation system (Fazal Mohammad 1989) depending on the patient and its dose of heparin. With higher ultrafiltration (as in HDF), a thick protein deposit on the membrane is induced by the additional phenomenon of polarization. This progressively reduces the membrane permeability. The thickness of the protein layer depends on the wall shear rate value and is very important for the membrane performance (Ronco et al. 1998).
Therefore the transfer of solute should be easier from dialysis fluid towards blood than from blood to dialysis fluid due to the membrane asymmetry and the protein concentration polarization. The phenomenon of concentration polarization is reversible because proteins move along the membrane.

Considering these two phenomena, HCO_3^- solute could be titrated by non bicarbonate buffer or could be trapped inside the membrane. Other phenomena that we did not identify could also interact with HCO_3^-.

3.4. Conclusions

This section gives hypotheses that we can not confirm due the lack of knowledge about HCO_3^- and its reactions. Nevertheless we highlight the problem of differences in HCO_3^- mass flow rates between blood and dialysis fluid.
This problem shows that the real mass flux of HCO_3^- crossing the hemodialyzer membrane is altered by phenomena that lead to a disappearance of HCO_3^- in blood. If we consider that no interactions occur in dialysis fluid, therefore Mdh should represent this amount of HCO_3^- crossing the hemodialyzer membrane.
Nevertheless, our HCO_3^- Mbh and Mbp calculated previoustly with blood concentrations and flow rates (as seen in section 2) are still correct because they represent the amount of HCO_3^- what the patient really gains during its dialysis session.

In order to quantify the amount of HCO_3^- gained or lost by the patient, an usual possibility is to calculate dialysances. As the amount of HCO_3^- transferred from dialysis fluid to blood can react with other solutes in blood, our calculation of dialysance will probably not represent the dialysance as defined by theory. The following section investigates the bicarbonate dialysance during *in vitro* and *in vivo* studies.

4. Bicarbonate dialysance

As urea clearance represents the volume of blood cleared from urea per minute, HCO_3^- dialysance should represent the volume of blood refilled with HCO_3^- per minute. It thus represents an interesting index for the clinicians allowing the quantification of the dialysis session. Dialysance is described by the change in solute content of incoming blood divided by the concentration driving force (Sargent and Gotch 1989). As the clearance, the dialysance is expected to be constant during the dialysis session and should be independent of Cbi and Cdi.

Authors in the literature have always reported constant values for bicarbonate dialysance: 130 mL/min for Ursino et al. for a blood flow of 300 mL/min. Gennari (1996) explained that bicarbonate dialysance is a measure of the rate of HCO_3^- movement across the dialysis membrane, expressed as a clearance in mL/min, and is dependent on the hemodialyzer characteristics and on blood and dialysis fluid flow. In HD treatment, with Qb = 200 mL/min, Qd = 400 mL/min and using a cellulose membrane of 1.8 m², HCO_3^- dialysance is found to be 131 mL/min.

Urea clearances are calculated using *in vitro* data and are presented in Annexe D. It can be seen that urea clearances stay quite stable as expected, during the first 20 minutes of the *in vitro* dialysis sessions.

4.1. Method for HCO_3^- dialysance estimation

For bicarbonate, dialysance has been used instead of clearance, as bicarbonate concentration in dialysis fluid is different from zero. Equation has been corrected by the Donnan factor, α (Chapter 1), because the measured blood concentration Cbi (deduced from the measured plasma concentration) is not the concentration that is effective in the concentration gradient which is the driving force for the diffusive transport. For bicarbonate, α has been taken as 1.05.

Equations V.6 give the possible means of hemodialyzer dialysance calculation:

$$D = \frac{QbiCbi - QboCbo}{\alpha Cbi - Cdi} = \frac{QdoCdo - QdiCdi}{\alpha Cbi - Cdi} = \frac{Mbh}{\alpha Cbi - Cdi} = \frac{Mdh}{\alpha Cbi - Cdi} \qquad \textbf{V. 6}$$

In this section, bicarbonate dialysances have only been calculated using blood concentrations and flow rates (and not using dialysis fluid values).

In HDF, due to the composition of the reinjection flow rate, Qr, the mass returning to the patient become QboCbo + QrCdi, and the dialysance become the 'patient dialysance':

$$Dp = \frac{QbiCbi - QboCbo - QrCdi}{\alpha Cbi - Cdi} \qquad \textbf{V. 7}$$

Using the notation of mass transfer equations, patient dialysance is also equal to:

$$Dp = \frac{-Mbp}{\alpha Cbi - Cdi} \qquad \textbf{V. 8}$$

According to Equation I.26 (relation between blood and plasma concentration), patient dialysance becomes:

$$Dp = \frac{QbiCpi(1 - Hi + HiK) - QboCpo(1 - Ho + HoK) - QrCdi}{\alpha Cpi(1 - Hi + HiK) - Cdi} \qquad \textbf{V. 9}$$

Where the subscripts i and o mean hemodialyzer inlet and outlet, respectively and K = 0.57.

This equation giving Dp has been applied for *in vitro* and *in vivo* data in HD mode (where Qr = 0) and in HDF postdilution mode.

In all equations, measured Cdi values have been taken rather than theoretical Cdi values programmed by the dialysis machine in order to be as close as possible to experimental tests.

In order to compare *in vitro* results with those of modeling, theoretical Dp have been also calculated knowing Cpi from the model results and Cpo from the linear relations between Cpi and Cpo (3rd section of Chapter III).

4.2. *In vitro* and theoretical calculations

The variation of instantaneous HCO_3^- patient dialysance in HD tests is depicted in Figure V.10.

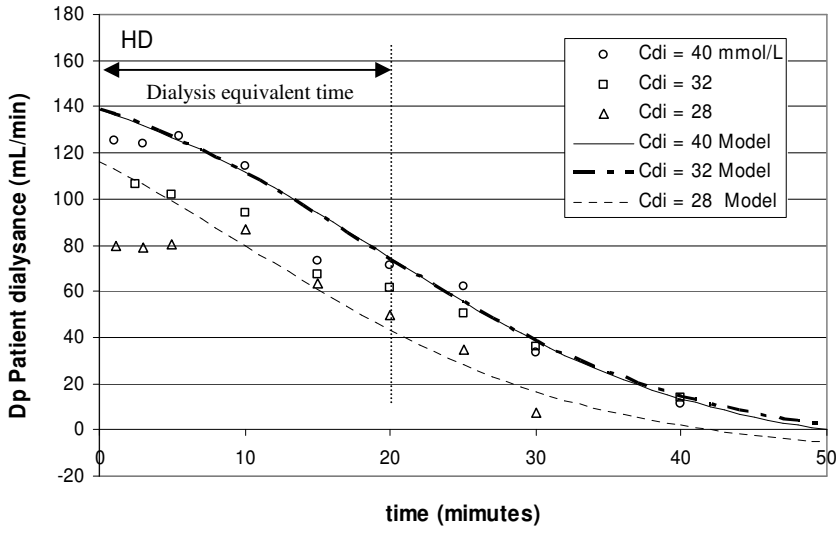

Figure V. 10 Patient HCO_3^- dialysance in HD tests

Dialysances unexpectively decay with time from 126 mL/min for test 40 HD and from 108 mL/min for test 32 HD to about 60 mL/min at t = 20 min (52% decreasing for 40 HD and 44% for 32 HD test). The fit between measured dialysance and that calculated by the model is good for test 40 HD, while the model overestimates data for 32 HD test at t<20 min.

Same results can be obtained for the 6 other *in vitro* tests.

4.3. *In vivo* HCO_3^- dialysance

All patients are dialysed using HCO_3^- dialysis fluid concentrations of 38 mmol/L, whereas the measured concentration is taken at 37.1 mmol/L for all dialysis machines.

Figures V.11 give the representation of HCO_3^- patient dialysance (Dp) variations with time for SG03 and LC04 patients.

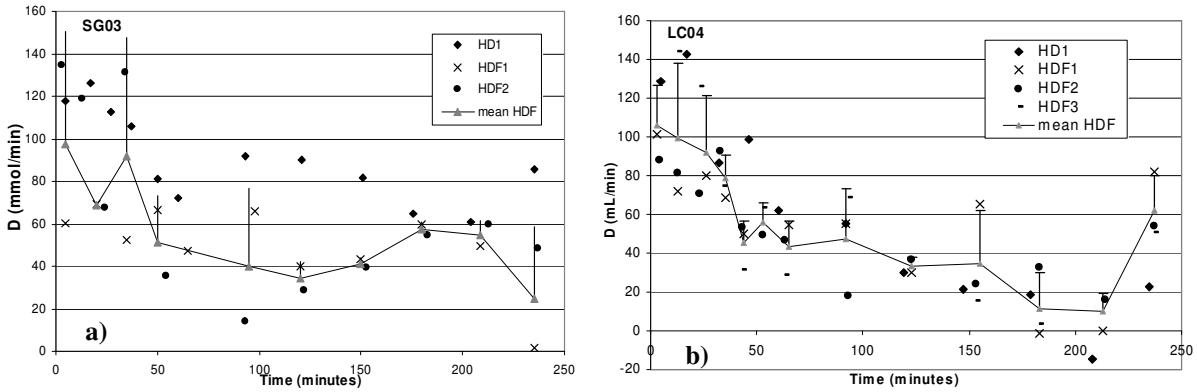

Figures V. 11 Bicarbonate dialysance (Dp) for SG03 (a)) and LC04 (b)) patient. Experimental linked marks in grey show mean values of the HDF sessions

HCO_3^- dialysances decrease with time during all dialysis sessions for both patients. This result can be found for all patients. In Chapter IV we have seen that plasma HCO_3^- concentrations time variations seem to increase until t = 100 minutes, and then remain stable. It could be the same for HCO_3^- dialysances with a decrease until t = 100 minutes and then HCO_3^- dialysances seem to reach a steady state (because of the fluctuations and the high standard deviation) but more data and patients are needed to confirm that observation.

4.4. Mathematical reason for dialysance decrease

In HD or HDF, there is a mass transfer across the hemodialyzer membrane if there is a concentration gradient (αCbi-Cdi). When approaching equilibrium during the dialysis treatment, the concentration gradient becomes smaller as αCbi becomes closer to Cdi. But this concentration gradient never reaches zero due to H and K correcting plasma concentration.

The HCO_3^- mass transfer (QbiCbi – QboCbo – QrCdi) decreases proportionally to the concentration gradient (αCbi - Cdi) as it exists a linear relation between the mass transfer and the concentration gradient. But the mass transfer decrease faster than the concentration gradient, therefore the patient dialysance given by the ratio of (QbiCbi – QboCbo – QrCdi) by (αCbi - Cdi) can not remain constant as seen in previous Figures (*in vitro* and *in vivo* results) and decreases with time.

For example for LC04 patient, at 92 minutes of its HDF1 session, |QbiCbi – QboCbo – QrCdi| decrease with time is 57% whereas that of |αCbi-Cdi| is 27% only. Nevertheless, this difference between |QbiCbi – QboCbo – QrCdi| and |αCbi-Cdi| seems to be constant after about 100 minutes dialysis session. But we need more dialysis sessions to confirm or not this hypothesis.

4.5. Conclusions

In our study, an unexpected result is that patient HCO_3^- dialysances are not constant, but decay with time towards zero for both HD and HDF during *in vitro* and *in vivo* studies.

As seen in section 3 of this chapter, for HCO_3^-, the mass transfers QbiCbi – QboCbo or QbiCbi – QboCbo – QrCdi does not represent the HCO_3^- mass flux through the membrane (J) due to the probably HCO_3^- reactions in plasma and red blood cell to regenerate non-bicarbonate buffer or due to HCO_3^- trapped inside the membrane: CbiQbi and CboQbo represent mass flow rate measured between the inlet and outlet of the hemodialyzer whereas dialysance is defined with J, the real mass flux through the hemodialyzer membrane.

Therefore the calculation of the dialysance using blood values is altered. Bicarbonate dialysances have been calculated using dialysis fluid concentration for 28 HD and 28 HDF 30 tests (tests presented in the 3rd section). Between the initial time of dialysis session and 20 minutes, dialysance with dialysis fluid values decrease about 17% for 28 HDF 30, and increase of about 7% for 28 HD test. With blood values, dialysance decrease about 61% for 28 HDF 30 and 40% for 28 HD test. Even if bicarbonate dialysance seems not to be stable using dialysis fluid values, the difference between initial time and 20 minutes is smaller than using blood values and is comparable to urea clearance also calculated for these two tests (Annexe D, Figures D.3).

We can write that J, the HCO_3^- mass flux that really passes through the hemodialyzer membrane should be higher than our J_{meas} measuring using blood and flow rate at hemodialyzer inlet and outlet. Therefore we should have:

$$D_{theo} = \frac{J}{\alpha Cbi - Cdi} > D_{cal} = \frac{QbiCbi - QboCbo - QrCdi}{\alpha Cbi - Cdi} \qquad \textbf{V. 10}$$

The calculated dialysance (D_{cal}) represented in Figures V.10 to V.11 would be then underestimated as compared to theoretical dialysance (D_{theo}), the one which can really estimate the efficiency of a hemodialyzer. This hypothesis still needs a deepened investigation.

To conclude on the bicarbonate dialysance, we can wonder if the dialysance concept is appropriate for bicarbonate as it can react with blood components inside the hemodialyzer.

5. Relationship between final and initial HCO_3^- concentration

In this section we represent the increase of HCO_3^- plasma concentration and the final HCO_3^- plasma concentration in function of the initial one for *in vitro* tests and *in vivo* dialysis sessions.
From these graphs we could deduce some experimental prediction of the increase of HCO_3^- plasma concentration or of the final HCO_3^- plasma concentration in function of the operating conditions and of the hemodialyzer characteristics in order to have an approximation of the patient HCO_3^- refilling.

This could help clinicians in their individualisation of the HCO_3^- dialysis fluid concentration.

5.1. ΔHCO_3^- plasma concentration as function of its initial value

5.1.1. *In vitro* study

Figure V.12 gives the rise of HCO_3^- plasma concentration (ΔHCO_3^- = final HCO_3^- plasma concentration – initial HCO_3^- plasma concentration) in function of its initial value for all *in vitro* tests without distinctions between HD and HDF sessions. Final HCO_3^- plasma concentrations have been taken at 20 minutes, the equivalent dialysis time and initial HCO_3^- plasma concentrations before the *in vitro* dialysis sessions.

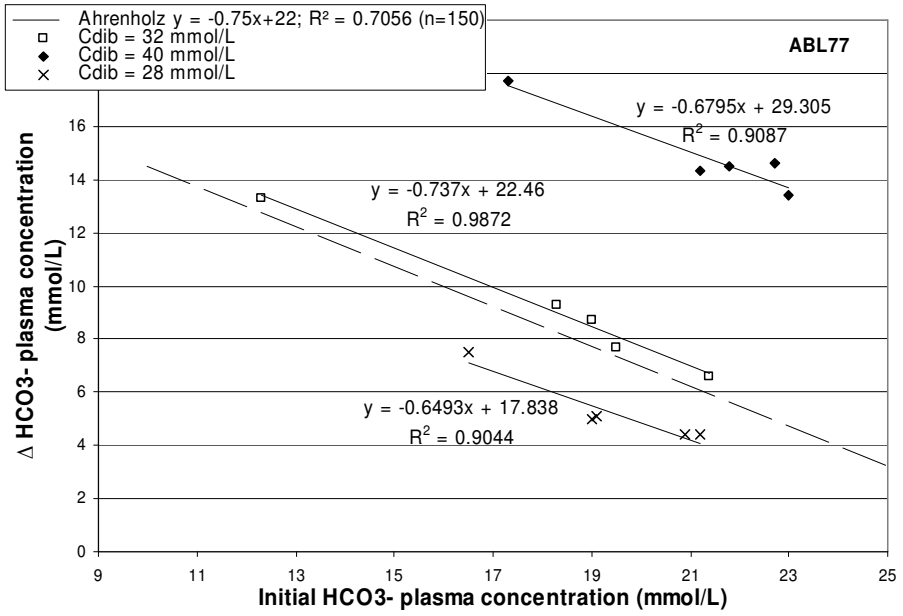

Figure V. 12 Rise of plasma HCO_3^- concentration in function of initial plasma HCO_3^- concentration. Ahrenholz correlation is given for dialysis fluid HCO_3^- concentration of 32 mmol/L. Cdi_b represents the dialysis HCO_3^- concentration of 28, 32 or 40 mmol/L

The increase in HCO_3^- plasma concentration during dialysis session depends on the initial HCO_3^- plasma concentration and on the HCO_3^- dialysis fluid concentration (28, 32 or 40 mmol/L).

No differences are observed between HD and HDF mode therefore Figure V.12 is given for HD and HDF sessions without any distinction.

The linear relationship between ΔHCO_3^- and initial HCO_3^- concentration means that the acid-base status of patients is corrected by hemodialysis without acid-base disturbance in HDF sessions. It can also be seen that the HCO_3^- dialysis fluid concentration determines the maximum plasma HCO_3^- concentration.

We found similar linear regressions as Ahrenholz et al. (1998). The Ahrenholz linear regression is given for 150 dialysis sessions in HD, in postdilution HDF and predilution HDF mode, using a HCO_3^- dialysis fluid concentration of 32 ± 1.5 mmol/L. It is very close to our *in vitro* results using also an HCO_3^- dialysis fluid concentration of 32 mmol/L.

5.1.2. *In vivo* study

Increases in plasma HCO_3^- concentrations have been represented in function of the initial one for the 23 dialysis sessions together with Ahrenholz et al. (1998) and Sepandj et al. (1996) correlations in Figure V.13.

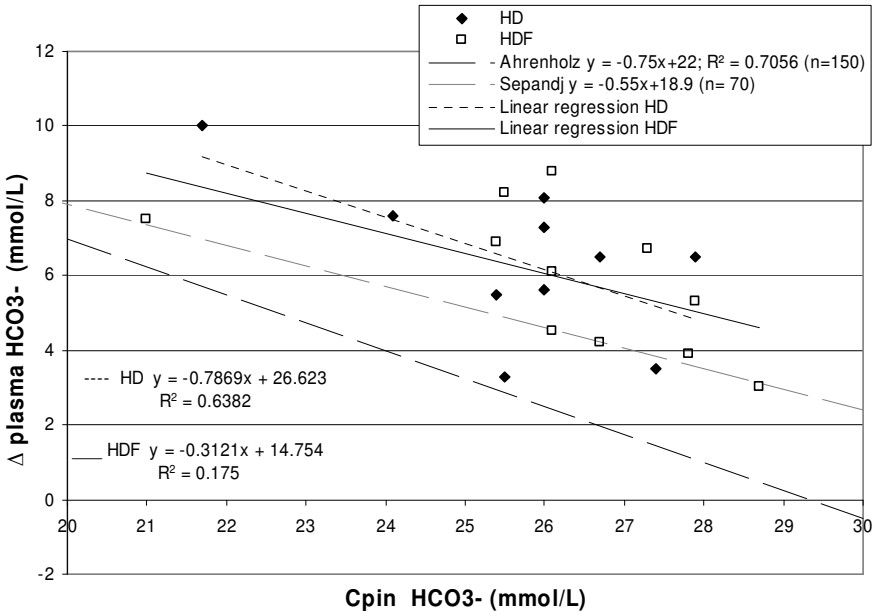

Figure V. 13 Rise of plasma HCO_3^- concentration in function of initial plasma HCO_3^- concentration. Ahrenholz linear regression is given for dialysis fluid HCO_3^- concentration of 32 mmol/L and Sepandj for 36 mmol/L.

Our findins are close to those of Sepandj in HD sessions with HCO_3^- dialysis fluid concentration of 36 mmol/L. They follow the same slope than Ahrenholz but ΔHCO_3^- is higher in our case since our HCO_3^- dialysis fluid concentration (38 mmol/L) is much higher than that used by Ahrenholz.

We observe the highest increase in plasma HCO_3^- concentration when initial plasma HCO_3^- concentration is the smallest. This means that in HD and HDF mode, acidosis is automatically corrected and that excessive compensation of the acid-base disturbance does not occur (Ahrenholz et al. 1998).
In Figure V.13 we do distinctions between HD and HDF sessions. HDF squared correlation coefficient is very low and we will need more HD and HDF sessions in order to conclude on differences between HD and HDF sessions.

If we compare Figure V.12 and V.13, we can observe that for the *in vivo* study, the ΔHCO_3^- is more dispersed than for the *in vitro* study. This is probably due to the larger patient distribution volume.

5.2. Can final HCO_3^- plasma concentration be estimated from the initial one?

5.2.1. *In vitro* study

In this section we have represented the final HCO_3^- plasma concentration as function of the initial one. Linear regressions between these two concentrations are given in Table V.2 for each HCO_3^- dialysis fluid concentration.

Dialysis fluid HCO_3^- concentration	Cdi_b = 28 mmol/L	Cdi_b = 32 mmol/L	Cdi_b = 40 mmol/L
Linear regression equations (mmol/L)	y = 0.35x +17.8 (R^2 = 0.734)	y = 0.26x + 22.4 (R^2 = 0.91)	y = 0.32x + 29.4 (R^2 = 0.69)

Table V. 2 Linear regression equations between inital (x) anf final (y) plasma HCO_3^- concentration

We can also propose a generalisation of the linear regressions given in Table V.2. As the mean slope of the 3 regressions is close to 0.31 and that the mean of differences between theoretical HCO_3^- dialysis fluid concentration and constant of the regressions is 10.1 mmol/L, the data suggest the following empirical correlation between the initial (Cpin) and final (Cpfin) HCO_3^- plasma concentration:

$$Cpfin = 0.31Cpin + (Cdi_b - 10.1) \qquad \textbf{V. 11}$$

Where Cdi_b is the theoretical HCO_3^- dialysis fluid concentration.

We prefer to use the theoretical HCO_3^- dialysis fluid concentration (programmed in the dialysis machine) than the measured HCO_3^- dialysis fluid concentration, since in practice HCO_3^- dialysis fluid concentration can not be measured.

This empirical correlation has been represented in Figure V.14 together with experimental results for the 17 *in vitro* tests.

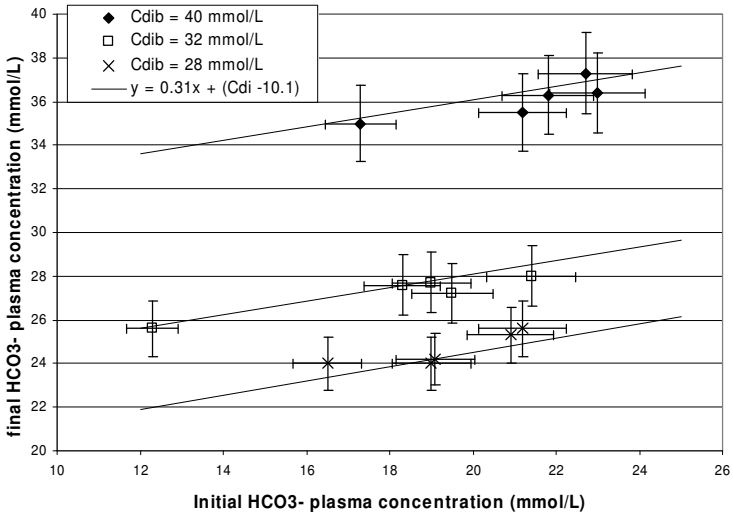

Figure V. 14 Final HCO_3^- plasma concentration in function of initial one. Cdi_b represents the HCO_3^- dialysis fluid concentration of 28, 32 or 40 mmol/L. The measurement errors are represented and are about 7% for HCO_3^- plasma concentration

We can observe that there is a good agreement between experimental results and the representation of Equation V.11. It can be seen that the maximum plasma concentrations remain always below the HCO_3^- dialysis fluid concentrations: the maximum HCO_3^- plasma concentration is about 37 mmol/L for Cdi of 40 mmol/L, 28 for Cdi of 32 and 25.8 for Cdi of 28.

5.2.2. *In vivo* study

For the 23 dialysis sessions, final plasma HCO_3^- concentrations have been represented in function of the initial one on Figure V.15.

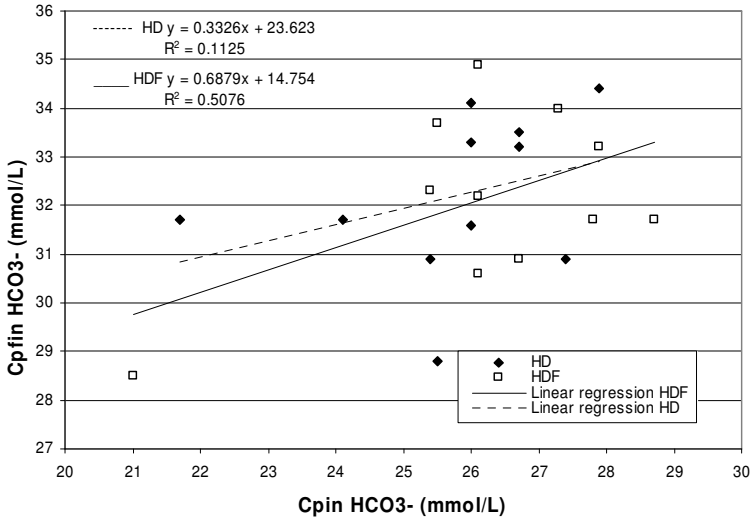

Figure V. 15 Final plasma HCO_3^- concentration (Cpfin) in function of the initial (Cpin) one for the 23 dialysis sessions

Figure V.15 shows that, even if initial plasma HCO_3^- concentrations are widely dispersed between 22 and 28 mmol/L for HD and between 21 and 29 mmol/L for HDF, there is a positive correlation between final and initial concentration with a higher slope for HDF than for HD. Nevertheless, the small squared correlation coefficient ($R^2 = 0.1125$) for HD sessions means that the linear regression can not be taken into account.

In HD sessions, mean initial and final HCO_3^- concentrations are 25.9 ± 1.65 mmol/L and 32.19 ± 1.68 mmol/L, respectively whereas in HDF sessions, mean initial and final HCO_3^- concentration are 26.24 ± 2.03 mmol/L and 32.15 ± 1.79 mmol/L respectively.

Even though patients are all dialysed using a 38 mmol/L dialysis fluid HCO_3^- concentration, final plasma HCO_3^- concentrations are well dependent of the initial one and also of each individual acid production and anion losses during dialysis session.

If we compare Figure V.14 and V.15 we can also observe the higher dispersion in final values for the *in vivo* study than for the *in vitro* study. We have tried to apply Equation V.11 to the *in vivo* study: no agreement can be found between the results of this equation and *in vivo* data, as *in vivo* final HCO_3^- concentration never reaches HCO_3^- dialysis fluid concentration contrary to *in vitro* data.

6. HCO_3^- plasma gain

Bicarbonate plasma gain during the entire dialysis session corresponds to the amount of plasma HCO_3^- that the patient receives during his dialysis session. It represents another parameter to quantify the final balance of dialysis sessions, and is often calculated by physicians.
In this section we propose to quantify this amount using *in vitro* tests and the *in vivo* data. The *in vitro* results are also compared to the modeling results.

6.1. *In vitro* study and modeling results

HCO_3^- plasma gains have been calculated by multiplying experimental values of Cpi and Cpo by initial and final plasma volumes of the *in vitro* tests. For all tests, initial and final blood volumes have been taken to 2 and 1.98 L respectively, as the final volume is calculated by subtracting samples volume taken during dialysis session from initial volume. Initial (Vp_in) and final (Vp_fin) plasma volumes (at 20 minutes of the dialysis *in vitro* sessions) have been calculated from initial and final hematocrit using: Vp_in = Vb_in(1- Hi + Hi*K) and Vp_fin = Vb_fin(1- Ho + Ho*K).

The results are presented in Table V.3 in mmol/test:

HCO_3^- dialysis fluid concentration (mmol/L) / Dialysis mode	40	32	28
HD	23.94	22.06	6.61
HDF 30	30.22	12.22	8.41
HDF 50	20.82	14.13	12.43
Mean	*24.99*	*16.14*	*9.15*

Table V. 3 HCO_3^- plasma gain in mmol/test for the 9 *in vitro* tests

The final balance of the tests shows differences in HCO_3^- plasma gain according to the 3 various HCO_3^- dialysis fluid concentrations (Cdi), with the highest values observed for Cdi of 40 mmol/L (23.94 in HD, 30.22 in HDF 30 and 20.82 mmol/session in HDF 50) and the lowest values for Cdi of 28 mmol/L (6.61 in HD, 8.41 in HDF 30 and 12.43 mmol/session in HDF 50). The HCO_3^- concentration in the dialysis fluid influences HCO_3^- plasma gains during the dialysis session.

These plasma gains also depend on the initial plasma concentration: for example for the 40 HDF 50 test, HCO_3^- plasma gain is low (20.82 mmol/session) compared to the 2 other tests using HCO_3^- in the dialysis fluid of 40 mmol/L. This test shows the highest initial HCO_3^- plasma concentration (23 mmol/L) and thus the difference between plasma concentration and targeted value (given by HCO_3^- dialysis fluid concentration) is small.

Using the kinetic modeling, we do a simulation using the same initial conditions (H = 30% and initial HCO_3^- plasma concentration = 21 mmol/L) for all configurations, in order to observe the influence of the dialysis mode independent of the initial conditions. Table V.4 summarises the results.

Dialysis mode \ HCO_3^- dialysis fluid concentration (mmol/L)	40	32	28
HD	27.4	13.45	8.4
HDF 30	27.9	13.62	8.5
HDF 50	28.13	13.68	8.54
Mean	*27.81*	*13.58*	*8.48*

Table V. 4 Theoretical HCO_3^- plasma gain in mmol/test calculated from the kinetic modeling using the same initial conditions (H = 30% and initial HCO_3^- plasma concentration = 21 mmol/L)

HCO_3^- plasma gain is slightly higher in HDF with a higher reinjection rate than in HD mode: for HCO_3^- dialysis fluid concentration of 32 mmol/L, the difference is 1.71% between HD and HDF50 mode. But this difference stay negligible and we can consider that there is no influence of the dialysis mode on our *in vitro* tests.

If we compare these data to the literature, it can be seen that our *in vitro* HCO_3^- plasma gains are very low compared to clinical data. This is due to our small blood volume 2L, compared to a HCO_3^- distribution volume between 30 and 40 L (depending of the body weight of the patient). HCO_3^- gains are generally given between 150 and 400 mmol/session (Feriani 1998, Pedrini et al. 2002) about 15 times more, corresponding to a volume 15 times larger. The following section presents the calculation of the HCO_3^- plasma gains using our *in vivo* data.

6.2. *In vivo* study

In dialysed patient, the HCO_3^- gain (BG) is difficult to quantify because HCO_3^- space is not constant during dialysis. Nevertheless this section attemps to estimate the plasma HCO_3^- gain using the *in vivo* resuls.

6.2.1. Method

As HCO_3^- Mbh transfers are calculated for all dialysis sessions. We can thus estimate the amount of HCO_3^- gained during HD sessions or lost during HDF sessions through the hemodialyzer by applying Equation V.12:

$$BGh = \int_{t0}^{t240} Mbh(t) \times dt \qquad \textbf{V. 12}$$

This integral from the beginning of the dialysis session (t0) until the end (t240) are estimated by trapezoidal rule for each segment where Mbh are calculated.

This amount (BGh) only represents the plasma HCO_3^- really gain or lost by the patient's blood (free dissolved HCO_3^-) after crossing the membrane of the hemodialyzer, as we can not estimate (if it exists) the amount of HCO_3^- used to generate the non-bicarbonate buffer or the HCO_3^- trapped inside the membrane.

In HD sessions, BGh is equal to BG as there is no reinjection rate. But in HDF session, the amount of HCO_3^- reinjected during HDF dialysis sessions (QBR) can be calculated by:

$$QBR = reinjection\ volume * HCO_3^-\ dialysis\ fluid\ concentration \quad \textbf{V. 13}$$

Where HCO_3^- concentration in dialysis fluid is 38 mmol/L for all *in vivo* sessions.

Therefore, HCO_3^- plasma gain (BG) is equal to

1) BG = BGh in HD sessions

2) BG = BGh + QBR in HDF sessions.

Table V.5 presents the HCO_3^- gain (BG) for each patient and each dialysis session.

Patient	Reinjection volume (L)	QBR = amount of bicarbonate reinjected (mmol/session)	BG (mmol/session)
PC01 HD3			268.99
PC01 HDF1	22	836	201.37
PC01 HDF2	19.1	725.8	na
MA02 HD1			288.87
MA02 HD3			265.2
MA02 HD4			na
MA02 HDF1	22.4	851.2	236.59
MA02 HDF2	22.7	862.6	208.09
MA02 HDF3	22.2	843.6	238.61
SG03 HD1			240.48
SG03 HDF1	20.6	782.8	174.36
SG03 HDF2	21.2	805.6	105.2
LC04 HD1			110.12
LC04 HDF1	24.1	915.8	112.99
LC04 HDF2	24.9	946.2	111.57
LC04 HDF3	24.2	919.6	138.25
GV05 HD1			159.99
GV05 HD2			203.0
GV05 HD3			179.18
LR06 HD1			148.13
LR06 HDF1	21.7	824.6	151.75
Mean ± SD **HD**			207.11 ± 62.15
Mean ± SD **HDF**			167.88 ± 51.37
Mean ± SD **All**	22.28 ± 1.69	846.71 ± 64.24	186.56 ± 58.67

Table V. 5 Amount of HCO_3^- reinjected in HDF postdilution sessions. Plasma bicarbonate gain, BG (in mmol/session). na = not available

In HDF the reinjection rate (Qr) differs for each patient (the nurse has to enter the total protein concentration for each patient). However the difference in QBR is low between sessions of the same patient.

It can also be seen that plasma HCO_3^- gains (BG) seem to have a higher average in HD than in HDF sessions: 207.11 ± 62.15 in HD and 167.88 ± 51.37 mmol/session in HDF sessions. It is not the case for all patients: for LC04 and LR06, BG are similar in HD as in HDF sessions whereas for SG03 and MA02, BG is higher in HD sessions than in HDF sessions. For the GV05 patient, its BG is very different from a session to another (there are 44 mmol/session between the highest and the smallest BG in HD sessions).
These differences may be due to the Mbh transfers unaccuracy. More data are necessary to conclude on differences in plasma HCO_3^- gain between HD and HDF sessions.

6.2.2. Apparent Bicarbonate Space (ABS)

The analysis of distribution volume for bicarbonate can be useful in order to quantify the base deficit in dialysed patients. The distribution volume for bicarbonate or apparent bicarbonate space (ABS) is calculated as the ratio of administered HCO_3^- (in mmol) to the observed change in plasma HCO_3^- concentration (in mmol/L).

Because the administrated HCO_3^- is dissipated by body buffers, the ABS has two components, an anatomical portion corresponding to extracellular water where HCO_3^- is freely diluted (dilutional space, DS) and a non-anatomical one where HCO_3^- is titrated by non-bicarbonate buffers (Titration space, TS). The ABS can be estimated in normal individuals as 40 to 50 % of the body weight as compared with an extracellular fluid volume of 20 % of the body weight (Adrogué et al. 1983).
By using the chemical laws of the buffering power, it is possible to extrapolate the following equation (Fernandez et al. 1989):

$$ABS = \frac{\text{Administrated}HCO_3^-}{\Delta HCO_3^- \text{ (P)}} = (0.4 + \frac{2.6}{HCO_3^-(P)}) \times W \qquad \textbf{V. 14}$$

Where the ABS volume is in L, HCO_3^- is plasma concentration (mmol/L) and W the body weight (kg). This equation can predict the distribution volume for HCO_3^- in any clinical condition. The ABS variation depends on the nature of the acid-base disorder.

Pedrini et al. (2002) have used this equation in order to estimate the plasma HCO_3^- gain (BG). BG is then calculated from the difference between the products of final and initial plasma HCO_3^- concentration by its final and initial apparent distribution volume:

$$BG_{pedrini} = Cpfin \times (0.4 + \frac{2.6}{Cpfin}) \times Wfin - Cpin \times (0.4 + \frac{2.6}{Cpin}) \times Win \quad \textbf{V. 15}$$

Where Cpfin and Cpin represent final and initial plasma HCO_3^- concentration (Cpi) and Wfin and Win the final body weight (after the dialysis session) and initial body weight.

But this method is not correct because Cpfin and Cpin only represent HCO_3^- freely diluted in plasma, while ABS represents the HCO_3^- in two components, diluted and titrated. Therefore this method has not been applied to our study.

Nevertheless initial and final ABS are estimated and Table V.6 presents the results together with percentage of the body weight. Initial ABS volume is calculated using Equation V.14 with initial weight (before the dialysis session) and initial HCO_3^- plasma concentration of each patient (at 3 minutes of the dialysis session). Final ABS volume is calculated using weight and HCO_3^- plasma concentration final values (3 minutes before the end of the dialysis session) for each patient. The initial and final ABS are estimated in percentage of the initial and final body weights respectively.

Patients	Initial ABS (L)	Initial ABS as % of the initial body weight	Final ABS (L)	Final ABS as % of the final body weight
PC01 HD3	35.65	50.79	31.91	48.2
PC01 HDF1	34.12	49.74	31.97	48.41
PC01 HDF2	36.14	52.38	32.42	49.12
MA02 HD1	45.03	49.32	41.9	47.56
MA02 HD3	45.36	50.24	42.17	48.41
MA02 HD4	44.61	49.74	41.55	47.76
MA02 HDF1	44.97	49.96	41.44	47.45
MA02 HDF2	45.23	50.2	41.8	47.72
MA02 HDF3	45.82	50.24	42.28	48.05
SG03 HD1	38.9	50	36.65	48.23
SG03 HDF1	39.01	49.32	36.35	47.83
SG03 HDF2	39.89	49.06	37.65	48.2
LC04 HD1	21	50	18.65	47.81
LC04 HDF1	20.78	49.96	19.16	48.5
LC04 HDF2	20.23	49.35	19.04	48.2
LC04 HDF3	20.68	49.96	18.99	48.07
GV05 HD1	27.32	49.49	24.79	48.41
GV05 HD2	27.56	50.2	25	49.03
GV05 HD3	26.56	49.74	24.39	47.83
LR06 HD1	43.75	50	40.11	47.62
LR06 HDF1	42.49	49.52	39.83	47.65
Mean ± SD **HD**	35.57 ± 9.26	49.95 ± 0.42	32.71 ± 8.89	48.09 ± 0.46
Mean ± SD **HDF**	35.4 ± 10.21	49.97 ± 0.88	32.81 ± 9.48	48.11 ± 0.47
Mean ± SD **All**	35.48 ± 9.52	49.96 ± 0.68	32.76 ± 8.97	48.10 ± 0.45

Table V. 6 Initial and final Apparent Bicarbonate Space (ABS) in L and their percentage of the initial and final weight respectively

Concerning the initial and final ABS values and their respective proportions of the body weight, there are no differences between HD and HDF tests. The initial ABS volume is higher than the final ABS one: 35.48 ± 9.52 L and 32.76 ± 8.97 L respectively.

As the initial weight of patient is higher than his final weight and since his initial HCO_3^- plasma concentration is smaller than the final one, results are coherent to find higher initial ABS than final ABS.

A statistical analysis (paired Student t-test) applied between initial and final ABS for the 21 dialysis sessions reveals that initial and final ABS are significantly different (under a significance level of 5%) with a p value < 0.05.

In patient suffering of severe metabolic acidosis, physicians can administrate a 'bolus' of sodium bicarbonate. Therefore they need to have an indication of the bicarbonate distribution volume: it is generally taken between 40 and 50% of the total body weight or approximately twice the extracellular fluid volume. By applying the Fernandez formula that can predit the distribution volume for bicarbonate in any clinical conditions, we find an encouraging result: our initial and final ABS represents nearly the same percentage of the body weight in all sessions (49.96 ± 0.68 % before and 48.1 ± 0.45 % after dialysis session).

7. Conclusions

This chapter was dedicated to the analysis of the bicarbonate transfers in blood and dialysis fluid during *in vitro* and *in vivo* tests. We have shown a good agreement between blood mass transfers in *in vitro* and theoretical data from the kinetic model and the same trends have been observed between *in vitro* and *in vivo* studies. Differences between HD and HDF transfers inside the hemodialyser are also observed. An unexpected result is the difference between mass flow rates through the hemodialyser calculated either from the blood or from the dialysis fluid side. This suggests the disappearance of bicarbonate in blood side. Another interesting result is that HCO_3^- dialysance seems to behave very differently from urea clearance, even though both solutes have similar molecular weight. HCO_3^- 'patient dialysance' decays with time during *in vitro* and *in vivo* dialysis sessions. This result suggests that, for bicarbonate, dialysance does not representing the amount of bicarbonate 'refilling' for the patient. This chapter concludes by presenting two concepts which can also quantify the 'refilling' of bicarbonate for the patient: the 1st is the experimental determination of the concentration of bicarbonate at the end of dialysis and the other is the plasma bicarbonate gain during the *in vitro* and *in vivo* sessions.

Chapter VI Conclusions and perspectives

1. Conclusions

This thesis focusses on the study during online hemodiafiltration (HDF) of the acid-base balance parameters: in order to quantify bicarbonate transfers during dialysis, a kinetic model, and an *in vitro* and *in vivo* analysis of its transfers have been undertaken.

The *in vitro* study is considered as a parametric study. Parameters (reinjection flow rate, dialysis mode and bicarbonate dialysis fluid concentration) have been varied in order to analyse their influence on the progress of the dialysis session. Our investigation revealed that different results can be obtained when measuring the same parameter in various methos (especially for bicarbonate concentration and hematocrit). The repeatability study about acid-base parameters for the *in vitro* tests shows very good results when using the same blood under the same experimental conditions. The analysis of the inlet dialysis fluid for the *in vitro* and *in vivo* tests, by our blood gas analyzer (ABL) shows that the standard deviation and the coefficient of variations are very low between tests and between dialysis machines. This important result indicates the consistency of our data and the reliability of dialysis fluid composition delivered by dialysis machines.

The implementation of the kinetic model (where the modeled system is the patient + hemodialyzer) has been achieved. The principal assumptions of this model are that the patient is modeled as a single compartment using mass balance equations and the mass transfers in hemodialyzer are calculated by a local model (Legallais et al. 2000) using diffusion and convection processes (and no chemical reactions). Initial and operating conditions are the one of the *in vitro* tests. Physical parameters have been found in the literature and other parameters such as membrane permeability or real ultrafiltration rate have been verified using the *in vitro* tests. The kinetic model has been validated: analysis of results confirms that our kinetic model is able to predict the *in vitro* intradialytic time (during dialysis session) of urea and HCO_3^- concentration with a good accuracy. We have found that HCO_3^- plasma concentration calculated by the kinetic model reaches the HCO_3^- dialysis fluid concentration, whereas the measured HCO_3^- plasma concentration always stays slightly below (the model predictions remain smaller than the 7% corresponding to experimental errors and blood gas analyzer accuracy). With urea, the kinetic model results fit well with the experimental results. We have seen that our *in vitro* study, although it represents the 'patient' by a small blood volume (2L), seems to reproduce adequately the kinetics of HCO_3^- and urea. The time to reach equilibrium is much smaller (20 min), than in a dialysis session. The *in vitro* results have been compared with literature data and these data show that our choice of scaled down blood volumes, blood flow rates (200 mL/min) and membrane area (0.6m²) leads to HCO_3^- kinetics close to those observed *in vivo*.

We have presented the methodology to analyse an *in vivo* preliminary study of 23 dialysis sessions for a total of 6 patients included. The statistical analysis of this preliminary study did not reveal any differences between HD and HDF sessions as far as initial and final states of the acid-base parameters are concerned. It can be concluded that the HDF technique is not likely to create more ionic unbalances than HD. Even if a larger number of dialysis sessions in HD and HDF mode would be needed in order to better appreciate acid-base parameter evolution, the investigation of the case study reveals that similar trends for acid-base parameters time variations are observed. An encouraging result is that time variations for each parameter in various sessions are consistent and are similar for different patients.

To pursue this analysis further, we then dedicated a chapter to the quantification of the *in vitro* and *in vivo* dialysis session regarding bicarbonate and calculated its mass transfers and dialysance. We found that *in vitro* and *in vivo* HCO_3^- hemodialyzer and patient mass flow rates, and dialysances follow the same time variations. Nevertheless, an important difference between these two studies concerns the final HCO_3^- plasma concentration: for the *in vitro* study, it reaches the HCO_3^- dialysis fluid concentration whereas for the *in vivo* study, it stays below even if the equilibrium has been already reached. When comparying bicarbonate mass transfer from both the blood and the dialysate sides, it was unexpectedly found that transfers from dialysis fluid were constantly higher, in both HD and in HDF modes, than those recorded on the blood side. This is probably due to the regeneration of the non-bicarbonate buffer by the HCO_3^- solute, some of the added bicarbonate is consumed in buffering the protons that are released from the non-bicarbonate buffers. Therefore the HCO_3^- dialysances usually calculated using blood HCO_3^- mass flux can not be a good parameter to quantify the 'refilling' of HCO_3^- by the patient. Both hemodialyzer and 'patient' dialysance calculated for the *in vitro* and *in vivo* studies are not constant, but decay with time towards zero for both HD and HDF.
HCO_3^- gain in plasma was calculated using the *in vitro* experiments results and the kinetic model: this HCO_3^- plasma gain is slightly higher in HDF with a higher reinjection rate than in HD mode but this difference is negligible and we can consider that there is no influence of the dialysis mode on our *in vitro* tests. However this gain depends on the bicarbonate dialysis fluid concentration: the plasma gain is 3.3 higher when bicarbonate dialysis fluid concentration is changed from 28 to 40 mmol/L. During the *in vivo* study, an encouraging result is that the final ABS (Apparent Bicarbonate Space) represents nearly the same percentage of the body weight in all sessions: 49.96 ± 0.68 % before dialysis session and 48.1 ± 0.45 % after dialysis session which is close to the literature data.

2. Perspectives

Although the described kinetic model can be a convenient tool to compare efficiencies of various HDF strategies or various hemodialyzers, it has only been applied and validated with our *in vitro* study. Consequently, in the following paragraph, suggestions are given for the extension of this kinetic modeling for application to *in vivo* data.
Other suggestions are also given to optimise the *in vivo* protocol as this clinical investigation could be extended.

2.1. Extension of the kinetic modeling applied to *in vivo* study

Our one compartment kinetic model applied for HCO_3^- has been validated using *in vitro* tests: with 2L blood plastic bag, which is assimilated to one compartment.
However in dialysis patients, it is not possible to represent the patient HCO_3^- pool by one compartement due to many interactions of HCO_3^- between extra and intracellular fluids.

Therefore we list the improvements that should be considered for a kinetic model applied for bicarbonate and extended for a dialysis patient:
- Two or more compartments for the representation of the patient HCO_3^- pool need to be examined: the sum has to represent the distribution volume of HCO_3^-. The problem of this HCO_3^- distribution volume is that it is variable and difficult to predict because of HCO_3^- interactions with buffer systems, both contained in intracellular and extracellular water and its elimination as CO_2 through the lungs. Nevertheless, we could try to use the Fernandez et al. equation (verified in our *in vivo* preliminary study) to predict the HCO_3^- distribution volume.

- As the local model (modified Legallais et al. model) describes HCO_3^- transfers between blood and dialysis fluid, it should be coupled with a chemical model in order to investigate the HCO_3^- reactions. The chemical model will have to take into account all equilibrium equations for HCO_3^- for the interactions between blood and dialysis fluid inside the hemodialyser.
Using experimental tests, we should calculate a rate of reaction Ri (mmol/s/L) to be included in the mass balance equation for the patient (presented in Chapter III):

$$\frac{d(Vb \times Cb)}{dt} = -QbiCbi + QboCbo + QrCdi + Vb(t)\sum_{i=1}^{n} Ri \qquad \textbf{IV.1}$$

In a recent paper of Choi and Lim (2009), a mathematical model of the reaction-diffusion kinetics of bicarbonate system in blood is presented. This work should be included in our model in order to explore the dynamics of the bicarbonate system. This enables to take into account the hidden mechanism of acid–base disorders in the clinical setting.

- To improve the knowledge of HCO_3^- transfers, other *in vitro* tests could be conducted using only plasma bags. Thus whole blood (as already done) and plasma transfers could be dissociated in order to separate the influence of the RBC on the HCO_3^- transfers.

- Then more *in vivo* data on blood and dialysis fluid transfers are necessary, in order to answer following questions: is the amount of blood bicarbonate lost independent of each patient or, on the contrary, also dependent on the patient physiology and its acid production or food uptake during the interdialytic period? Is this amount of trapped (or generated) bicarbonate constant during dialysis session? Or is it higher at the beginning than after 100 minutes (times from which we observe the stable plasma HCO_3^- concentration in the *in vivo* study) due to the regeneration of plasma and blood buffers first?

2.2. Suggestions for optimising the *in vivo* protocol

The *in vivo* study is going to continue from January 2010 in collaboration with the Nephrology and Pharmacy departments of Amiens Hospital. Patients have to be monitored during 3 consecutives HD and 3 consecutives HDF sessions (except on Monday or Tuesday to avoid the influence of the week-end).

- For few HD and in HDF dialysis sessions, samples of dialysis fluid at hemodialyzer outlet should be taken in order to compare HCO_3^- blood and dialysis fluid transfers.
We think that one of the 5008 dialysis machines of Amiens Hospital could be equipped by an additional sampling site on dialysis fluid line at hemodialyzer outlet.
We propose to collect outlet dialysis fluid samples for one patient (during its 3 HD and 3 HDF sessions to test the reproducibility of the data) at the same time when blood inlet and outlet samples are taken.
This procedure has to be repeated on at least 5 other patients (but during one of HD and one of the HDF sessions) in order to see if differences between patients can occur.

- Urea concentration should be analysed in inlet and outlet blood samples two times per dialysis session (30 minutes after the beginning and 30 minutes before the end) in order to calculate urea clearances and to compare them to urea clearance from OCM. This repetition will permit to verify if the urea clearance stays constant during dialysis session. This procedure should be realised on one patient during its 3 HD and 3 HDF sessions.

- Thanks to the high number of sampling, the preliminary study presented in this document shows high precision in HCO_3^- time variations and transfers. In future tests, fewer samples could be taken: +3 min,

+13 min, +23 min, +33 min, +43 min, +53 min, +90 min, +150 min, +210 min, +237 min. It will be important to respect this time sampling to order to compare concentrations between patients.

- ABL blood gas analyzer also analyse Na+, Cl-, K^+ and Ca^{2+} concentrations. These concentrations have been analysed but not commented in this preliminary study; they could be analysed in the future following a larger study for the ionic state.

For example, in case of acidosis, K^+ generally moves out of the cells and hydrogen (H+) ions enter the cells. During dialysis, acidosis is compensated by HCO_3^- uptake by blood from dialysis fluid. Then blood pH rises, causing K^+ to return to the cell in exchange for hydrogen ions. Therefore changes in acid-base balance affect the distribution of potassium in the body (Grassmann et al. 2000).

- Using the electrolyte concentrations, anion gap should also be calculated: anion gap (AG) is another tool for evaluating the acid-base disorders. It can be calculated by the difference between the sum of charges from plasma anions and cations and represents the concentration of all the unmeasured anions in the plasma. For all dialysis sessions of the 6 included patients, we have observed that the AG decreases during the dialysis sessions. This result is normal but should be compared between HD and HDF sessions. It is possible that the AG in an HDF session highly decreases (between intial and final values) due to the higher ultrafiltration than in an HD session (for the same patient). This assumption should be verified and analysed during the continuation of the project.

References

Abbott HJ and Ward RA. Acid-base Homeostasis in dialysis patients (Chapter 20). In Clinical Dialysis. 4th edition. McGraw-Hill Medical 2005

Adams AP and Hahn CEW. Blood-gas electrodes (Chapter 7; p49-63). In Principles and practice of blood-gas analysis. 2nd edition. Churchill Livingstone 1982

Aday LA, Cornelius LJ, and Cohen SB. Designing and Conducting Health Surveys: A Comprehensive Guide. 3rd edition. Jossey-Bass Inc U.S. 2006

Adrogué HJ, Brensilver J, Cohen JJ and Madias NE. Influence of steady-state alterations in acid-base equilibrium on the fate of administered bicarbonate in the dog. J Clin Invest 1983. 71(4):867–883

Ahrenholz P, Winkler RE, Ramlow W, Tiess M, Müller W. On-line hemodiafiltration with pre- and post-dilution: a comparison of efficacy. Int J Artif Organs 1997. 20(2):81-90

Ahrenholz P, Winkler RE, Ramlow W, Tiess M, Thews O. Online Hemodiafiltration with pre- and postdilution: impact on the acid-base status. Int J Artif Organs 1998. 21(6):321-7

BEH (Bulletin épidémiologique hebdomadaire) n°37-38 2005. L'insuffisance rénale chronique. http://www.invs.sante.fr/beh/2005/37_38/beh_37_38_2005.pdf

Bhagavan NV. Medical biochemistry. 4th edition. Jones & Bartlett Publishers 1992

Boure T and Vanholder R. Which dialyser membrane to choose? Nephrology Dialysis Transplantation 2004. 19(2): 293-6

Braconnier F, Dupeyrat A, Odelut P. Évaluation et utilisation de l'analyseur de gaz du sang Radiometer ABL77. Spectra biologie 2003. 22(133):63-65

Bray J, Cragg PA, Macknight ADC, Mills RG. Lecture notes on human physiology. 4th edition. Wiley-Blackwell 1999

Canaud B, Bosc JY, Leray H, Stec F, Argiles A, Leblanc M, and Mion C. Online hemodiafiltration: state of the art. Nephrology Dialysis Transplantation 1998. 13(S5):3-11

Canaud B, Morena M, Leray H, Chalabi L, and Cristol JP. Overview of clinical studies in hemodiafiltration; what do we need now? Hemodialysis International 2006. 10(S):5-12

Canaud B, Bragg-Gresham JL, Marshall MR , Desmeules S , Gillespie BW, Depner T, Klassen P and Port FK. Mortality risk for patients receiving hemodiafiltration versus hemodialysis: European results from the DOPPS. Kidney International 2006. 69:2087–2093

Capdevila M, Martinez Ruiz I, Ferrer C, Monllor F, Ludjvick C, García NH, Juncos LI. The efficiency of potassium removal during bicarbonate hemodialysis. Hemodialysis International 2005. 9(3):296-302

Chandran KB, Yoganathan AP, Rittgers SE. Biofluid Mechanics: The Human Circulation. CRC Press Inc. 2007

Chamney PW. Recirculation and dialysis access (Chapter 5). In Dialysis access: current practice edited by Akoh JA and Hakim NS. Imperial college Press 2001

Choi SJ, Lim J. Stability of the bicarbonate system in the blood. J. Math. Anal. Appl. 2009. 356:145-153

Circulaire DGS/DH/AFSSAPS n° 311 du 7 juin 2000, relative à relative aux spécifications techniques et à la sécurité sanitaire de la pratique de l'hémofiltration et de l'hémodiafiltration en ligne dans les établissements de santé

Coli L, Ursino M, Dalmastri V, Volpe F, La Manna G, Avanzolini G, Stefoni S, Bonomini V. A simple mathematical model applied to selection of the sodium profile during profiled haemodialysis. Nephrol Dial Transplant 1998. 13(2):404-16

Colton CK, Smith KA, Merrill EW, Reece JM. Diffusion of organic solutes in stangnant plasma and red cell suspension. Chem Eng Prog Symp Ser 1970. 99(66):85–100

Colton CK and Lowrie EG. Hemodialysis: Physical principles and technical considerations. In The Kidney, 2nd edition. Brenner BM Rector FC 1981. II:2425–2489

Combarnous F, Tetta C, Cellier CC, Wratten ML, Custaud, De Catheu T, Fouque D, David S, Carraro G, Laville M. Albumin loss in on-line hemodiafiltration. Int J Artif Organs 2002. 25(3):203-9

Coulter W. High Speed Automatic Blood Cell Counter and Cell Size Analyzer. Proc. National. El. Conf. 1956

Craddock PR, Fehr J, Dalmasso AP, Brighan KL, and Jacob HS. Hemodialysis leukopenia. Pulmonary vascular leukostasis resulting from complement activation by dialyzer cellophane membranes. J Clin Invest 1977. 59(5):879–888

Daugirdas JT, Depner TA. A nomogram approach to hemodialysis urea modeling. American journal of kidney diseases 1994. 23(1):33-40

De Broe M, Lins RR and De Backer WA. Pulmonary aspects of dialysis patients (Chapter 38; p827). In Replacement of renal function by dialysis. 3rd edition. Edited by Maher JF. Kluwer Academic Publishers 1989

Deane N and Wineman RJ. Multiple use of hemodialyzers (Chapter 18; p400-416). In Replacement of renal function by dialysis. 3rd edition. Edited by Maher JF. Kluwer Academic Publishers 1989

Depner TA. Assessing adequacy of hemodialysis: Urea modeling. Kidney International 1994. 45:1522–1535

Doumas BT. Standards for Total Serum Protein Assays — A Collaborative Study. Clinical Chemistry 1975. 21:1159-1166

Engelhardt I, Flemming B, Glatzel E, and Precht K. Determination of the acid-base status in blood of patients on chronic hemodialysis and of bicarbonate in dialysate: comparison of three techniques and their mathematically derived values. Nephrology Dialysis Transplantation 1988. 3:641-646

Eschbach JW. Hematological problems of dialysis patients. (Chapter 40; p859). In Replacement of renal function by dialysis. 3rd edition. Edited by Maher JF. Kluwer Academic Publishers 1989

Fazal Mohammad S. Extracorporeal thrombogenesis: mechanisms and prevention. In Replacement of renal function by dialysis. 3rd edition. Edited by Maher JF. Kluwer Academic Publishers 1989

Feriani M. Behaviour of acid-base control with different dialysis schedules. Nephrology Dialysis Transplantation 1998. 13(6):62-65

Feriani M, Fabris A and La Greca G. Acid-base in dialysis (Chapter 28; p829-847). In Replacement of renal function by dialysis. 5th edition. Edited by Hörl WH, Koch KM, Lindsay RM, Ronco C, Winchester JF. Kluwer Academic Publisher 2004

Fernandez PC, Cohen RM and Feldman GM. The concept of bicarbonate distribution space: The crucial role of body buffers. Kidney International 1989. 36:747–752

Gennari FJ. Acid-Base Homeostasis in End-Stage Renal Disease. Seminars in Dialysis 1996. 9(5):404 - 411

Gennari FJ and Feriani M. Acid-base problems in hemodialysis and peritoneal dialysis. (Chapter 19; p361). In Complications of dialysis. Edited by Lameire N and Mehta RL. Marcel Dekker Inc 2000

Ghezzi PM and Ronco C. Excebrane®: Hemocompatibility studies by the Intradialytic Monitoring of Oxygen Saturation. In Vitamin E-Bounded Membrane: A Further Step in Dialysis Optimization. Ronco C La Greca G. Contributions to Nephrology 1999. 127: 177-191

Grassmann A, Uhlenbusch-Körwer I, Bonnie-Schorn E, Vienken J. Composition and Management of Hemodialysis Fluids. Pabst Science Publishers. Lengerich (Germany) 2000

Heineken FG, Brady-Smith M, Haynie J, Van Stone JC. Prescribing dialysate bicarbonate concentrations for hemodialysis patients. Int J Artif Organs 1988. 11(1):45-50

Henderson LW. Biophysics of ultrafiltration and hemofiltration (Chapter 13; p300). In Replacement of renal function by dialysis. 3rd edition. Edited by Maher JF. Kluwer Academic Publishers 1989

Jaffrin MY, Ding L and Laurent JM. Simultaneous Convective and Diffusive Mass Transfers in a Hemodialyzer. J. Biomech. Eng 1990. 112(2): 212- 229

Jaffrin MY, Gupta BB, Malbrancq JM. A one-dimensional model of simultaneous hemodialysis and ultrafiltration with highly permeable membranes. J. Biomech. Eng 1981. 103:261–266

Jaffrin MY. Convective mass transfer in hemodialysis. Artif. Organs 1995. 19(11):1162-1171

Johner C, Chamney P, Schneditz D and Kramer M. Evaluation of an ultrasonic blood volume monitor. Nephrology Dialysis Transplantation 1998. 13(8):2098-2103

Kallenbach JZ, Gutch CF, Stoner MH, Corea AL. Review of hemodialysis for nurses and dialysis personnel. 7th edition. Mosby 2005

Kerr PB, Argilés A, Flavier JL, Canaud B and Mion CM. Comparison of hemodialysis and hemodiafiltration: a long-term longitudinal study. Kidney International 1992. 41:1035-1040

Kunimoto T, Lowrie EG, Kumazawa.S, O'Brien M, Lazarus JM, Gotlieb MN, Merrill JP. Controlled ultrafiltration (UF) with hemodialysis (HD): analysis of coupling between convective and diffusive mass transfer in a new HD-UF system. Trans ASAIO 1977. 23:234-241

La Greca G, Fabris A, Feriani M, Chiaramonte S and Ronco C. Acid base homeostasis in clinical dialysis (Chapter 37; p808). In Replacement of renal function by dialysis. 3rd edition. Edited by Maher JF. Kluwer Academic Publishers 1989

Laplanche A, Com-Nougué C, Flamant R. Méthodes statistiques appliquées à la recherche clinique. Flammarion médecines sciences 1989

Latchford K, Cowperthwaite J. Shortness of breath during dialysis- A role of bicarbonate in dialysis fluid? Journal of Renal Care 2008. 34 (1):2-4

Leber HW, Wizemann V, Goubeaud G, Rawer P, Schütterle G. Hemodiafiltration: a new alternative to hemofiltration and conventional hemodialysis. Artificial Organs 1978. 2(2):150-3

Ledebo I. Principles and practice of hemofiltration and hemodiafiltration. Artificial Organs 1998. 22(1):20-25

Ledebo I. Acid-base correction and convective dialysis therapies. Nephrol Dial Transpl 2000. 15 (2): 45-8

Legallais C, Catapano G, Von Harten B and Baurmeister U. A theoretical model to predict the in vitro performance of hemodiafilters. J Membr Sci 2000. 168: 3-15

Locatelli F, Di Filippo S, Manzoni C. Hemodialysis fluid composition (Chapter 21; p585-596). In Replacement of renal function by dialysis. 5th edition. Edited by Hörl WH, Koch KM, Lindsay RM, Ronco C, Winchester JF. Kluwer Academic Publisher 2004

Maduell F, del Pozo C, Garcia H, Sanchez L, Hdez-Jaras J, Albero M, Calvo C, Torregrosa I and Navarro V. Change from conventional haemodiafiltration to on-line haemodiafiltration. Nephrology Dialysis Transplantation 1999. 14(5):1202-1207

Maduell F. Hemodiafiltration. Hemodialysis International 2005. 9(1): 47-55

Mann H and Stiller S. Sodium modeling. Kidney International 2000. 76:79-88

Man NK, Ciancioni C, Perrone B, Chauveau P, Jehenne G. Renal Biofiltration. ASAIO Transactions 1989. 35:8-13

Marieb EN and Hoehn K. Human Anatomy and Physiology. 7th edition. Pearson International Edition 2007 (p856)

Mason RL, Gunst RF, Hess JL. Statistical Design and Analysis of Experiments: With Applications to Engineering and Science. 2nd edition. John Wiley & Sons Inc 2003 (p56)

Maton A, Hopkins J, Johnson S, William C, Quon Warner M, LaHart D, Wright JD. In Human Biology and Health. New Jersey: Prentice Hall 1995 (p108-118)

Merlo S, Donadey A, Coevoet B and Legallais C. Générateurs d'hémodialyse : état du marché français. IRBM 2007. 28(3-4):150-168

Métais P. Biochimie clinique. Vol. 1 – Biochimie analytique. Simep edition. 1980

Mineshima M, Hoshino T, Era K, Agishi T, Ota K. Diffusive and convective mass transport characteristics in β2-M removal. Trans. ASAIO 1987. 33:103-106

Mion CM, Hegstrom RM, Boen ST and Scribner BH. Substitution of sodium acetate for sodium bicarbonate in the bath fluid for hemodialysis. Trans Am Soc Artif Intern Organs 1964. 10:110-5

Mockros LF, Leonard R. Compact cross-flow tubular oxygenators. Trans Am Soc Artif Intern Organs 1985. 31:628-633

Moline J. Manuel de sémiologie médicale. Editions Masson 1992

Norris KA, Atkinson AR and Smith WG. Colorimetric Enzymatic Determination of Serum Total Carbon Dioxide, as Applied to the Vickers Multichannel 300 Discrete Analyzer. Clinical Chemistry 1975. 21:1093-1101

Paganini EP. General Application of continuous therapeutic techniques (Chapter 9; p103). In Principles and Practice of Dialysis. Edited by Henrich WL. Philadelphia: LippincottWilliams &Wilkins 1994

Passlick-Deetjen J and Pohlmeier R. Online Hemodiafiltration: gold standard or top therapy? Contribution Nephrology 2002. 137:201-211

Pedrini LA, De Cristofaro V, Pagliari B, and Sama F. Mixed predilution and postdilution online hemodiafiltration compared with the traditional infusion modes. Kidney International 2000. 58:2155-2165

Pedrini LA, De Cristofaro V, Pagliari B. Effects of the infusion mode on bicarbonate balance in on-line hemodiafiltration. Int J Artif Organs 2002. 25(2):100-6.

Pedrini LA, Ponti R, Faranna P, Cozzi G, and Locatelli F. Sodium modeling in hemodiafiltration. Kidney International 1991. 40:525–532

Pellet MV. Physiologie humaine. I. Milieu intérieur compartiments liquidiens. Paris: SIMEP 1977 (p92)

Petitclerc T. Do dialysate conductivity measurements provide conductivity clearance or ionic dialysance? Kidney International 2006. 70:1682–86

Polaschegg HD. Automatic, noninvasive intradialytic clearance measurement. Int J Artif Organs 1993. 16(4):185-91

Prakash S, Reddan D, Heidenheim AP, Kianfar C, Lindsay RM. Central, peripheral, and other blood volume changes during hemodialysis. ASAIO Journal 2002. 48(4):379-382

Ravel R. Clinical Laboratory Medicine: Clinical Application of Laboratory Data. (Chapter 24; p394). 6th edition. Mosby 1995

Röckel A, Hertel J, Fiegel P, Abdelhamid S, Panitz N and Walb D. Permeability and secondary membrane formation of a high flux polysulfone hemofilter. Kidney International 1986. 30:429-432

Ronco C, Fabris A, Chiaramonte S, De Dominicis E, Feriani M, Brendolan A, Bragantini L, Milan M, Dell'Aquila R, La Greca G. Comparison of four different short dialysis techniques. Int J Artif Organs 1988. 11(3):169-74

Ronco C, Ghezzi PM, Brendolan A, Crepaldi C and La Greca G. The haemodialysis system: basic mechanisms of water and solute transport in extracorporeal renal replacement therapies. Nephrology Dialysis Transplantation 1998. 13(6):3-9

Ronco C, Ghezzi PM, Bowry SK. Membranes for hemodialysis (Chapter 13; p301-323). In Replacement of renal function by dialysis. 5th edition. Edited by Hörl WH, Koch KM, Lindsay RM, Ronco C, Winchester JF. Kluwer Academic Publishers 2004

Santoro A, Canova C, Mancini E, Deppisch R, Beck W. Protein Loss in On-Line Hemofiltration. Blood Purif 2004. 22:261-268

Santoro A, Ferrari G, Spongano M, Cavalli F, and Zucchelli P. Effects of pK variability on bicarbonate balance evaluation in dialysis patients. Artificial Organs 1987. 11(6):491-495

Sargent JA, Gotch FA. Principles and biophysics of dialysis (Chapter 4; p88-143). In Replacement of renal function by dialysis. 3rd edition. Edited by Maher JF. Kluwer Academic Publishers 1989

Sepandj F, Jindal K, Kiberd B, and Hirsch D. Metabolic acidosis in hemodialysis patients: a study of prevalence and factors affecting intradialytic bicarbonate gain. Artificial Organs 1996. 20(9):976-980

Sigdell JE. Calculation of combined diffusive and convective mass transfer. Int. J. Artif. Organs 1982. 5:361-372

Siggaard-Andersen O, Wimberley PD, Fogh-Andersen N, Gothgen IH. Measured and derived quantities with modern pH and blood gas equipment: calculation algorithms with 54 equations. Scand J Clin Lab Invest 1988. 48(189):7-15

Siggaard-Andersen O. The acid-base status of the blood. 4th edition. Copenhagen: Munksgaard 1974

Schmidt-Nielsen K. Animal Physiology: Adaptation and Environment. 5th edition. Cambridge University Press 1997 (p82)

Schneditz D. Technological aspect of hemodialysis and Peritoneal Dialysis (Chapter 3). In Clinical Dialysis. 4th edition. McGraw-Hill Medical 2005

Sombolos KI, Bamichas GI, Christidou FN, Gionanlis LD, Karagianii AC, Anagnostopoulos TC, Natse TA. pO_2 and pCO_2 in post dialyser blood: the role of dialysate. Artificial Organs 2005. 29(11):892-8

Steuer RR., Harris DH, Conis JM. A new optical technique for monitoring hematocrit and circulating blood volume: its application in renal dialysis. Dialysis & transplantation 1993. 22(5):260-265

Stiller S, Mann H, Brunner H. Backfiltration in hemodialysis with highly permeable membranes. Contrib Nephrol 1985. 46:23-32

Story DA, Poustie S, Bellomo R. Comparison of three methods to estimate plasma bicarbonate in critically ill patients: Henderson-Hasselbalch, enzymatic, and strong-ion-gap. Anaesth Intensive Care 2001. 29(6):585-90

Story DA, Poustie S. Agreement between two plasma bicarbonate assays in critically ill patients. Anaesth Intensive Care 2000. 28(4):399-402

Symreng T, Flanigan MJ and Lim VS. Ventilatory and metabolic changes during high efficiency hemodialysis. Kidney International 1992. 41:1064–1069

Tannen RL. Potassium and Acid-base balance (Chapter 10). In Potassium Transport: Physiology and Pathophysiology. Giebisch G. Academic Pr. 1987

Thews O, Hutten H. A comprehensive model of the dynamic exchange processes during hemodialysis. Med Prog Technol 1990. 16(3):145-61

Thews O. Model-based decision support system for individual prescription of the dialysate bicarbonate concentration in hemodialysis. Int J Artif Organs 1992. 15(8):447-55

Thews O. Simulation analysis of the influence of hemodialysis control parameters on exchange processes during therapy. Int J Artif Organs 1992. 15(4):213-21

Uhlenbusch-Körwer I, Bonnie-Schorn E, Grassmann A, Vienken J. Understanding Membranes and Dialysers. Science Publishers. Lengerich (Germany) 2004

Ursino M, Coli L, Brighenti C, Chiari L, De Pascalis A, and Avanzolini G. Prediction of solute kinetics, acid-base status and blood volume changes during profiled hemodialysis. Ann Biomed Eng 2000. 28:204-216

Ursino M, Coli L, Brighenti C, De Pascalis A, Chiari L, Dalmastri V, La Manna G, Mosconi G, Avanzolini G, and Stefoni S. Mathematical modeling of solute kinetics and body fluid changes during profiled hemodialysis. Int J Artif Organs 1999. 22:94-107

Ursino M, Coli L, La Manna G, Cicilioni MG, Dalmastri V, Giudicissi A, Masotti P, Avanzolini G, Stefoni S, Bonomini V. A simple mathematical model of intradialytic sodium kinetics: “in vivo validation during hemodialysis with constant or variable sodium”. Int J Artif Organs 1996. 19(7):393-403

Van Laecke S, De Wilde K, and Vanholder R. Online hemodiafiltration. Artificial Organs 2006. 30(8):579-585

Vanholder R, De Smet R, Glorieux G et al. Review on uremic toxins: Classification, concentration, and interindividual variability. Kidney International 2003. 63:1934-1943

Vienken J and Bowry S. Quo vadis dialysis membrane? Artif Organs 2002. 26(2):152-9

Waniewski J. Mathematical modeling of fluid and solute transport in hemodialysis and peritoneal dialysis. Journal of Membrane Science 2006. 274(1-2):24-37

Watson PE, Watson ID and Batt RD. Total body water volumes for adult males and females estimated from simple anthropometric measurements. American Journal of Clinical Nutrition 1980. 33:27-39

Werynski A and Wanieski J. Theoretical description of mass transport in medical membrane devices. Artif. Organs 1995. 19(5):420–427

Wieth JO, Andersen OS, Brahm, J, et al. Chloride bicarbonate exchange in red blood cells: physiology of transport and chemical modification of binding sites. Phil Trans Roy Soc London Ser B 1982. 299:383-99

Wizemann V, Külz M, Techert F, Nederlof B. Efficacy of haemodiafiltration. Nephrology Dialysis Transplantation 2001. 16(s4):27-30

Wüpper A, Woermann D, Dellanna F, Baldamus CA. Retrofiltration rates in high-flux hollow fiber hemodialyzers: analysis of clinical data. J. Membr. Sc 1996. 121:109-11

Zeman LJ and Zydney AL. Microfiltration and Ultrafiltration: Principles and Applications. Marcel Dekker Inc. 1996

Ziolko M, Pietrzyk JA, Grabska-Chrzastowska J. Accuracy of hemodialysis modeling. Kidney International 2000. 57(3):1152-1163

Publications and communications

PUBLICATION

In vitro tests and modelisation of bicarbonate kinetics and mass transfers during online hemodiafiltration
Hélène MOREL, Michel Y. JAFFRIN, Patrick PAULLIER, Cécile LEGALLAIS
The International Journal of Artificial Organs (in press)

COMMUNICATIONS

June 2008: Séminaire d'été de la société francophone de dialyse (*Compiègne*)
Modélisation des transferts de bicarbonate en HD et HDF postdilution
H. Morel, M.Y. Jaffrin, et C. Legallais

September 2008: 33ème CONGRES annuel de la Société de BIOMECANIQUE (*Compiègne*)
In vitro bicarbonate and urea kinetics during hemodialysis and online hemodiafiltration
H. Morel, M.Y. Jaffrin, C. Legallais and J. Vienken

September 2008: XXXV Annual Meeting for European Society for Artificial Organs, ESAO (*Geneva*)
BICARBONATE AND UREA KINETICS MODELING DURING HEMODIALYSIS AND ONLINE POSTDILUTION HEMODIAFILTRATION
H. Morel, M. Jaffrin, J. Vienken, C. Legallais

May 2009: World Congress of Nephrology (*Milan*)
IN VITRO TESTS AND MODELISATION OF BICARBONATE KINETICS DURING ONLINE HEMODIAFILTRATION
Helene Morel, Michel Y. Jaffrin, Joerg Vienken, Patrick Paullier and Cecile Legallais

September 2009: XXXVI Annual meeting for European Society for Artificial Organs, ESAO (*Compiègne*)
EFFECT OF DIALYSIS FLUID BICARBONATE CONCENTRATION ON ACID-BASE BALANCE IN HEMODIAFILTRATION: *in vitro* and mathematical model
H. Morel, M.Y. Jaffrin, J. Vienken, P. Paullier, and C. Legallais

September 2009: World congress for Medical physics and biomedical engineering (*Munich*)
In vitro online postdilution hemodiafiltration: effect of various bicarbonate dialysis fluid concentrations on acid-base status
H. Morel, M. Y. Jaffrin, P. Paullier, J. Vienken and C. Legallais

Annexes

A: Legallais et al. paper

Legallais C, Catapano G, Von Harten B and Baurmeister U. A theoretical model to predict the in vitro performance of hemodiafilters. J Membr Sci 2000. 168:3-15

ELSEVIER

Journal of Membrane Science 168 (2000) 3–15

journal of MEMBRANE SCIENCE

www.elsevier.nl/locate/memsci

A theoretical model to predict the in vitro performance of hemodiafilters

Cecile Legallais [a,*], Gerardo Catapano [b], Bodo von Harten [c], Ulrich Baurmeister [c]

[a] *Technological University of Compiegne, UMR CNRS 6600, BP 20259, 60205 Compiegne Cedex, France*
[b] *Department of Chemical and Materials Engineering, University of Calabria, I-87030 Arcavacata di Rende (CS), Italy*
[c] *Membrane GmbH, Oehder Str. 28, D-42289 Wuppertal, Germany*

Received 22 June 1999; received in revised form 16 August 1999; accepted 30 August 1999

Abstract

In vitro tests with saline or plasma replacing the blood are generally used in the development of membranes and membrane modules for hemodiafiltration (HDF) and for quality control purposes. Theoretical models predicting performance of a hemodiafilter based on module geometry, membrane properties and operating conditions are needed, but are not yet available, to distinguish to what extent membrane properties and module fluid dynamics both affect module clearance.

In this paper, we report on the development of a simple predictive model for hemodiafiltration which still accounts for those phenomena that most profoundly affect performance of hemodiafilters, such as: the dependence of mass transport coefficients on the actual flow conditions; concentration polarization; the actual water filtration flux along the hemodiafilter length. The model was validated with respect to data in literature. Model predictions for low to high molecular weight solute clearance were within 10% of experimental data when saline replaces the blood and within 20% when plasma replaces the blood, at blood flow rates ranging from 100 to 500 ml/min and net overall filtration flow rates from 0 to 60 ml/min. Under all conditions, the model predicted clearances were in better agreement with experimental data than those predicted by other, non-predictive models for HDF. ©2000 Elsevier Science B.V. All rights reserved.

Keywords: Hemodiafiltration; Mass; Membrane; Momentum; Transport

1. Introduction

Enhancing the quality of treatment of chronic renal failure still calls for the development of membrane modules and clinical procedures that ensure the removal of low (LMW) to high molecular weight (HMW) solutes as efficiently as in the natural kidney. As compared to conventional hemodialysis, the hemofiltration treatment enhances removal of HMW solutes although at the expense of lower urea clearance. In hemodiafiltration (HDF), toxic solutes are removed by a combination of diffusion and convection [1] resulting in higher clearance of HMW solutes without noticeable reduction of LMW solute clearance. Evidence is accumulating that the efficacy of such treatment may benefit chronic renal patients and HDF is regaining a certain popularity with the introduction of on-line substitution fluid [2]. As a result, high flux membranes and membrane modules are being developed for HDF with the aim of effecting even better clearances than those obtained so far. Before reaching the clinics, newly developed membranes and membrane modules are generally optimized by testing their performance in vitro with saline and

* Corresponding author. Tel.: +33-3-44-23-44-01; fax: +33-3-44-20-48-13.
E-mail address: cecile.legallais@utc.fr (C. Legallais).

PII: S0376-7388(99)00297-5

plasma. In vitro tests are also widely used for quality control purposes. In either case, unless a feasible description of transport phenomena in the membrane module used for the test is available, it is difficult to distinguish to what extent membrane transport properties and module fluid dynamics both contribute to effecting module clearance. A transport model able to predict the clearance spectrum of a hemodiafilter based on module and membrane geometry, membrane transport properties and operating conditions would also help to direct the development of new membranes and modules for HDF, as well as to reduce development costs. It should also be considered that manufacturers often provide their hemodiafilters with specification sheets generally reporting only the clearance of LMW solutes at low net overall filtration flow rates (i.e., from 0 to 10 ml min^{-1}). A model able to reliably predict clearances of middle molecular weight (MMW) or HMW solutes at high net overall filtration flow rates (e.g., up to 60 ml min^{-1}) would also be a precious tool for clinicians to tailor HDF treatment to the patient's need.

Over the past 20 years, efforts have been made to develop models aimed at describing transport phenomena in hemodiafilters [3–13]. Most models have been based on simplifying assumptions, which have sometimes made it possible to obtain analytical solutions to the conservation equations: the water filtration flux J_V, is often assumed constant [3,5,6,8,10]; accumulation of partially rejected solutes at the membrane wall is also generally neglected [3,4,6,8]. Solute transport from the blood bulk to the membrane, across the membrane wall and from the membrane to the dialysate bulk is generally described in terms of a lumped overall mass transfer coefficient K_{ov}, whose value is assumed equal to membrane diffusive permeability [7,10,12,13] or is estimated for a given solute in a given hemodiafilter under given operating conditions from the experimental clearance of that solute [3,8]. As a result, K_{ov} is often dealt with as an adjustable parameter and models are rather used to establish semi-empirical correlations for the hemodiafilter clearance of a solute under varying operating conditions. Some authors [5,6,9,11] provided a more detailed description of how solute transfer across the membrane occurs and is related to module geometry, membrane properties and operating conditions. However, they neither accounted for the effective J_V profile that establishes along the module length, as a result of the hydrostatic and the osmotic pressure profiles in the blood and dialysate compartment, nor did they account for the change of the mass transport coefficient on either side of the membrane along the module length with the actual flow conditions. Besides, such models were not validated experimentally [6] or their predictions were proven satisfactory only for LMW solutes, such as urea [5].

In this paper, we report on the development of a model that predicts the performance of hemodiafilters based on module geometry, membrane transport and separation properties and the actual operating conditions. The model accounts for solute transport across the membrane by both a diffusive and convective mechanism; for concentration polarization of partially or totally rejected species at the membrane wall; for the change of the mass transport coefficient on either side of the membrane and of the water filtration flux along the module length with the actual flow conditions. The model computes concentration, flow rate and pressure profiles in both compartments of a hemodiafilter. Model predictions were validated with respect to experimental clearances of LMW to HMW solutes reported in literature at increasing net overall filtration flow rates and blood flow rates. The predicted clearance enhancements were also compared to the best-fit values of other, non-predictive models.

2. Theory

The theoretical model for solute transport in hemodiafilters was developed under the following assumptions:

1. operation at steady state (in particular membrane transport and separation properties do not change with time) in counter-current mode;
2. flow rates, concentrations and pressures are uniformly distributed over the module cross-section and vary only along the module length;
3. axial diffusion is negligible with respect to axial convection;
4. uniform distribution of fibers in the module;
5. solute partition coefficient between the membrane and the surrounding fluids is equal to 1 (i.e., solute concentration profile is continuous across phase boundaries);

6. fluids in the blood and dialysate compartment are Newtonian;
7. plasma proteins are completely rejected by the membrane;
8. kinetics of solute adsorption is neglected;
9. membrane hydraulic permeability is the same as saline flows from the blood compartment to the dialysate compartment and in the opposite direction.

2.1. Conservation equations and boundary conditions

Conservation equations for mass and momentum in the blood and dialysate compartment were written with respect to the bundle of N fibers in the control volumes shown in Fig. 1: in addition to the conservation of the overall mass, mass balances of permeable and rejected solutes were taken into account.

2.1.1. Continuity equations

Part of the liquid flowing in the blood compartment (hereafter referred to as the blood) is removed by filtration, as follows:

$$\frac{dQ_B}{dx} = -N\pi d_B J_V(x) \quad (1)$$

and enriches the liquid flowing in the dialysate compartment (hereafter referred to as the dialysate):

$$\frac{dQ_D}{dx} = -N\pi d_B J_V(x) \quad (2)$$

The local water filtration flux $J_V(x)$ is expressed as a function of the local transmembrane pressure difference as follows [14]:

$$J_V(x) = L_p[P_B(x) - P_D(x) - \Pi(x)] \quad (3)$$

where Π is the local oncotic pressure on the blood side and L_p is membrane hydraulic permeability. Boundary conditions are set by the flow rates at the blood and dialysate inlet:

$$x = 0 \qquad Q_B(0) = Q_{Bin};$$
$$x = L \qquad Q_D(L) = Q_{Din} \quad (4)$$

2.1.2. Mass balance of permeating species

Permeable solutes are removed from the blood at a rate J_s, as follows:

$$\frac{d[Q_B C_B]}{dx} = -N\pi d_B J_s(x) \quad (5)$$

and are transferred into the dialysate:

$$\frac{d[Q_D C_D]}{dx} = -N\pi d_B J_s(x) \quad (6)$$

The local transmembrane solute flux J_s, accounting for both diffusive and convective transport is expressed according to Zydney [15], as follows:

$$J_s(x) = K_0(C_B(x) - C_D(x)) + J_V(x)S_\infty(f_B(x)C_B(x) + f_D(x)C_D(x)) \quad (7)$$

f_B and f_D are the local blood and dialysate concentration factors, respectively, and are expressed as a function of membrane transport properties and operating conditions as follows:

$$f_B = \frac{\exp[(S_\infty J_V/P_m) + (J_V/K_B) + (J_V/K_D)]}{(1 - S_\infty)\exp(J_V/K_D)\left[\exp(S_\infty J_V/P_m) - 1\right] + S_\infty \exp[(S_\infty J_V/P_m) + (J_V/K_B) + (J_V/K_D)] - S_\infty} - \frac{K_0}{J_V S_\infty} \quad (8)$$

$$f_D = \frac{-1}{(1 - S_\infty)\exp(J_V/K_D)[\exp(S_\infty J_V/P_m) - 1] + S_\infty \exp[(S_\infty J_V/P_m) + (J_V/K_B) + (J_V/K_D)] - S_\infty} + \frac{K_0}{J_V S_\infty} \quad (9)$$

Eqs. (7)–(9) have been obtained by integration of the local solute mass balances under steady state conditions at the membrane and the adjacent boundary

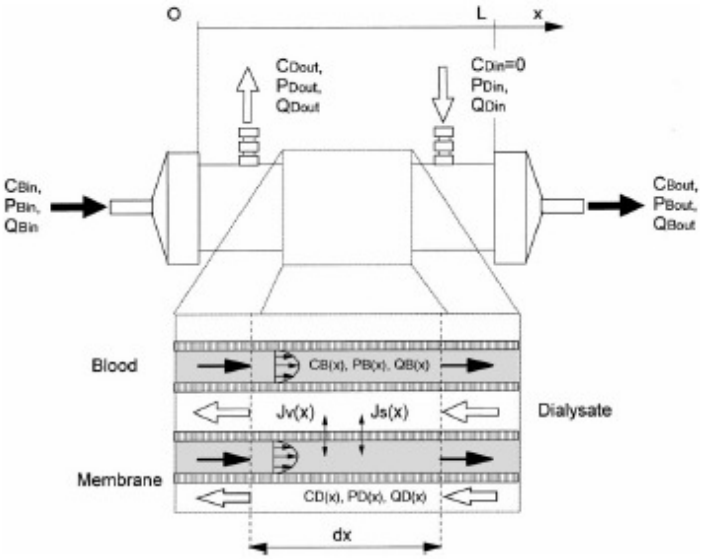

Fig. 1. Scheme of the membrane hemodiafilter evidencing the control volume to which balances are referred.

layers on both sides. These equations account for the combined effects of convection and diffusion, and for the accumulation of partially rejected solutes at the membrane wall (i.e., concentration polarization). To the best of our knowledge, they have never been used before to predict clearance of clinical-scale hemodiafilters. The overall mass transfer coefficient K_0 with respect to the inner membrane surface area, under null water filtration flux, is expressed according to a series resistance model, as follows:

$$\frac{1}{K_0} = \frac{1}{K_B} + \frac{1}{P_m} + \frac{1}{K_D} \tag{10}$$

Each term is the reciprocal mass transport resistance in the blood compartment, the membrane and the dialysate compartment, respectively. K_D also takes into account the fiber geometry. K_B dependence on module geometry, fluid properties and operating conditions was evaluated according to the Graetz theory [16]; K_D was estimated according to [17] with reference to the hydraulic diameter of the equivalent cylindrical tube. The value of S_∞ for each membrane/solute pair was estimated as described in Section 3.2. The local concentration factors, f_B and f_D, at each position in the membrane module were evaluated according to Eqs. (8) and (9) based on the actual water filtration flux and mass transport coefficients at that same position, for the given module geometry and operating conditions. Boundary conditions are set by the permeable solute concentrations at the blood and dialysate inlet:

$$x = 0 \qquad C_B(0) = C_{Bin};$$
$$x = L \qquad C_D(L) = C_{Din} = 0 \tag{11}$$

2.1.3. Mass balance of rejected species

Plasma proteins are completely rejected by the HDF membrane and are retained in the blood, thus:

$$\frac{d[Q_B C_p]}{dx} = 0 \tag{12}$$

The boundary condition is set by the plasma protein concentration at the blood inlet:

$$x = 0 \qquad C_p(0) = C_{pin} \tag{13}$$

2.1.4. Momentum conservation

Values of the Reynolds number under clinical operating conditions for commercial hemodiafilters

suggested making reference to the Hagen–Poiseuille equation, or modifications thereof, to correlate the pressure drop to the membrane (versus module) geometry and the actual blood (versus dialysate) linear velocity. Pressure in the blood compartment is assumed to drop along the hemodiafilter length according to the Hagen–Poiseuille equation, as follows:

$$\frac{dP_B}{dx} = -\frac{128\,\mu_B}{N\pi d_B^4} Q_B \tag{14}$$

where μ_B is the local blood viscosity.

Axial pressure drop in the dialysate compartment was expressed in terms of a modified form of the Hagen–Poiseuille equation [18] with reference to the equivalent cylindrical tube, as follows:

$$\frac{dP_D}{dx} = \frac{-32\mu_D}{S_{eq}(d_{eq})^2} Q_D \tag{15}$$

where μ_D is the local dialysate viscosity and

$$S_{eq} = \frac{\pi {d_{case}}^2}{4} - \frac{N\pi(d_B + 2\delta)^2}{4} \tag{16}$$

$$d_{eq} = \frac{4S_{eq}}{(N\pi(d_B + 2\delta) + \pi d_{case})} \tag{17}$$

where d_{case} is the inner diameter of the housing and δ membrane thickness. Boundary conditions are set by the pressure at the blood inlet and by the set net overall filtration flow rate:

$$x = 0 \qquad P_B(0) = P_{Bin}; \qquad Q_f = Q_{f_{exp}} \tag{18}$$

2.2. Parameter estimation

2.2.1. Fluid viscosity

Viscosity of saline at actual operating conditions was assumed equal to that of water. When plasma is assumed to flow in the blood compartment, its relative viscosity was assumed to depend on the actual protein concentration according to Pallone et al. [19], as follows:

$$\frac{\mu_B}{\mu_w} = 1 + \left(\frac{\mu_{pR}}{\mu_w} - 1\right)\frac{C_p}{C_{pR}} \tag{19}$$

where $\mu_{pR} = 1.22 \times 10^{-3}$ Pa s; $C_{pR} = 70\,g\,l^{-1}$.

2.2.2. Oncotic pressure

Oncotic pressure develops only in the presence of proteins in the blood compartment. Hence, in the case that saline replaces the blood it was neglected throughout. For plasma, oncotic pressure dependence on protein concentration was expressed according to Landis and Pappenheimer's semi-empirical correlation [20]:

$$\Pi(x) = 0.21C_p(x) + 1.6 \times 10^{-3}C_p(x)^2 + 9 \times 10^{-6}C_p(x)^3 \tag{20}$$

where C_p is in $g\,l^{-1}$ and Π in mm Hg.

3. Methods

3.1. Model validation

The model was validated with respect to hemodiafilters operated at increasing Q_B and Q_f by comparing model predicted clearances with experimental in vitro data reported in literature. Despite the great number of papers on the in vitro characterization of hemodiafilter performance, only in few cases detailed information on the membrane and module characteristics, and the operating conditions are available and module clearance is reported for LMW to HMW solutes. When saline solution is used in substitution of the blood, we validated the model predictions with respect to the experimental results reported by Bosch et al. [21] for the F60 Fresenius polysulfone module (membrane area $\approx 1.25\,m^2$) and by Jaffrin et al. [9] for the Hospal Filtral 12 AN69HF module (membrane area $\approx 1.15\,m^2$). We validated the model predictions also when plasma is used in substitution of the blood to check the model capacity to predict the effect of the oncotic pressure on the filtration flux profile and solute removal: to this end, we referred to data reported by Bosch et al. [21]. Hereafter, the hemodiafilter clearance is defined as follows:

$$CL = \frac{Q_{Bin}C_{Bin} - Q_{Bout}C_{Bout}}{C_{Bin}} \tag{21}$$

Such a definition holds true for hemodialysis as well as for post-dilutional hemodiafiltration: in fact, blood dilution downstream from the module does not affect its clearance but only flow rate and concentration on the blood side.

Table 1
Geometric characteristics[a] of the membrane modules used for clearance predictions

Module type	Effective length (cm)	Number of fibers	Fiber diameter (μm)	Fiber thickness (μm)	Case diameter (cm)	Membrane area (m^2)
Fresenius F60	22	9000	200	40	4.0	1.25
Hospal Filtral 12	20	8500	220	45	3.9	1.15

[a] Data from the manufacturer.

3.2. Parameter estimation

The model predicts performance of a particular hemodiafilter under given conditions provided that module geometry, membrane transport and separation properties are known. Values of geometrical parameters (e.g., the fiber effective length and diameter, the housing inner diameter, etc.) for the hemodiafilters which are considered were gathered from specifications of the module manufacturer. Membrane hydraulic permeability L_p, depends on the liquid replacing the blood in the in vitro experiments: L_p values for the Fresenius F60 and the Hospal Filtral 12 AN69HF membranes were obtained either from literature or from specifications of the module manufacturer. The diffusive permeability P_m, of the considered membranes towards the given solute were obtained from literature or from specifications of the module manufacturer. In the absence of data, membrane P_m for a given solute was inferred from the experimental clearances reported in literature [9,21] by adjusting the P_m value to yield model predicted clearances at a null net overall filtration flow rate to match the reported ones. This value was then used to obtain model predictions at increasing net overall filtration flow rates. The membrane sieving coefficient towards a given solute required in Eqs. (8) and (9) is the infinite sieving coefficient S_{∞}. In the experiments reported in [9,21] hemodiafilters were operated at water filtration fluxes at which the actual sieving coefficient S_a is close to S_{∞}: consequently, we assumed S_{∞} equal to S_a which was estimated from the apparent sieving coefficient according to Langsdorf et al. [22]. Values of the relevant parameters used for clearance prediction are reported in Tables 1 and 2.

3.3. Integration procedure

A custom made, two-step numerical code was written to integrate the set of conservation and constitutive equations together with the set boundary conditions, based on a 4th order Runge–Kutta procedure. In the first step, the program integrates the set of Eqs. (1), (2), (13) and (14) to yield pressure and flow rate profiles in both compartments. In the second step, Eqs. (5) and (6) are solved for solute concentrations in both compartments based on the flow rate and pressure profiles obtained in the previous step. Counter-current operation of the membrane module provides boundary conditions for each pair of variables at opposite ends of the module. This makes it impossible to integrate each set of differential equations with techniques 'marching' from one end of the module, where boundary conditions on all variables are assigned, to the opposite

Table 2
Transport and separation characteristics[a] of membranes in the modules used for clearance predictions. Sieving coefficient and diffusive permeability are estimated in saline solution

Module type	Membrane material	L_p [ml/(h m^2 mm Hg)] w/water	w/plasma	Creatinine S_a[–]	P_m (cm min^{-1})	Vit. B12 S_a[–]	P_m (cm min^{-1})	Inulin S_a [–]	P_m [cm/s]	Myoglobin S_a [–]	P_m (cm s^{-1})
Fresenius F60	Polysulfone	121	39[*]	1.0	–	1.0	–	0.99[*]	–	–	–
Hospal Filtral 12	AN 69 HF	27	–	1.0	3.2×10^{-2}[**]	1.0	1.35×10^{-2}[**]	0.77	–	0.7[#]	$2.2 \cdot \times 10^{-3}$[*]

[a] Data from the manufacturer except for [*]: By Bosch et al. [21]; [**]: By fitting model predicted clearances to experimental ones at $Q_B = 200$ ml min^{-1}, $Q_f = 0$ ml min^{-1}; [#]: By Jaffrin et al. [9].

end. Our code integrates each set of differential equations according to a trial-and-error technique known as 'shooting technique'. According to this technique, a tentative value is assigned to the unknown variable at one end of the module (e.g., C_{Dout}) and the set of differential equations is integrated 'marching' from this end to the opposite end. The technique iteratively seeks the tentative value of that variable that yields a value at the opposite end (e.g., C_{Din}) matching that given as the boundary condition. The shooting technique integrates Eqs. (1), (2), (13) and (14) by seeking the pressure at the outlet that yields the required net overall filtration flow rate. By doing so, the code mimics the procedure according to which most dialysis monitors realize the set Qf. Eqs. (5) and (6) are integrated by seeking the solute concentration at the dialysate outlet that yields a null solute concentration at the dialysate inlet. Once the concentration profiles of all solutes are obtained, the code computes the module clearance of the given solute.

4. Results and discussion

4.1. Flow rate, pressure and concentration profiles

The model predicts sound profiles of flow rate, water filtration flux, pressure and solute concentration along the length of a Fresenius F60 hemodiafilter operated with saline under zero net overall filtration flow rate. As one would expect for as permeable a membrane as the polysulfone type used in the F60, in the first half of the module (i.e., from $x = 0$–$L/2$) about 2.5% of saline fed to the blood compartment (i.e., Q_B) is filtered into the dialysate as a result of the higher pressure in the blood compartment than that in the dialysate compartment. Pressure drop in either compartment results in water filtration fluxes linearly decreasing towards the module half length. In the second half of the module (i.e., from $x = L/2$–L) the pressure drop makes blood pressure lower than that in the dialysate compartment and saline is filtered back into the blood compartment. Counter-current operation under a null net overall filtration flow rate causes flow rates in both compartments to decrease in a parabolic fashion along the module length with a minimum at the module half-length. Comparison of model predictions with experimental data reported by Bosch et al. [21] for the F60 under identical operating conditions shows that the model predicted blood pressure drop is in excellent agreement with the experimental data, whereas the predicted pressure drop in the dialysate compartment is somewhat lower than that reported. The latter discrepancy is possibly to be blamed on the placement of the pressure sensors at a distance from the module shell, which is likely to occur when pressure is measured with the sensors placed on the dialysate line in the dialysis monitor. In such a case, the pressure drop in the line and the dialysate headers would add to that in the module shell and would result in higher experimental pressure drops than those predicted by the model.

Fig. 2 shows the model predicted concentration profiles for a LMW solute (e.g., urea) and a HMW solute (e.g., β2-microglobulin) along the module length. Urea concentration in the blood compartment decreases very rapidly in the first half of the module and quite slowly in the second half yielding an axial concentration profile with an upward concavity. Correspondingly, urea concentration in the dialysate increases from the dialysate inlet to the outlet resulting in a transmembrane urea concentration difference rapidly decreasing from blood inlet to the outlet (Fig. 2a). The polysulfone membrane in the F60 features a sieving coefficient equal to 1 and a high diffusive permeability towards urea. Fig. 2a soundly suggests that urea is transported into the dialysate mostly by diffusion: in fact, about 50% of urea entering the module is cleared in the first quarter of the module length where the transmembrane concentration difference is high; the last quarter of the module close to the blood outlet contributes to the overall clearance by removing only 5% of the inlet urea concentration. The predicted axial concentration profile according to the model for the less permeable β2-microglobulin (β2M) is quite different (Fig. 2b). β2M concentration in the blood compartment decreases slowly and in a near-linear fashion along the length of the module. β2M concentration in the dialysate increases from the dialysate inlet to the outlet: in spite of the constant transmembrane concentration difference, β2M concentration in the dialysate leaving the module is only 10% that of β2M in the inlet blood stream. The 0.79 sieving coefficient and the low diffusive permeability of the F60 towards β2M (i.e., $P_m = 7 \times 10^{-3}$ cm min^{-1}) suggest

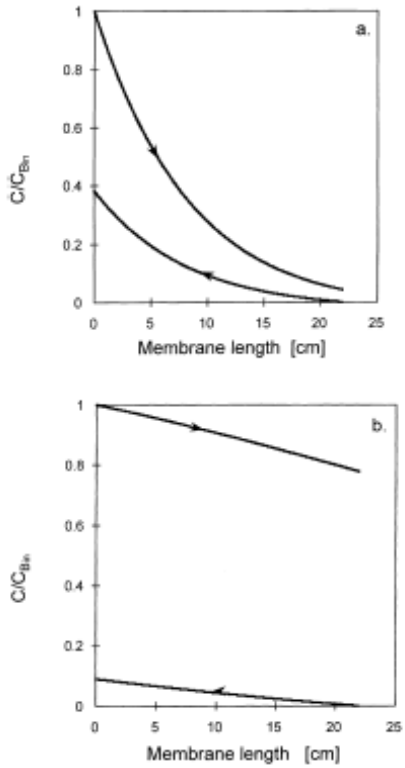

Fig. 2. Permeable solute concentration profile in the blood (——) and the dialysate (– – –) compartment of a Fresenius F60 hemodiafilter where saline replaces blood, which is operated at $Q_{Bin} = 200\,ml\,min^{-1}$, $Q_{Din} = 500\,ml\,min^{-1}$, $Q_f = 0\,ml\,min^{-1}$: (a) urea; (b) β2-microglobulin.

that β2M is mostly removed by a convective mechanism, which explains its relatively low, nonetheless significant, clearance of $40\,ml\,min^{-1}$.

4.2. Effect of blood flow rate on clearance

Model predictions for the effect of blood flow rate on solute clearance were validated with respect to the experimental work by Jaffrin et al. [9] with a Hospal Filtral 12 AN69HF module using saline in substitution of the blood. We referred to three solutes whose MWs are representative of the expected clearance MW spectrum of the AN69HF membrane: creatinine

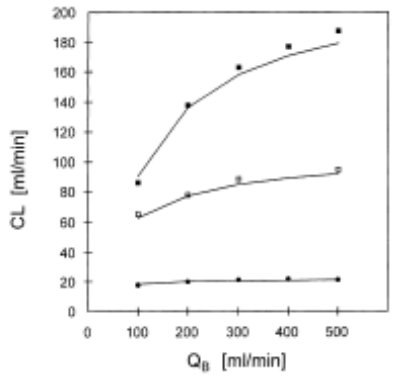

Fig. 3. Effect of blood flow rate on the clearance of permeable solutes by a Hospal Filtral 12 AN69HF hemodiafilter where saline replaces blood, which is operated at $Q_{bin} = 200\,ml\,min^{-1}$, $Q_{Din} = 500\,ml\,min^{-1}$; $Q_f = 0\,ml\,min^{-1}$: (■) creatinine; (□) vitamin B12; (●) myoglobin. Model predictions are reported as continuous lines. Experimental data from [9].

(MW = 113); vitamin B12 (MW = 1355); myoglobin (MW = 15 000). Reliable values of the diffusive permeability of the membrane towards each solute were not found in literature. As described in the Methods section, P_m was estimated for each solute as the P_m value yielding the best match between the model predicted and the reported experimental solute clearance at $Q_B = 200\,ml\,min^{-1}$ under a null net overall filtration flow rate. Fig. 3 shows that the model soundly predicts that increasing blood flow rate from 100 to $500\,ml\,min^{-1}$ enhances creatinine clearance from about 91 to $180\,ml\,min^{-1}$: in fact, increasing blood flow rates would reduce the resistance to creatinine transport from the blood bulk to the membrane which significantly contributes to the total transmembrane resistance to mass transfer. As solute MW increases to 1355 (i.e., for vitamin B12), increasing Q_B from 100 to $500\,ml\,min^{-1}$ produces only a 45% clearance increase. In the case of larger solutes, such as myoglobin, their low permeability across the membrane makes the membrane property limit mass transport: under such circumstances, increasing Q_B has no effect on solute clearance as Fig. 3 shows. Fig. 3 shows also the excellent agreement between experimental data and model predictions under all conditions, the latter always being within 6% of the experimental clearance.

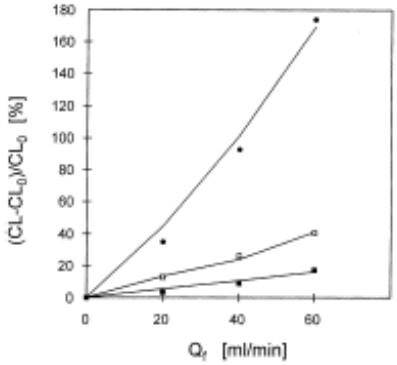

Fig. 4. Clearance enhancement with increasing net overall filtration flow rate as compared to that under null Q_f for solutes with different molecular weight: (■) creatinine; (□) vitamin B12; (●) myoglobin. Data refer to a Hospal Filtral 12 AN69HF hemodiafilter where saline replaces blood, which is operated at $Q_{Bin} = 200\,ml\,min^{-1}$, $Q_{Din} = 500\,ml\,min^{-1}$. Model predictions are reported as continuous lines. Experimental data from [9].

4.3. Effect of filtration flow rate on clearance

Model predictions of solute clearance at increasing net overall filtration flow rate were also validated with respect to the experimental investigation reported in [9]. Model predicted clearances of creatinine, vitamin B12 and myoglobin were obtained at $Q_B = 200\,ml\,min^{-1}$, $Q_D = 500\,ml\,min^{-1}$. Fig. 4 shows that the model soundly predicts that increasing the net overall filtration flow rate from 0 to $60\,ml\,min^{-1}$ would result in enhanced myoglobin clearances: clearance enhancement with respect to operation under a null net overall filtration flow rate E, increases with Q_f and attains a remarkable 170% value at $Q_f = 60\,ml\,min^{-1}$, consistent with a mechanism where solute is transported mostly by convection. As solute MW decreases (e.g., for vitamin B12), solute transport across the membrane by diffusion becomes appreciable: as a result, increasing Q_f from 0 to $60\,ml\,min^{-1}$ yields only small enhancements of vitamin B12 clearance (e.g., $E \approx 40\%$ at $Q_f = 60\,ml\,min^{-1}$) that do not increase as rapidly with Q_f as in the case of myoglobin. LMW solutes, such as creatinine, are mainly transported across the membrane by diffusion: the model soundly predicts that creatinine clearance is not affected to a large extent by operation under high Q_f, yielding a maximal 16% clearance enhancement at $Q_f = 60\,ml\,min^{-1}$. Fig. 4 shows that also in this case model predictions are in excellent agreement with the experimental results, predicted clearances always being within 7% of the experimental values.

4.4. Effect of the substitution fluid properties on clearance

In the in vitro characterization of membranes (versus membrane modules) for HDF, plasma is often used in substitution of the blood to account for the effects of plasma proteins on membrane transport and separation properties, as well as on the actual water filtration flux. In fact, plasma protein adsorption on the membrane generally reduces its L_p [21] and may profoundly alter its sieving coefficient spectrum [23]. Moreover, dynamic accumulation of rejected proteins at the membrane wall develops an axial oncotic pressure profile that reduces the effect of the existing transmembrane hydrostatic pressure difference on water flux as shown in Eq. (3). Model predictions when plasma in used in in vitro tests in substitution of the blood were validated with respect to the experimental work by Bosch et al. [21]. Estimates of the diffusive permeability of the polysulfone membrane used in [21] towards creatinine and inulin in plasma could not be found in literature. P_m values of $7.5 \times 10^{-2}\,cm\,min^{-1}$ and $3.8 \times 10^{-2}\,cm\,min^{-1}$ for creatinine and inulin, respectively, were estimated by adjusting P_m to yield model predicted clearances at $Q_B = 200\,ml\,min^{-1}$, $Q_f = 0\,ml\,min^{-1}$ matching the experimental ones reported in [21] in saline solution. Other parameter values were as in Tables 1 and 2. Model predicted clearance was obtained for creatinine and inulin (MW = 5200) at $Q_f = 0$ and $50\,ml\,min^{-1}$. Consistent with experimental data, the model predicts higher clearances when saline replaces the blood than when plasma is used. Fig. 5 shows that the model also soundly predicts that increasing Q_f generally results in a greater clearance enhancement when plasma is used. Clearance enhancement is also more significant for higher MW solutes (e.g., for inulin). Analysis of the model predicted filtration flux profile which establishes in the hemodiafilter shows that, when saline replaces the blood and the hemodiafilter is operated under null Q_f, a large volume of water is recircu-

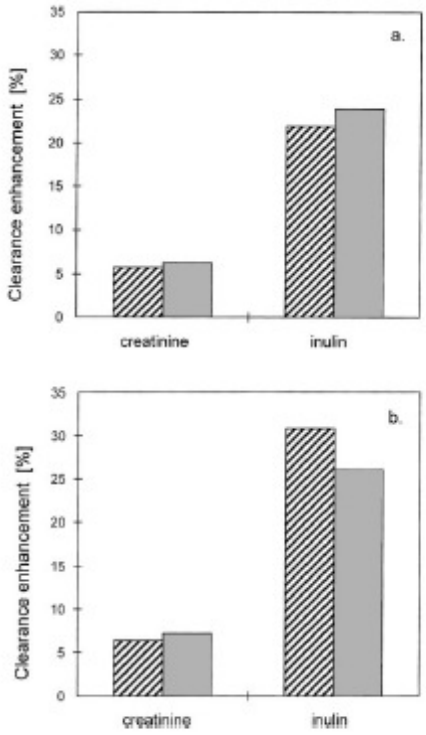

Fig. 5. Enhancement of creatinine and inulin clearance as compared to that at null Q_f for a Fresenius F60 hemodiafilter operated at $Q_{Bin} = 200\,ml\,min^{-1}$, $Q_{Din} = 500\,ml\,min^{-1}$ and $Q_f = 50\,ml\,min^{-1}$ where different fluids replace blood: (a) saline; (b) plasma. Experimental data from [21] is reported as shaded bars; model predictions are reported as closed bars.

lated from the blood into the dialysate and back, thus improving removal of MMW to HMW solutes. When plasma is used, both lower membrane L_p and oncotic pressure reduce the water volume which is internally recirculated eventually resulting in lower MWM to HMW solute clearance than with saline. Under such circumstances, increasing Q_f may be expected to result in a more significant enhancement of MMW to HMW solute clearance when plasma replaces the blood, as the model soundly predicts. Fig. 5 shows also that model predictions are in good agreement with experimental data, since differences never exceed 15%. When plasma replaces the blood, the agreement is not as good as when saline is used. This is possibly to be blamed on the simplifying assumptions that we made when we considered that only rejected albumin contributes to oncotic pressure. Further model refinement would require accounting for the presence and the effect of all plasma proteins. The increased model complexity would have to be weighted against obtainable accuracy on the basis of the difficult characterization of plasma composition.

4.5. Comparison with other proposed models

In the preceding sections, we showed that the model proposed in this paper accurately predicts in vitro LMW to HMW solute clearances in hemodiafiltration under different operating conditions. Clearance predicted by the model for a given hemodiafilter can be effectively compared to that by other models proposed in literature with respect to the main feature of the hemodiafiltration process, i.e., solute clearance enhancement (with respect to that under a null net overall filtration flow rate) resulting from operation under increasing net overall filtration flow rates. Models proposed in literature have often been used to establish semi-empirical correlations for clearance enhancement as a function of the net overall filtration flow rate [3,4,8,9]. Clearance enhancement is generally related to clearance under a null net overall filtration flow rate CL_0; the net overall filtration flow rate; sometimes, the overall mass transfer coefficient K_{ov} and the apparent sieving coefficient. The enhancement of creatinine and myoglobin clearance predicted for a Hospal Filtral 12 AN69HF by the model presented in this paper at increasing net overall filtration flow rates is reported in Tables 3 and 4 and is compared to experimental clearances and predictions of other models in literature. The agreement of model predicted clearances with experimental values over the considered Q_f range is measured in terms of the sum of squared residuals (SSR), which is reported in the last row of both the tables.

In all cases, increasing net overall filtration flow rates are associated with enhanced removal, hence clearance, of larger solutes. Tables 3 and 4 show that the model proposed by Sargent and Gotch for low flux membranes (which is mainly focused on urea removal) yields clearance enhancements in good agreement with experimental data over the whole range of J_V only for LMW solutes [4]. The model proposed by

Table 3
Enhancement of creatinine clearance at increasing net filtration flow rates predicted by different models as compared to experimental clearances. Data for a Hospal Filtral 12 module operated with saline solution at $Q_{Bin} = 200\,ml\,min^{-1}$, $Q_{Din} = 500\,ml\,min^{-1}$ [a]

Q_f ($ml\,min^{-1}$)	$(CL - CL_0)/CL_0$ [–]					
Model	Experimental	Sargent et al.	Jaffrin et al.	Kunitomo et al.	Chang et al.	This paper
Reference	[9]	[4]	[9]	[3]	[8]	
20	0.033	0.045	0.065	0.100	0.071	0.053
40	0.087	0.090	0.134	0.200	0.143	0.107
60	0.173	0.0135	0.209	0.300	0.214	0.160
SSR		1.64×10^{-3}	4.52×10^{-3}	4.25×10^{-2}	6.24×10^{-3}	9.68×10^{-4}

[a] SSR: sum of squared residuals evaluated with respect to experimental clearances.

Table 4
Enhancement of myoglobin clearance at increasing net filtration flow rates predicted by different models as compared to experimental clearances. Data for a Hospal Filtral 12 module operated with saline solution at $Q_{Bin} = 200\,ml\,min^{-1}$, $Q_{Din} = 500\,ml\,min^{-1}$ [a]

Q_f ($ml\,min^{-1}$)	$(CL - CL_0)/CL_0$ [–]					
Model	Experimental	Sargent et al.	Jaffrin et al.	Kunitomo et al.	Chang et al.	This paper
Reference	[9]	[4]	[9]	[3]	[8]	
20	0.350	0.900	0.447	0.100	0.752	0.450
40	0.930	1.800	0.926	0.200	1.504	1.015
60	1.740	2.700	1.439	0.300	2.256	1.695
SSR		1.98	9.97×10^{-2}	8.96	7.58×10^{-1}	1.93×10^{-2}

[a] SSR: sum of squared residuals evaluated with respect to experimental clearances.

Kunitomo et al. [3] leads to a constant enhancement factor specific for each solute and yields clearance enhancements quite different from the experimental data, similar to those yielded by Chang and Lee's model [8]. Jaffrin et al. [9] averaged the estimated clearance enhancement for different MW solutes and concluded that clearance increases proportionally to the half of the net overall filtration flow rate, independent of solute MW: as a result, their model yields clearance enhancements in close agreement with experimental data only for MMW solutes (e.g., vitamin B12). The SSR values of these models show that the assumptions that were made in their development simplify solution to the conservation equations but make the models reliable only in a narrow range of solute MW and operating conditions.

In the development of the model presented in this paper we accounted for those phenomena that more profoundly affect performance of hemodiafilters, such as: the dependence of mass transport coefficients on the actual flow conditions; concentration polarization of rejected species; the dependence of J_V on the actual hydrostatic and osmotic pressure profiles along the hemodiafilter length. The SSR values for such a model show that it predicts clearance enhancements in closer agreement with experimental data than those of other models and further validate its accuracy in predicting performance of hemodiafilters under a broad range of operating conditions.

5. Conclusions

In this paper, we presented a one-dimensional model for transport in hemodiafilters aimed at predicting their clearance spectrum based on module geometry, membrane transport properties and operating conditions. The model was developed to be as simple as possible, yet it accounts for those phenomena that more profoundly affect performance of hemodiafilters, such as: the dependence of mass transport coefficients on the actual flow conditions; concentration polarization of rejected species; the dependence of the water filtration flux on the actual hydrostatic and osmotic pressure profiles along the hemodiafilter length. The model was validated with respect to data in literature. Model

predicted clearances of LMW to HMW solutes agree very well with in vitro experimental data obtained by using saline and plasma in substitution of the blood, under a broad range of blood and net overall filtration flow rates. The model also yields more accurate predictions of clearance enhancement at increasing net overall filtration flow rates than other models proposed in literature for hemodiafiltration.

We conclude that, although simple, the model accurately predicts the clearance spectrum of hemodiafilters based on their module geometry, membrane transport properties and actual operating conditions. The model also provides pressure, flow rate, water filtration flux and solute concentration profiles along the hemodiafilter length both in the blood and the dialysate compartment. We believe that such a model can be used as a rational tool to predict the occurrence of backfiltration and to direct the development of more effective membrane and membrane modules for hemodiafiltration.

6. List of symbols

A	hemodialyser surface area [L^2]
C	solute concentration [ML^{-3}]
CL	clearance [L^3T^{-1}]
d_B	inner fiber diameter [L]
d_{case}	inner diameter of housing [L]
$E = (CL - CL_0)/CL_0$	clearance enhancement, –
f	concentration factor, –
J_s	permeable solute filtration flux [ML^2T]
J_v	water filtration flux [LT^{-1}]
K_i	mass transport coefficient in compartment i [LT^{-1}]
K_{ov}	overall mass transfer coefficient [LT^{-1}]
K_0	overall mass transfer coefficient under null water filtration flux [LT^{-1}]
L	fiber length [L]
L_p	membrane hydraulic permeability [$M^{-1}L^2T$]
N	number of fibers
P	pressure [$ML^{-1}T^{-2}$]
P_m	membrane diffusive permeability [LT^{-1}]
Q	flow rate [L^3T^{-1}]
Q_f	net overall filtration flow rate [L^3T^{-1}]
S_a	actual sieving coefficient, –
S_∞	sieving coefficient at infinite filtration flux, –
x	space coordinate [L]

6.1. Subscripts

0	null net overall filtration flow rate
B	blood compartment
D	dialysate compartment
f	filtration
in	inlet
out	outlet
p	protein
w	water

6.2. Greek letters

δ	membrane thickness [L]
μ	viscosity [$ML^{-1}T^{-1}$]
Π	oncotic pressure [$ML^{-1}T^{-2}$]

References

[1] M. Mineshima, T. Hoshino, K. Era, T. Agishi, K. Ota, Diffusive and convective mass transport characteristics in β2-M removal, Trans. ASAIO 33 (1987) 103–106.
[2] P. Ahrenholz, R.E. Winkler, W. Ramlow, M. Tiess, W. Müller, On-line hemodiafiltration with pre- and post-dilution: a comparison of efficacy, Int. J. Artif. Organs 20 (2) (1997) 81–90.
[3] T. Kunimoto, E.G. Lowrie, Kumazawa et al., Controlled ultrafiltration (UF) with hemodialysis (HD): analysis of coupling between convective and diffusive mass transfer in a new HD-UF system, Trans. ASAIO, vol. 23, 1977 pp. 234–241.
[4] J.A. Sargent, F.A. Gotch, Principles and biophysics of dialysis, in: W. Drukker, F.M. Parsons, J.F. Maher (Eds.), Replacement of renal function by dialysis, Martinus Nijhoff Medical Division, The Hague, 1978, pp. 38–68.
[5] M.Y. Jaffrin, B.B. Gupta, J.M. Malbrancq, A one-dimensional model of simultaneous hemodialysis and ultrafiltration with highly permeable membranes, J. Biomech. Eng. 103 (1981) 261–266.
[6] J.E. Sigdell, Calculation of combined diffusive and convective mass transfer, Int. J. Artif. Organs 5 (1982) 361–372.

[7] S. Stiller, H. Mann, H. Brunner, Backfiltration in hemodialysis with highly permeable membranes, Contr. Nephrol. 46 (1985) 23–32.
[8] Y.L. Chang, C.J. Lee, Solute transport characteristics in hemodiafiltration, J. Membr. Sci. 39 (1988) 99–111.
[9] M.Y. Jaffrin, L.H. Ding, J.M. Laurent, Simultaneous convective and diffusive mass transfer in a hemodialyser, J. Biomech. Eng. 112 (1990) 212–219.
[10] A. Werynski, J. Wanieski, Theoretical description of mass transport in medical membrane devices, Artif. Organs 19 (5) (1995) 420–427.
[11] M.Y. Jaffrin, Convective mass transfer in hemodialysis, Artif. Organs 19 (11) (1995) 1162–1171.
[12] A. Wüpper, D. Woermann, F. Dellanna, C.A. Baldamus, Retrofiltration rates in high-flux hollow fiber hemodialysers: analysis of clinical data, J. Membr. Sci. 121 (1996) 109–116.
[13] A. Wüpper, F. Dellanna, C.A. Baldamus, D. Woermann, Local transport processes in high-flux hollow fiber dialyzers, J. Membr. Sci. 131 (1997) 181–193.
[14] W.F. Blatt, A. Dravid, A.S. Michaels, L. Nelsen, Solute polarization and cake formation: causes, consequences, and control techniques, in: J.E. Flinn (Ed.), Membrane Science and Technology, Plenum Press, New York 1970, pp. 47–97.
[15] A.L. Zydney, Bulk mass transport limitations during high flux hemodialysis, Artif. Organs 17 (11) (1993) 919–924.
[16] L. Wolf, S. Zaltman, Optimum geometry for artificial kidney dialysers, in: R.L. Dedrick, K.B. Bischoff, E.F. Leonard (Eds.), The Artificial Kidney, Chem. Eng. Prog. Symp. Series 84(LXIV) AIChE, New York, 1968, pp. 104–111.
[17] C. Gostoli, A. Gatta, Mass transfer in a hollow fiber dialyser, J. Membr. Sci. 6 (1980) 133–148.
[18] N. Hosoya, K. Sakai, Backdiffusion rather than backfiltration enhances endotoxin transport through highly permeable dialysis membranes, Trans. ASAIO 36 (1990) M311–M313.
[19] T.L. Pallone, J. Petersen, A mathematical model of continuous arteriovenous hemofiltration predicts performance, Trans. ASAIO 33 (1987) 304–308.
[20] E.M. Landis, J.R. Pappenheimer, Handbook of Physiology, Section 2: Circulation, Am. Phys. Soc., Washington, DC, 1963, vol. II, p. 961.
[21] T. Bosch, B. Schmidt, W. Samtleben, H.J. Gurland, Effect of protein adsorption on diffusive and convective transport through polysulfone membranes, Contr. Nephrol. 46 (1985) 14–22.
[22] L.J. Langsdorf, A.L. Zydney, Diffusive and convective solute transport through hemodialysis membranes: a hydrodynamic analysis, J. Biomed. Mat. Res. 28 (1994) 573–582.
[23] P. Feldhoff, T. Turnham, E. Klein, Effect of plasma proteins on the sieving spectra of hemofilters, Artif. Organs 8 (2) (1984) 186–192.

B: Example of the experimental determination of the Hagen-Poiseuille law for one *in vitro* test

40 HDF 30 test using a reinjection flow rate of Qr = 30 mL/min is considered as a reference test since ΔP_{meas} = 173.6 mmHg stays constant during dialysis session (Figure III.12). We propose to calculate ΔP_{hp} using experimental data of viscosity and the Hagen-Poiseuille law and to compare this value with ΔP_{meas}.

Viscosity measurement

We describe two methods to access to blood viscosity. The first one is to use from literature, empirical linear relations between blood hematocrit and viscosity (two examples of these linear relations are given) whereas the second one is to use the Casson model.

Linear empirical correlations between hematocrit and viscosity

Stiller et al. (1985) proposed Equation B.1 where the blood viscosity is given as function of its hematocrit:

$$\mu_S = 1.2 + 3.175 \times (H - 0.1) - 1.8748 \times (H - 0.1)^2 + 15.208 \times (H - 0.1)^3 \quad \textbf{B.1}$$

Where H is the decimal hematocrit.

While Mockros et al. (1985) found the following Equation B.2:

$$\mu_M = \mu p \times e^{0.0235H} \quad \textbf{B.2}$$

Where μp is the plasma viscosity (1.3 10^{-3} Pa.s) and H is hematocrit in %.

With Hi = 0.24 and Ho = 0.29 at hemodialyzer inlet and outlet, respectively for 40 HDF 30 test (with Qf= Qr = 30 mL/min), we obtain the results in Table B.1:

Method	μis (Pa.s)	μos (Pa.s)	μim (Pa.s)	μom (Pa.s)
Values	1.65 10^{-3}	1.84 10^{-3}	2.28 10^{-3}	2.57 10^{-3}
Viscosity increase at hemodialyzer outlet	12% increase		13% increase	
Mean values	1.75 10^{-3}		2.43 10^{-3}	

Table B.1 Blood viscosity from Stiller and Mockros equations at hemodialyzer inlet and outlet. Mean viscosities are calculated between hemodialyzer inlet and outlet

The mean viscosity is derived from the measured inlet and outlet hemodialyzer viscosities.

It can be seen that blood viscosity is strongly dependent of hematocrit and that these 2 empirical relations give very different blood viscosities.

Casson model

The 40 HDF 30 test bovine blood viscosity has been measured (before dialysis) at 20°C using a rheometer RheoStress 1 (Thermo Haake, Germany). The measurement has been measured three times to check reproducibility.

Figure B.1 illustrates the variation of dynamic viscosity with increasing shear rate.

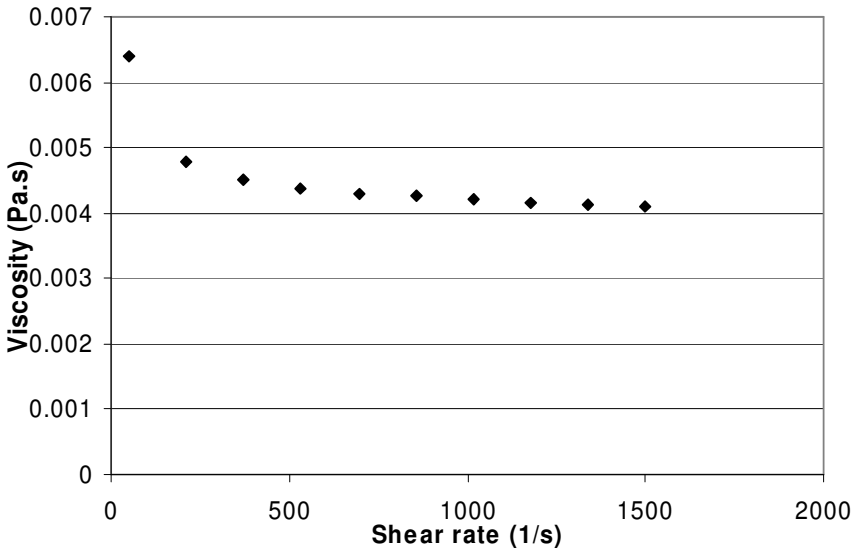

Figure B.1 Blood viscosity for 40 HDF 30, H = 24%, t = 20°C

The Casson equation is the most popular model for representation of non-Newtonian behaviour of blood over share rates (Chandran 2007) and is given by:

$$\sqrt{\tau} = \sqrt{\mu} \times \sqrt{\dot{\gamma}} + \sqrt{\tau_0} \qquad \textbf{B.3}$$

Where τ is the shear stress (Pa), μ the apparent viscosity (Pa.s), $\dot{\gamma}$ the shear rate (1/s) and τ_0 the yield stress.

For the 40 HDF 30 test, the linear regression between $\sqrt{\tau}$ and $\sqrt{\dot{\gamma}}$ is given by:

$$\sqrt{\tau} = 0.0606 \times \sqrt{\dot{\gamma}} + 0.1309 \qquad \textbf{B.4}$$

Therefore by identification the viscosity can be calculated: μ = 3.67 10^{-3} Pa.s and τ_0 = 0.0171 Pa.

As viscosity is strongly dependent on temperature, blood viscosity increases with decreasing temperature. Our viscosity has been measured at 20°C although blood viscosity is generally given at 37°C.

To obtain the blood viscosity in order to use Equation III.18 (Hagen-Poiseuille equation) and to calculate ΔP_{hp}, we have chosen Casson model rather than empirical mathematical relations between blood viscosity and hematocrit. This choice has been done, first due to the lack of precision of

hematocrit measurements (as seen in section 5.2 of the Chapter II) and secondly, due to the very different empirical mathematical relations between blood viscosity and hematocrit.

Application of the Hagen-Poiseuille law to the 40 HDF 30 test to calculate ΔP_{hp}

With Qbi = 200 mL/min and due to the ultrafiltration rate of 30 mL/min, mean blood flow rate has been taken for the Hagen-Poiseuille law to 185 mL/min (or 3.08 10^{-6} m^3/s).

With μ = 3.67 10^{-3} Pa.s (Casson model), and an estimated increase of blood viscosity of 12% at the hemodialyzer outlet for this test (as seen in Table B.1), viscosity has been taken for the Hagen-Poiseuille law to 4.11 10^{-3} Pa.s.

Using L = 25.5 cm (fibres length including potting), r = 92.5 µm, and N = 4588, ΔP_{hp} can be calculated from Hagen-Poiseuille law:

$$\Delta P_{hp} = \frac{8\mu L}{\pi r^4 N} Qb = 24473 Pa = 184 mmHg \qquad \textbf{B.5}$$

This value is very close to ΔP_{meas} = 173.6 mmHg measured with pressure transducers and is inferior to the ± 10% of the pressure errors measurements. The difference (5.4 %) can be attributed to experimental errors, devices precision, or blood viscosity measurements.

C: *In vivo* urea clearance and percentage of recirculation

Effect of the dialysis mode (HD/HDF) on urea clearance

Urea clearances are recorded in dialysis machine 5008 using Online Clearance Monitor (OCM) described in Chapter II and are periodically registered during the entire dialysis session.

Values in Table IV.1 correspond to mean values during the entire dialysis session: in HD sessions, CL_{HD} = 200.83 ± 8.35 mL/min and in HDF sessions, CL_{HDF} = 219.3 ± 13.69 mL/min. Paired student t-test applied for the comparison of HD and HDF clearance gives significant difference under a significant level of 5 % with p = 0.00023 < 0.05.

This result is also found in the literature: Kerr et al. (1992) have observed that the clearance of urea was significantly improved with HDF, which provide 10 to 15% better clearances of small molecules, such as urea, with the use of similar dialysers and dialysis time (between HD and HDF).

Jaffrin et al. (1990) have proposed the empirical correlation for the HDF clearance:

$$CL_{HDF} = CL_{Qf=0} + 0.46 \times Qf \quad \textbf{C.1}$$

Where Qf is the ultrafiltration flow rate, CL_{HDF} the clearance in HDF model and $CL_{Qf=0}$ the clearance at Qf = 0.

This correlation has been validated for medium solutes (creatinine, vitamine B12 and myoglobin) and using AN69 HF hemodialyzer of 1.15 m² with membrane permeability of about 30 mL/h/mmHg.

Applying this relation to our *in vivo* results, it can be found that the HDF clearance should be:

$$CL_{HDF} = CL_{Qf=0} + 0.46 \times 106.73 \approx 243.75 mL/\min \quad \textbf{C.2}$$

with $$CL_{Qf=0} = CL_{HD} - 0.46 \times 13.44 \approx 194.65 mL/\min \quad \textbf{C.3}$$

This result (243.75 mL/min) is overestimated compared to our urea HDF clearance measured.

Recirculation

Recirculation has been recorded using the Blood Temperature Monitor (BTM) with temperature sensors, explained in Chapter II.

Recirculation of blood directly to the extracorporeal circuit reduces the efficiency of a dialysis session because cleaned blood can be mixed with blood from the patient. It is imperative that the blood filtered returns back into the general circulation (in the body) and not in the extracorporeal circuit, or the dialysis session will be done in closed circuit. Recirculation percentage evaluates the potential presence of this phenomenon.

Mean total recirculation percentage has been recorded in our 23 dialysis sessions to be: 15.18 ± 5.9%. Patient MA02 and LC04 have higher percentage of recirculation than other patients. Paired student t-test applied for the comparison of HD and HDF recirculation gives not significant difference under a significant level of 5 % with $p = 0.96 > 0.05$.

In the literature Kerr et al. (1992) did not find any significant changes between recirculation in HD (15.3 ± 1.3%) and in HDF (15.6 ± 1.4%). Our mean results are very close in the two dialysis modes: we found a percentage of recirculation in HD of 14.64 ± 6.39 and in postdilution HDF, 15.72 ± 5.62.

D: *In vitro* urea mass transfer and clearance

Urea is a waste product formed in the liver during the metabolic breakdown of proteins and is removed by the kidney. In ESRD patients, urea is eliminated by dialysis techniques. Urea clearance is an important indicator of hemodialysis efficiency for physicians since it represents the blood flow rate cleared from urea. As already seen, urea clearance is now monitored by dialysis machine (see the beginning of Chapter IV).

This section is dedicated to urea transfers and urea clearance. Comparisons have been made between experimental data (*in vitro* tests) and theoretical data from the kinetic modeling. As laboratory urea concentrations are measured in plasma, they need to be multiplied by (1- H + HK) with K = 0.86 for urea to obtain blood concentrations.

1. Urea Mbh/Mdh comparison

Urea Mbh (plasma mass transfer through the hemodialyzer) and urea Mdh (dialysis fluid mass transfer through the hemodialyzer) should be equal as there is no accumulation or loss of urea inside the hemodialyzer.

In order to check the consistency of experimental urea mass transfer calculations, we have plotted in Figure D.1 the urea Mdh transfers calculated using dialysis fluid concentrations with the corresponding urea mass transfer in plasma, Mbh for the 9 *in vitro* tests.

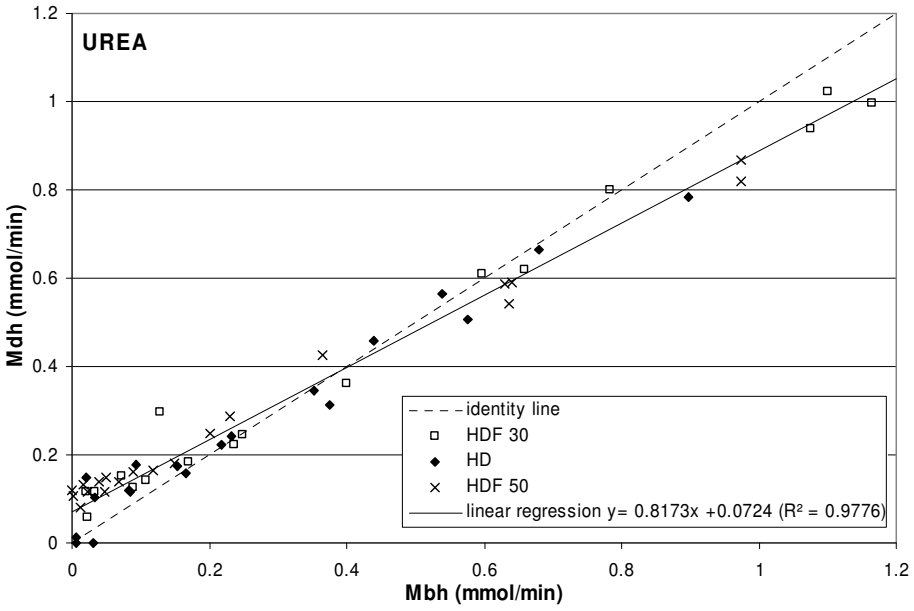

Figure D.1 Urea Mdh as function of Mbh (mmol/min)

Distinctions have been made between the dialysis mode, HD, HDF with Qr = 30 mL/min, and HDF with Qr = 50 mL/min. But no influence of the dialysis mode can be observed from the repartition of the points.

Mean value of differences between Mbh and Mdh is -0.017 ± 0.073 mmol/min.

The regression equation writes that Mdh = 0.82Mbh + 0.072, with a squared correlation coefficient of 0.98. It can be seen that the intercept point at the origin is 0.072 mmol/min which is very low.

This regression means that Mdh transfer is slightly larger than Mbh transfer for Mbh < 0.4 mmol/min and a slightly smaller Mbh for Mbh > 0.4 mmol/L. As Mbh and Mdh decrease with time, the values at the end of the dialysis session are situated between 0 and 0.2 mmol/min in Figure D.1. Values of mass transfer below 0.2 mmol/min need to be taken with caution as the limit detection of urea concentration (1 mmol/L) has been reached and this increases the error.

Nevertheless there is good agreement between instantaneous mass transfers measured in dialysate and in plasma, confirming the consistency of our urea calculation.

2. Urea mass transfers

Figure D.2 shows that urea mass flow rate through the hemodialyzer (Mbh) remain positive and decrease until zero (at 60 minutes) as blood urea has been completely eliminated in dialysis fluid.

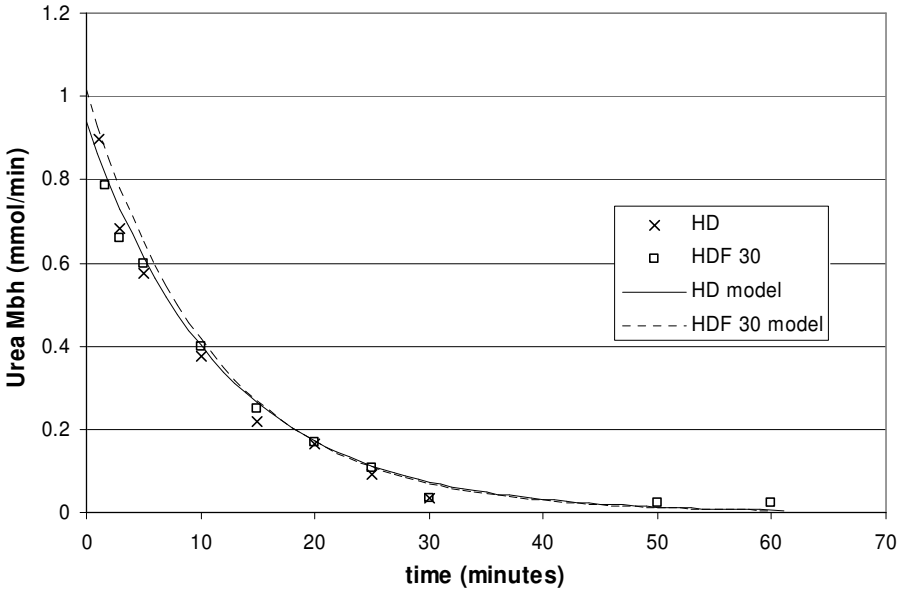

Figure D.2 Urea Mbh for 28 HD and 28 HDF 30 tests

There is only a small difference between the two dialysis modes in urea mass transfers through the hemodialyzer. This difference is due to the difference between initial urea concentrations between the two tests. As for urea time variation (as seen in Chapter III), good agreement is obtained between experimental and theoretical data.

3. Urea clearance

Urea clearance is independent on the urea plasma concentration and only depends on the operating conditions and on the hemodialyzer characteristics. According to the manufacturer data, using a FX 40 with a blood flow rate (Qb) of 200 mL/min and a dialysis fluid flow rate (Qd) of 500 mL/min leads to urea clearance of 170 mL/min (under blood specifications: H = 32%, proteins = 6% and T = 37°C) whatever the initial urea plasma concentration. Therefore urea clearance should be constant during dialysis session if the operating conditions stay the same during dialysis session.

Experimental urea clearances have been calculated by two different methods. The first one consists in calculating urea clearance from the urea mass transfer through the hemodialyzer using the 'traditional' definition of urea clearance. The second one is to determine urea clearance from the slope of the curve representing the logarithm of the experimental ratio of urea Cpi/Cpinitial. This section also presents urea clearances calculation from the kinetic model.

3.1. Experimental urea clearance time variation

Urea clearances (CL) have been calculated using Equation D.1.

$$CL = \frac{QbiCbi - QboCbo}{Cbi} = \frac{Mbh}{Cbi} \qquad \textbf{D.1}$$

Where Cbi = Cpi (1-Hi + HiK) and Cbo = Cpo (1-Ho + HoK). Cpi and Cpo are measured in samples taken at the hemodialyzer inlet and outlet, respectively. Hi and Ho are measured by ABL in samples taken at the hemodialyzer inlet and outlet, respectively.

Figures D.3 give urea clearance time variation during dialysis session of two HD and three HDF 30 tests.

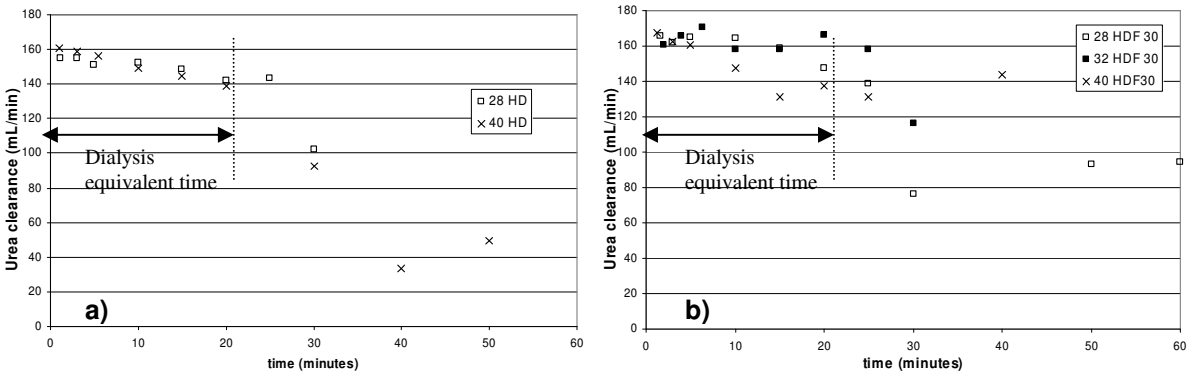

Figures D.3 Urea clearance time variation for two HD (a)) and three HDF 30 (b)) tests

Urea clearance slightly decreases with time until 25 minutes and then drops sharply. As urea concentrations become under the device detection limit (1 mmol/L) generally after 25-30 minutes, urea clearance calculations can not be valid and must not be taken into account. Nevertheless, until 25

minutes, urea clearance decrease about 8 % for HD tests and 16% for 28 HDF 30 test. Urea clearance decrease is more related to blood quality than to operating conditions which have been stable during all *in vitro* tests. For the 32 HDF 30 test, urea clearance stays quite stable with an ultrafiltration of 30 mL/min.

In practice during dialysis session of dialysis patient, it is known that urea clearance decrease about 10%.

It can also be seen that at the beginning of the dialysis session, urea clearance is higher in HDF 30 (with Qr = Qf = 30 mL/min) than in HD tests: for 40 HD test, CL = 160.8 mL/min and for 40 HDF 30 tests, CL = 168 mL/min (or an increase of 4.5%). The relatively low difference is due to the small ultrafiltration rate and to the mainly diffusive transfer.

3.2. Mean experimental urea clearance over dialysis session

Urea mass balance (in HD and in HDF, since Cdi = 0 for urea) can be written, according to equation presented in Chapter III (Figure III.1):

$$\frac{d(VbCb)}{dt} = QboCbo - QbiCbi = -CL \times Cbi \qquad \textbf{D.2}$$

Where CL is urea hemodialyzer clearance in HD or in HDF.

Then as Vb(t) = -Qw*t + Vbin (seen in Chapter II, section 4.4), where Qw is the weight loss rate and Vbin the initial blood volume, Equation D.2 becomes:

$$\frac{dCbi}{dt} = \frac{(Qw - CL) \times Cbi}{Vb(t)} \qquad \textbf{D.3}$$

An analytical solution can be obtained if Vb = Vbin = constant (Qw = 0, since it is the case of our *in vitro* tests):

$$Cb(t) = Cbin \times e^{\frac{-CL \times t}{Vbin}} \text{ for HD and HDF mode} \qquad \textbf{D.4}$$

Leading to:

$$CL \times t = -Vbin \times \ln \frac{Cb(t)}{Cbin} \qquad \textbf{D.5}$$

Therefore CL, the urea hemodialyzer clearances in HD as in HDF mode are experimentally determined by the slope of the curves Vbin* ln(Cb(t)/Cbin) for the 9 *in vitro* tests. The slopes of the curves are only determined over the first 15-20 minutes of the dialysis session when the urea clearances are quite stable.

Figure D.4 shows the good linearity between CL * t and time for 40 HD, 32 HDF 30 and 28 HDF 50 tests. Nevertheless for 28 HDF 50 test, the urea clearance is 216.9 mL/min which is impossible since the *in vitro* blood flow rate is 200 mL/min.

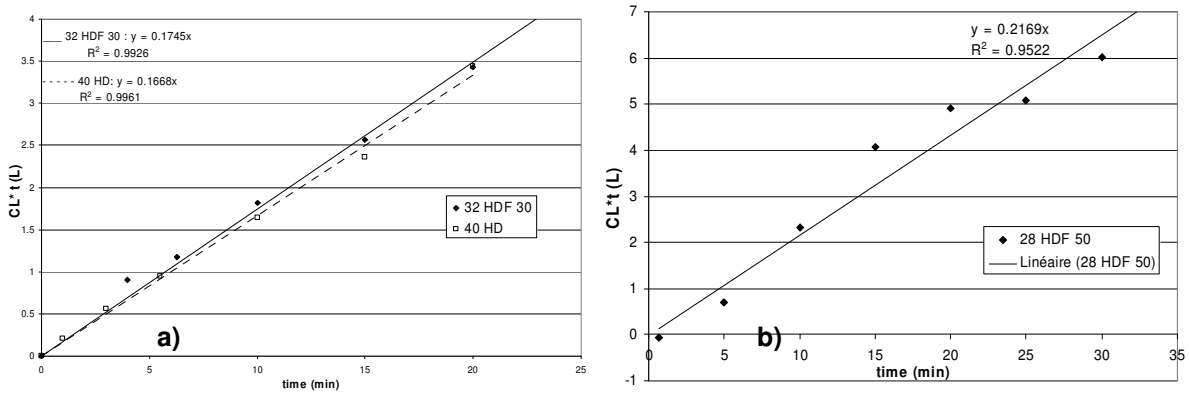

Figures D.4 Example of urea hemodialyzer clearance determined by the slope of the curve Vbin* ln(Cb(t)/Cbin) for 40 HD, 32 HDF 30 (a) and 28 HDF 50 (a) tests

Table D.1 presents the results of urea hemodialyzer clearance for the 9 *in vitro* tests. These results must be taken with caution since some values have been calculated higher than the blood flow rate of 200 mL/min which is impossible. This can be due to measurements errors in urea concentration or to blood and reinjection pump errors.

	28 HD	32 HD	40 HD	28 HDF 30	32 HDF 30	40 HDF 30	28 HDF 50	32 HDF 50	40 HDF 50
Urea clearance, CL (mL/min)	156	na	167	191.1	174.5	205.6	216.9	200.6	168.1
R^2	0.99	na	0.996	0.989	0.993	0.94	0.952	0.96	0.963
Mean ± sd	161.5 ± 7.8			190.4 ± 15.56			195.2 ± 24.84		

Table D.1 Mean urea hemodialyzer clearance. na = not available

It can be seen that mean urea hemodialyzer clearance is lower in HD tests than in HDF tests. This is consistent with the clinical literature which reports higher urea clearance in HDF mode than in HD as already seen in the previous section.

3.3. Urea clearance by kinetic modeling

If we compare these values of urea clearance calculated from experimental data, with data from the kinetic modeling, urea clearance is found to be CL = 170 mL/min in HD and 177.7 mL/min in HDF 30, or an increase of 4.6 % between the two modes, and 182.5 mL/min for HDF 50 mode. As the modeling does not take into account blocked fibres during dialysis session, these values stay constant during the entire dialysis session.

In the Chapter III, we have shown that blood clotting could block a significant number of fibres during dialysis sessions. Using the kinetic modeling, we have tried to evaluate the effect of the decrease of the number of active fibres (or decrease of active membrane area) on the urea clearance. This calculation follows the 4th section of Chapter III where a modeling approach is presented to evaluate the number of blocked fibres.

Combined with the kinetic modeling, the Legallais et al. model (2000) uses the Graetz theory to calculate blood mass transfer coefficient (Kb). This law depends on module geometry, blood properties and operating conditions. Blood and dialysate mass transfer coefficients allow the calculation of the local transmembrane solute flux which is used in the mass balance of solute in order to determine the solute concentration profile between inlet and outlet hemodialyzer. Then urea clearance is calculated knowing concentrations and hematocrit at the hemodialyzer inlet and outlet.

If we number of fibres decrease, we can see an impact on the available surface area which decrease and an impact on the blood velocity in the remaining active fibres which increase. This increase leads to an increase of the blood mass transfer coefficient Kb.

Table D.2 shows the urea clearance calculated with the local model in function of the number of active fibres in HD mode.

Number of active fibres and percentage of blocked fibres	N = 4588	N = 4359 (5%)	N = 4129 (10%)	N = 3670 (20%)	N = 2294 (50%)
Urea clearance (Qf = 0) mL/min	170.2	167.3	163.7	155.3	120.3
Percentage of urea clearance decrease	Initial status	1.7%	3.8%	8.7%	29.3%

Table D.2 Effect of blocked fibres on urea hemodialyzer clearance in HD mode. The operating conditions are the same as for *in vitro* tests: FX40 hemodialyzer geometry, Qb = 200 mL/min, Qd= 500 mL/min

Urea clearance decreases when the number of active fibres decreases. However, this decrease is not linear: when no ultrafiltration is applied, a 20% loss of fibres leads to a urea clearance decrease of 8.7%. It seems that ultrafiltration has a small influence on it: using Qf = 30 mL/min, a 20 % loss of fibres leads to a urea clearance decrease of 7.4%.

Using these results of calculated urea clearance, we can conclude that a decrease of the number of active fibres (due to blocked fibres) until 20% does not have a significant impact on urea clearance (a decrease < 10%).

3.4. Conclusions on urea clearance

In this paragraph we have shown that *in vitro* urea clearance can be calculated by the 2 methods with a good agreement with urea clearance calculated with the kinetic modeling. The first method gives an indication on urea clearance time variations during the *in vitro* tests and the second one allows calculation of mean urea clearance during the first 20 minutes of the dialysis session. Even if some results show impossible urea clearance, the other results are in good agreement with literature and with kinetic modeling and are quite stable during dialysis session.